

School of Chemistry
Cardiff University



**Triazine Based N-Heterocyclic Carbenes -
Synthesis, Coordination and Catalysis**

Mohammed M. Hasson

**A thesis submitted to Cardiff University
in accordance with the requirements for the degree of
Doctor of Philosophy**

July 2015

DECLARATION

This work has not been submitted in substance for any other degree or award at this or any other university or place of learning, nor is being submitted concurrently in candidature for any degree or other award.

Signed (candidate) Date.....9/07/2015.....

STATEMENT 1

This thesis is being submitted in partial fulfilment of the requirements for the degree of PhD.

Signed..... (candidate) Date.....9/07/2015.....

STATEMENT 2

This thesis is the result of my own independent work/investigation, except where otherwise stated. Other sources are acknowledged by explicit references. The views expressed are my own.

Signed..... (candidate) Date.....9/07/2015.....

STATEMENT 3

I hereby give consent for my thesis, if accepted, to be available for photocopying and for inter-library loan, and for the title and summary to be made available to outside organisations.

Signed..... (candidate) Date..... 9/07/2015.....

STATEMENT 4: PREVIOUSLY APPROVED BAR ON ACCESS

I hereby give consent for my thesis, if accepted, to be available online in the University's Open Access repository and for inter-library loans after expiry of a bar on access previously approved by the Academic Standards & Quality Committee.

Signed (candidate) Date 9-7-2015.....

ACKNOWLEDGMENTS

In the name of Allah, Most Gracious,

To Allah, my God you have promised to help those who need you. So I have deep faith that you will not abandon me.

First of all I would like to thank my supervisors: Dr. Athanasia Dervisi for her support and expert leadership and for giving me this opportunity to study under her supervision. Without her care and timely guidance I could not have achieved my goals. Dr. Ian Fallis for the assistance, encouragement and valuable suggestions you have provided to aid me in overcoming the difficulties that I've faced during the course of this work. A huge thank you to the academic staff in the school of chemistry, particularly Dr. Angelo Amoroso, Dr. Benjamin D. Ward and Dr. Benson Kariuki for their advice and support. I would also like to thank the technical staff at Cardiff University; Robin for his patience with mass spectrometry and Dr Rob Jenkins for his help and keeping NMR machines online. A great thank you has to go to everyone past and present who have been in the inorganic section. Steve, Owen, Lenali, Thomas, Brendan, Ollie, Emily Langdon-Jones, Emily Stokes Mauro, Ali Al-Riyahee, Mohammed Bahili, Geraint, Andy and Seni, for making my time during my PhD so enjoyable and their sincere support. I would like thank my friend Mark Driver for his help throughout this thesis. I wish to thank my family for their love, kindness and unlimited support, my brother and sisters for their unconditional encouragement during my study and my lovely children Abd Allah and Abd Al-kareem for their love, support and for keeping me going. Without you all I would not have been able to complete my goals.

I would like to give special thanks to the Establishment of Martyrs Iraq who take care of the families of Martyrs for a postgraduate scholarship.

ABBREVIATIONS

NHC	N-hetrocyclic carbene
DMSO	Dimethyl sulfoxide
DMF	Dimethylformamide
NaOAc	Sodium acetate
SMe ₂	dimethyl sulfide
DCM	Dichloromethane
t-BuOK	Potassium <i>tert</i> -butoxide
THF	Tetrahydrofuran
<i>p</i> -cymene	1-Methyl-4-isopropyl benzene
PEPPSI	pyridine-enhanced pre-catalyst, preparation, stabilization and initiation
NMR	nuclear magnetic resonance
py	pyridine
<i>et al</i>	and others
Choral	CCl ₃ CHO
Mes	Mesityl (1,3,5-trimethylphenyl)
HHM	hexamethylmelamine
ORTEP	Oak-Ridge thermal ellipsoid plot
TON	Turnover number
C _{NHC}	Carbene carbon
Hz	Hertz
TON	Turnover number
TOF	T urnover frequency

Abstract

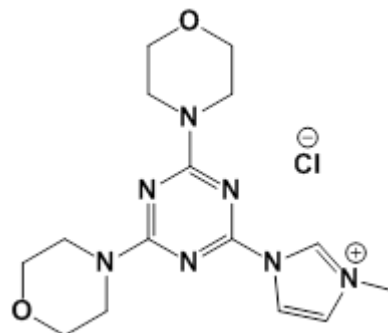
This thesis describes the synthesis and characterization (^1H , ^{13}C NMR, CHN, and X-ray) of new NHC ligands incorporating a triazine core and their complexation with Ag(I), Pd(II) and Ru(II) metals. Imidazolium salts **[2.4H]I** – **[2.7H]Br** and **[2.10H]** - **[2.15H]Br** were obtained by reaction of 2,4-diamino-6-chloro-1,3,5-triazine (diamino = morpholine, piperidine, diethylamine, or dimethylamine) with H- imidazole followed by alkylation with a variety of alkyl halides such as propyl, butyl, octyl bromides or isopropyl iodide. While the imidazolium salts **[2.3H]Cl**, **[2.8H]Cl**, **[2.9H]Cl** and **[2.13H]Cl** were prepared by reaction of N-substituent imidazole (mesityl, phenyl ethyl, and methyl) with 2,4-diamino-6-chloro-1,3,5-triazine (diamino = morpholine or dimethylamine). Silver complexes were prepared from the reaction of Ag_2O with an NHC precursor salt using in situ deprotonation techniques giving the desired structures in good yield. X-ray studies with other spectral and analytical studies reveal the formation monodentate complexes of the NHC ligands. The coordination geometry at Ag is slightly distorted from the idealised linear geometry. The Ag(I)-NHC complexes were used as NHC transfer reagents to prepare Ru(II) and Pd(II) complexes.

New monodentate Pd (II) complexes were prepared by in situ deprotonation of the NHC ligand by K_2CO_3 in the presence of PdCl_2 . The catalytic activity of the complexes in the Suzuki reaction was explored with conversions of up to 100 % being observed. Bis(carbene)Pd(II) complexes were prepared by transmetalation from the silver complexes with $\text{Pd}(\text{MeCN})\text{Cl}_2$. X-ray crystallography shows a distorted square planar geometry around the palladium metal centre for both complex types.

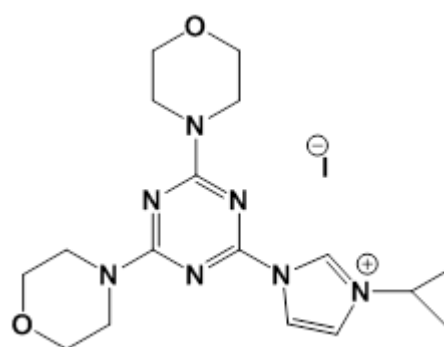
A series of Ru (II) complexes were prepared by transmetalation techniques using the silver complexes as transfer reagents with $[\text{Ru}(\eta^6\text{-arene})\text{Cl}_2]_2$ in dichloromethane. Single crystal studies along with other spectral and analytical studies reveal the coordination of the triazine-NHC ligand in a chelating mode where both the carbene and one of the N-donors of the triazine group ligate the metal. The complexes are active for the transfer hydrogenation of ketones with conversions up to 96%.

New NHC Salts

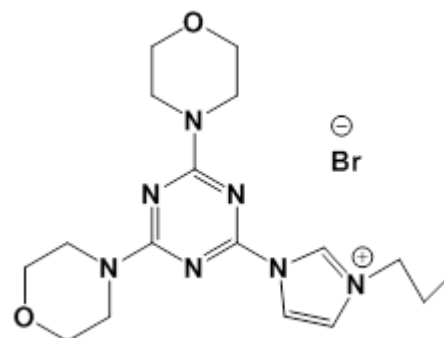
[2.3H]Cl [1-TzMorph₂-3-Me- Im]Cl



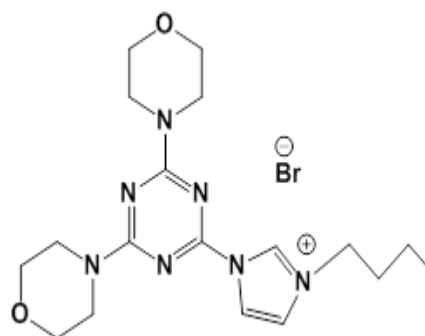
[2.4H]I [1-TzMorph₂-3-IPr- Im]I



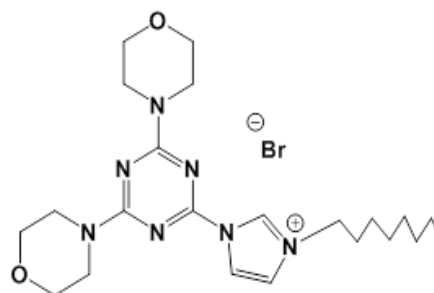
[2.5H]Br [1-TzMorph₂-3-Pr- Im]Br



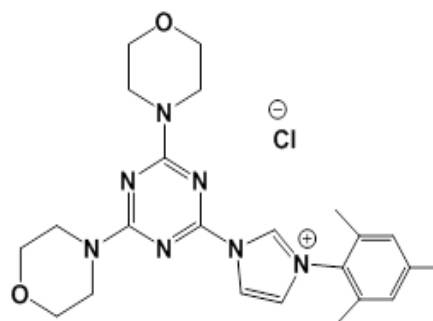
[2.6H]Br [1-TzMorph₂-3-Bu- Im]Br



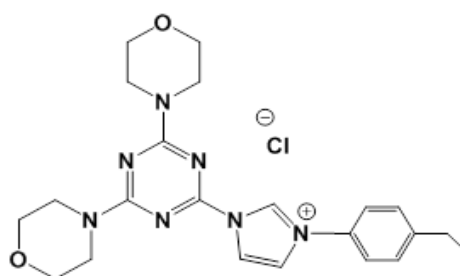
[2.7H]Br [1-TzMorph₂-3-octyl-Im]Br



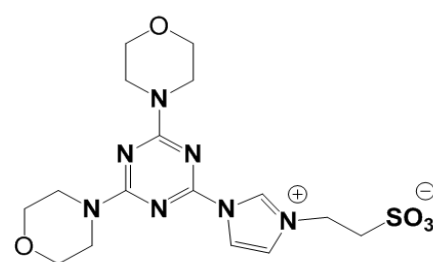
[2.8H]Cl [1-TzMorph₂-3-mes-Im]Cl



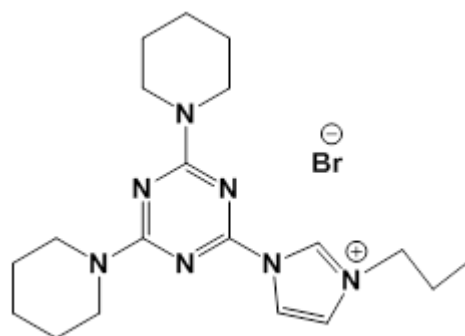
[2.9H]Cl [1-TzMorph₂-3-PhEt-Im]Cl



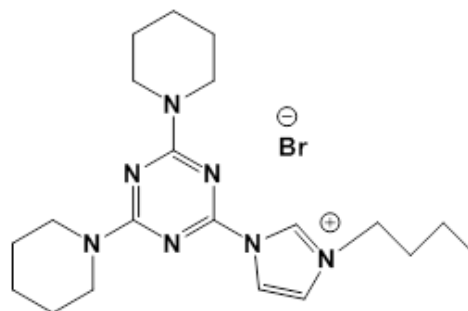
[2.10H] [1-TzMorph₂-3-sulfonat-Im]



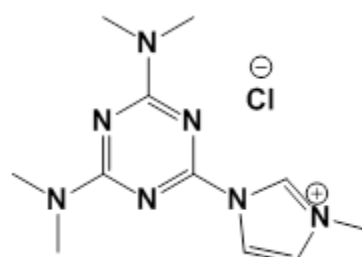
[2.11H]Br [1-TzPip₂-3-Pr-Im]Br



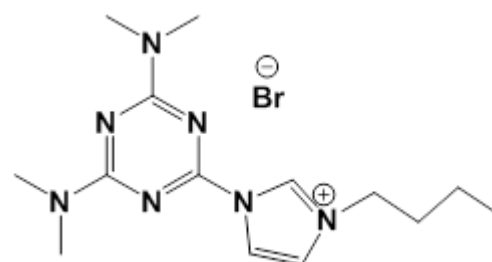
[2.12H]Br [1-TzPip₂-3-Bu-Im]Br



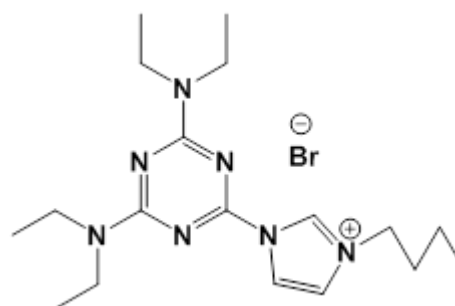
[2.13H]Cl [1-Tz(NMe₂)₂-3-Me-Im]Cl



[2.14H]Br [1-Tz(NMe₂)₂-3-Bu-Im]Br

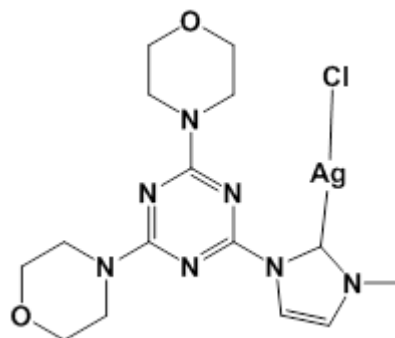


[2.15H]Br [1-Tz(NEt₂)₂-3-but-Im]Br

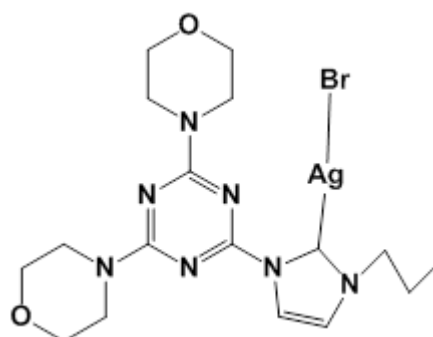


Ag Complexes

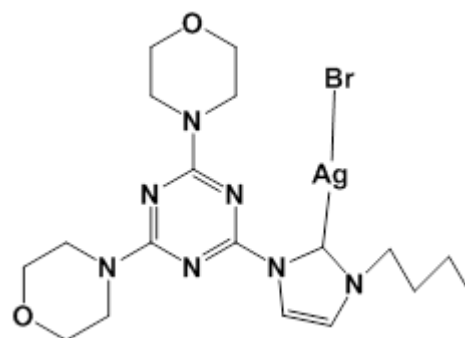
3.1 [AgCl(2.3)]



3.2 [AgBr(2.5)]

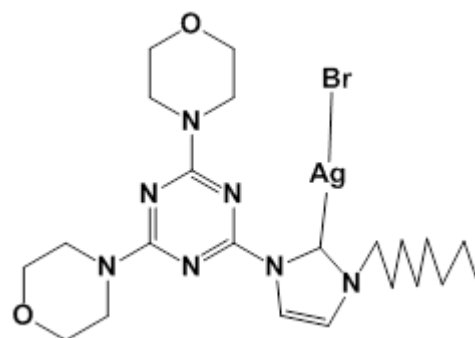


3.3 [AgBr(2.6)]



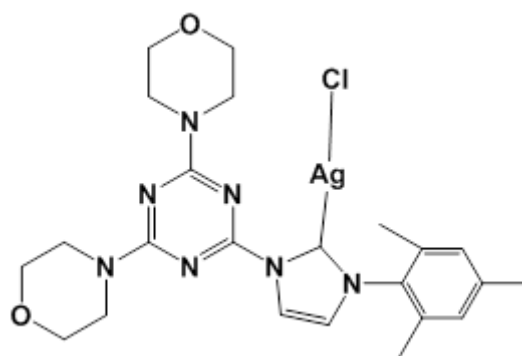
3.4

[AgBr(2.7)]



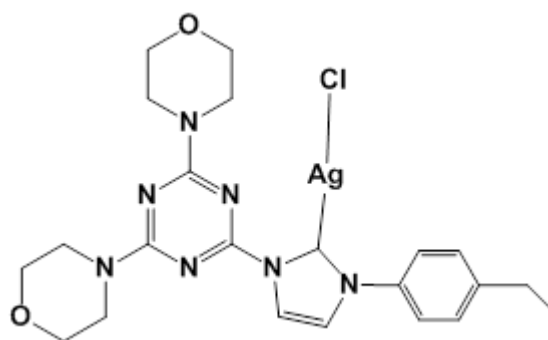
3.5

[AgCl(2.8)]



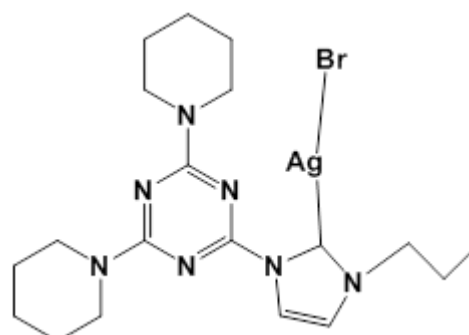
3.6

[AgCl(2.9)]



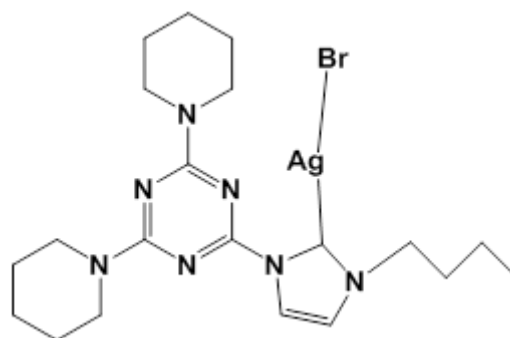
3.7

[AgBr(2.11)]



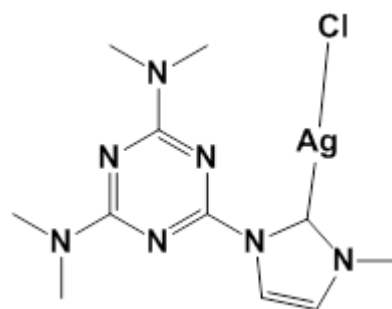
3.8

[AgBr(2.12)]



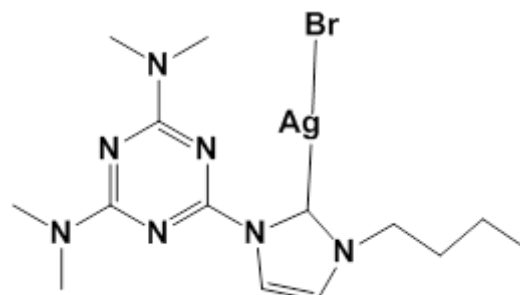
3.9

[AgCl(2.13)]



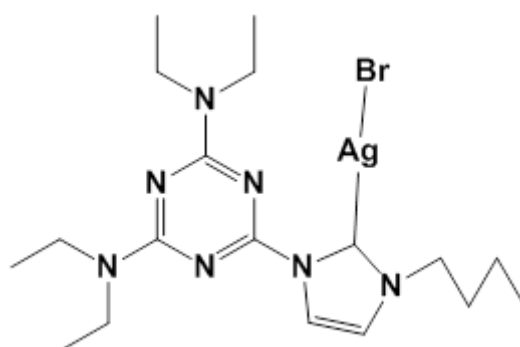
3.10

[AgBr(2.14)]



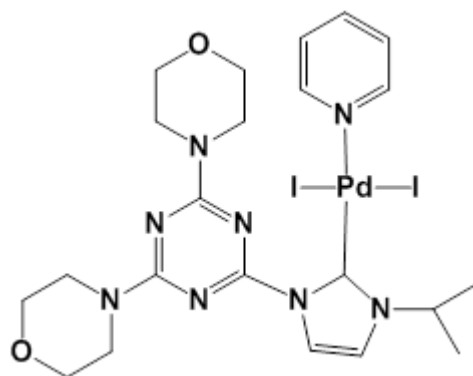
3.11

[AgBr(2.15)]

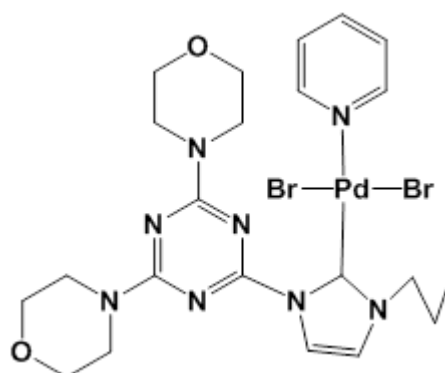


Pd Complexes

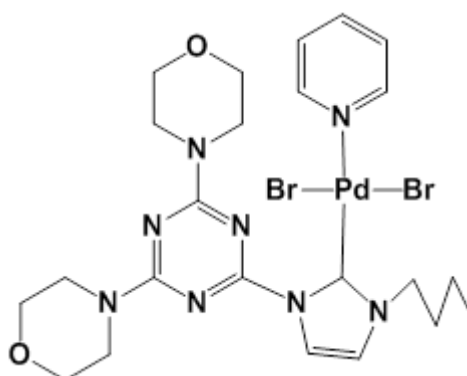
4.1 [Pd(py)I₂(2.4)]



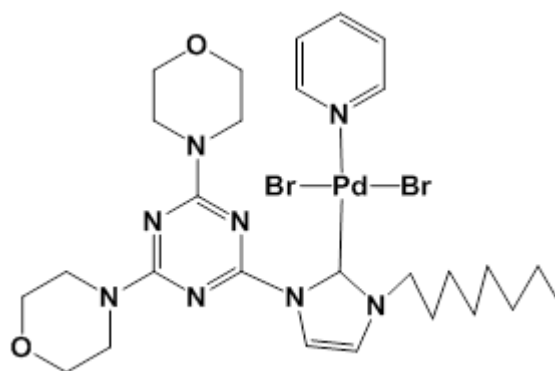
4.2 [Pd(py)Br₂(2.5)]



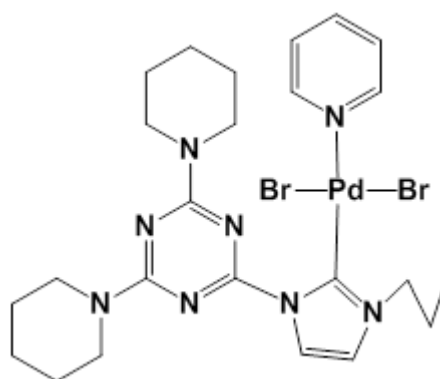
4.3 [Pd(py)Br₂(2.6)]



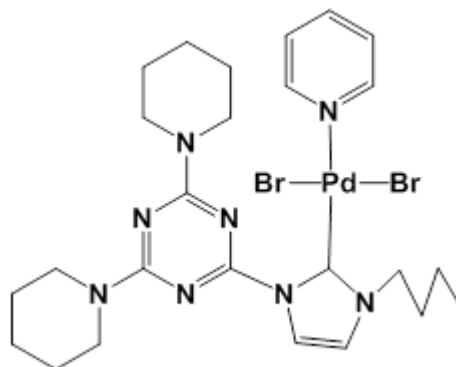
4.4 [Pd(py)Br₂(**2.7**)]



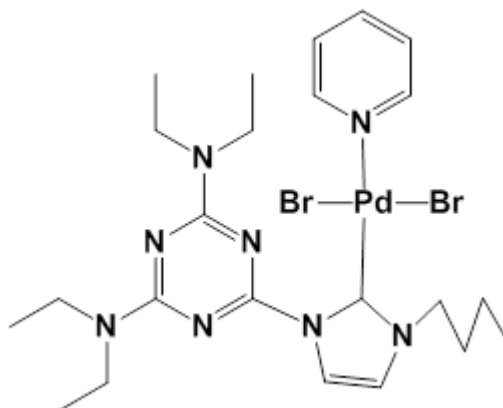
4.5 [Pd(py)Br₂(**2.11**)]



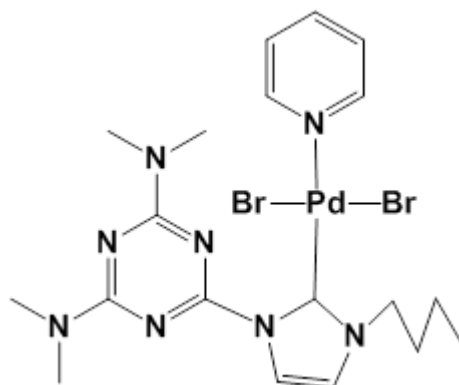
4.6 [Pd(py)Br₂(**2.12**)]



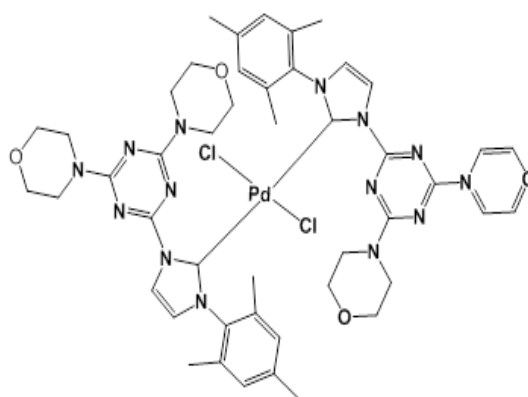
4.7 [Pd(py)Br₂(**2.15**)]



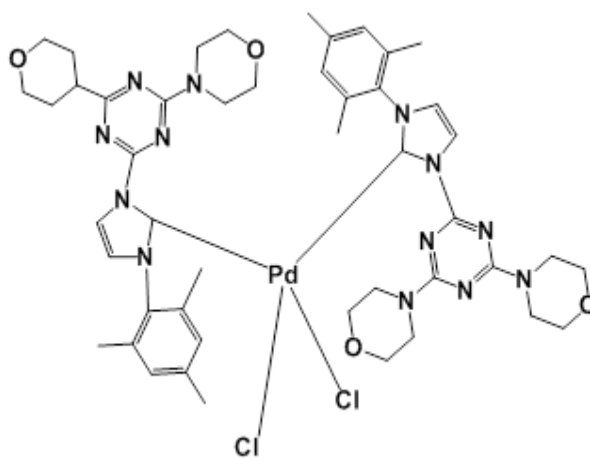
4.8 [Pd(py)Br₂(**2.14**)]



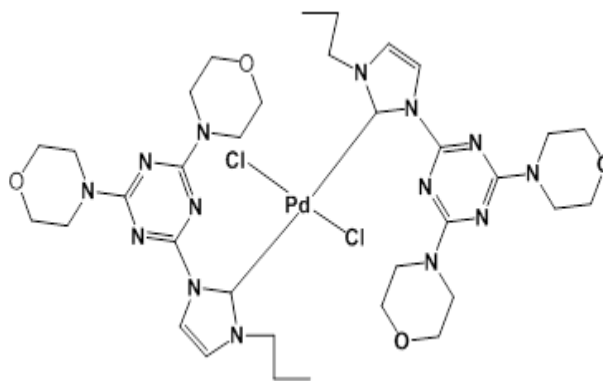
4.9a *trans*-[PdCl₂(**2.8**)₂]



4.9b *Cis*-[PdCl₂(**2.8**)₂]

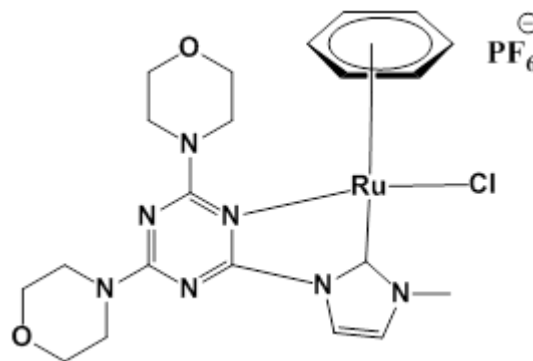


4.10 [Pd(Cl₂(2.5)₂)]

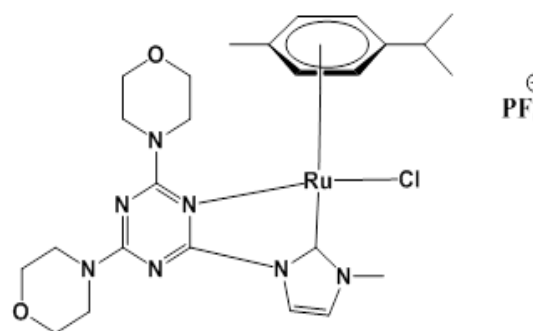


Ru Complexes

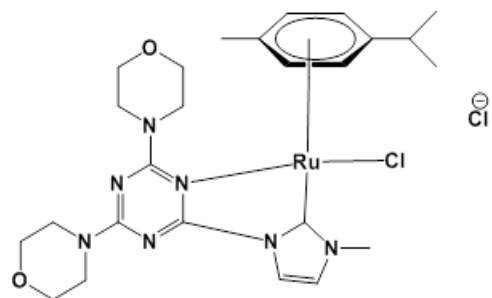
5.1 [Ru(C₆H₆)Cl(2.3)] PF₆[⊖]



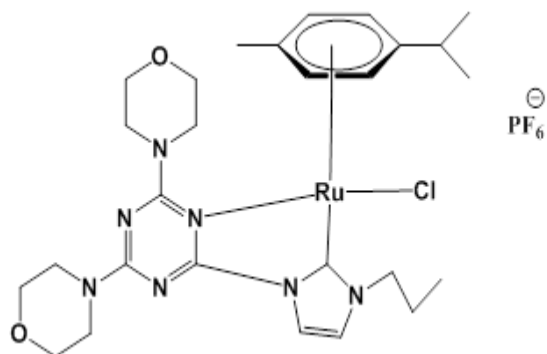
5.2 [Ru(*p*-cymene)Cl(2.3)] PF₆[⊖]



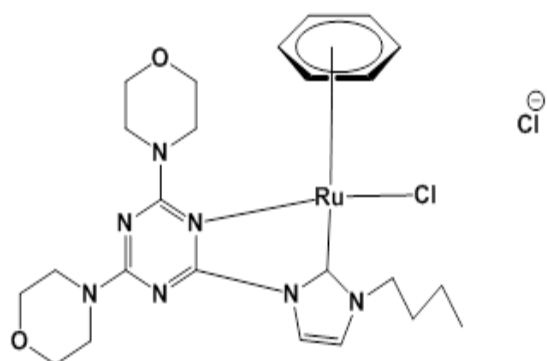
5.3 [Ru(*p*-cymene)Cl(2.3)] Cl



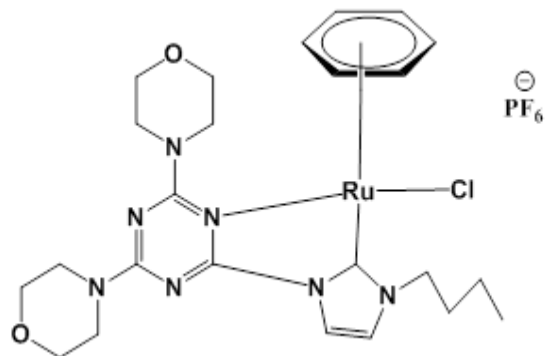
5.4 [Ru(*p*-cymene)Cl(2.5)] PF₆



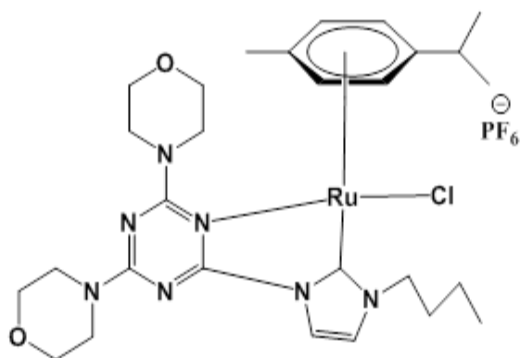
5.5 [Ru(C₆H₆)Cl(2.6)] Cl



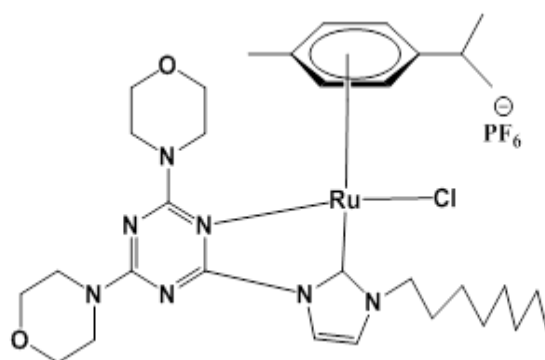
5.6 [Ru(C₆H₆)Cl(2.6)] PF₆



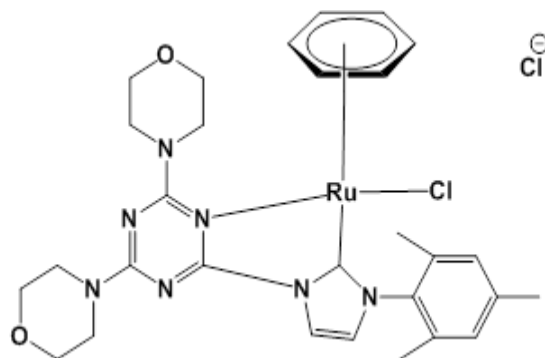
5.7 [Ru(*p*-cymene)Cl(2.6)] PF₆



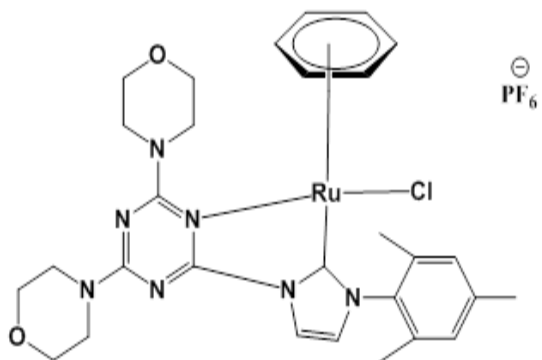
5.8 [Ru (*p*-cymene)Cl(2.7)] PF₆



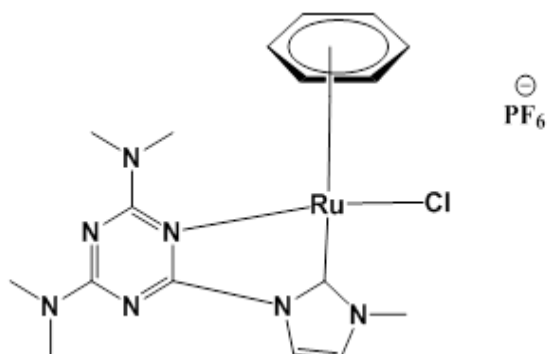
5.9 [Ru(C₆H₆)Cl(2.8)] Cl



5.10 [Ru(C₆H₆)Cl(2.8)] PF₆[⊖]



5.11 [Ru(C₆H₆)Cl(2.13)] PF₆[⊖]



5.12 [Ru(C₆H₆)Cl(2.14)] PF₆[⊖]

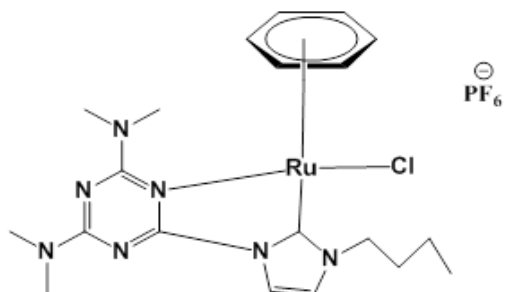


Table of Contents

Chapter 1	1
1.1- Carbenes definition	1
1.2-Type of carbene ligands	2
1.2.1-Fischer carbenes	3
1.2.2-Schrock carbene	3
1.2.3-NHC carbene	4
1.3-N-Heterocyclic carbene complexes	7
1.4-Preparation of NHC complexes	8
1.4.1-In situ deprotonation of imidazolium salt	8
1.4.2-Preparation of complexes via free carbene	10
1.4.3-Transmetalation method.....	12
1.5-Triazine	14
1.6-NHC complexes as Catalysts	17
1.6.1-Suzuki cross coupling reaction.....	18
1.7- Transfer hydrogenation reaction	20
1.8-Aims and objectives of this research	22
1.9-References	24
Chapter 2	30
Synthesis and characterization of new NHC ligands incorporating a triazine core	30
2.1-Introduction	30

2.1.1-Imidazoles and Imidazolium salts	30
2.1.2-Synthesis of imidazolium salts	31
2.1.2.1- Substitution on the imidazole ring	32
2.1.2.2-Synthesis of imidazolium ring	32
2.1.3-What is a triazine?	33
2.1.4-Strategy for Designing New NHC Ligands incorporating a triazine core	39
2.2- Results and discussion	41
2.2.1-Synthesis of 2, 4-diamino-6-chloro -1, 3, 5-triazine	41
2.2.2- Synthesis of 2, 4-di amino-6-(1 <i>H</i> -imidazol-1-yl)-1, 3, 5-triazine....	42
2.2.3- Synthesis of imidazolium salts.....	42
2.2.4-Solid state structural studies.....	47
2.3-Experimental	51
2.4-References	68
Chapter3.....	71
Synthesis and characterization of new N-heterocyclic carbene complexes of Ag (I).....	71
3.1-Introduction.....	71
3.1.1-Synthesis of Ag-NHC complexes	71
3.1.2-Structural variation of Ag-NHC complexes.....	74
3.1.3-Aims	78
3.2 - Results and discussion	79

3.2.1-Synthesis of silver complexes (3.1-3.11)	79
3.2.2 - X-ray Structural Determination.....	82
3.3-Experimental	88
General procedure of synthesis of Ag(I)NHCs.....	89
3.4-References	97
Chapter 4.....	100
Synthesis and characterization of new Pd(II)-NHC complexes and their application in catalysis	100
4.1-Introduction.....	100
4.1.1-Synthesis of Pd-NHC complexes	100
4.1.2- NHC–Pd cross-coupling catalysis.....	105
4.1.3-Summary	112
4.2-Results and discussion	114
4.2.1-Synthesis of Pd-NHC complexes	114
4.2.2-X-ray Structural Determination.....	121
4.2.3-Catalytic activity of Pd(NHC)(py)Cl ₂	130
4.3-Experimental	134
4.4-References	144
Chapter 5.....	148
Synthesis and characterization of new Ru(II)-NHC complexes and their application in transfer hydrogenation reactions	148
5.1-Introduction.....	148

5.1.1-Types of Ru-NHC complexes	148
5.1.1.1-NHC–Ru arene complexes	149
5.1.2-Transfer hydrogenation application	154
5.1.3-Aims	159
5.2-Results and discussion	161
5.2.1-Synthesis of Ru-NHC complexes.....	161
5.2.2-X-ray Structural Determination.....	165
5.2.3-Catalytic Transfer Hydrogenation of Acetophenone	175
5.3-Experimental	181
5.4-References	191
Chapter 6.....	195
6.1-Conclusions	195
Publication from this Thesis	200
X-Ray crystal structure data	201

Chapter 1: Introduction

1.1- Carbenes definition

Carbenes have been known for over 100 years. [1] They are neutral molecules containing at least one carbon atom with 6 electrons in its valence shell. [2-4] The carbon atom bears two sigma bonds in addition to the two remaining electrons in a non-bonding orbital (Figure1-1).

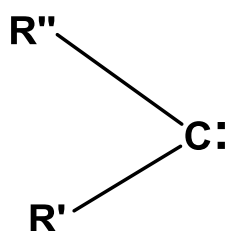


Figure (1-1) General formula of a carbene

Depending on the multiplicity of the unshared electrons, the carbene can be classified as either a singlet or triplet ground state. The singlet ground state occurs when the unshared electrons occupy the same σ or π orbital with anti-parallel spin. Whereas the triplet ground state occurs when the electrons are unshared, occupying the σ - and π -orbitals with parallel spins (Figure 1-2).

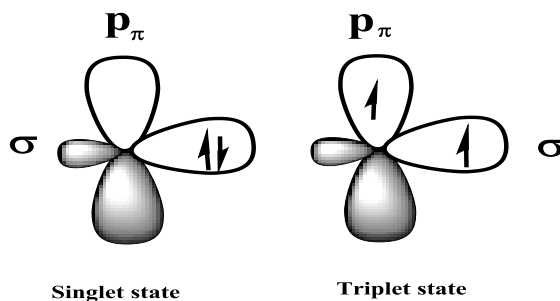


Figure (1-2) Ground states of carbenes

The geometry of the carbene carbon atom can be either bent or linear. The bent shape implies sp^2 hybridization, with the P_y orbital retaining pure p character, this orbital called P_π . Likewise, the S character increases in the P_x orbital and this orbital forms the σ -orbital. These differences lead to a loss of degeneracy between these orbitals. The linear shape adopts sp hybridization with two non-bonding degenerate orbitals (P_x and P_y , Figure 1-3). [3, 5]

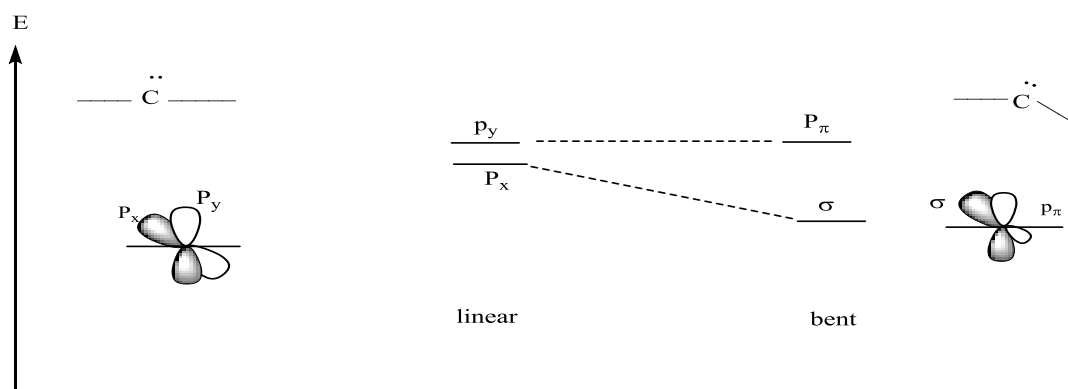


Figure (1-3) Diagram illustrating the loss of degeneracy of carbene orbitals

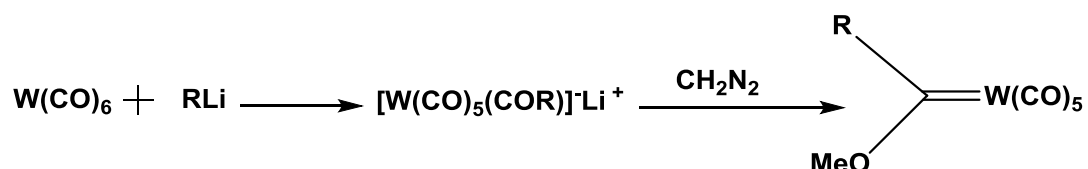
The ground state is determined by the relative energies of σ and $p\pi$ orbitals, when the gap between them is greater than 2 eV the singlet ground state is preferred, while if the gap is less than 1.5 eV the triplet state is more stable. [6, 7]

1.2-Type of carbene ligands

Carbene ligands can be classified into three categories according to their structure and reactivity towards a metal ion; Fischer carbenes, Schrock carbenes and Arduengo or N-heterocyclic carbenes.

1.2.1-Fischer carbenes

Fischer prepared the first complex of this type in 1964. The tungsten complex was synthesised by the reaction of tungsten (0) hexacarbonyl with an alkyl lithium, followed by treatment with diazomethane (Scheme 1-1). [8]



Scheme (1-1) preparation of first Fischer complex

Fischer carbenes display a singlet ground state, the carbene is bonded to a metal by the lone pair located in the sp^2 orbital to form a σ bond, the metal can then back-bond to the empty p_π orbital of the carbene to form a π bond. This type of carbene forms complexes with a low oxidation state, with middle and late transition metals such as Cr(0), Fe(0), Mn(0) and Co(0) (Figure 1-4).

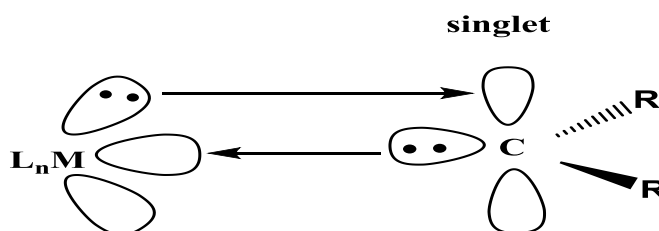
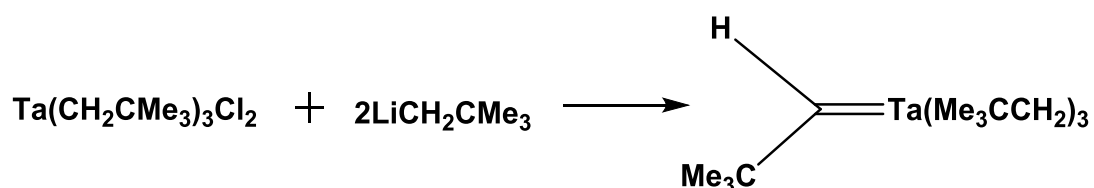


Figure (1-4) Bonding in the Fischer carbene

1.2.2-Schrock carbene

This type of carbene was first synthesised by Schrock in 1974 via treatment of dichlorotris(neopentyl)tantalum with neopentyl lithium (Scheme 1-2). [9-11] Schrock carbenes occur in the triplet ground state and are found with high oxidation state,

early transition metals. Schrock carbenes do not have the π -acceptor ligands, and are nucleophilic complexes.



Scheme (1-2) Synthesis of the first Schrock carbene

Schrock complexes can be described as having two covalent bonds between the carbene and metal. As the carbon atom is more electronegative than the metal, the covalent bonds tend to be partially polarized and thus the carbene centre is nucleophilic.

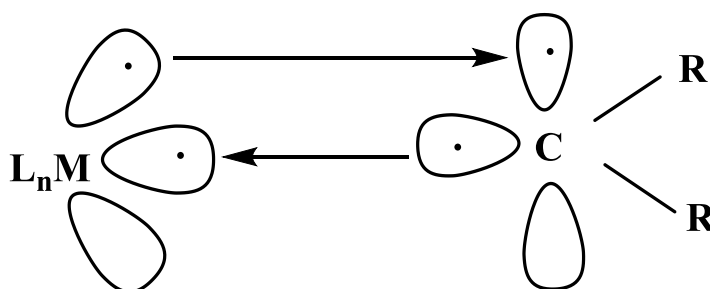


Figure (1-5) Bonding in Schrock carbene

1.2.3-NHC carbene

N-Heterocyclic carbenes refer to cyclic compounds derived from deprotonation of azolium salts. There are similarities between NHC complexes and those of Fischer carbenes where the lone pair is donated by the NHC to the metal to form a strong sigma bond. [12] However in the case of NHCs the π acceptor interaction does not occur (Figure 1-6).

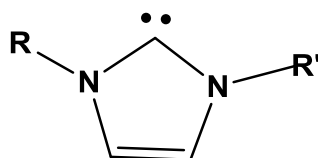


Figure (1-6) a N-heterocyclic carbene

There are two main differences between NHCs and both Fischer and Schrock complexes, the metal-carbene bond of an N-heterocyclic carbene complex is less reactive than both Fischer and Schrock carbenes and their ability to coordinate with many transition metals regardless of their oxidation state.

The exceptional stability in this type of carbene has been attributed to the existence of two nitrogen atoms adjacent to the carbene carbon. This stabilises the carbene via σ bonding (an inductive effect) and π bonding (a resonance effect). The nitrogen atoms donate a lone pair of electrons into the empty p orbital of the carbene and pull the electron density from the carbene by an inductive effect (Figure 1-7).

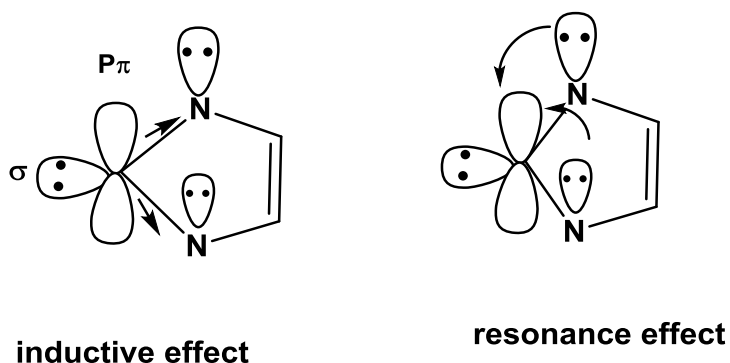
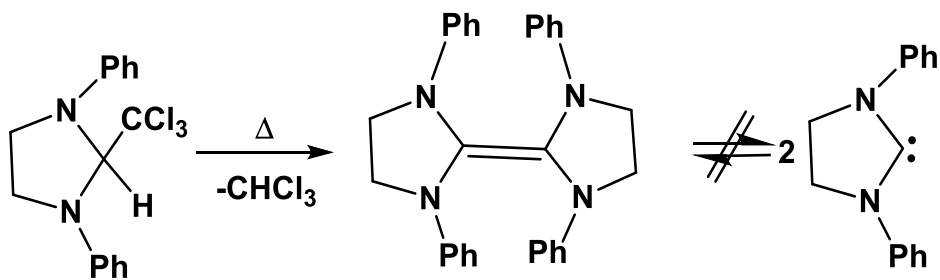


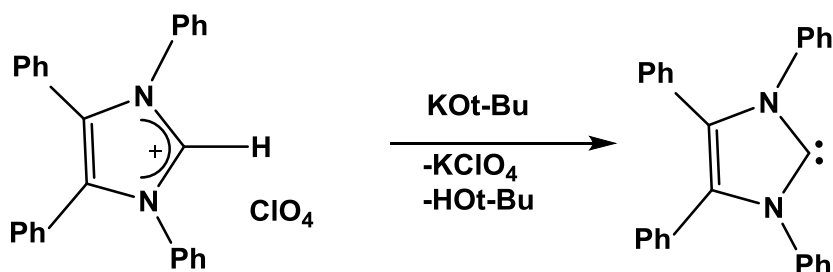
Figure (1-7) Electronic effect of NHC

Wanzlick *et al* tried to prepare a free NHC using α -elimination of chloroform from a saturated imidazole. [13] However, he recovered dimer instead of the free carbene. He assumed that dimer cleavage is the main path to form free carbenes, but cross metathesis experiments did not support this assertion (Scheme1-3).



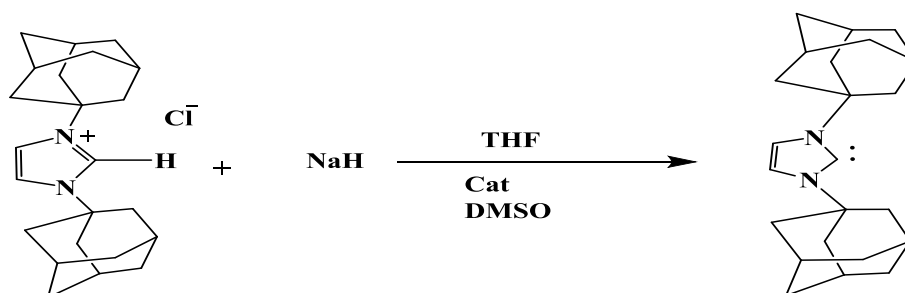
Scheme (1-3) attempted isolation of a free carbene by α -elimination

Wanzlick also tried to deprotonate tetraphenyl imidazolium perchlorate using KOtBu but was unable to isolate the free NHC (Scheme 1-4). [14-15]



Scheme (1-4) Wanzlick's attempted synthesis of a free NHC

Widespread interest in NHC's began in 1991 when Arduengo synthesised the first free carbene by deprotonation of 1,3-adamantyl imidazolium chloride (Scheme 1-5). [16] The deprotonation was conducted using NaH with catalytic amounts of KOtBu or DMSO anions. Arduengo proved that the carbene is thermally stable (mp 240-241 °C without decomposition).



Scheme (1-5) Arduengo free carbene

1.4-Preparation of NHC complexes

The use of NHC's as ligands is of interest as a result of their strong metal coordination properties. Several methods have been utilized in the preparation of NHC metal complexes. Generally three methods are used for the preparation of these complexes under specific reaction conditions. [19-21] The selection of which method to be used depends on the ease with which the carbene can be prepared and manipulated.

1.4.1-In situ deprotonation of imidazolium salt

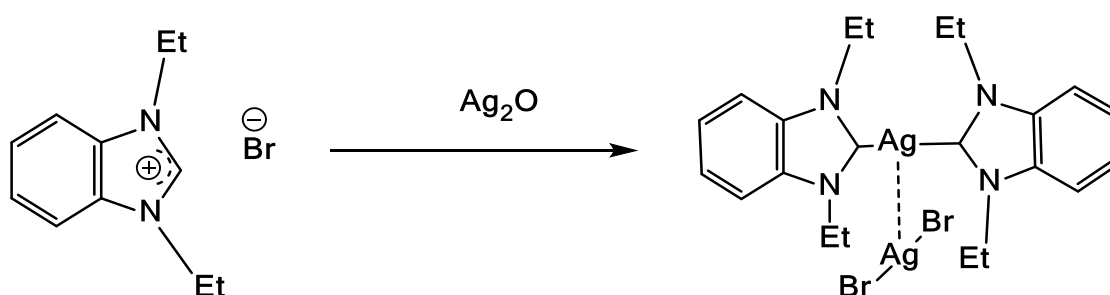
The pioneers of this method are Öfele and Wanzlick. [17, 18] In this route the generation of the free carbene and complexation with metal can be accomplished in a one pot reaction. Deprotonation of the azolium salt in the presence of a metal ion provides a direct route to NHC-transition metal complexes. The advantage of this method is the fact that isolation of the free carbene is not necessary.

This method is suitable when difficulties are encountered obtaining the free carbene due to their instability. The deprotonation of azolium salts can be achieved via one of two methods:

1- The use of an external base. The deprotonation of azolium salts is conducted using a strong base prior to addition of the metal forming the NHC complexes. Several bases have been used for deprotonation, such as NaH, t-BuOK, t-BuOLi and NaOAc.[22-25]

2- The use of a basic metal as an internal base. In this method both deprotonation and complexation can be accomplished simultaneously.

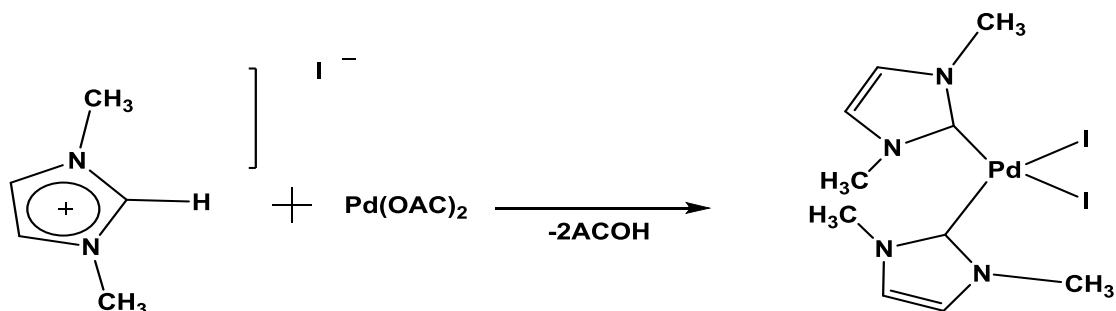
The reaction can be carried out using a basic metal sources such as Ag_2O , Ag_2CO_3 , $\text{Hg}(\text{OAc})_2$, $\text{Pd}(\text{OAc})_2$ or $\text{Au}(\text{SMe}_2)\text{Cl}$ to produce NHC metal complexes. AgOAc has been used to prepare many silver carbene complexes in this way. Lin *et al* used Ag_2O to prepare silver complexes of 1, 3-diethylbenzimidazol-2-ylidene, high yields of up to 89% were obtained at ambient temperature in dichloromethane solution. [26] X-ray diffraction showed a neutral complex with an interaction between two silver atoms (Scheme 1-8). The reaction was controlled by removing insoluble Ag_2O . [27-29]



Scheme (1-8) synthesis of $\text{Ag}(\text{NHC})$ via in situ deprotonation method

Danopoulos *et al* have prepared silver-NHC complexes using Ag_2CO_3 for the deprotonation of imidazolium salts in refluxing dichloromethane over 2 days. [30]

The first Pd-NHC complexes were prepared by Herrmann *et al* in 1995. The complexes were obtained by reacting 1,3-dimethylimidazolium iodide or 3,3'-dimethyl-1,1'-methylenediimidazolium iodide with $\text{Pd}(\text{OAc})_2$. Palladium acetate was used as a source of both Pd and base for the deprotonation of the azolium salts (Scheme 1-9). [31]

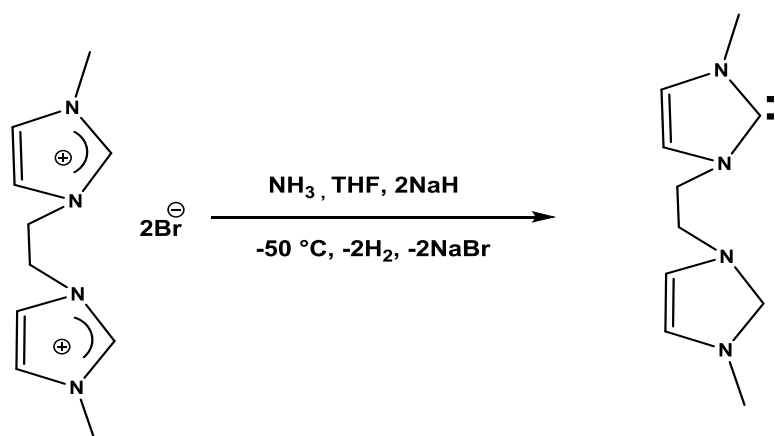


Scheme (1-9) synthesis of Pd-NHC via in situ deprotonation

Various solvents have been utilized for the synthesis of Ag and Pd NHC complexes using this method such as DCM, DCE, DMF, methanol, acetonitrile, acetone and DMSO.

1.4.2-Preparation of complexes via free carbene

This method for the synthesis of metal-NHC complexes has attracted much attention after the first free carbene was isolated by Arduengo in 1991. [16] Several strong bases including NaH, *t*-BuOK and dimsyl anion have been used to deprotonate azoliums to generate the free carbene. [32] The first bidentate free carbene was isolated by Herrmann *et al* using liquid ammonia at $-50\text{ }^{\circ}\text{C}$ in THF, obtaining up to 95% yields. This was used in the synthesis of bis-NHC complexes of Ru(II), Pd(II), Os(II), Ir(I) and Rh(I) (Scheme 1-10).[33]

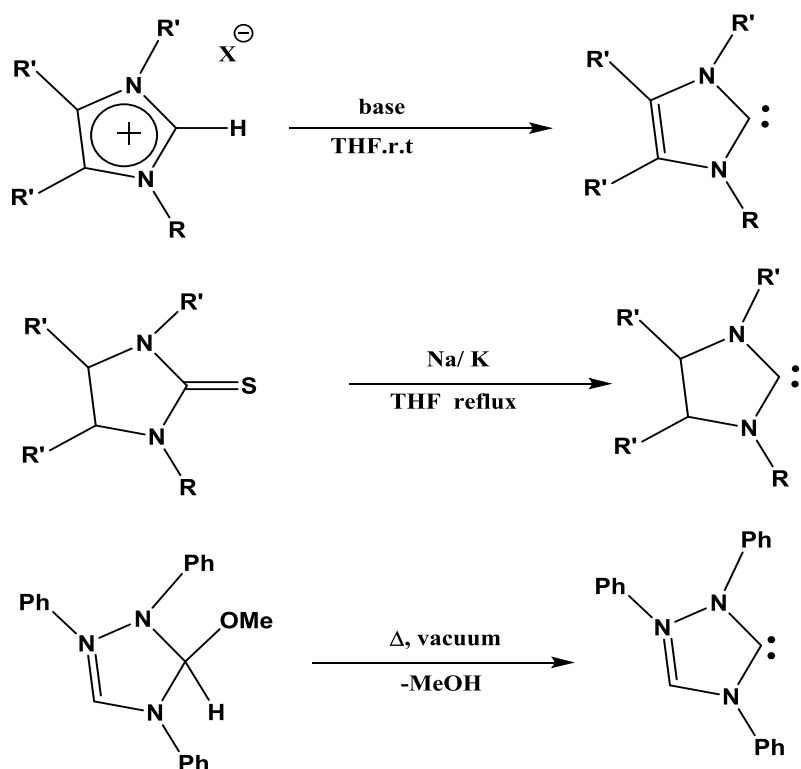


Scheme (1-10) first bidentate free carbene

α -Elimination of small molecules has been used to form thermally stable carbenes. Small molecules such as methanol [34] or 5-methyl-triazole [35] can be removed from suitably designed imidazolium precursors although this method is limited to producing only thermally stable NHC's.

Another route to free NHC's involves the reduction of thiones. In this method imidazole 2- thiones are reduced by potassium in boiling THF, typically achieving good yields. Kuhn and Kratz [36] have successfully prepared free NHC's by using this method (Scheme-11).

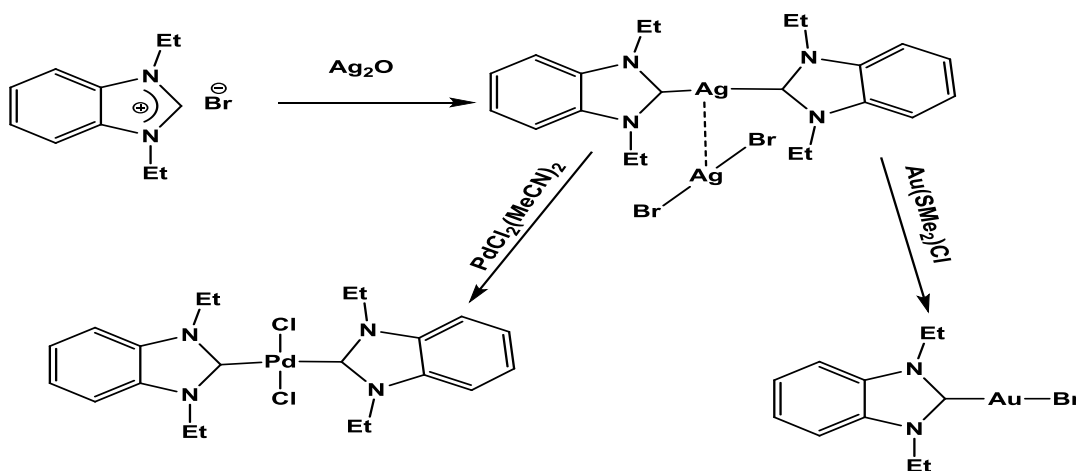
One advantage of this method is that many transition metal complexes can be prepared regardless of their oxidation state. Most free carbenes are sensitive towards both air and moisture. Preparation of the carbene by this method often leads to decomposition or dimerisation of the carbene.



Scheme (1-11) preparation of free NHCs

1.4.3-Transmetalation method of carbene ligand into other metal

Transmetalation has been widely used in organometallic chemistry for the synthesis of metal-NHC complexes. In this method basic metals are used to deprotonate the azolium salts to produce metal NHC complex, after that transmetalation can be utilized to transfer the ligand onto another metal centre to produce analogous NHC complexes of the desired metal. Silver bases such as Ag_2O , Ag_2CO_3 or AgOAc are used for the preparation of silver-NHC complexes. The lability and fluxional behavior of Ag(I)NHC complexes has led to their use as ligand transfer agents to prepare many complexes with metals such as Au(I) , Pd(I) , Cu(I) , Cu(II) , Ni(II) , Pt(II) , Ru(II) and Ru(III) . [37] This method proved its utility when Wang *et al* successfully prepared $\text{Pd}(\text{Et}_2\text{-Bimy})_2\text{-Cl}_2$, $\text{Au}(\text{Et}_2\text{-Bimy})\text{Br}$ and $[\text{Au}(\text{Et}_2\text{-Bimy})_2]\text{PF}_6$ via transmetalation from $[\text{Ag}(\text{Et}_2\text{-Bimy})_2][\text{AgBr}_2]$ and $[\text{Ag}(\text{Et}_2\text{-Bimy})_2]\text{PF}_6$. (Scheme 1-12). [26]



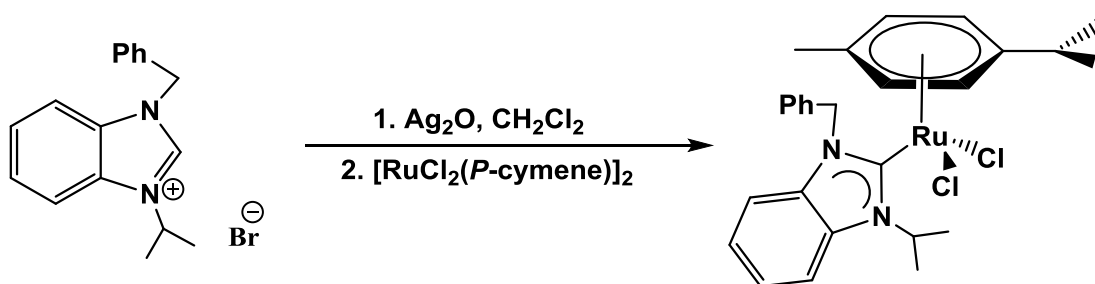
Scheme (1-12) First synthesis of Pd(II) and Au(II) complexes by transmetalation from a Ag(I) NHC complex. [26]

Transmetalation offers many advantages such as air stability and greater scope as there is no requirement for the addition of base and deprotonation of the azolium salts only occurs at the C2 position leaving other acidic protons in the azolium salts intact.

This method was used to avoid the harsh conditions required by other techniques and can be used to obtain the desired complexes when the direct reaction is unsuccessful. The transmetalation reaction can be conducted in air and moisture need not be rigorously removed; although, care must be taken to exclude all light from the reaction mixture in order to avoid decomposition of the silver species.

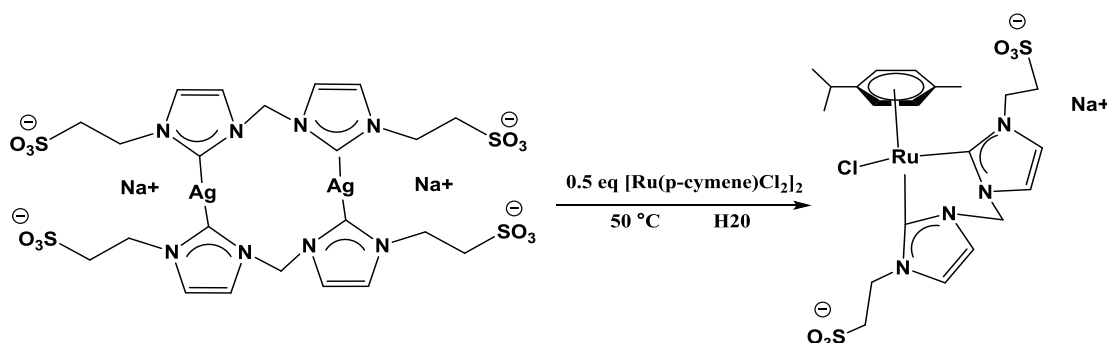
For the preparation of Pd-NHC complexes the source of palladium is usually $\text{PdCl}_2(\text{MeCN})_2$, $\text{PdBBr}_2(\text{MeCN})_2$, $\text{Pd}(\text{COD})\text{Cl}_2$, PdCl_2 or $\text{PdCl}_2(\text{PhCN})_2$. [38-42]

Many Ru-NHC complexes have also been prepared *via* transmetalation from the corresponding Ag-NHC complexes using $[\text{Ru}(p\text{-cymene})\text{Cl}_2]_2$ or $[\text{Ru}(\text{benzene})\text{Cl}_2]_2$ as the ruthenium source. [43-45] Asymmetrical benzimidazolium salts react with Ag_2O in CH_2Cl_2 furnishing the air and moisture stable silver complex. The formation of the complex was confirmed by the absence of the NCHN peak in the ^1H NMR spectrum and a peak corresponding to the Ru-C was observed at 189 ppm in the ^{13}C NMR spectrum. X-ray crystallography further confirmed the expected molecular structure (Scheme 1-13). [46]



Scheme (1-13) Synthesis of Ru complex *via* transmetalation method

A ruthenium-NHC complex bearing sulfonate side arms was prepared by treatment of the silver bis(NHC) complex with $[\text{Ru}(p\text{-cymene})\text{Cl}_2]_2$ in water at $50\text{ }^\circ\text{C}$ to produce $[\text{Ru}(\text{NHC})(p\text{-cymene})\text{Cl}]\text{PF}_6$ as a yellow powder in 86% yield. The carbene was observed at 173.4 ppm in the ^{13}C NMR spectrum (Scheme 1-14). [47]



Scheme (1-14) Synthesis of Ru complex with sulfonate chain by transmetalation

1.5-Triazine

1,3,5-Triazines are six-membered heterocyclic rings comprised of alternating carbon and nitrogen atoms connected by single and double bonds. This isomer of triazine is usually called s-triazine. The numbering for these compounds is starting with a nitrogen atom as a number one. It is thermally stable up to 600 °C and readily undergoes nucleophilic substitution [48, 49]

1,3,5-triazine was synthesized by Nef in 1895 by reacting hydrogen cyanide with ethanol in an ether solution saturated with hydrogen chloride. The resultant mixture was then treated with base and distilled to produce 1,3,5-triazine in low yields of 10 % (Figure 1- 8). [50]

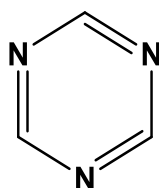
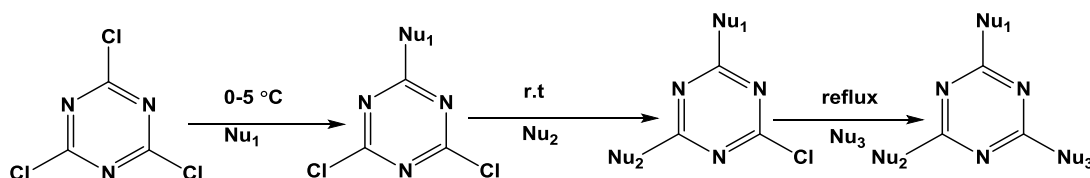


Figure (1- 8) 1,3,5- Triazine structure

Triazine derivatives have received great attention and have found applications in different fields, for example herbicide production, polymers and photostabilisers. Their biological properties have also been studied for example hexamethylmelamine

(HMM) and 2-amino-4-morpholino-s-triazine were used to treat lung cancer and ovarian cancer respectively. [51]

Cyanuric chloride is a derivative of 1,3,5-triazine and has the formula $N_3C_3Cl_3$. It has received much attention due to the reactivity of its chlorine atoms, commercial availability and low cost. [52] Temperature plays an important role in the substitution of the chlorine atoms, where the replacement of the first chlorine atom occurs at 0-5 °C and the second substitution occurs at approximately room temperature, the third chloride needs high temperature at 70 - 100 °C in order to react (Scheme 1-15). [53]



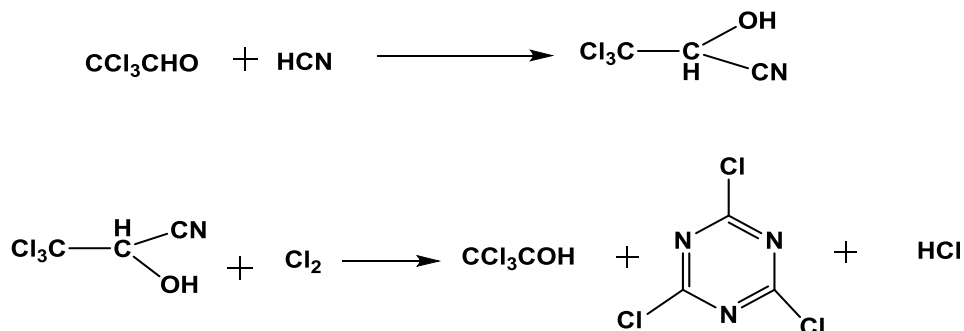
Scheme (1-15) Replacement of chlorine atoms

Cyanuric chloride is a colourless crystalline solid, it melts at 145 °C and boils at 198 °C. It is soluble in many organic solvents such as acetonitrile, acetone, ethanol, heptane and acetic acid. It is insoluble in cold water and undergoes hydrolysis in water above 10 °C. Cyanuric chloride is commonly prepared by one of three methods:

1- Trimerization of cyanogen chloride. The reaction is conducted in a chloroform-dioxane mixture in the presence of catalytic hydrogen chloride at 0 °C. The product can be readily isolated due to solubility of cyanuric chloride in chloroform. On the other hand, dioxane dissolves the hydrogen chloride but not cyanuric chloride. [54]

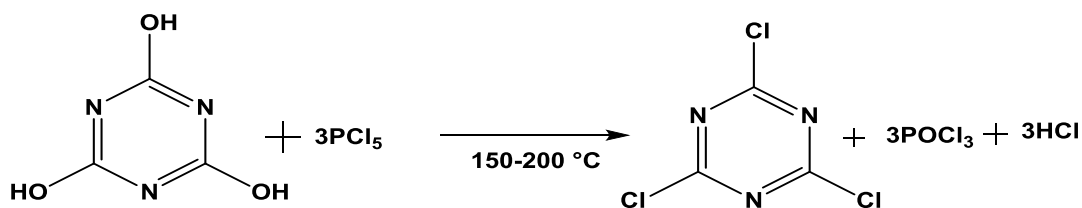
2- From Hydrocyanic Acid. The procedure consists of adding chlorine and hydrogen chloride to a solution of hydrogen cyanide in cold chloroform which contains a trace

of alcohol to produce chloral which serves as an intermediate. Chloral reacts with HCN to form the addition compound which then decomposes in the presence of chlorine to give cyanuric chloride (Scheme 1-16). [54, 55]



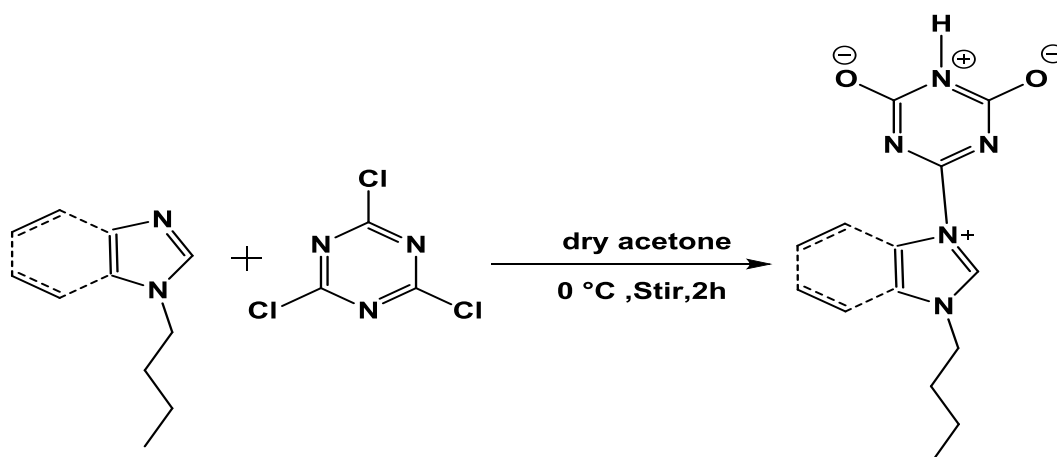
Scheme (1- 16) Synthesis of cyanuric chloride

3- From cyanuric acid. Cyanuric chloride can be obtained by reaction of cyanuric acid with phosphorous pentachloride (Scheme1-17). [56]



Scheme (1-17) Synthesis of cyanuric chloride via cyanuric acid

In 2015 Endud *et al* prepared a set of NHC ligands derived from imidazole and benzimidazole by reacting cyanuric chloride with 1-butylimidazole and benzimidazole. The reactions were conducted in dry acetone and stirred at room temperature. Unfortunately, all attempts to prepare silver and palladium complexes of these salts failed due to the low acidity of the C2 protons (Scheme 1- 18).[57]



Scheme (1-18) Synthesis of triazine benzimidazolium, imidazolium salts

1.6-NHC complexes as Catalysts

Cross coupling reactions have important roles in the synthesis of many pharmaceuticals, optical devices, natural products and industrially important starting materials. [58, 59]

The main reasons for the use of NHC complexes in Pd catalysed cross coupling reactions are the remarkable ability of NHC's to promote oxidative addition as a result of their sigma donating ability, the steric bulk of the NHC ligand makes the reductive elimination easier in comparison with common phosphine ligands and the strong Pd-carbene bond protects the complexes from decomposition. Furthermore, Pd-NHC complexes are easily accessible, stable to heat, oxygen and moisture and are less wasteful to produce compared to phosphine analogues as only stoichiometric quantities of the ligand need be used. [60, 61] Carbenes have found considerable success in C-C and C-heteroatom coupling reactions including the Suzuki [62-64], Heck reactions [65], Kumada Negishi, and Buchwald-Hartwig amination reactions. The formation of C-C bonds is a key step to build complex molecules.

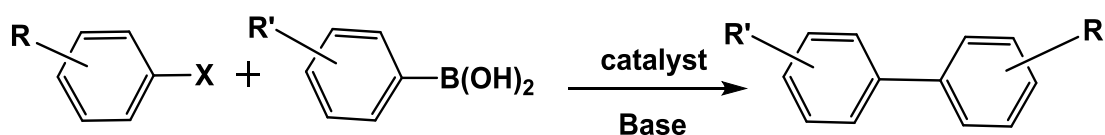
Generally, the mechanism of the cross coupling reactions is similar. The mechanism consists of oxidative addition, transmetalation and reductive elimination. The

oxidative addition step consists of cleavage of the Ar-X bond of an aromatic halide and formation of two bonds to the palladium centre from the halide and aryl moieties. This is the rate determining step of the reaction and is highly dependent on the halide. The transmetalation step involves the reaction of this species with an organometallic substrate to produce intermediate compound which can then undergo reductive elimination to produce the product and reform the active palladium catalyst.

The real potential of NHC ligands in catalysis was realized by Hermann and co-workers in 1995 [31] who observed coupling of a variety of aryl bromide and aryl chlorides with palladium complexes. Almost full conversion of the halide substrate was obtained with catalyst loadings of only 0.001 mol% for aryl bromides and 0.1-1 mol% for aryl chlorides.

1.6.1-Suzuki cross coupling reaction

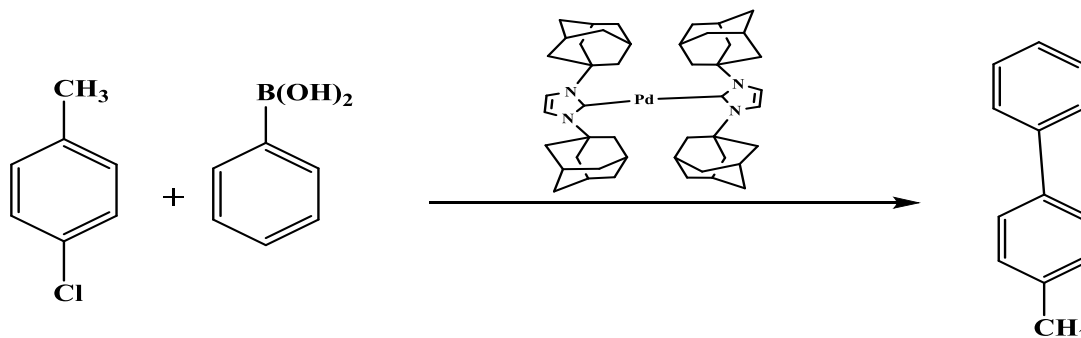
The Suzuki reaction has become widely used for the synthesis of many biaryl systems. The reaction takes place between aryl or vinyl halides with aryl or vinyl boronic esters and acids. (Scheme 1-19). [66, 67] Boronic acids are used as the transmetalating partner due to the commercial availability of numerous substrates, their stability toward moisture and air and non-toxic by-products that can be disposed of easily. [68, 69]



Scheme (1-19) General Suzuki coupling reaction

Suzuki cross coupling reactions have been demonstrated with numerous different substrates and there are many factors that can affect the outcome such as base, solvent, temperature and palladium source.

The generation of the active catalyst can be either isolated prior to reaction or generated in situ. The latter is useful as it avoids the isolation of the free carbene but the stoichiometry and composition of the active catalyst may be more difficult to elucidate leading to wasted metal source and/or ligand precursor. For this reason, many researchers prefer to isolate the catalyst species prior to the reaction. For example, Herrmann and co-workers [70] revealed high activity for Suzuki cross coupling reactions catalysed by a bis (NHC)-Pd(0) (Scheme1-20).



Scheme (1 - 20) Suzuki reaction coupling of aryl chloride with boronic acid

NHC–Pd–PEPPSI complexes (PEPSI = pyridine-enhanced pre-catalyst, preparation, stabilization and initiation) have proven highly active in Suzuki coupling reactions of a wide range of aryl halides with boronic acids. For example, the typical NHC-Pd-PEPPSI complexes **1**, **2**, and **3** are highly active with catalyst loadings of just 0.35 mol %. These complexes involve one NHC ligand, two anionic ligands (e.g, Cl, Br, OAc) and pyridine or its derivatives. The high activity of these catalysts can be attributed to the presence of pyridine as a good throw - away ligand (Figure 1-9). [71]

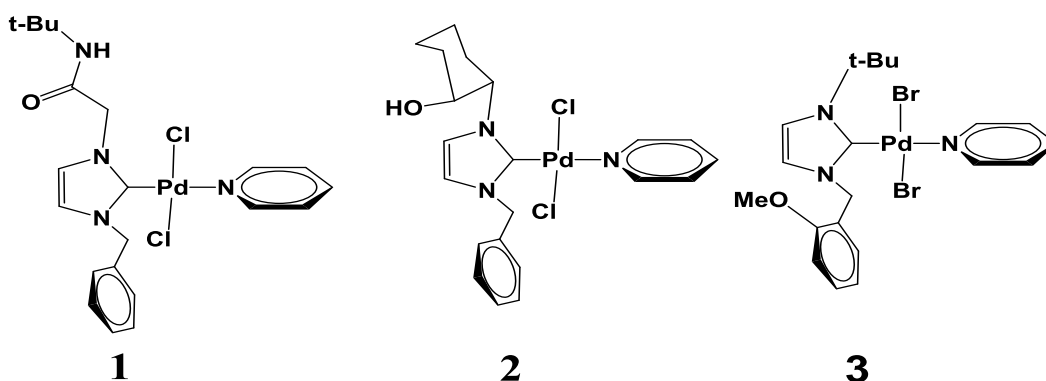
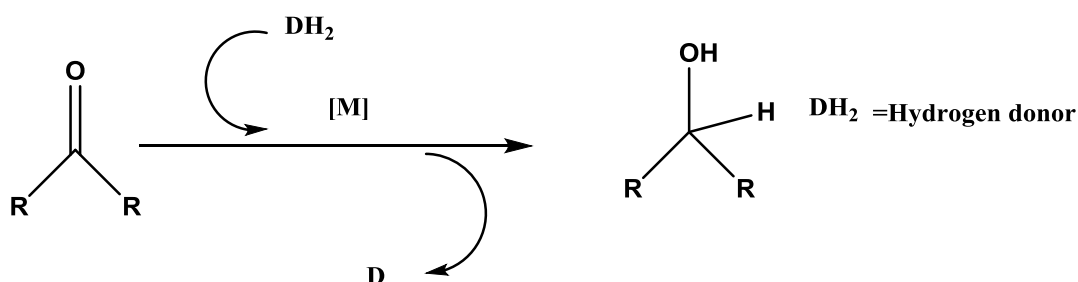


Figure (1-9) NHC–Pd–PEPPSI complexes

1.7- Transfer hydrogenation reaction

Transfer hydrogenation is a valuable tool for the reduction of aldehydes and ketones to produce the corresponding primary and secondary alcohols. [72, 73] The reaction can also be conducted with other unsaturated compounds, such as imines, alkenes and alkynes, with proton donor sources, such as isopropanol, which is usually present in excess as the reaction solvent (Scheme 1-21).



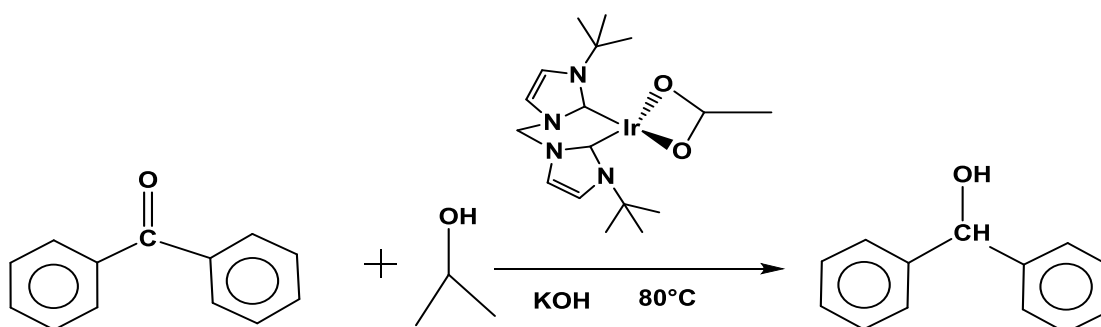
Scheme (1-21) General equation for transfer reaction

Isopropanol is often used as a source of hydrogen because of its favourable properties such as stability, low toxicity and cost, and ability to dissolve many organic compounds.

For transfer hydrogenation catalysts bearing NHC ligands, rhodium and iridium are the most commonly used, although ruthenium-based catalysts have the advantage of lower costs. [74, 75] Indeed, ruthenium-NHC catalysts have shown much promise in transfer hydrogenations for a number of types of unsaturated substrate. [76, 77]

The first use of a metal-NHC complexes in transfer hydrogenation was reported by Nolan *et al* in 2001. [78] His team prepared three Ir complexes which proved to be active catalysts for the reduction of ketones to the corresponding alcohol using isopropanol with KOH at 80 °C. 100 % conversion was obtained for benzophenone within 10 minutes.

Substituents on the NHC ligand play an important role for tuning the catalyst activity. Crabtree *et al.* [79] prepared a series of Ir-bis(NHC) complexes bearing a range of different alkyl side arms such as methyl, butyl, isopropyl and neopentyl groups. The results clearly showed that the nature of the substituent influence the catalyst activity, where 98% conversion was obtained for the reduction of benzophenone in 4 minutes with neopentyl substituents (Scheme 1-22).



Scheme (1-22) Reduction of benzophenone via transfer hydrogenation

NHC–Ru arene complexes $[\text{Ru}(\text{arene})(\text{NHC})\text{Cl}_2]$ have been employed as catalysts for transfer hydrogenation in the preparation of many alcoholic compounds. This type of ruthenium complex has proven highly efficient in transfer hydrogenation of ketones to their corresponding alcohols.

Cyclometalated ruthenium complexes bearing bidentate carbene/ NH_2 and iodide ligands have been tested as transfer hydrogenation catalysts for the reduction of acetophenone using isopropanol in presence of NaOtBu at 80 °C. Over 90% conversions were obtained within 30 minutes, while no conversion was recorded at 20 °C even after 72 hours which demonstrates the important role of temperature in this reaction. [45]

1.8-Aims and objectives of this research

The aim of this work has been to explore the incorporation of bis (dialkylamino) triazine substituents into a range of novel imidazolium salts and their conversion to NHC's and subsequent synthesis of Ag(I), Pd(II) and Ru(II) complexes. These complexes were investigated as potential catalysts in Suzuki cross coupling and transfer hydrogenation reactions.

In order to highlight the goals of this work, the thesis was divided into five chapters according to the sequence of work.

The current chapter provides an overview of the nature of carbenes and common methodologies for the synthesis of both imidazolium salts and NHC complexes. A brief introduction to two potential catalytic applications of such complexes is also discussed. Additionally, an explanation of the properties of triazine and previous work to synthesise 2,4-diamino- cyanuric chloride is provided.

Chapter 2 describes the preparation and characterisation of imidazolium salts required as precursors to the respective NHC ligands. The imidazolium salts were prepared by either reacting cyanuric chloride derivatives with imidazole and subsequent substitution at the 3-position or by building up the imidazole ring with the desired alkyl side chain followed by reaction with cyanuric chloride derivatives.

Chapter 3 describes the synthesis and characterisation of a new range of Ag(I)NHC complexes from Ag₂O and the imidazolium salts described in chapter 2. Many of these structures have been crystallographically characterised allowing for a discussion of the solid state structures. Preparation of these complexes represents one of our key

goals in order for them to be used as ligand transfer agents for the synthesis of ruthenium and palladium.

Chapter 4 discusses the synthesis and solid state structures of a new set of Pd(II) complexes. Mono-NHC palladium complexes $[\text{Pd}(\text{NHC})(\text{py})\text{X}_2]$ were prepared via deprotonation of the imidazolium salt using an external base with PdCl_2 in pyridine in a one pot procedure. Bis-carbene palladium complexes $[\text{Pd}(\text{NHC})_2\text{Cl}_2]$ were synthesized from the reaction of the corresponding silver complexes with $\text{Pd}(\text{MeCN})_2\text{Cl}_2$ in dichloromethane via a transmetallation reaction. The potential of these complexes to act as catalysts in Suzuki cross coupling reactions is investigated.

In chapter 5, the synthesis and characterisation of a new range of Ru(II) complexes are described. All the complexes have been prepared via transmetallation from the silver complexes described in chapter 3 with $[\text{Ru}(\text{p-cymene})\text{Cl}_2]_2$ or $[\text{Ru}(\text{benzene})\text{Cl}_2]_2$. The study of these complexes in transfer hydrogenation reactions is a goal of this work, their catalytic activity in this application is discussed.

1.9-References

- (1) E. Buchner and T. Curtius, *Ber. Dtsch. Chem. Ges.* 1885, **8**, 2377.
- (2) W. A. Herrmann and C. Köcher, *Angew. Chem. Int. Ed. Engl.* 1997, **36**, 2162.
- (3) D. Bourissou, O. Guerret, F. P. Gabbai and G. Bertrand, *Chem. Rev.* 2000, **100**, 39.
- (4) W. V. E. Doering and L. H. Knox, *J. Am. Chem. Soc.* 1956, **78**, 494.
- (5) G. Schuster, *Adv. Phys. Org. Chem.* 1986, **22**, 311.
- (6) R. Hoffmann, *J. Am. Chem. Soc.* 1968, **90**, 1475
- (7) F. E. Hahn and M. C. Jahnke, *Angew. Chem. Int. Ed.* 2008, **47**, 3122.
- (8) E. O Fischer and A. Maasböl, *Angew. Chem. Int. Ed. Engl.* 1964, **3**, 580.
- (9) R. R. Schrock, *J. Am. Chem. Soc.* 1974, **96**, 6796.
- (10) R. R. Schrock, *J. Chem. Soc. Dalton Trans.* 2001, 2541.
- (11) R. R. Schrock and P. R. Sharp, *J. Am. Chem. Soc.* 1978, **100**, 2389.
- (12) R. H. Crabtree, *The Organometallic Chemistry of the Transition Metals*, Wiley. International: New York, 2001.
- (13) H. W. Wanzlick, *Angew. Chem. Int. Ed. Engl.* 1962, **1**, 75.
- (14) H. J. Schoenherr and H. W. Wanzlick. *Liebigs Ann. Chem.* 1970, **731**, 176.
- (15) H. J. Schoenherr and H. W. Wanzlick. *Chem. Ber.* 1970, **103**, 1037.
- (16) A. J. Arduengo, III; R. L. Harlow and M. Kline, *J. Am. Chem. Soc.* 1991, **113**, 361.
- (17) K. Öfele, *Organometallics* 1968, **12**, 42.

H:W. Wanzlick and H. J. Schoenherr, *Angew. Chem, Int .Ed.* 1968, **7**,.141.

- (18) T. Weskamp, V. P. W. Böhm and W. A. Herrmann, *Organometallics* 2000, **600**, 12.
- (19) D. Enders and H. Gielen, *Organometallics* 2001, **617–618**, 70.
- (20) E. Peri and R. H. Crabtree, *Comptes. Rendus. Chimie.* 2003, **6**, 33.
- (21) M. Alcarazo, S. J. Roseblade, A. R. Cowley, R. Fernandez, J. M. Brown and J. M. Lassaletta, *J. Am. Chem. Soc.* 2005, **127**, 3290.
- (22) C. Kocher and W.A. Herrmann. *J. Am. Chem. Soc.* 1997, **532**, 261.
- (23) M. V. Baker, S. K. Brayshaw, B. W. Skelton, A. H. White and C. C. Williams, *J. Am. Chem. Soc.* 2005, **690**, 2312.
- (24) K. Öfele, W. A. Herrmann, D. Mihalios, M. Elison, E. Herdtweck, W. Scherer and J. Mink, *Organometallics* 1993, **954**, 177.
- (25) H. M. J. Wang and I. J. B. Lin. *Organometallics* 1998, **17**, 972
- (26) C. K. Lee, C. S. Vasam, T.W. Huang, H. M. J. Wang, R.Y. Yang, C.S. Lee, and I. J. B. Lin, *Organometallics* 2006, **25**, 3768.
- (27) R. S Simons, P Custer, C. A. Tessier, and W. Youngs. *Organometallics* 2003, **22**, 1979.
- (28) X. Wang.and S. Liu, *Organometallics* 2004, **23**, 6002.
- (29) A. A. D. Tulloch, A. A. Danopoulos, S. Winston, S. Kleinhenz, and G. Easthams, *J. Chem. Soc, Dalton Trans.* 2000, 4499.
- (30) W. A. Herrmann, M. Elison, J. Fisher, C. Kocher, G. R. J. Artus, *Angew. Chem. Int. Ed Engl.* 1995, **34**, 2371.
- (31) A. J. Arduengo, III, H. V. R Dias, R. L Harlow, M. Kline, *J. Am. Chem Soc.* 1992, **114**, 5530.
- (32) W. A. Herrmann. *Angew. Chem. Int. Ed.* 2002, **41**, 1290.

- (33) D. Ender, K. Bruer, G. Raabe, J. Runsink, J. H. Teles, J. P. Melder, K. Ebel and S. Brode, *Angew. Chem. Int. Ed.* 1995, **34**, 1021.
- (34) J. H. teles, J. P. Medler, K. Ebel, R. Schbeider, E. Gehrler, W. Harder and S. Brode. *Helv. Chem. Acta.* 1996, **79**, 61.
- (35) N. Kuhm and T. Kratz, *Synthesis.* 1993, 561.
- (36) P. L. Arnold. *Heteroatom Chemistry.* 2002, **13**, 534.
- (37) V. César, S. Bellemin-Laponnaz and L. H. Gade, *Organometallics* 2002, **21**, 5204.
- (38) M. Frøseth, M. Dhindsa, H. Røise and M. Tilset, *Dalton Trans.* 2003, **23**, 4516.
- (39) M. Frøseth, K. A. Netland, K. W. Törnroos, A. Dhindsa and M. Tilset, *Dalton. Trans.* 2005, **9**, 1664.
- (40) A. A. D. Tulloch, S. Winston, A. A. Danopoulos, G. Eastham and M. B. Hursthouse, *Dalton. Trans.* 2003, 699.
- (41) W. A. Herrmann, S. K. Schneider, K. Öfele, M. Sakamoto, and E. Herdtweck, *Organometallics* 2004, **689**, 2441.
- (42) M. Poyatos, A. Maise-Franc-ois, S. Bellemin-Laponnaz, E. Peris and L. H. Gade, *Organometallics* 2006, **691**, 2713.
- (43) P. Mathew, A. Neels and M. Albrecht, *J. Am. Chem. Soc.* 2008, **130**, 13534.
- (44) W. B. Cross, C. G. Daly, Y. Boutadla and K. Singh, *Dalton. Trans.* 2011, **40**, 9722.
- (45) S. P. Shan, X. Xiaoke, B. Gnanaprakasam, T. T. Dang, B. Ramalingam, H. V. Huynh and A. M. Seayad, *RSC. Adv.* 2015, **5**, 4434.

- (46) D. Jantke, M. Cokoja, A. Pöthig, W. A. Herrmann and F. E. Kühn. *Organometallics* 2013, **32**, 741.
- (47) E.M. Smolin, and L. Rapoport, s-Triazines and Derivatives. *Interscience publishers*. New York, 1959, Vol.**13**, p 644
- (48) H. Neunhoeffer, P. F. Wiley, Chemistry of 1, 2, 3-Triazines and 1, 2, 4-Triazines, Tetrazines, and Pentazines. *John Wiley & Sons, Inc*; New York, 1978; Vol.**33**, p 1335.
- (49) J. M. E. Quirke, *Comprehensive Heterocyclic Chemistry*. Pergamon press: Oxford, 1984: Vol. **3**, P 457
- (50) Z. Brzozowski and F. Saczewski, *Eur. J. Med. Chem.* 2002, **37**,709.
- (51) G. Blotny, *Tetrahedron*. 2006, **62**, 9507.
- (52) T. Thurston, J. R. Dudley, D. W. Kaiser, I. Hechenbleikner, F. C. Schaefer and D. Hølem-Hansen, *J. Am. Chem. Soc.* 1951, **73**, 2981
- (53) H. F. David and M. Matter, *J. SOCD. yers and Colourists*. 1937, **53**, 424.
- (54) O. Diels. *Ber. Dtsch. Chem. Ges.* 1899, **32**, 691
- (55) F. Beilstein, *Justus. Liebigs. Ann. Chem.* 1860, **116**, 357.
- (56) A. w. Salman, G. U. Rehman, N. Abdullah, s. Budagumpi, S. Endud, H. H. Abdullah, and W.Y. Wong, *polyhedron*, 2015, **81**, 499.
- (57) G. C. Fortman and St. P. Nolan, *Chem. Soc. Rev.* 2011, **40**, 5151
- (58) J. P. Corbet and G. R. Mignani, *Chem. Rev.* 2006, 106, 2651.
- (59) R. Amengual, V. Michelet and J. Genet, *Tetrahedron Letters*. 2002, **43**, 5905.
- (60) G. Altenhoff, R. Goddard, C. W. Lehmann and F. Glorius. *J. Am. Chem. Soc.* 2005, **126**, 15195.

- (61) G. A. Grassa, M. S. Viciu, J. Huang, C. Zhang, M. L. Trudell and S. P. Nolan, *Organometallics* 2002, **21**, 2866.
- (62) N. Hadei, E. A. B. Kantchev, C. J. OVBrien, M. G. Organ, *Org. Lett.* 2005, **7**, 1991.
- (63) W. A Herrmann, C.-P. Reisinger and M Spiegler, *Organometallics* 1998, **557**, 93.
- (64) K. C. Nicolaou, P. G. Bulger and D. Sarlah, *Angew. Chem, Int. Ed.* 2005, **44**, 4442.
- (65) A. Suzuki, *Organometallics* 1999, **576**, 147.
- (66) S. Kotha, K. Lahiri and D. Kashinath, *Tetrahedron*, 2002, **58**, 9633.
- (67) A. F. Littke and G. C. Fu, *Angew. Chem. Int. Ed.* 2002, **41**, 4176.
- (68) C. M. Crudden and D. P. Allen, *Coord. Chem. Rev.* 2004, **248**, 2247.
- (69) C. W. K. Gstöttmayr, V. P. W. Böhm, E. Herdtweck, M. Grosche and W. A. Herrmann, *Angew. Chem. Int. Ed.* 2002, **41**, 8, 1363.
- (70) L. Ray, M. M. Shaikh and P. Ghosh, *Dalton Trans.* 2007, 4546.
- (71) G. Brieger and T. J. Nestrick, *Chem. Rev.* 1974, **74**, 567
- (72) R. A. W. Johnstone, A. H. Wilby and I. D. Entwistle, *Chem. Rev.* 1985, **85**, 129
- (73) Gnanamgari, E. L. O. Sauer, N. D. Schley, C. Butler, C. D. Incarvito and R. H. Crabtree, *Organometallics* 2009, **28**, 321.
- (74) D. Gnanamgari, A. Moores, E. Rajaseelan and R. H. Crabtree, *Organometallics* 2007, **26**, 1226.
- (75) S. Diez-Gonzalez, N. Marion and S. P. Nolan, *Chem. Rev.*, 2009, **109**, 3612.

- (76) V. Dragutan, I. Dragutan, L. Delaude and A. Demonceau, *Coord. Chem. Rev.* 2007, **251**, 765.
- (77) A. C. Hillier, H M Lee, E D. Stevens and S P. Nolan. *Organometallics* 2001, **20**, 4246.
- (78) M Albrecht, J. R. Miecznikowski, A Samuel, J W. Faller and R. H. Crabtree, *Organometallics* 2002, **21**, 3596.

Chapter 2

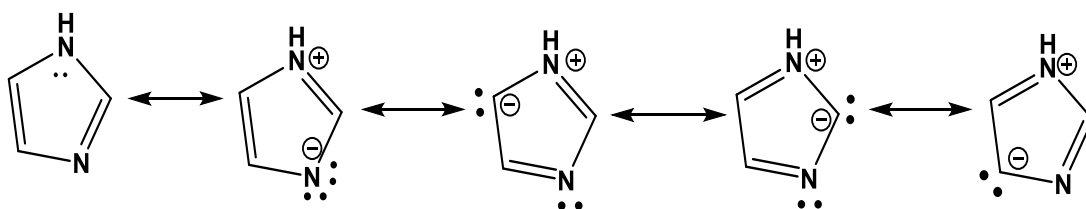
Synthesis and characterization of new NHC ligands incorporating a triazine core

2.1-Introduction

2.1.1-Imidazoles and Imidazolium salts

Imidazole is a planar five membered heterocyclic ring with the formula $C_3H_4N_2$. It is a highly polar compound and is highly soluble in water. Imidazole has aromatic properties due to the presence of a sextet of π -electrons which come from a pair of electrons from the protonated nitrogen atom, and one from each of the other atoms in the ring (Scheme 2-1). Its 1H NMR spectrum shows two peaks in the range 7.2-7.7 ppm for the imidazole protons, reflecting their aromatic nature. Imidazole has amphoteric properties which allow use as both an acid and a base, it is found in many natural products such as histamine, histidine, and serine.

Imidazole has two tautomeric forms, *1H*-imidazole, and *3H*-imidazole depending on the position of the H atom on the nitrogen atoms in the heterocyclic ring.

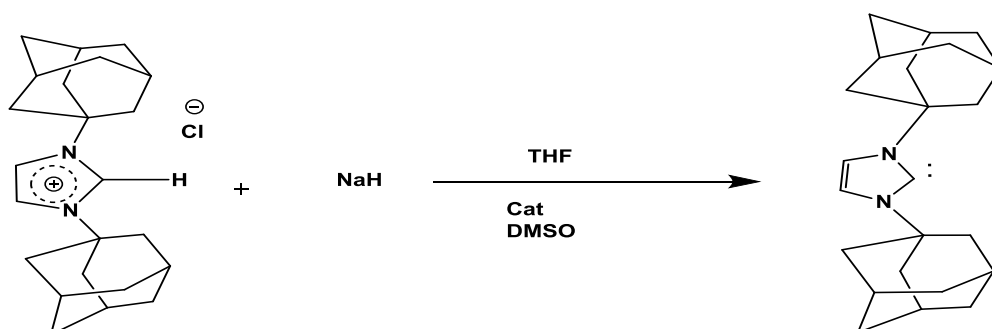


Scheme (2-1) Resonance structures of imidazole

Imidazole derivatives have found applications in medicinal chemistry and have been used in the synthesis of a large number of novel chemotherapeutic agents. [1]

Previous investigations of imidazole derivatives have shown that they have pharmacological activity as antifungal, [2] antibacterial, [3] anticancer, [4] antiviral, [5] anti-inflammatory, and analgesic drugs. [6]

Substitution on both of the nitrogen atoms of an imidazole ring by various functional groups yields imidazolium salts. [7] Since the first free N-Heterocyclic carbene (NHC) compound was isolated by Arduengo in 1991 (Scheme 2-2), [8] NHC ligands derived from imidazolium salts have received a lot of attention due to the ease of their synthesis. These ligands synthesized through the modification of the substituents on the nitrogen atoms. Many compounds can be obtained with a variety of steric properties and asymmetric environments. Moreover, multidentate NHC ligands can be obtained by use of appropriate donor groups on the nitrogen substituents. [9]



Scheme (2-2) Arduengo's free carbene

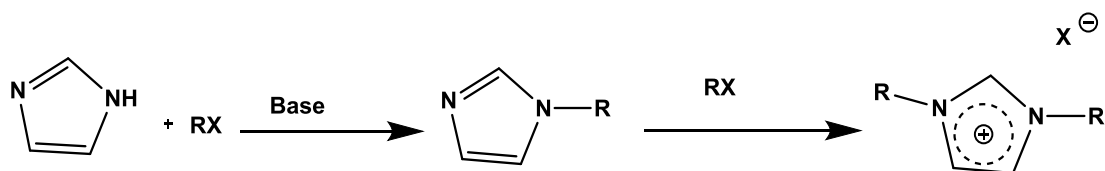
2.1.2-Synthesis of imidazolium salts

Imidazolium salts are widely used as starting materials for the synthesis of N-heterocyclic carbene ligands. The lack of commercial availability, storage difficulties and high cost associated with many imidazolium salts has led to the development of many protocols for their synthesis, as mentioned in chapter one. In this work, two common methods were used to obtain the desired imidazolium salts; substitution on

the imidazole ring and generation of the imidazole ring with the substituent to produce an N-substituted imidazoles.

2.1.2.1 - Substitution on the imidazole ring

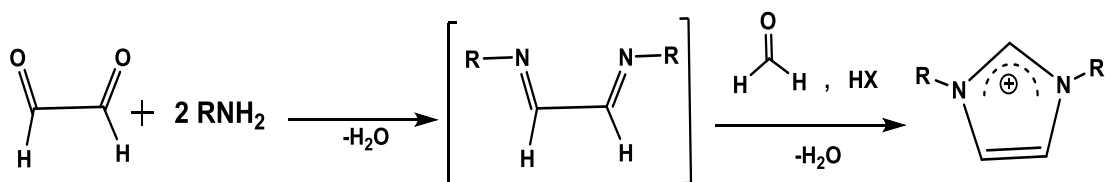
This method is based on the deprotonation of imidazole with a strong base, usually sodium or potassium hydroxide, followed by reaction of the salt with 1 equivalent of an alkyl halide to produce an N-alkyl imidazole. [10] Further substitution is conducted by reaction with 1 equivalent of an alkyl halide. The symmetrical NHC can be accessed by stepwise alkylation or in a one pot synthesis by introducing 2 equivalents of an alkyl halide in the presence of base, furthermore, unsymmetrically substituted NHC's can be obtained by using different alkyl halides in a stepwise process [11-18]. This method is limited to the use of primary alkyl halides to produce imidazolium salts (Scheme 2-3).



Scheme (2-3) Substitution of imidazole

2.1.2.2 - Synthesis of imidazolium ring

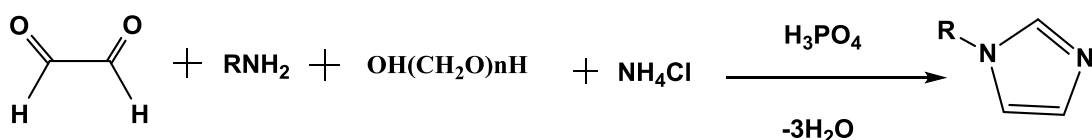
This method is used when substituents other than primary alkyl groups are wanted, especially aromatic substituents. Symmetrical imidazolium salts are generated from glyoxal with 2 eq of a primary amine and formaldehyde in the presence of acid. Initially, condensation of the primary amine with glyoxal forms the corresponding Schiff base, while the second condensation with formaldehyde leads to the imidazolium salts. Symmetrical N, N'-substituted imidazolium salts with various alkyl and aryl substituents can be prepared by this method (Scheme 2-4). [19]



R= aryl, alkyl

Scheme (2-4) One-pot synthesis of imidazolium salts

The reaction of glyoxal, ammonium chloride, paraformaldehyde and one equivalent of primary amine produces N-substituted imidazoles, which go on to react with alkyl halides to produce unsymmetrical imidazolium salts (Scheme 2-5). [20]



Scheme (2-5) Synthesis of N-substituted imidazole ring

This method is not applicable for the synthesis of imidazolium salts where the C4 and C5 positions are substituted.

2.1.3-What is a triazine?

Triazine is an aromatic organic heterocyclic compound similar to benzene but three carbon atoms are replaced by nitrogen atoms. So there are three isomers occurring depending on the position of their nitrogen atoms; 1,2,3-triazine, 1,2,4-triazine and 1,3,5-triazine (Figure 2-1).

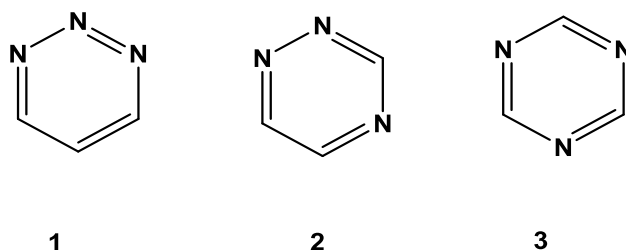


Figure (2-1) Isomers of triazine

Due to the higher symmetry, the 1, 3, 5,-triazine has been extensively studied. [21, 22]. It has been first synthesized by Nef in 1895 through the reaction of hydrogen cyanide with ethanol in ether saturated with hydrogen chloride. [23]

1,3,5-triazine or s-triazine was used as a core in the synthesis of many compounds due to its reactivity towards nucleophilic substitution and the increased stability of the ring (82.5 Kcal/mol) compared to that of the benzene (39 Kcal/mol). [24]

Triazine derivatives have received great attention and have found applications in numerous different fields, for example herbicide production, polymers and photostabilizers. Their biological properties have also been studied for example hexamethylmelamine (HMM), and 2-amino-4-morpholino-s-triazine have been used to treat lung cancer and ovarian cancer (Figure 2-2) respectively. [25]

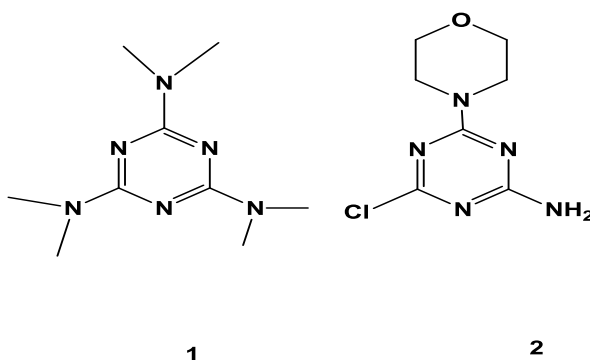
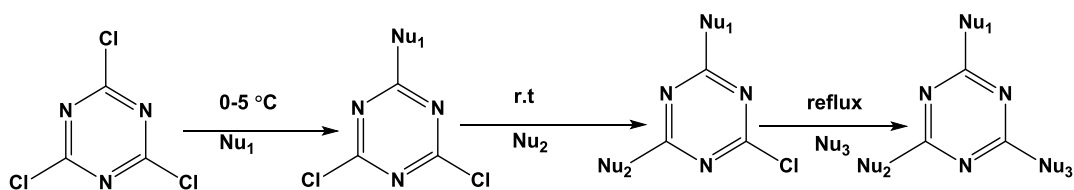


Figure (2-2) Structures of HMM, and 2-amino-4-morpholino-s-triazine

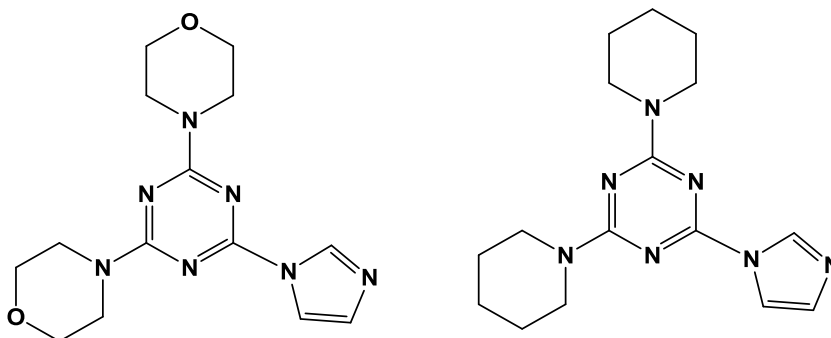
Due to the reactivity of its chlorine atoms, commercial availability and low cost [26] cyanuric chloride was used as a core to prepare many compounds, for example, by reacting with different amino compounds in the presence of base (sodium carbonate, bicarbonate, hydroxide or tertiary amines). Temperature plays an important role in the replacement of the chlorine atoms, where the replacement of the first chlorine atom occurs at 0-5 °C and the second substitution occurs at approximately room

temperature, the third chloride needs high temperature at 70 - 100 °C in order to react (Scheme 2-6). [27]



Scheme (2-6) Replacement of chlorine atoms

Kato *et al.* have synthesized a series of imidazolyl 1,3,5-triazine derivatives. These compounds include morpholine, thiomorpholine, diethylamine and piperidine moieties. The compounds were proven as antitumor agents for breast cancer through inhibition of aromatase placental microsomes and cytochrome (Figure 2-3).

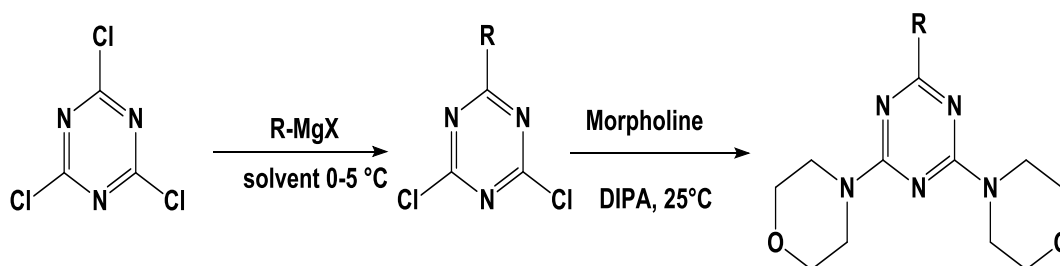


Figure(2-3) 2,4-Dimorpholine-6-imidazolyl-s-triazine(left),2,4-dipiperidine-6-imidazolyl-s-triazine(right)

Cyanuric chloride was used to prepare these compounds. Mono substitution was conducted in the presence of water and acetone as a solvent while second and third substitutions were conducted in DMF at varying temperatures. [28]

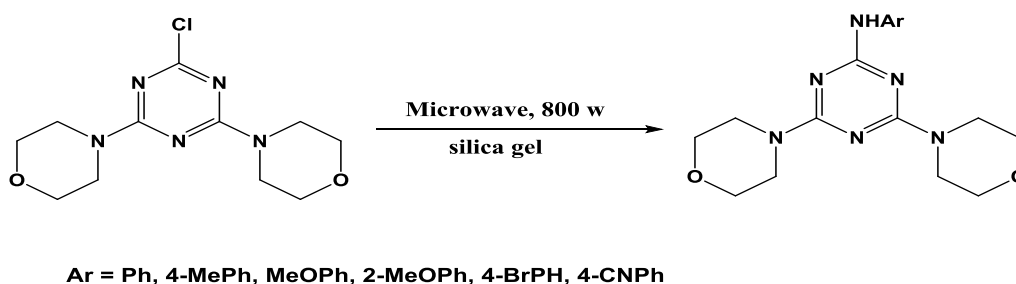
A series of Grignard reagents were used to prepare 2-alkyl-4,6-morpholinyl-1, 3, 5-triazine compounds by reaction of either phenylethylmagnesium bromide, benzylmagnesium chloride, isopropylmagnesiumchloride or S-2-methyl butyl

magnesium chloride with cyanuric chloride under stirring for 3 hours at 0-5 °C then at 25 °C, until the first chloride atom of cyanuric chloride was replaced. The products react with an excess of morpholine to substitute the other chlorine atoms in 1,4-dioxane with diisopropylamine as a base at room temperature between 15-48 hours. These compounds have proven to be good antifungal agents (Scheme 2-7). [29]



Scheme (2- 7) Synthesis of 2-alkyl-4,6-dimorpholine -1, 3, 5-triazine compounds

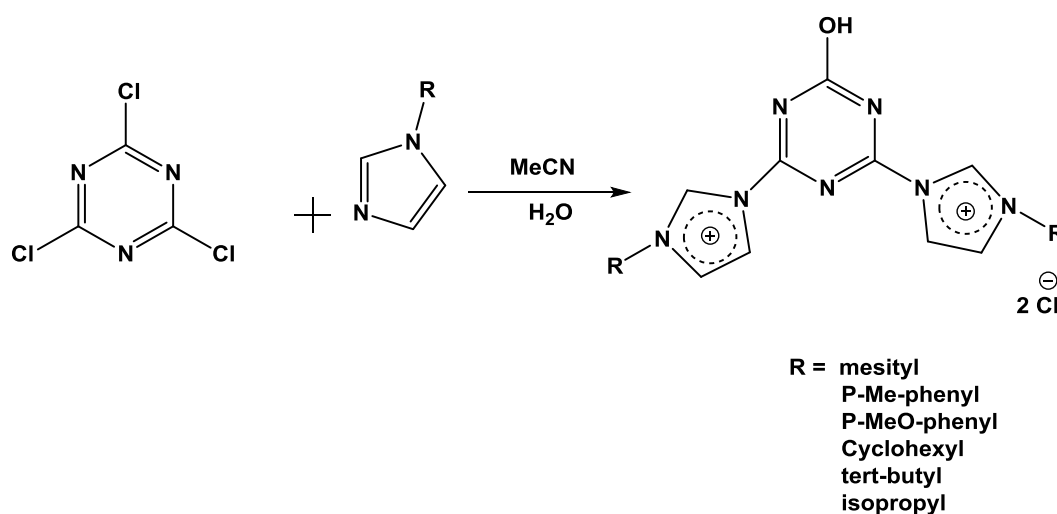
To avoid the harsh conditions used in the replacement of the third chlorine atom on cyanuric chloride a microwave oven in presence of silica gel was used. Many advantages were apparent in using this method including reduced reaction time, no solvent usage, low cost and energy savings. Ivanova and co-workers prepared a series of melamine compounds by reacting 2,4-dimorpholine-6-chloro triazine with various aromatic amines in the presence of silica gel under microwave irradiation at 800W power, 99% yields were obtained in only three minutes. The efficiency of this method is independent of the bulk of the amine used (Scheme 2-8). [30]



Scheme (2-8) Synthesis of melamine compounds

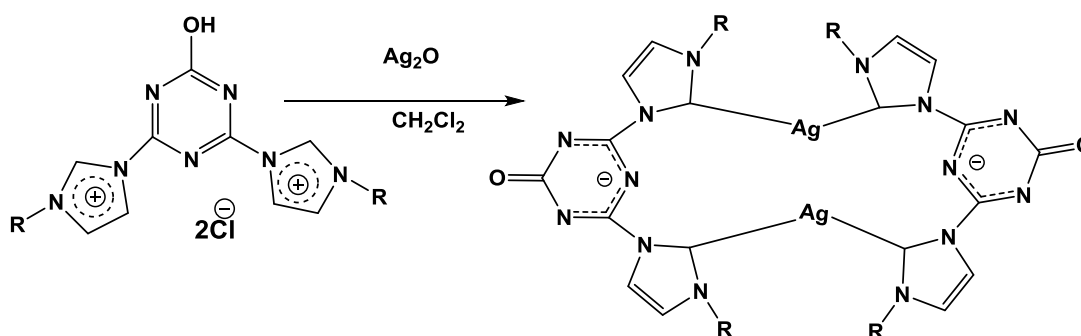
1, 3, 5-Triazine derivatives were incorporated into a substituted imidazole for the synthesis of NHC ligands. Large numbers of NHC complexes have been synthesized by using this methodology.

A series of bisimidazolium salts were obtained by reacting cyanuric chloride with an excess of various N-substituted imidazoles in a CH₃CN/H₂O solvent mixture (Scheme 2-9).



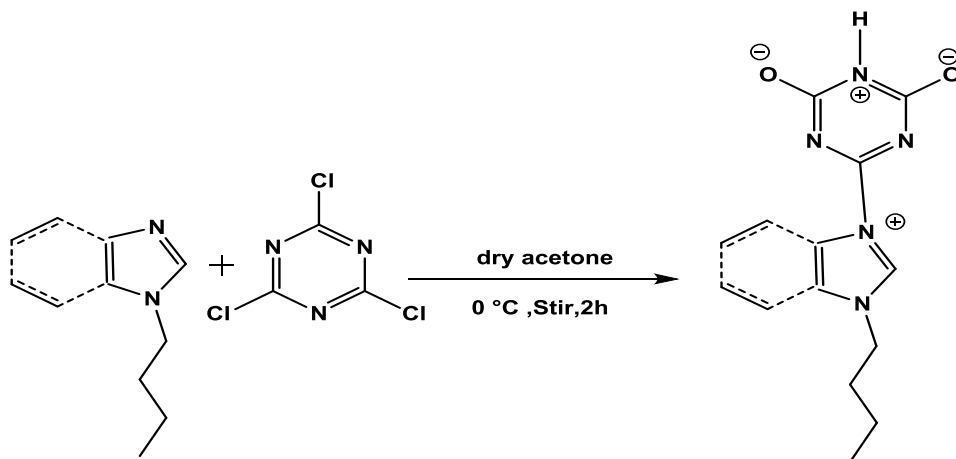
Scheme (2-9) Synthesis of bis imidazole triazine

Silver complexes were obtained by reacting silver oxide with these pro-ligands at room temperature in the dark (Scheme 1-10). [31]



Scheme (2-10) silver complexes

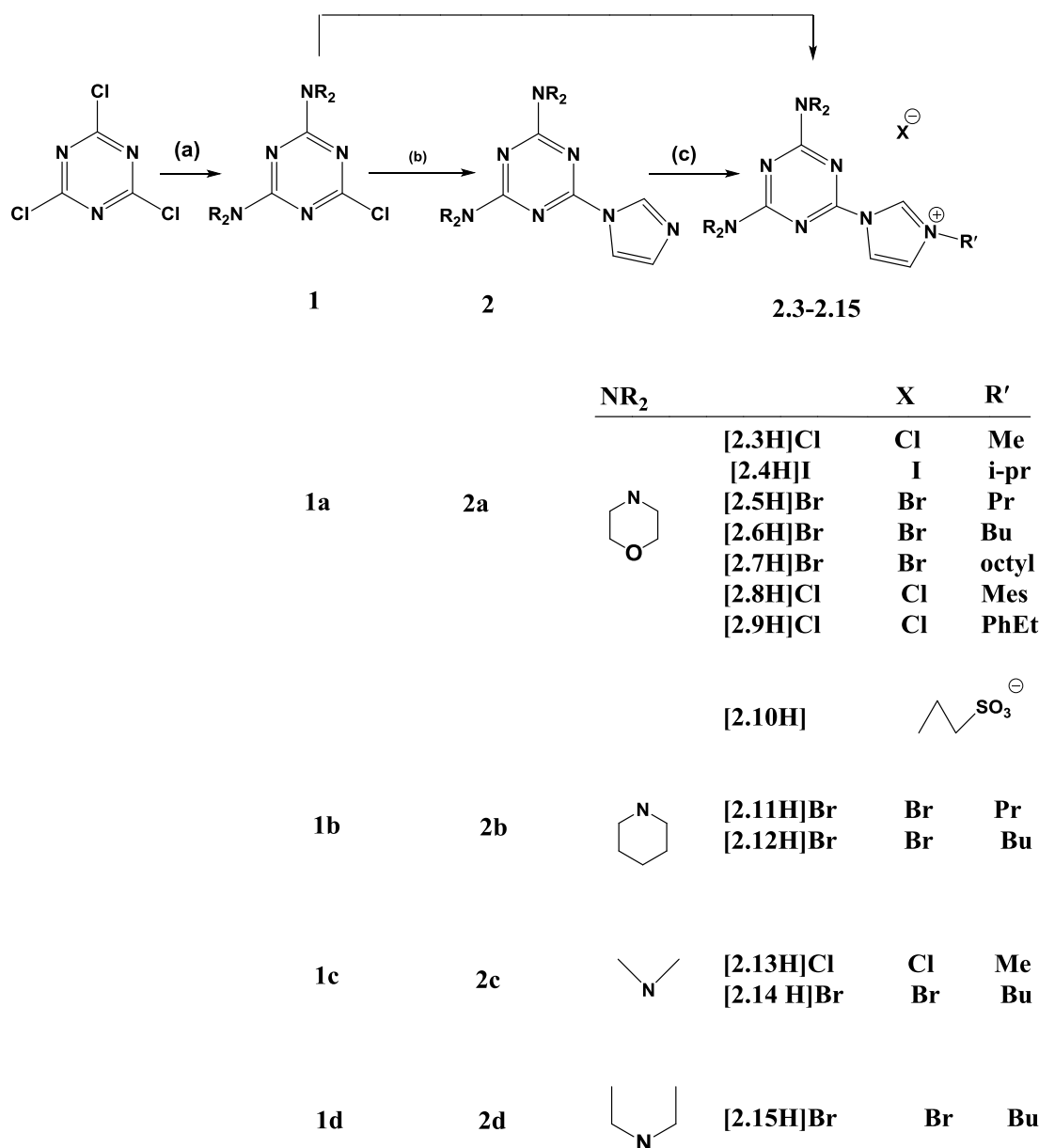
Cyanuric chloride was reacted with 1-butyl imidazole, and benzimidazole to afford imidazolium and benzimidazolium salts. The reactions were conducted in dry acetone and stirred at room temperature. Unfortunately, all attempts to prepare silver and palladium complexes of these salts failed because of the low acidity of C2 protons (Scheme 2-11). [32]



Scheme (2 - 11) Synthesis of triazine benzimidazolium and imidazolium salts

2.1.4-Strategy for Designing New NHC Ligands incorporating a triazine core

A range of novel imidazolium salts were prepared incorporating cyanuric chloride derivatives as a core. Similar methods as those discussed above were used to conduct substitution of cyanuric chloride (Scheme 1-1). Dichlorotriazine derivatives **1a**, **1b**, **1c**, and **1d** were prepared by the reaction of morpholine, piperidine, diethylamine, and dimethylamine respectively with cyanuric chloride under mildly basic aqueous conditions, while the third chloride was replaced by the reaction with either 1*H*-imidazole or *N*-substituted-imidazole. Imidazolium salts have been obtained by reaction of a variety of alkyl halides with **2a**, **2b**, **2c**, and **2d**. Imidazolium salts containing aryl derivatives at the site of the imidazole ring have been prepared by reacting the cyanuric derivatives with *N*-aryl imidazole compounds at high temperature (Scheme 2-12).



Scheme (2-12) Synthesis of imidazolium salts. Reagents and conditions: (a) (1a, 1b, 1c, 1d) 1 equiv. cyanuric chloride, 2 equiv. amine, Na₂CO₃, acetone-H₂O, (0-5) °C for the first 2hrs followed by Rt overnight; (b) (2a, 2b, 2c, 2d) 1equiv. (1a, 1b, 1c, 1d), 1.5 eq. KOH, 1 eq. imidazole, 140 °C, DMF; (c) [2.3H]Cl, [2.13H]Cl 1eq N-methylimidazole, 1 eq. 1a, 1c, 140 °C; (d) [2.4H]I, [2.10H] 1 eq. 1a, excess isopropyl iodide, 1,3- propanesulfonate, CH₃CN, reflux; (e) [2.5H]Br, [2.6H]Br, [2.7H]Br, [2.11H]Br, [2.12H]Br, [2.14H]Br, [2.15H]Br 1 eq. 2a, excess 1-bromo propyl, 1-bromo butyl, 1-bromo octyl, DMF, 120 °C; (f) [2.8H]Cl, [2.9H]Cl 1eq. 1a, N-mesityl imidazol, N-ethylphenylimidazol, 140 °C.

2.2- Results and discussion

2.2.1-Synthesis of 2, 4-diamino-6-chloro -1, 3, 5-triazine

Secondary diamino –chlorotriazines **1a**, **1b**, **1c**, and **1d** were synthesised according to the previously known methods under basic conditions (Scheme 2-12). [27, 33] Due to the differing reactivity of the cyanuric chlorides with respect to nucleophilic substitution reactions the first substitution is carried out between 0-5 °C during the first 2 hours, while the second substitution occurs at room temperature overnight. The reactions were carried out in aqueous solvent allowing the products to be isolated easily and in high yield. [34] Recrystallization from hot ethanol afforded the products as white crystalline solids in 62-72% yields.

The ^1H NMR spectrum for **1a** shows a multiplet at 3.7-2.95 ppm with integration of 16H corresponding to the methylene groups of the morpholine moieties. Four peaks appear in the ^{13}C NMR spectrum, two for morpholine and two more for the triazine core. The ^1H NMR spectrum of compound **1b** shows three multiplets centred at 3.94, 1.87 and 1.79 ppm integrating to 8H, 4H and 8H respectively. These correspond to the methylene groups of the piperidine moieties. Five peaks were observed in the ^{13}C NMR spectrum; two peaks at 169.4, 164.1 ppm for the triazine, and three peaks at 44.4, 25.3, 24.6 ppm for the piperidine.

Due to a restricted rotation about the diamino–triazine bond. The ^1H NMR spectrum for C1 showed two singlet peaks at 3.05, and 3.07 ppm integrating to 6H each as expected for two methyl groups. The ^{13}C NMR spectrum of C1 showed 3 peaks at 167.8, 163.8 for triazine, and 35.3 ppm for The methyl groups.

^1H NMR analysis of compound **1d** shows two broad peaks centred at 3.46 and 1.10 ppm integrating to 8H and 12H respectively corresponding to the ethyl groups. ^{13}C NMR spectroscopy shows four peaks, two peaks for triazine at 168.9, 163.9 ppm, and two peaks for ethyl groups at 41.2, 13.3 ppm.

2.2.2- Synthesis of 2, 4-di amino-6-(1*H*-imidazol-1-yl)-1, 3, 5-triazine.

Due to the low activity of mono-chlorotriazine towards nucleophilic substitution reactions compounds **2a**, **2b**, **2c** and **2d** were synthesised by heating **1a**, **1b**, **1c** or **1d** with 1 equivalent of imidazole in DMF at 120 °C for 48 h. KOH was used to deprotonate the imidazole prior to substitution and water added to the mixture to produce white solids. Purification by column chromatography (ethyl acetate/ hexane 9:1) afforded white products in 63-84 % yields. [28]

The formation of compounds **2a**, **2b**, **2c**, and **2d** was confirmed by ^1H NMR and ^{13}C NMR spectroscopy as well as mass spectrometry. Additional sharp peaks appeared in the ^1H NMR spectra at around 8.4 ppm, as well as two peaks around 7.7 and 7.0 ppm. Each of these peaks integrates to 1H; indicative of an imidazole group. Furthermore, ^{13}C NMR analysis showed an additional three peaks around 136.1, 129.6 and 116.1 ppm corresponding to the imidazole group.

2.2.3- Synthesis of imidazolium salts

The imidazolium salts [**2.3H**]**Cl**, [**2.13H**]**Cl** were obtained by mixing **1a** or **1c** with *N*-methylimidazole without solvent at 140 °C for overnight. [35] White solids of [**2.3H**]**Cl** and [**2.13H**]**Cl** were obtained in 83 and 80% yields respectively. Comparison of the ^1H NMR spectra of **1a** and **1c** with the products show new peaks integrating to imidazole protons and methyl group at 10.20, 8.47, 7.92, 3.69 ppm for [**2.3H**]**Cl**, and 7.94, 7.46, 4.31 ppm for [**2.13H**]**Cl**. ^{13}C NMR spectroscopy also

confirmed the formation of the. **[2.3H]Cl** and **[2.13H]Cl** as the observed peaks at 137.4, 125.1 and 119.1 ppm assigned to imidazole ring and 37.2 ppm corresponding to the methyl group that attached to the imidazole group.

[2.4H]I was prepared by the reaction of 2,4-dimorpholine-6-imidazole-1,3,5-triazine **2a** with excess isopropyl iodide in refluxing acetonitrile. Long reaction times were necessary to complete the reaction [35]. Product formation was accompanied by a downfield shift of the imidazole peaks in the ^1H NMR spectrum from 7.02 to 7.6 ppm and from 8.46 to 10.36 ppm alongside the appearance of two peaks centred at 5.25 (multiplet) and 1.57 ppm (doublet) ppm. The integrals and chemical shifts are consistent with the attachment of an isopropyl group at nitrogen. This assignment is corroborated by the appearance of two peaks at 55.2 ppm and 23.3 ppm in the ^{13}C NMR spectrum corresponding to the CH and methyl groups respectively.

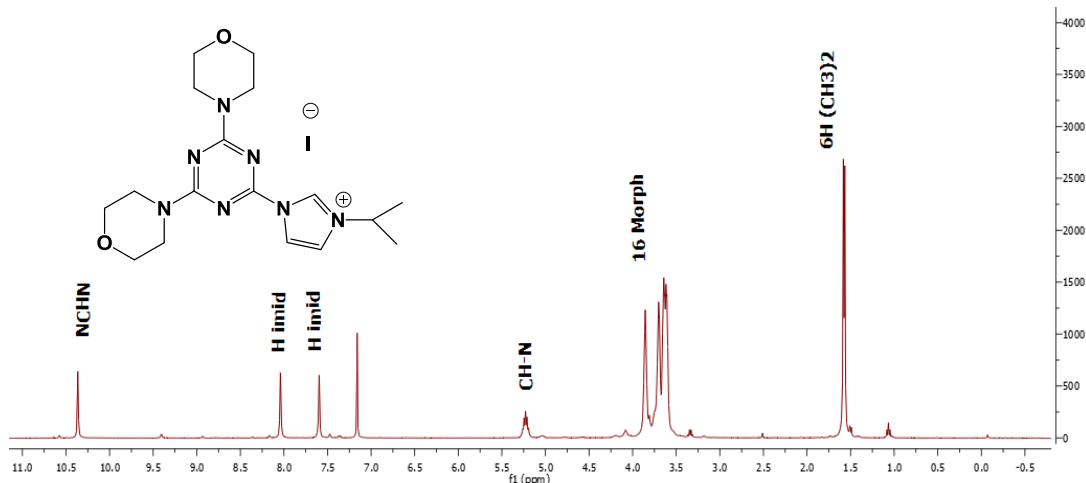


Figure (2- 4) ^1H NMR spectrum of 1-(2, 4-di (morpholino-1,3,5-triazine-2-yl)- 3-isopropyl-1*H*-imidazol-3-ium iodide, **[2.4H]I**

Salts of **[2.5H]Br**, **[2.6H]Br**, **[2.7H]Br**, were obtained by reaction of 2,4-dimorpholine-6-imidazole-1,3,5-triazine **2a** with excess propyl bromide, butyl bromide and octyl bromide respectively, in DMF. The mixtures were heated at 120

°C for 48 hours. Purification was achieved by recrystallisation from dichloromethane/diethyl ether. The formation of salts was confirmed by a downfield shift of the imidazole peak in the ^1H NMR spectrum from 7.02 to 7.49, 7.72 and 7.63 ppm for **[2.5H]Br**, **[2.6H]Br**, and **[2.7H]Br** respectively alongside the appearance of new peaks for the propyl, butyl, and octyl chains which correspond with the previous literature [36]. ^{13}C NMR spectroscopy also confirmed formation of the salts as new peaks emerged corresponding to propyl, butyl and octyl groups.

The ^1H NMR spectra for the imidazolium salts **[2.11H]Br**, and **[2.12H]Br** displayed new peaks at 4.64, 1.98 and 0.99 or 4.74, 1.92, 1.32 and 0.98 ppm corresponding to the propyl and butyl chains respectively. Also ^{13}C NMR spectroscopy confirmed product formation as new peaks corresponding to the propyl and butyl chain were observed at 52.0, 23.9 and 10.7 or 49.8, 31.3, 18.5, and 12.6 ppm respectively.

The synthesis of **[2.14H]Br**, and **[2.15H]Br**, were carried out under the same conditions as described above. **[2.14H]Br** was synthesised from 2,4-di(dimethyl)-6-imidazole-1,3,5-triazine with an excess of butyl bromide and **[2.15H]Br** was prepared using 2,4-di(diethylamine)-6-imidazole-1,3,5-triazine with excess of butyl bromide. NMR spectroscopy confirmed the introduction of propyl, and butyl chains to the imidazole unit. Peaks attributed to the imidazole protons were shifted downfield as a result of salt formation.

The ^1H NMR of **[2.14H]Br**, Figure (2-5), showed two peaks for the protons dimethyl amino groups. This is in consistent with a rotational barrier about the amine–triazine bonds which is due to the extended π -conjugation network between the amino N-atoms and the triazine ring.

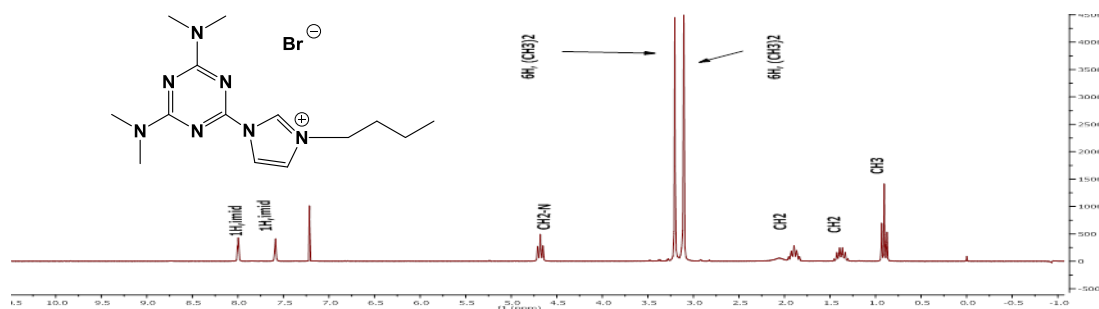
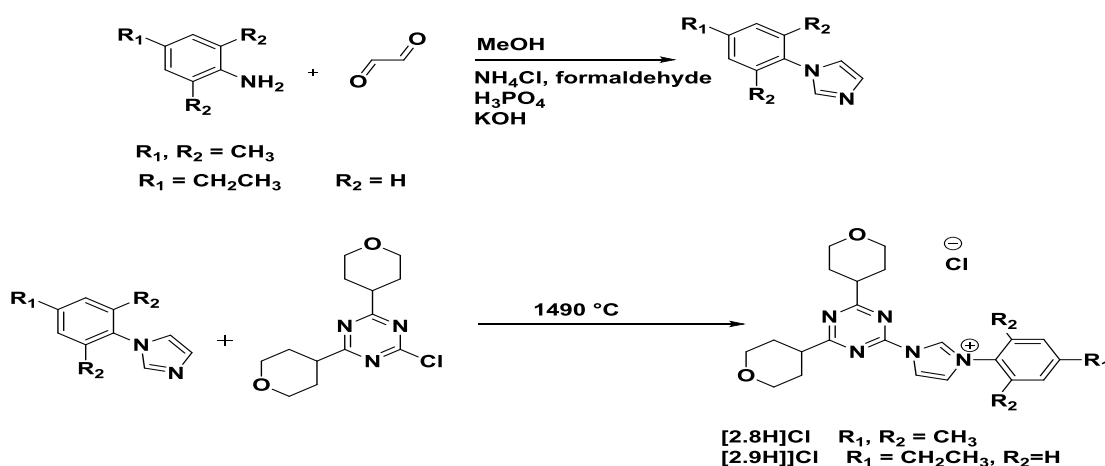


Figure (2- 5) ^1H NMR spectrum of 1-(2, 4-dimethylamino-1,3,5-triazine-2-yl)-butyl-1*H*-imidazol-3-ium bromide, **[2.14H]Br**.

In order to prepare the N-aryl substituted salts **[2.8H]Cl**, and **[2.9H]Cl**, 1-mesitylimidazole and ethyl phenyl imidazole were prepared by reaction of 2,4,6-trimethylaniline and 4-ethylaniline respectively with glyoxal in methanol according to the literature procedures (Scheme 2-13). [19, 37] Imidazolium salts **[2.8H]Cl** and **[2.9H]Cl** were synthesised by reaction of **1a** with 1-mesitylimidazole and 1-(4-ethylphenyl) imidazole in a pressure tube in the absence of solvent at 140 °C overnight.

The product was dissolved in dichloromethane and diethyl ether was added to obtain a white precipitate. New peaks were observed by ^1H NMR spectroscopy for **[2.8H]Cl** at 8.56 and 7.70 ppm for the imidazole protons, 7.02 ppm (2H) for the aromatic protons and peaks at 2.34 ppm (3H) and 2.15 ppm (6H) are consistent with the presence of a pendant mesityl group. ^{13}C NMR analysis confirmed formation of the product; four peaks were detected in the range 141.2 - 125.9 ppm corresponding to the aromatic mesityl atoms (in addition to the three imidazolium peaks) and two peaks at 21.0 and 17.8 ppm corresponding to the three methyl groups. In the ^1H NMR spectrum of **[2.9H]Cl** three peaks for the imidazole were found at 10.59, 8.75, and 8.52 ppm as well as peaks at 7.87 and 7.52 ppm corresponding to the aromatic protons and two peaks for the ethyl group at 2.72 (2H) and 1.23 (3H) ppm. ^{13}C NMR spectroscopy also confirmed formation of **[2.9H]Cl**, new peaks emerged

corresponding to imidazolium carbon atoms and the phenyl group were found in the range 147.2-119.4 ppm, in addition to peaks at 28.4 and 15.1 ppm for the ethyl group.



Scheme (2-13) Synthesis of [2.8H]Cl and [2.9H]Cl imidazolium salts

[2.10H] was obtained by reaction of an excess of 1,3-Propanesultone with **2a** in acetonitrile. A white precipitate was obtained for [2.10H] after purification from ethanol/diethyl ether. The ^1H NMR spectrum in D_2O shows three peaks at 4.38 (2H), 2.87 (2H), and 2.29 ppm ($\text{CH}_2\text{-S}$). Elemental analysis confirmed the formation of [2.10H] while the ^{13}C NMR spectrum shows three peaks at 49.06, 44.13 and 25.37 ppm corresponding to the propyl group. The results are compatible with the previous literature. [38]

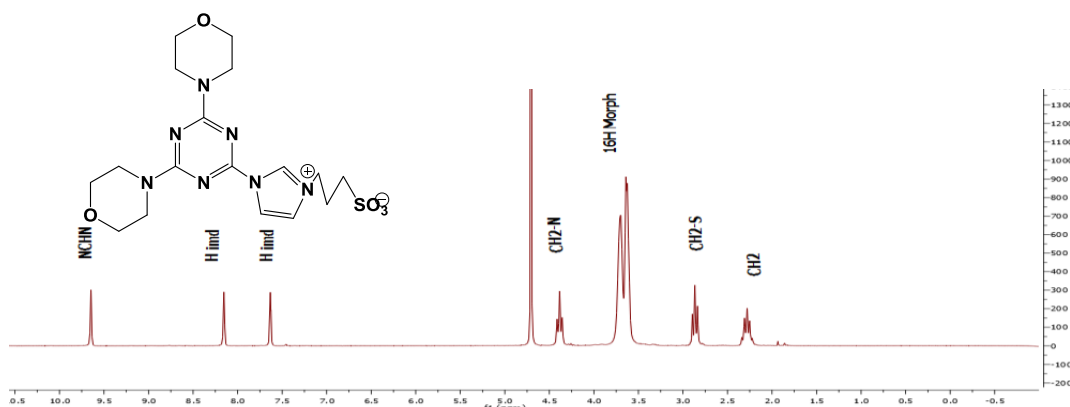


Figure (2- 6) ^1H NMR spectrum of 1-(2, 4-dimorpholino-1, 3, 5-triazine-2-yl)-1H-imidazol-3-ium propane-1-sulfonate [2.10H]

2.2.4-Solid state structural studies

The molecular structures of the [2.4H]I, [2.6H]Br and [2.10H] were determined by single crystal X-ray diffraction. The crystals of salt [2.4H]I were grown by the slow evaporation of a concentrated solution in acetonitrile at ambient temperature. Selected bond lengths and angles are listed in Table (2-1). The structure consists of 1-(2,4-di(morpholine-1,3,5-triazine)-3-isopropyl imidazolium as a cation and one iodide anion (Figure 2-7).

The imidazole C2-C3 bond length of 1.349 (3) Å is close to the reported value of 1.32 Å for C (sp²) - C (sp²) bonds. This suggests a localized carbon-carbon double bond in the imidazole ring. The N1-C1 and N2-C1 bond lengths of 1.321(3) and 1.340 (3) Å are between the expected values of 1.28 Å for C (sp²) -N (sp²) double bonds and 1.38 Å for C (sp²) -N (sp³) single bonds which is consistent with a delocalized double bond system in the NCN unit of the imidazole rings. The angle between the triazine unit and the imidazolium is twisted out of the plane by 8.96(18)°(torsion angle N5-C7-N2-C1).

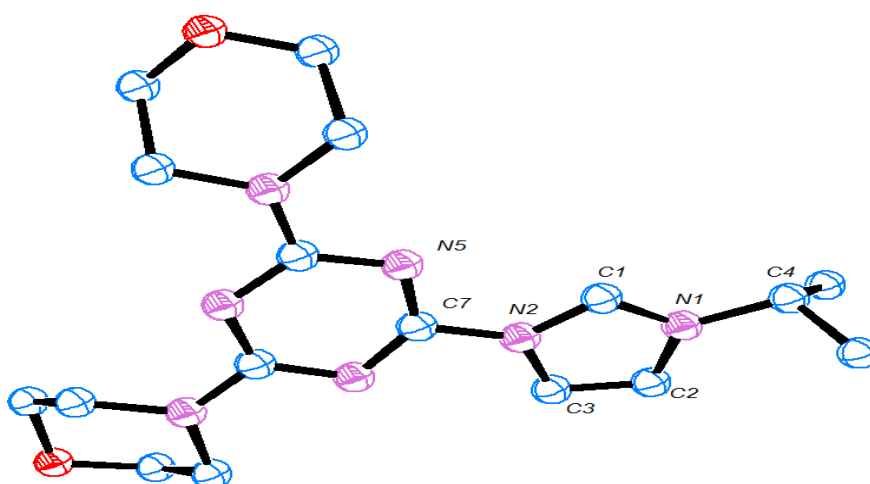


Figure (2 - 7) ORTEP ellipsoid plot at 50% probability of molecular structure of [2.4H]I. H atoms, counter ion and solvent omitted for clarity.

Table (2 - 1) Selected bond lengths and angles for **[2.4H]I**

Bond Angles (°)		Bond lengths (Å)	
N1-C1-N2	108.16(18)	C1-N1	1.321(3)
C1-N1-C2	109.05(17)	C1-N2	1.340(3)
C1-N2-C3	109.05(17)	C3-C2	1.349(3)
N2-C3-C2	106.46(18)	N1-C4	1.485(3)
N1-C3-C2	107.27(17)	N2-C7	1.432(2)
C1-N1-C4	124.95(18)	N1-C2	1.390(3)
C1-N2-C7	124.61(17)	N2-C3	1.388(2)

Suitable crystals of **[2.6H]Br** were obtained from vapour diffusion of diethyl ether into chloroform solutions. The structure consists of 1-(2,4-di(morpholine-1,3,5-triazine)-3-butyl imidazolium as a cation and one bromide as an anion (Figure 2-8). Selected bond lengths and angles are listed in Table (2-2).

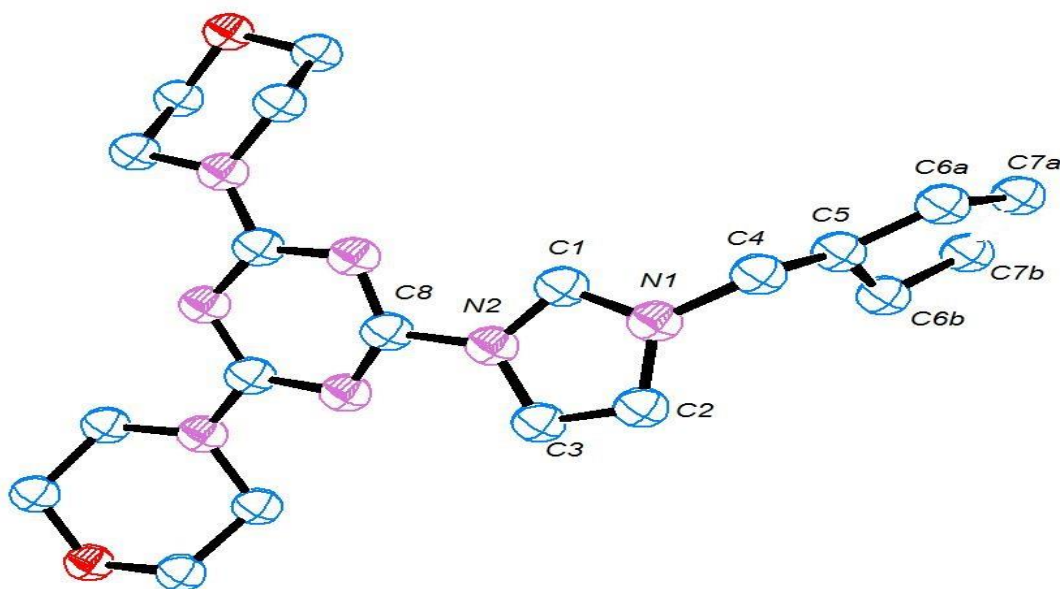


Figure (2 - 8) ORTEP ellipsoid plot at 50% probability of molecular structure of **[2.6H]Br**, H atoms, counter ion and solvent omitted for clarity

The crystal structure of [2.6H]Br showed that C6 and C7 of the butyl group are distorted. some in the butyl chain. The positional probability of the distorted atoms are C_6 (C_{6a} 0.623, C_{6b} 0.377) and C_7 (C_{7a} 0.623, C_{7b} 0.377). All structural parameters are consistent with and comparable to the previously discussed data for the similar ligand 2.4. The imidazole C-C bond length of 1.345(4) Å is close to the reported value of 1.32 Å for C (sp^2) - C (sp^2) bonds. This suggests a localized carbon-carbon double bond in the imidazole ring. The N1-C1 and N2-C1 bond lengths of 1.324(4) and 1.332(4) Å are between the expected values of 1.28 Å for C (sp^2) - N (sp^2) double bonds and 1.38 Å for C (sp^2) - N (sp^3) single bonds [25] which is consistent with a delocalized double bond system in the NCN unit of the imidazole rings. The angle between the triazine unit and the imidazolium is twisted out of the plane by 9° (torsion angles N3-C8-N2-C3).

Table (2-2) Selected bond lengths and angles for [2.6H]Br

Bond Angles (°)		Bond lengths (Å)	
N1-C1-N2	108.2(3)	C1-N1	1.324(4)
C1-N1-C2	108.5(3)	C1-N2	1.332(4)
C1-N2-C3	109.4(3)	C3-C2	1.345(4)
N1-C3-C2	108.4(3)	N1-C4	1.468(4)
N2-C3-C2	105.5(3)	N2-C8	1.444(4)
C1-N1-C4	124.4(3)	N1-C2	1.379(4)
C1-N2-C8	124.6(2)	N2-C3	1.392(3)

Single crystals of [2.10H] were obtained from diffusion of diethyl ether into ethanol solutions. The molecular structure is shown in Fig (2-9). The solid state structure of the neutral compound shows that the imidazolidinyl-triazine heterocyclic moiety adopts a planar geometry. Structural data shows similarities with previous data for

[**2.4H**]Br and [**2.6H**]Br with regards to imidazole bond lengths and bond angles [35, 39].

Table (2-3) Selected bond lengths and angles for [**2.10H**].

Bond Angles (°)		Bond lengths (Å)	
N1-C1-N2	107.56(14)	C1-N1	1.324(2)
C3-C2-N2	106.92(14)	C1-N2	1.3425(19)
C1-N1-C3	109.59(13)	C3-C2	1.348(2)
C1-N2-C2	10.12(14)	N1-C4	1.4804(19)
N1-C3-C2	107.82(15)	N2-C7 _{triazine}	1.4355(19)
C1-N1-C4	124.19(13)	N1-C3	1.358(2)
C1-N2-C7	125.28(14)	N2-C2	1.382(2)
		O1-S1	1.4529(12)
		O2-S1	1.4467(13)
		O3-S1	1.318(14)

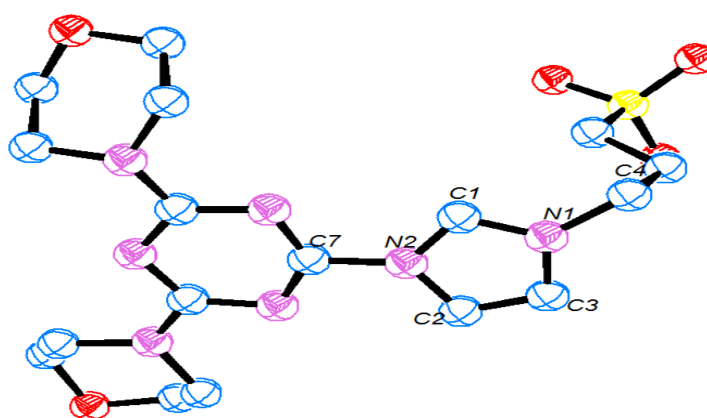


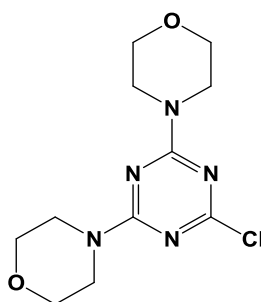
Figure (2-9) ORTEP ellipsoid plot at 50% probability of molecular structure of [**2.10H**] H atoms, counter ion and solvent omitted for clarity

2.3-Experimental

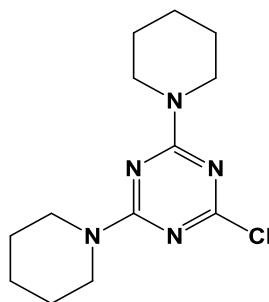
General remarks.

All manipulations were performed using standard glassware under aerobic conditions. Solvents of analytical grade were purified using a Braun-SP Solvent purification system (DMF, MeCN). Chemical reagents (cyanuric chloride, morpholine, piperidine, diethylamine, dimethylamine, imidazole, N-methylimidazole, isopropyl iodide, propyl bromide, butyl bromide, octyl bromide, Ammonium chloride, 1,3,5-trimethyl aniline, 4-phenyl aniline, glyoxal, Paraformaldehyde were used as received. NMR spectra were obtained on either a Brüker 500 Ultrashield, Brüker Avance AMX 400, Brüker Avance or 250 spectrometer. The chemical shifts are given as dimensionless σ values and are frequency referenced relative to TMS. Coupling constants J are given in hertz (Hz) as positive values regardless of their real individual signs. The multiplicities of the signals are indicated as s, d, and m for singlets, doublets, and multiplets, respectively. The abbreviation br is given for broadened signals, mass spectra and high resolution mass spectra were obtained in electrospray (ES) mode unless otherwise reported, on Waters LCT Premier XE instrument. Elemental Analysis worked by Elemental Analysis Service Science Centre London Metropolitan University.

X-Ray crystallographic data for [2.4H]I, [2.6H]Br, and [2.10H] collected using Rigaku AFC12 goniometer equipped with an enhanced sensitivity (HG) Saturn724+ detector mounted at the window of an FR-E+ SuperBright molybdenum rotating anode generator with HF Varimax optics (100 μ m focus). Structural solution and refinement was achieved using SHELXS97, SHELXL-2013 or SHELXL97 software, and absorption correction analysed using CrystalClear-SM Expert software.

Synthesis of 2,4-dimorpholine-6-chloro-1,3,5-triazine, 1a

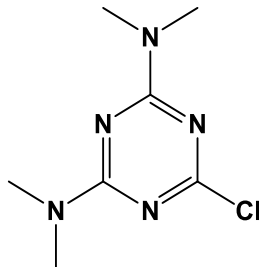
In a round bottom flask cyanuric chloride (9.22 g, 50 mmol) was dissolved in acetone (200 mL) and ice water (200 mL). Morpholine (8.7 g, 100 mmol) was added to the reaction gradually with Na_2CO_3 (10.69 g, 100 mmol). The mixture was stirred for 2 hours at 0-5 °C, followed by stirring at room temperature for 24 hours. The white precipitate formed was isolated by filtration and recrystallised from hot ethanol. Yield = 8.8g (30 mmol) 62 %, ^1H NMR (250 MHz, CDCl_3 , ppm) δ_{H} = 3.74 (m, 8 H, morpholine), 3.59 (br, 4 H, morpholine), 2.95 (br, 4 H, morpholine), ^{13}C NMR (101 MHz, CDCl_3 , ppm) δ_{C} = 170.1, 164.2 (3 \times C, triazine), 67.1 (4 \times C, morpholine), 44.6, 44.2 (4 \times C, morpholine), MS (ES^+) for $[\text{M}+\text{H}]$, $\text{C}_{11}\text{H}_{17}\text{O}_2\text{N}_5\text{Cl}$ 286.10 (100%). These data are consistent with those previously reported. [27, 33]

Synthesis of 2,4-dipiperidine-6-chloro-1,3,5-triazine, 1b

Prepared similarly from cyanuric chloride (9.22 g, 50 mmol), piperidine (8.5 g, 100 mmol), Na_2CO_3 (10.69 g, 100 mmol) Yield = 9 g (32 mmol) 64 %. ^1H NMR (400 MHz, CDCl_3 , ppm) δ_{H} = 3.94 (m, 8 H, N- CH_2), 1.87 (m, 4 H, $\text{NCH}_2\text{CH}_2\text{CH}_2$), 1.79 (m, 8 H, NCH_2CH_2). ^{13}C NMR (63 MHz, CDCl_3 , ppm) δ_{C} = 169.4, 164.1 (3 \times C,

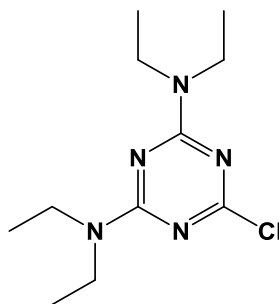
triazine), 44.4 (CH₂), 25.3 (CH₂), 24.6 (CH₂). MS (ES⁺) for [M+H], C₁₃H₂₁N₅Cl 282.16 (90%). These data are consistent with those previously reported. [27, 33]

Synthesis of 2,4-dimethylamine-6-chloro-1,3,5-triazine, 1c

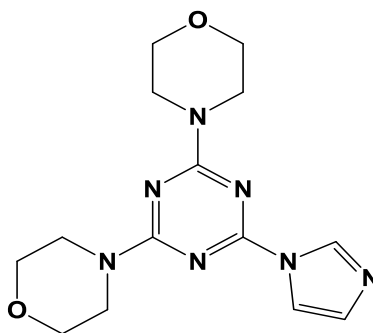


Prepared similarly from cyanuric chloride (9.22 g, 50 mmol), dimethylamine (4.50 g, 100 mmol), with Na₂CO₃ (10.69 g, 100 mmol) were used. Yield = 7.28 g (43 mmol) 72 %. ¹H NMR (250 MHz, CDCl₃, ppm) δ = 3.05 (s, 6 H, N-CH₃), 3.07 (s, 6 H, N-CH₃), ¹³C NMR (101 MHz, CDCl₃, ppm) δ = 167.8, 163.8 (3 × C, triazine), 35.3 (4 × CH₃), MS (ES⁺) for [M+H], C₇H₁₃N₅Cl 202.09 (100%). These data are consistent with those previously reported. [27, 33]

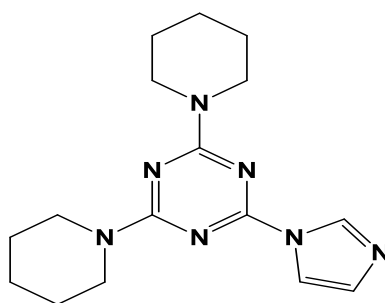
Synthesis of 2,4-diethylamine-6-chloro-1,3,5-triazine, 1d



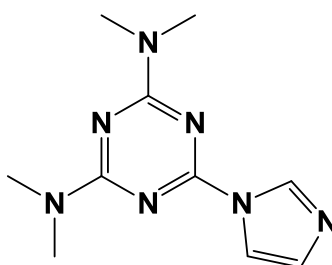
Prepared similarly from cyanuric chloride (9.22 g, 50 mmol), diethyl amine (7.3 g, 100 mmol) Na₂CO₃ (10.69 g, 100 mmol), Oily product. Yield = 8.5 g (33 mmol) 66 %. ¹H NMR (400 MHz, CDCl₃, ppm) δ_H = 3.46 (m, 8 H, N-CH₂), 1.10 (m, 12 H, NCH₂CH₃). ¹³C NMR (63 MHz, CDCl₃, ppm) δ_C = 168.9, 163.9 (3 × C, triazine), 41.2 (N-CH₂), 13.3 (CH₃). MS (ES⁺) for [M+H], C₁₁H₂₁N₅Cl 258.14 (70%). These data are consistent with those previously reported. [27, 33]

Synthesis of 2, 4-di (Morpholine) -6-(1*H*-imidazol-1-yl)-1, 3, 5-triazine, 2a

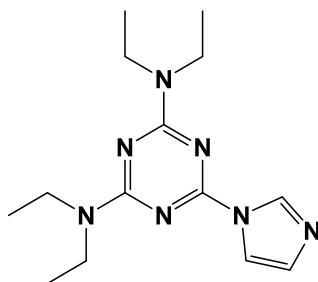
In a round bottomed flask, KOH (0.84 g, 15 mmol) was dissolved in DMF (10 mL). Imidazole (0.68 g, 10 mmol) was added to the solution and stirred at room temperature for 1 h. **1a** (2.85 g, 10 mmol) was added to the solution and heated to 120 °C for 48 hours. The solution was diluted with distilled water (80 ml) and the product immediately precipitated as a pearlescent solid. After filtration the product was dried *in vacuo*. The product was purified by column chromatography (silica, AcOEt / hexane 9:1) affording a colourless solid. Yield = 2.0 g (6.2 mmol) 63 %. ¹H NMR (400 MHz, CDCl₃, ppm) δ_H = 8.43 (s, 1H, NCHN), 7.69 (d, *J* = 1.2 Hz, 1 H, C₅), 7.02 (d, 0.9, 1 H, C₄), 3.79 (s, 8 H, morpholine), 3.78 - 3.61 (br, 8 H, morpholine), ¹³C NMR (101, MHz, CDCl₃, ppm) δ_C = 165.2, 160.5 (3 × C, triazine), 136.1 (NCHN, imid), 129.8, 116.3 (2 × C, imid) 66.6 (4 × C, morpholine), 43.7, 44.2 (4 × C, morpholine), MS (ES⁺) for [M+H]⁺, C₁₄H₂₀O₂N₅ (318.16) (100%). These data are consistent with those previously reported. [27, 33]

Synthesis of 2,4-di(piperidine)-6-(1H-imidazol-yl)-1,3,5-triazine, 2b

The **2b** was prepared similarly from KOH (0.58 g, 10.6 mmol), Imidazole (0.48 g, 7.1 mmol) and **1b** (2 g, 7.1 mmol). Yield = 1.5 g (5.4 mmol) 67 %. ^1H NMR (400 MHz, CDCl_3 , ppm) δ_{H} = 8.44 (s, 1 H, NCHN), 7.72 (br, 1 H, imid), 7.00 (br, 1 H, imid), 3.72 (m, 8 H, N- CH_2), 1.62-1.53 (m, 12 H, $\text{NCH}_2\text{CH}_2\text{CH}_2\text{CH}_2$). ^{13}C NMR (63 MHz, CDCl_3 , ppm) δ_{C} = 164.8, 160.5 (3 \times C, triazine), 136.2 (NCHN), 129.6, 116.4 (2 \times C, imid), 44.4 (CH_2), 25.8 (CH_2), 24.8 (CH_2), MS (ES^+) for $[\text{M}+\text{H}]^+$. $\text{C}_{16}\text{H}_{23}\text{N}_7$ (313.12) (100%). These data are consistent with those previously reported. [27, 33]

Synthesis of 2,4-di(dimethylamine)-6-(1H-imidazol-1-yl)-1,3,5-triazine, 2c

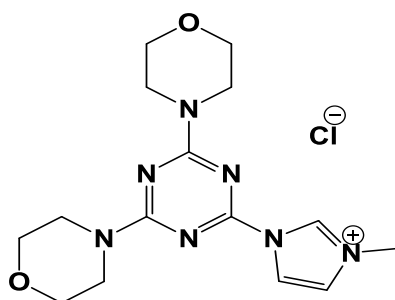
The **2c** prepared similarly from KOH (0.84 g, 15.0 mmol), imidazole (0.68, 10 mmol) and **1c** (2.01 g, 10 mmol). Yield = 1.6g (6.9 mmol) 69 %, ^1H NMR (400 MHz, CDCl_3 , ppm) δ_{H} = 8.46 (s, 1 H, NCHN), 7.73 (br, 1 H, imid) 7.01 (br, 1 H, imid) 3.09 (s, 6 H, N- CH_3), 3.08 (s, 6 H, N- CH_3), ^{13}C NMR(101 MHz, CDCl_3 , ppm) δ_{C} = 165.7, 160.1 (3 \times C, triazine), 136.45 (NCHN, imid), 129.9, 116.6 (2 \times C, imid) 36.3 (4 \times CH_3), MS (ES^+) for $[\text{M}+\text{H}]^+$, $\text{C}_{10}\text{H}_{16}\text{N}_7$ 234.17 (70%). These data are consistent with those previously reported. [27, 33]

Synthesis of 2, 4-di (diethylamine)-6-(1*H*-imidazol-1-yl)-1, 3, 5-triazine, 2d

The **2d** prepared similarly from KOH (0.98 g, 17.5 mmol), imidazole (0.79g, 11.6 mmol) and **2d** (3 g, 11.6 mmol). Yield = 2.8 g (9.68 mmol) 83 %. ¹H NMR (400 MHz, CDCl₃, ppm) δ_H = 8.46 (s, 1H, NCHN), 7.72 (br, 1H, imid), 7.01 (br, 1H, imid), 3.51 (m, 8H, N-CH₂), 1.11 (m, 12H, N-CH₂CH₃). ¹³C NMR (63 MHz, CDCl₃, ppm) δ_C = 164.6, 160.1 (3 × C, triazine), 136.1 (NCN), 129.6, 116.3 (2 × C, imid), 41.6 (CH₂), 13.65, 12.65 (CH₃), MS (ES⁺) for [M+H]⁺, C₁₄H₂₃N₇ (289.20) (80%).

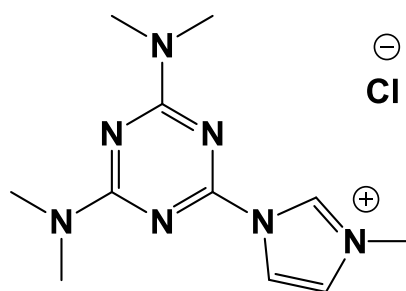
General procedure for the synthesis of the methyl imidazolium salts [2.3H]Cl, [2.13H]Cl.

In a high pressure tube, **1a** or **1c** was mixed with 1-methyl imidazole (1 eq). The mixture was heated to 140 °C and left stirring overnight. After cooling to room temperature the reaction mixture was triturated with diethyl ether and the precipitated product was collected by filtration. Recrystallisation from CH₂Cl₂ and Et₂O afforded the clean product.

Synthesis of 1-(2,4-dimorpholino-1,3,5-triazine-2-yl)-methyl-1*H*-imidazol-3-ium chloride, [2.3H]Cl.

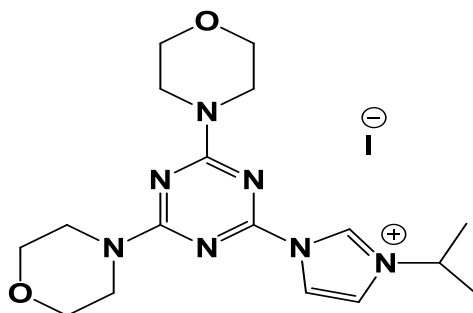
1a (0.5 g, 1.75 mmol) and 1 - methyl imidazole (0.143 g, 1.75 mmol). Yield = 0.48 (1.47 mmol) 83 %, ^1H NMR (400 MHz, DMSO, ppm) δ = 3.68 - 3.89 (m, 16 H, morpholine), 3.96 (s, 3H, N-CH₃), 7.92 (d, 1 H, J = 1.8, imid), 8.47 (d, 1 H, J = 1.8, imid), 10.20 (s, 1 H, NCHN). ^{13}C NMR (75 MHz, DMSO, ppm) δ_{C} = 164.4, 159.2 (3 \times C, triazine), 137.4 (NCHN, imid), 125.1, 119.1 (2 \times C, imidazole), 66.5, 66.3, 44.4, 45.9 (8 \times C, morpholine) 37.2 (CH₃-N), MS (ES⁺) for [M-Cl]⁺, C₁₅H₂₂N₇O₂ 332.18 (100%).

Synthesis of 1-(2,4-dimethylamino-1,3,5-triazine-2-yl)-methyl-1H-imidazol-3-ium chloride, [2.13]Cl



The [2.13]Cl was prepared similarly from **1c** (0.5 g, 2.48 mmol) and 1- methyl imidazole (0.203 g, 2.48 mmol). Yield = 0.49 g (1.97 mmol) 80 %, ^1H NMR (250 MHz, CDCl₃, ppm) δ = 7.94 (br, 1H, imid), 7.46 (br, 1 H, imid), 4.31 (s, 3 H, N-CH₃), 3.24 (s, 6 H, N-CH₃) 3.11 (s, 6 H, N-CH₃) . ^{13}C NMR (63 MHz, CDCl₃, ppm) δ_{C} = 166.7, 160.2 (3 \times C, triazine), 136.1 (NCHN, imid), 125.9, 120.4 (2 \times C, imid), 50.6 (CH₃-N), 37.7, 37.1, 37.1 (4 \times CH₃), MS (ES⁺) for [M-Cl]⁺, C₁₁H₁₈N₇ 248.17 (100%).

Synthesis of 1-(2,4-dimorpholino-1,3,5-triazine-2-yl)-isopropyl-1*H*-imidazol-3-ium iodide, [2.4H]I.

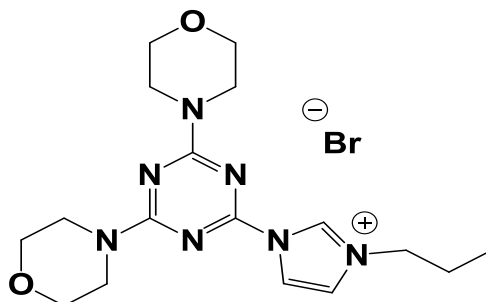


In a round bottom flask compound **2a** (1.0 g, 3.1 mmol) was dissolved in acetonitrile (25 mL). Isopropyl iodide (5.27 g, 31 mmol) was slowly added and the mixture was refluxed for 72h. The solvent was removed *in vacuo* and the crude product recrystallised (CHCl₃ / Et₂O) to give a brown precipitate. Yield = 1.22 g (2.50 mmol) 80 %. ¹H NMR (400 MHz, CDCl₃, ppm) δ = 10.36 (s, 1H, NCHN), 8.04 (br, 1H, imid), 7.6 (br, 1H, imid), 5.23 (m, 1H, N-CH), 3.86 (m, 8H, morpholine), 3.7-3.62 (m, 8H, morpholine), 1.57 (d, 6H, CH-(CH₃)₂) ppm. ¹³C NMR (101 MHz, CDCl₃, ppm) δ_C = 164.4, 159.0 (3 × C, triazine), 134.6 (NCN), 120.95, 119.46 (2 × C, imid) 66.7 (4 × C, morpholine), 44.7, 44.2 (4 × C, morpholine), 55.2 (C-(CH₃)₂), 23.3 (2 × CH₃), HRMS (ES⁺, CH₃CN), calcd mass for [M⁺-I], C₁₇H₂₆O₂N₇ 360.2150, measured 360.2148.

General procedure for synthesis [2.5H]Br, [2.6H]Br, [2.7H]Br, [2.11H]Br, [2.12H]Br, [2.14H]Br, [2.15H]Br

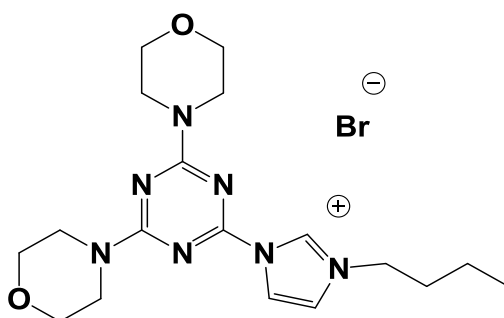
2a, 2b, 2c, 2d was dissolved in DMF (20 mL), alkyl halides (10 eq) were added to the solution. The mixture was heated at 120 °C for 2 days. After cooling, diethyl ether was added resulting in immediate precipitation of the product. The product was filtered and recrystallised by (CHCl₃ / ether) to afford a white solid.

Synthesis of 1-(2, 4-dimorpholino-1,3 ,5-triazine-2-yl)- 3-propyl-1*H*-imidazol-3-ium bromide, [2.5H]Br



2a (1.4 g, 4.4 mmol) and 1-bromo propane (5.41 g, 44 mmol). Yield = 1.64 g (3.73 mmol) 84 %, ^1H NMR (250 MHz, CDCl_3 , ppm) δ_{H} = 7.97 (br, 1 H, imid), 7.49 (br, 1 H, imid), 4.62 (t, J = 7.2, 2 H, N- CH_2), 3.95 (m, 4 H, morpholine), 3.72 (m, 12H, morpholine), 1.95 (m, 2H, N CH_2CH_2 , propyl), 0.97 (t, J = 7.3 Hz, 3H, CH_3 , propyl) ^{13}C NMR (63 MHz, CDCl_3 , ppm) δ_{C} = 164.4, 158.8 (3 \times C, triazine), 137.1 (NCHN, imid), 122.9 , 118.3 (2 \times C, imidazole), 66.8, 64.4, 44.5, 44.3 (8 \times C, morpholine), 52.1 (N- CH_2) 36.3 (CH_2), 23.8 (CH_2), 10.7 (CH_3) HRMS (ES^+ , CH_3CN), calcd mass for [M^+ - Br], $\text{C}_{17}\text{H}_{26}\text{O}_2\text{N}_7$ 360.2148, measured 360.2148.

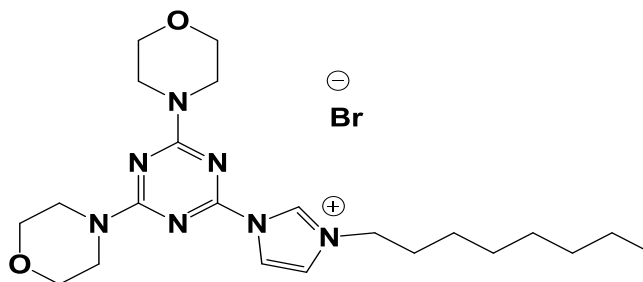
of 1-(2, 4-di (morpholino-1,3,5-triazine-2-yl)- 3-butyl-1*H*-imidazol-3-ium bromide, [2.6H]Br.



The [**2.6H**]Br was prepared from **2a** (1.0 g, 3.14 mmol) and 1- bromo butane (4.3 g, 31.4 mmol). Yield = 1.21 (2.6 mmol) 84 %, ^1H NMR (250 MHz, CDCl_3 , ppm) δ = 9.29(s, 1 H, NCHN), 8.09 (br, 1 H, imid), 7.72 (br, 1 H, imid), 4.63 (t, J = 7.20, 2 H,

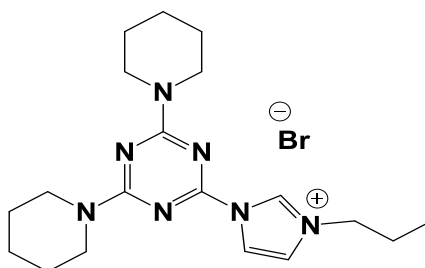
N-CH₂), 3.95 (m, 4 H, morpholine), 3.91-3.45 (m, 12 H, morpholine), 2.11(m, 2 H, NCH₂CH₂), 1.56 (m, 2 H, NCH₂CH₂CH₂CH₂), 0.98 (t, *J* = 7.25 Hz, 3 H, CH₃) ¹³C NMR (63 MHz, CDCl₃, ppm) δ_C = 164.3, 158.7 (3 × C, triazine), 136.1 (NCHN, imid), 123.1, 118.5 (2 × C, imidazole), 66.7, 66.7, 44.3, 43.9 (8 × C, morpholine), 50.9 (N-CH₂) 32.1 (CH₂), 19.4 (CH₂), 13.5 (CH₃). HRMS (ES⁺, CH₃CN), calcd mass for [M⁺-Br], C₁₈H₂₈N₇O₂ 374.2288, measured 374.2304.

Synthesis of 1-(2,4-dimorpholino-1,3,5-triazine-2-yl)- 3-octyl-1*H*-imidazol-3-ium bromide [2.7H]Br.



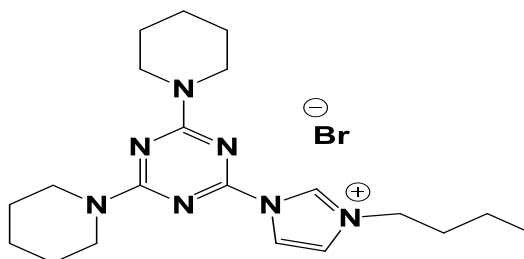
The [2.67H]Br was prepared from **2a** (1.0 g, 3.14 mmol) and 1-bromo octane (6.0 g, 31.4 mmol). Yield = 1.25 (2.45 mmol) 78 %, ¹H NMR (250 MHz, CDCl₃, ppm) δ_H = 8.08 (br, 1H, imid), 7.63 (br, 1H, imid), 4.66 (t, *J* = 7.1, 2 H, N-CH₂), 4.01 (m, 4 H, morpholine), 3.77 (m, 12 H, morpholine), 1.98 (m, 2 H, octyl), 1.25 (m, 10 H, octyl), 0.87 (t, *J* = 6.3, 3 H, CH₃), ¹³C NMR (63 MHz, CDCl₃, ppm) δ_C = 164.4, 158.7 (3 × C, triazine), 136.7 (NCHN, imid), 123.1, 118.4 (2 × C, imid), 66.8, 64.3, 44.4, 43.9 (8 × C, morpholine), 50.6 (N-CH₂, octyl), 31.1, 30.4, 28.9, 26.1, 22.5 (6 × CH₂, octyl), 13.90 (CH₃). HRMS (ES⁺, CH₃CN), calcd mass for [M⁺-Br], C₂₂H₃₆N₇O₂ 430.2918, measured 430.2930.

Synthesis of 1-(2,4-di(piperidin-1-yl)-1,3,5-triazine-2-yl)-3-propyl-1*H*-imidazol-3-ium bromide, **2.11**



The [**2.11H**]**Br** was prepared from **2b** (0.5 g, 1.59 mmol) and 1-bromopropane (1.95 g, 1.59 mmol). Yield = 0.57 g (1.3 mmol) 82 %. ^1H NMR (400 MHz, CDCl_3 , ppm) δ_{H} = 8.01 (br, 1 H, imid), 7.71 (br, 1 H, imid), 4.64 (t, $J = 7.6$ Hz, N- CH_2 , propyl), 3.84 (m, 4 H, N- CH_2), 3.73 (m, 4 H, N CH_2), 1.98 (m, 2 H, CH_2 , propyl), 1.63 (m, 4 H, N $\text{CH}_2\text{CH}_2\text{CH}_2$), 1.57 (m, 8 H, N CH_2CH_2), 0.99 (t, $J = 6.8$ Hz, 3 H, CH_3). ^{13}C NMR (63 MHz, CDCl_3 , ppm) δ_{C} = 163.9, 158.7 (3 \times C, triazine), 136.0 (NCN), 123.1, 118.4 (2 \times C, imid), 52.0 (C-N, propyl), 45.0 (CH_2), 44.6 (CH_2), 23.9 (CH_2 , propyl), 25.8 (CH_2), 23.9 (CH_2), 10.7 (CH_3 , propyl) ppm. HRMS (ES^+ , CH_3CN), calcd mass for [M^+ -Br], $\text{C}_{19}\text{H}_{30}\text{N}_7$ 356.2559, measured 356.2563.

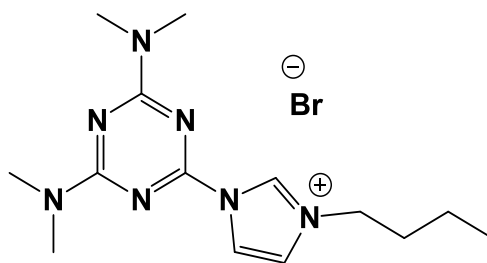
Synthesis of 1-(2,4-di(piperidin-1-yl)-1,3,5-triazine-2-yl)-3-butyl-1*H*-imidazol-3-ium bromide **2.12**



The [**2.12H**]**Br** was prepared from **2b** (0.5 g, 1.59 mmol) and 1-bromobutane (2.1g, 15.9 mmol). Yield = 0.44 g (0.97 mmol) 61%. ^1H NMR (400 MHz, CDCl_3 , ppm) δ_{H} = 10.65 (s, NCHN), 8.05 (br, 1H, imid), 7.67 (br, 1 H, imid), 4.74 (t, $J = 7.0$ Hz, 2 H,

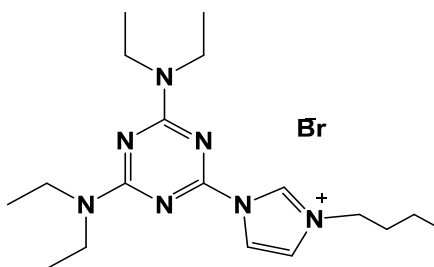
CH₂-N), 3.83 (m, 4 H, N-CH₂), 3.72 (m, 4 H, N-CH₂), 1.92 (m, 2 H, CH₂-but), 1.76 (m, 4 H, NCH₂CH₂CH₂), 1.67 (m, 8 H, NCH₂CH₂), 1.32 (m, 2 H, CH₂ butyl), 0.98 (t, $J = 7.2$ Hz, 3 H, CH₃-but). ¹³C NMR (63 MHz, CDCl₃, ppm) $\delta_C = 163.0, 159.0$ (3 \times C, triazine), 134.7 (NCHN), 122.2, 117.5 (2 \times C, imid), 49.8 (CH₂-N, but), 44.0 (CH₂), 43.6 (CH₂), 31.3 (CH₂, but), 24.9 (CH₂), 24.7 (CH₂), 23.4 (CH₂), 18.5 (CH₂, but), 12.6 (CH₃, butyl). MS (ES⁺) for [M-Br]⁺, C₂₀H₃₂N₇ (370) (100%).

Synthesis of 1-(2,4-dimethylamino-1,3,5-triazine-2-yl)-butyl-1H-imidazol-3-ium bromide, 2.14.



The [2.14H]Br was prepared from **2c** (1g, 4.29 mmol) and 1-bromo butane (5.87 g, 42.9 mmol). Yield = 1.27 g (3.45 mmol) (79 %), ¹H NMR (250, MHz, CDCl₃, ppm) $\delta_H = 7.99$ (br, 1 H, imid), 7.59 (br, 1 H, imid), 4.68 (t, $J = 7.5$, 2 H, N-CH₂), 3.20 (s, 6 H, N-CH₃) 3.11 (s, 6 H, N-CH₃) 1.90 (m, 2 H, NCH₂CH₂), 1.36 (m, 2 H, NCH₂CH₂CH₂), 0.90 (t, $J = 6$, 3 H, CH₃, butyl), ¹³C NMR (63, MHz, CDCl₃, ppm) $\delta_C = 164.9, 158.3$ (3 \times C, triazine), 136.2 (NCHN, imid), 123.5, 118.5 (2 \times C, imidazole), 50.5 (CH₂-N), 37.0, 36.6 (4 \times CH₃), 32.6, 19.6, (2 \times CH₂) 13.7 (CH₃), MS (ES⁺) for [M-Br]⁺, C₁₄H₂₄N₇ (290.27) (100%).

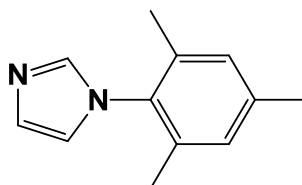
Synthesis of 1-(2,4-diethylamino-1,3,5-triazine-2-yl)-butyl-1*H*-imidazol-3-ium bromide, **2.15**



The [**2.15H**]**Br** was prepared from **2d** (2.8 g, 9.68 mmol) and 1-bromobutane (13.2 g, 96.8 mmol). Yield = 2.2g (5.16 mmol) 53%. ^1H NMR (400 MHz, CDCl_3 , ppm) δ_{H} = 10.77 (s, NCHN), 7.98 (br, 1 H, imid), 7.56 (br, 1 H, imid), 4.69 (br, 2 H, $\text{CH}_2\text{-N}$, butyl), 3.62 (m, 4 H, NCH_2CH_2), 3.53 (m, 4 H, NCH_2CH_2), 1.92 (m, 2 H, NCH_2CH_2 , Butyl), 1.41 (m, 2 H, $\text{NCH}_2\text{CH}_2\text{CH}_2$, butyl), 1.13 (m, 12 H, $4 \times \text{CH}_3$), 0.92 (t, $J = 7.2$ Hz, 2 H, CH_3 , butyl). ^{13}C NMR (63 MHz, CDCl_3 , ppm) δ_{C} = 163.7, 158.2 ($3 \times \text{C}$, triazine), 135.7 (NCN), 123.7, 118.4 ($2 \times \text{C}$, imid), 50.8 (N-C, butyl), 41.9 ($4 \times \text{CH}_2$), 32.3 (CH_2 , butyl), 19.4 (CH_2 , butyl), 13.5 ($4 \times \text{CH}_3$), 12.8 (CH_3 , butyl). MS (ES^+) for $[\text{M-Br}]^+$, $\text{C}_{18}\text{H}_{32}\text{N}_7$ (347.25) (100%).

Synthesis of 1-(2,4-dimorpholino-1,3,5-triazine-2-yl)-methyl-1*H*-imidazol-3-ium chloride, [**2.8H**]**Cl**.

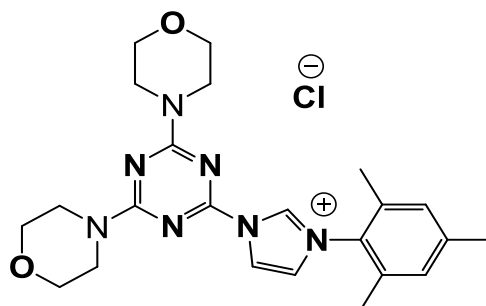
Synthesis of 1-mesityl-1*H*-imidazol



2,4,6-Trimethylaniline (6.8 g, 0.05 mol) in MeOH (25 mL) was stirred with 30 % aqueous glyoxal (8.1 mL, 0.05 mol) for 16 h at room temperature. A bright yellow mixture was formed. NH_4Cl (5.4 g, 0.1 mol) was added followed by 37 % aqueous

formaldehyde (8 mL, 0.1 mol). The mixture was diluted with MeOH (200 mL) and refluxed for 1 h. H₃PO₄ (7 mL, 85 % soln) was added over a period of 10 min. The resulting mixture was then stirred overnight. After removal of solvent, the dark residue was poured onto ice (200 g) and treated with aqueous 40 % KOH solution until pH9. The resulting mixture was extracted with EtOAc (2 × 200 mL) and the organic phases were combined and washed sequentially with H₂O and brine before drying with anhydrous MgSO₄. After filtration, the solvent was removed and the residue purified by distillation on a Kugelrohr under vacuum at 240 °C. ¹H NMR (250, MHz, CDCl₃, ppm) δ_H =: 7.45 (s, NCHN), 7.20 (br, 1H, imid) 6.95 (s, 2 H, mesityl), 6.84 (br, 1H, imid), 2.32 (s, 3H), 1.99 (s, 6H). These data are consistent with previously reported. [40]

Synthesis of [2.8H]Cl.

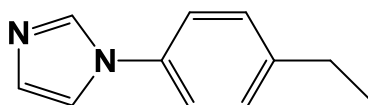


In high pressure tube, a mixture of the 1-(mesityl)-1*H*-Imidazole (0.65 g, 3.5 mmol) and **1a** (1 g, 3.5 mmol) was stirred neat at 140 °C for 16 h. After cooling the mixture was dissolved in CH₂Cl₂ (20 mL) and Et₂O (100 mL) added. A white precipitate was formed. Yield = 1.37 g (2.96 mmol) 85 %. ¹H NMR (500 MHz, CDCl₃, ppm) δ_H = 10.55 (s, NCHN), 8.56 (br, 1H, imid), 7.70 (br, 1 H, imid) 7.02 (s, 2 H, mesityl), 4.21-3.74 (m, 16 H, morpholine), 2.34 (s, 3 H, CH₃), 2.15 (s, 6 H, 2 × CH₃). ¹³C NMR (101MHz, CDCl₃, ppm) δ_C = 164.4, 158.9 (3 × C, triazine), 141.2, 136.7,

134.1, 130.9, 129.8 (6 × C, Ar), 125, 120.4 (2 × C, imid), 66.8, 66.4 (4 × C, morpholine), 44.5, 44.0 (4 × C, morpholine), 21.2 (CH₃), 17.8 (2 × CH₃). HRMS (ES⁺, CH₃CN), calcd mass for [M⁺-Cl], C₂₃H₃₀N₇O₂ 436.2445, measured 436.2461.

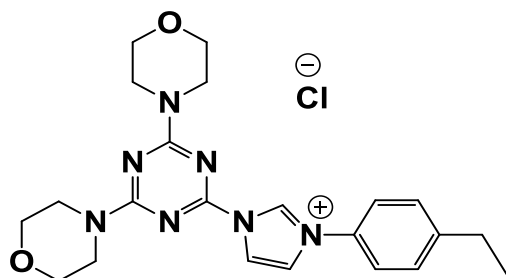
Synthesis of 1-(2,4-dimorpholino-1,3,5-triazine-2-yl)-ethylphenyl-1*H*-imidazol-3-ium chloride, 2.9

Synthesis of 1-(4-ethylphenyl) 1*H*-imidazole



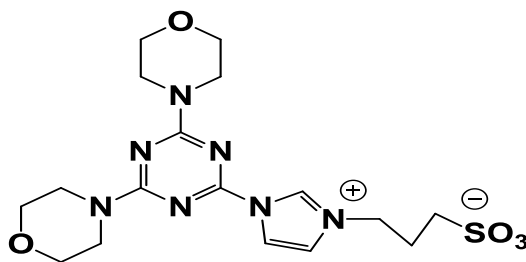
4-ethylaniline (6.05 g, 0.05 mol) in MeOH (25 mL) was stirred with 30 % aqueous glyoxal (8.1 mL, 0.05 mol) for 26 h at room temperature. A bright yellow mixture was formed. NH₄Cl (5.4 g, 0.1 mol) was added followed by 37 % aqueous formaldehyde (8 mL, 0.1 mol). The mixture was diluted with MeOH (200 mL) and the resulting mixture was refluxed for 1 h. H₃PO₄ (7 mL, 85% soln) was added over a period of 10 min. The resulting mixture was then stirred overnight. After removal of the solvent, the dark residue was poured onto ice (200 g), and treated with aqueous 40% KOH solution until pH9. The resulting mixture was extracted with EtOAc (2 × 200 mL) and the organic phases were combined and washed sequentially with H₂O and brine before drying with anhydrous MgSO₄. After filtration, the solvent was removed and residue was purified by distillation on a Kugelrohr under vacuum at 240 °C. (250, MHz, DMSO, ppm) δ_H =: 8.25 (br, 1H), 7.60 (br, 1H), 7.55 (d, *J* = 8.4, 2 H, phenyl), 7.35 (d, *J* = 8.4, 2 H, phenyl), 2.65 (m, 2, CH₂), 1.15 (t, *J* = 8 Hz, 3H, CH₃).

Synthesis of [2.9H]Cl



In high pressure tube, a mixture of the 1-(4-ethyl)-1*H*-Imidazole (0.3 g, 1.75 mmol) and **1a** (0.5 g, 1.75 mmol) was stirred neat at 140 °C for 16 h. After cooling the mixture was dissolved in CH₂Cl₂ (20 mL) and Et₂O (100 mL) added. A white precipitate was formed. Yield = 0.62 (1.35 mmol) (75 %), ¹H NMR (250 MHz, DMS, ppm) δ_H = 10.5 (s, NCHN) 8.75 (br, 1 H, imid), 8.52 (br, 1 H, C₄), 7.87 (d, *J* = 8.4, 2 H, phenyl) 7.52 (d, *J* = 8.4, 2 H, phenyl) 3.96-3.44 (m, 16 H, morpholine), 2.72 (m, 2 H-CH₂), 1.23 (t, *J* = 8 Hz, 3H, CH₃). ¹³C NMR (63, MHz, CDCl₃, ppm) δ_C = 164.4, 158.8 (3 × C, triazine), 147.2, 134.5, 131.9, 129.7, 122.4, 122.2, 119.47 (6 × C, Ar, imid), 28.4 (CH₂), 15.1 (CH₃), MS (ES⁺) for [M-Cl]⁺, C₂₂H₂₈N₇O₂ (422.22) (100%).

Synthesis of 1-(2, 4-dimorpholino-1,3,5-triazine-2-yl)-isopropyl-1*H*-imidazol-3-ium propane-1-sulfonate, [2.10H]



In a round bottomed flask equipped with a reflux condenser **2a** (0.623g, 2 mmol) and 1,3-propanesulfonate (0.24 g, 2.0 mmol) were dissolved in dry acetonitrile (30 mL). The mixture was left under reflux for 72 hours. The filtrate was collected and dried under vacuum before recrystallization from ethanol/diethyl ether to afford the product as a white solid (0.65 g, 1.48 mmol) 75%. ^1H NMR (400 MHz, D_2O , ppm) $\delta_{\text{H}} = \delta 9.5$ (s, 1H, NCHN), 8.16 (d, $J = 2.0$ Hz, 1 H, imid), 7.60 (d, $J = 2.0$ Hz, 1 H, imid), 4.38 (t, $J = 7.1$ Hz, 2 H, $\text{CH}_2\text{-N}$), δ 3.76 (s, 8 H, $\text{CH}_2\text{-N}$, morpholine), 3.66 (m, 8 H, $\text{CH}_2\text{-N}$, morpholine), 2.87 (t, $J = 7.3$ Hz, 2 H, $\text{CH}_2\text{-S}$), 2.29 (d, $J = 6.9$ Hz, 2 H, CH_2) ^{13}C NMR (101 MHz, D_2O , ppm) $\delta_{\text{C}} = 164.75$, 159.39 ($3 \times \text{C}$, triazine), 143.63 (NCHN), 122.8, 119.0 ($3 \times \text{C}$, imidazole), 66.6 ($4 \times \text{C}$, morpholine), 49.06 ($\text{CH}_2\text{-N}$), 47.5 ($4 \times \text{C}$, morpholine), 44.1 ($\text{CH}_2\text{-S}$), 25.3 (CH_2). MS (ES^+) for $[\text{M}+\text{H}]$, $\text{C}_{17}\text{H}_{25}\text{O}_5\text{SN}_7$ 440.17 (100%). Anal. Calcd for $\text{C}_{17}\text{H}_{25}\text{O}_5\text{SN}_7$: C, 46.46; H 5.73; N 22.31 Found: C, 46.31; H, 5.84; N, 22.27.

2.4-References

- (1) D. H. Romero, V. E. T Heredia, O. G. Barradas, Ma. E. M. López and E. S. Pavón, *J. Chem. and Biochemistry*. 2014, **2**, 45.
- (2) R. V. Shingalapur and K. M. Hosamani, R. S. Keri, *Eur. J. Med. Chem.* 2009, **44**, 4244.
- (3) D. Sharam, B. Narasimhan, P. Kumar, R. Narang, E. De Clercq and J. Balzarini, *Eur. J. Med. Chem.* 2009, **44**, 2347.
- (4) H. M. Refaat, *Eur. J. Med. Chem.* 2010, **45**, 2949.
- (5) M. Tonell, M. Simone, B. Tasso, F. Novelli, V. Boido, F. Sparatore, G. Paglietti, S. Pricl, G. Giliberti, S. Blois, C. Ibba, G. Sanna, R. Loddo and P. L Colla, *Bioorg. Med. Chem.* 2010, **18**, 2937.
- (6) K. C. S. Achar, K.M. Hosamani and H. R. Seetharamareddy, *Eur. J. Med. Chem.* 2010, **45**, 2048.
- (7) W. A. Hermann and C. Kocher, *Angew. Chem. Int. Ed. Engl.* 1997, **36**, 2162.
- (8) A. J. Arduengo, R. L. Harlow and M. Kline, *J. Am. Chem. Soc.* 1991, **113**, 362.
- (9) A. Danopoulos, N. Tsoureas, J. Wright and M. Wright, *J. Am. Chem. Soc.* 2004, **23**, 166.
- (10) P. Fourman, P. de Conitet and E. Laviron, *Bull. Chem. Soc. Fr.* 1968, 2438.
- (11) W. A. Herrmann and L. J. Goosen, M. Spiegler, *J. Organomet.Chem.* 1997, **547**, 357.
- (12) F. E. Hahn, B. Heidrich, T. Lugger and T. Pape, *Z. Naturforsch.* 2004, **59b**, 1519.

- (13) F. E. Hahn, B. Heidrich, T. Pape, A. Hepp, M. Martin, E. Sola and L. A. Oro, *Inorg. Chim. Acta.* 2006, **359**, 4840.
- (14) B. C. Etinkaya, S. Demir, I. Özdemir, L. Toupet, D. Semeril, C. Bruneau and P. H. Dixneuf, *Chem. Eur. J.* 2003, **9**, 2323.
- (15) I. Özdemir, S. Demir, B. C. etinkaya, L. Toupet, R. Castarlenas, C. Fischmeister and P. H. Dixneuf. *Eur. J. Inorg. Chem.* 2007, **18**, 2862.
- (16) L. R. Moore, S. M. Cooks, M. S. Anderson, H. Schanz, Scott T. Griffin, R. D. Rogers, M. C. Kirk and K. H. Shaughnessy, *Organometallics* 2006, **25**, 5151.
- (17) D.S. McGuinness, W. Mueller, P. Wasserscheid, K. J. Cavell, Brian W. Skelton, Allan. H. White and U. Englert, *Organometallics* 2002, **21**, 175.
- (18) N. Gonsior, F. Mohr, and H. Ritter, *Beilstein, J. Org. Chem.* 2012, **8**, 390.
- (19) A. J. Arduengo III, US Patent No. 5 077 414 (DuPont), 1991.
- (20) A. A. Gridnev, and I. M. Mihaltseva, *Synth. Commun.* 1994, **24**, 1547.
- (21) E. M. Smolin, L. Rapaport and Lawrence, *s-Triazines and Derivatives. Interscience publishers, Inc.*; New York, 1959, **13**, 644.
- (22) H. Neunhoeffer; P. F. Wiley, Chemistry of 1, 2, 3-Triazines and 1, 2, 4-Triazines. *John Wiley Sons, Inc.*; New York, 1978; **33**, 1335.
- (23) J. M. E. Quirke., *Comprehensive Heterocyclic Chemistry.* Oxford, 1984. **3**, 457.
- (24) L. Pauling and J. H. Sturdivant, *Proc. Natl. Acad. sci.* 1937. **23**; 615.
- (25) Z. Brzozowski and F. Saczewski, *Eur. J. Med. Chem.* 2002, **37**, 709.
- (26) G. Blotny, *Tetrahedron.* 2006, **62**, 9507.
- (27) J. T. Thurston, J. R. Dudley, D. W. Kaiser, I. Hechenbleikner, F. C. Schaefer and D. Hølem-Hansen, *J. Am. Chem. Soc.* 1951, **73**. 2981.

- (28) T. Matsuno, M Kato, Y. Tsuchida, M. Takahshi, S. Yaguchi and S. Terada, *Chem. Pharm. Bull.* 1997, **45**, 291.
- (29) R. Menicagli, S. Samaritani and V. Zucchelli, *Tetrahedron*. 2000, **56**, 9705.
- (30) K. Doktorov, V B. Kurteva, D. Ivanova and I Timtcheva, *ARKIVOC*. 2007, **15**, 232.
- (31) A. Poethig and T. Strassner, *Organometallics* 2011, **30**, 6674.
- (32) A. w. Salman, G. U. Rehman, N. Abdullah, S. Budagumpi, S. Endud, H. H. Abdullah and W.Y. Wong, *Polyhedron*. 2015, **81**, 499.
- (33) V. B. Kurteva and C. A. M. Afonso, *Green.Chem.* 2004, **6**,183.
- (34) A. M. Venkatesan, C. M.dehnhardt, E. D. Santos, Z .Cheng, O. D. Santons, S. Kaloustian ,G. Khafizovas , N. Brooijmans , R. Mallon, I. Hollander and L. Feldberg, *J. Med. Chem.* 2010, **53**, 2636.
- (35) F. Almalioti, J. Macdougall, S. Hughes, M. M. Hasson, R. Jenkins, B. D. Ward, G. J. Tizzard, S. J. Coles, D. W. Williams, S. Bamford, I. A. Fallis and A. Dervisi, *Dalton Trans*, 2013, **42**, 12370.
- (36) N. Gonsior, F. Mohr, and H. Ritter, Beilstein, *J. Org. Chem.* 2012, **8**, 390.
- (37) J. Liu, J. Chen, J. Zhao, Y. Zhao, L. Li and H. Zhang, *Synthesis*. 2003, **17**, 2661.
- (38) A. Alm-assy, C. E. Nagy, A. C. B-enyei and F. Jo-o, *Organometallics* 2010, **29**, 2484.
- (39) M. B. Smith, J. Marches, *Advanced Organic chemistry, John Wiley Sons: New York*. 2001,20.
- (40) G. Occhipinti, V. R. Jensen, K. W. Törnroos, N. Frøystein and H. Bjørsvik, *Tetrahedron* 2009, **65**, 7186

Chapter 3

Synthesis and Characterization of new N-Heterocyclic Carbene

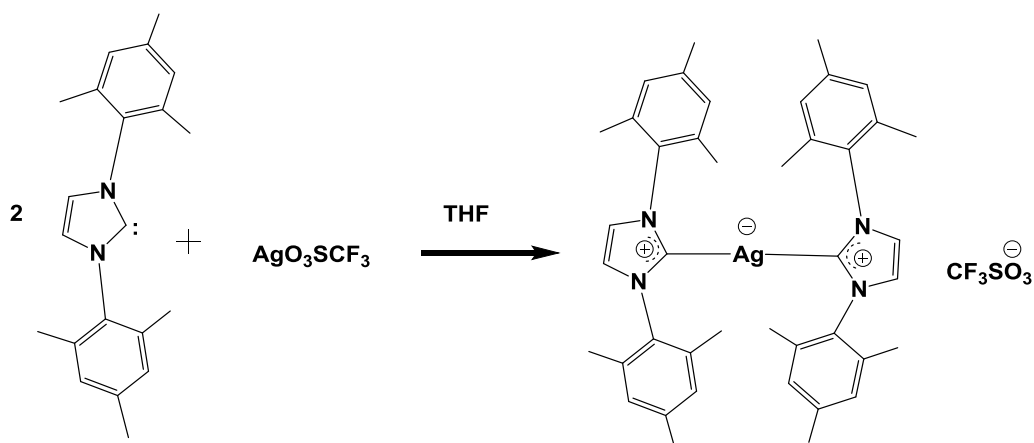
Complexes of Ag (I)

3.1-Introduction

3.1.1-Synthesis of Ag-NHC complexes

The synthesis of silver complexes containing nucleophilic N-heterocyclic carbenes has received increased attention in the recent past. [1] This is due to the ease of synthesis, stability and structural diversity of the complexes, as well as their usefulness in various applications, especially as carbene transfer agents for the preparation of many other transition metal-NHC complexes.

The first silver-NHC complex was synthesised in 1993 by Arduengo and co-workers. The NHC, 1,3-dimesityl imidazol-2-ylidene, was reacted in situ with silver triflate under a dry nitrogen atmosphere at room temperature to produce the homoleptic complex in 80 % yield (Scheme 3- 1).[2]

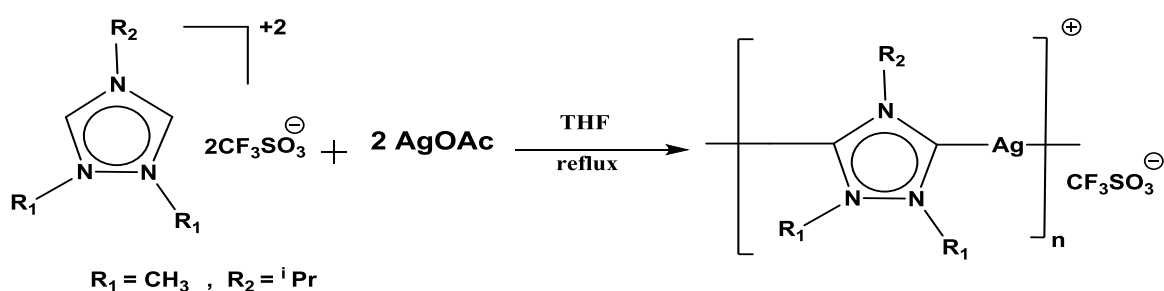


Scheme (3-1) Synthesis of Arduengo silver complex

Limited numbers of silver complexes have been obtained [3-5] by this method because of the difficulty in preparing free carbenes due to their sensitivity to moisture, air and heat, which leads to decomposition. [6, 7, 2]

To overcome the difficulties of obtaining free carbenes, Bertrand and his workers in 1997 described an alternative synthetic method for the preparation of silver-NHC complexes using basic silver sources in the deprotonation of triazolium salts. 2 equivalents of silver (I) acetate was treated with a triazolium salt in refluxing THF for 2 hours to obtain the first polymeric silver(I)-NHC compound. In the solid state structure, the silver atoms are linearly coordinated (Scheme 3-2). [8]

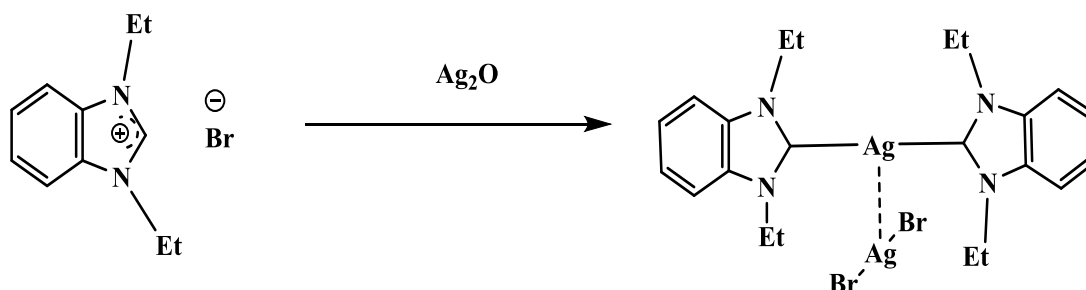
Danopoulos *et al* have prepared silver-NHC complexes using silver (I) carbonate for the deprotonation of imidazolium salts in refluxing dichloromethane over 2 days. The formation of complexes was confirmed by the appearance of a resonance at 165 ppm in the ^{13}C NMR spectra and absence of the 2H-imidazolium protons around 9 ppm in the ^1H NMR spectrum. [9]



Scheme (3-2) Synthesis of silver NHC complexes with silver acetate

Lin *et al* used Ag_2O for the synthesis of silver (I)-NHC complexes, high yields of up to 96 % were obtained at ambient temperature in dichloromethane. X-ray diffraction

showed a neutral complex with an interaction between two silver atoms (Scheme 3-3). [10]



Scheme (3-3) Preparation of Lin's complex

This method has been used in the synthesis of many silver-NHC complexes due to the straightforward procedure, high yield, ambient conditions, stability toward air and the ability to protect acidic hydrogen atoms other than C2-H. On the other hand, Arduengo's method for the deprotonation of imidazolium salts sometimes fails due to the presence of other acidic protons and instability of the free carbenes. [11]

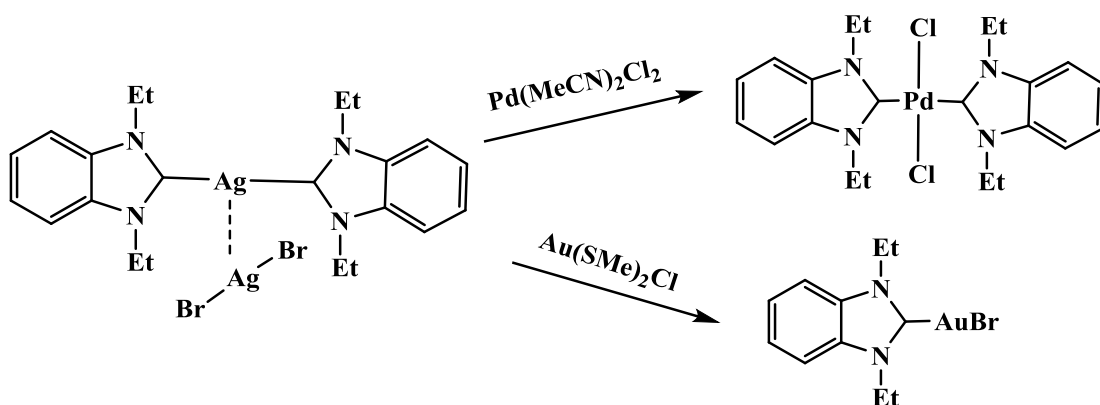
Although there are other ways to prepare silver(I)-NHC complexes, such as the reaction of imidazolium salts with silver salts in the presence of a base [10] or transmetalation [12, 13, 14], the use of Ag_2O proved successful and has been used more often than other routes.

Due to the labile nature and fluxional behaviour [10, 15] of silver (I)-NHCs, these complexes have been used as ligand transfer agents for the synthesis of NHC complexes with Au(I), Pd(II), Cu(II), Ni(II), Pt(II), Ru(II) and Ru(III).[16-21] The transfer method also depends on the nature of the metal and reaction conditions.

The first application of Ag(I)-NHC complexes as a transmetalating agent was by Lin and co-workers in 1998. [7] An Ag(I)-NHC complex was first produced by reacting

Ag_2O with benzimidazolium salts in CH_2Cl_2 at room temperature. Reaction of this Ag-NHC complex with $\text{Pd}(\text{MeCN})_2\text{Cl}_2$ or $\text{Au}(\text{SMe}_2)\text{Cl}$ in dichloromethane at room temperature gives the Pd and Au complexes in high yield (87, 91% respectively) (Scheme 3-4). [10]

Transmetalation can be achieved using isolated silver complexes or alternatively the Ag (NHC) species can be prepared in situ by reacting Ag_2O with an imidazolium salt followed by addition of the desired metal in a one pot procedure. Application of silver-NHC complexes as transfer agents will be covered in chapter 5.



Scheme (3-4) Synthesis of Pd (II), Au (I) complexes by transmetalation

3.1.2-Structural variation of Ag-NHC complexes

Diverse structures for silver-NHC complexes have been observed in the solid state dependant on the steric bulk of the NHC involved, reaction conditions and nature of the counter ion. The structural differences can be due to the ability of silver to coordinate to one or more NHC ligands or anions as well as Ag-Ag interactions. Combinations of these factors lead to multiple different structures in the solid state.

There are two types of silver-NHC complexes observed in the solid state depending on the nature of the counter anions. The first type involves non-coordinated counter anions such as PF_6^- , which lead to coordination of two NHC ligands to silver (Figure 3-1). [22, 23, 18]

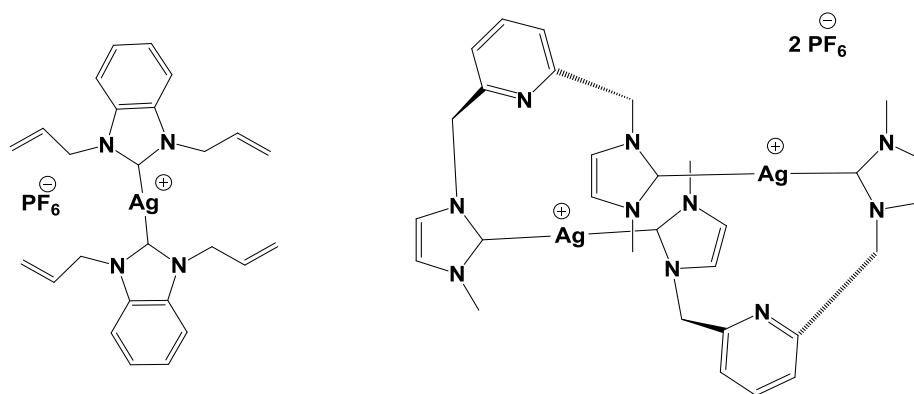


Figure (3-1) Silver complexes with non-coordinating anions

The second type occurs when neutral silver-NHC complexes form, usually with a coordinated halide. Five structural forms have been characterized in the solid state; (**C-Ag-X**) these complexes are neutral and linear structures with the silver ion bound to both a carbene and a halide atom (Figure 3-2). [9, 24]

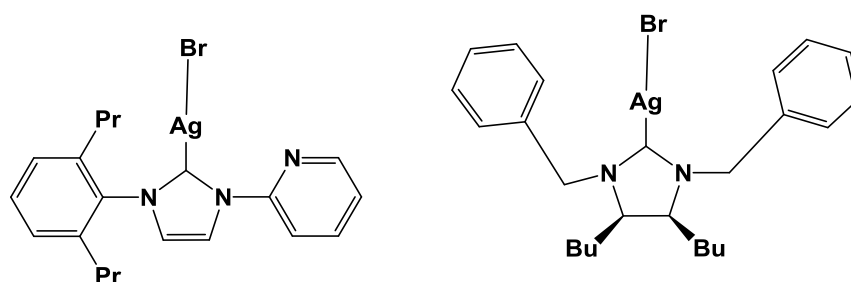


Figure (3-2) Silver complexes with coordinating anion

Other complexes form dimers with bridging halides (**C-Ag-X**)₂. The solid state structure shows formation of a bridged complex with two Ag atoms connected by two halide atoms. Neutral dimeric complexes were obtained (Figure 3-3). [9, 24]

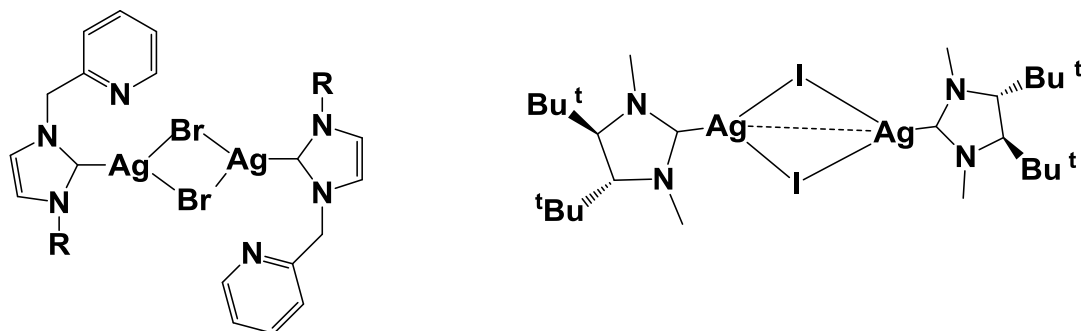


Figure (3-3) Silver complexes bridging $(C-Ag-X)_2$

Some silver complexes have had $C-Ag-X_3$ structures in the solid state. The silver cations are tetracoordinate with silver bound by one N-heterocyclic carbene and three bridging halides (Figure 3-4). [25]

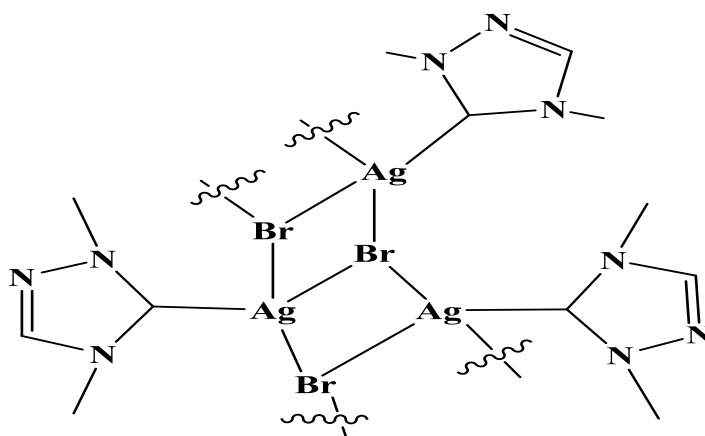


Figure (3-4) Structure of silver complexes $(C-Ag-X_3)$

Other structures have also been observed in the solid state; complexes of the type $[AgX_2]^- (C_2-Ag)$ and $[Ag_2X_4]^{2-} (C_2-Ag-AgX_3)$ have been reported, both types are placed in the same category due to the similarities of their structural features. Both types show interactions between multiple silver atoms. In $[AgX_2]^- (C_2-Ag)$ complexes, the silver ion is connected to two carbene moieties and the charge is balanced by an anionic $[AgX_2]^-$ species. The two silver atoms are connected through silver-silver interaction perpendicular to the silver biscarbene axis. Silver-NHC

complexes of the type $[\text{Ag}_2\text{X}_4]^{-2}$ ($\text{C}_2\text{-Ag-AgX}_3$) are stabilized by silver-silver interactions and are supported by three donor groups (scheme 3-5). [25- 29]

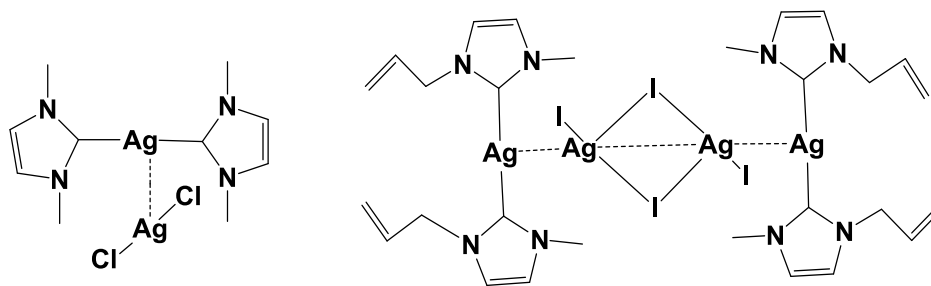
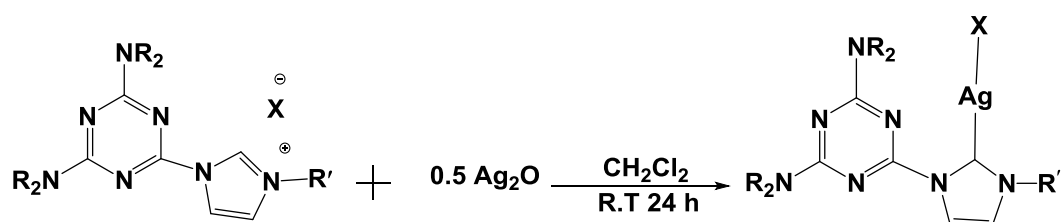


Figure (3-5) Structure of silver complex types $[\text{AgX}_2]^{-}$ ($\text{C}_2\text{-Ag}$) and $[\text{Ag}_2\text{X}_4]^{-2}$ ($\text{C}_2\text{-Ag-AgX}_3$)

3.1.3-Aims

This chapter discusses the synthesis and characterization of Ag(I)-NHC complexes via reaction of Ag_2O with triazine-functionalized imidazolium salts. NMR spectroscopy and mass spectrometry, as well as elemental analyses and X-ray crystallography were used to confirm the formation of complexes.



Ligand	NR_2	R'	X	Comp
[2.3H]Cl		Me	Cl	3.1 AgCl(2.3)
[2.5H]Br		Pr	Br	3.2 AgBr(2.5)
[2.6H]Br		Bu	Br	3.3 AgBr(2.6)
[2.7H]Br		Octyl	Br	3.4 AgBr(2.7)
[2.8H]Cl		mes	Cl	3.5 AgCl(2.8)
[2.9H]Cl		4-EtPh	Cl	3.6 AgCl(2.9)
[2.11H]Br		Pr	Br	3.7 AgBr(2.11)
[2.12H]Br		Bu	Br	3.8 AgBr(2.12)
[2.13H]Br		Me	Cl	3.9 AgCl(2.13)
[2.14H]Br		Bu	Br	3.10 AgBr(2.14)
[2.15H]Br		Bu	Br	3.11 AgBr(2.15)

Scheme (3-5) Synthesis of silver complexes Reagents and conditions: 1 equiv. preligand, 0.5 equiv. Ag_2O , CH_2Cl_2 , room temperature, overnight.

3.2 - Results and discussion

3.2.1-Synthesis of silver complexes (3.1-3.11)

The silver complexes [Ag(NHC)X] (**3.1** - **3.11**) were synthesized via an in situ technique according to previous literature. [10] The reaction was conducted using the imidazolium salts [2.3H]Cl – [2.15H]Br with Ag₂O in a 2:1 molar ratio in dichloromethane. The synthetic procedure is shown in scheme (3-5).

All reactions were conducted at room temperature overnight. Silver complexes were manipulated in the dark to avoid photodecomposition. The reactions were worked up by filtration through a pad of celite, the filtrates were dried under vacuum to obtain white solids. The products were purified by slow diffusion of diethyl ether into concentrated chloroform solutions of the crude products. Suitable crystals were obtained for some silver complexes which were analysed using single crystal X-ray diffraction.

The deprotonation of the imidazolium moieties was evidenced by the disappearance of the peak centred at around 10 ppm in the ¹H NMR spectra. Additionally, peaks attributed to the imidazolium C4 and C5 positions were shifted upfield as a result of coordination to Ag(I).

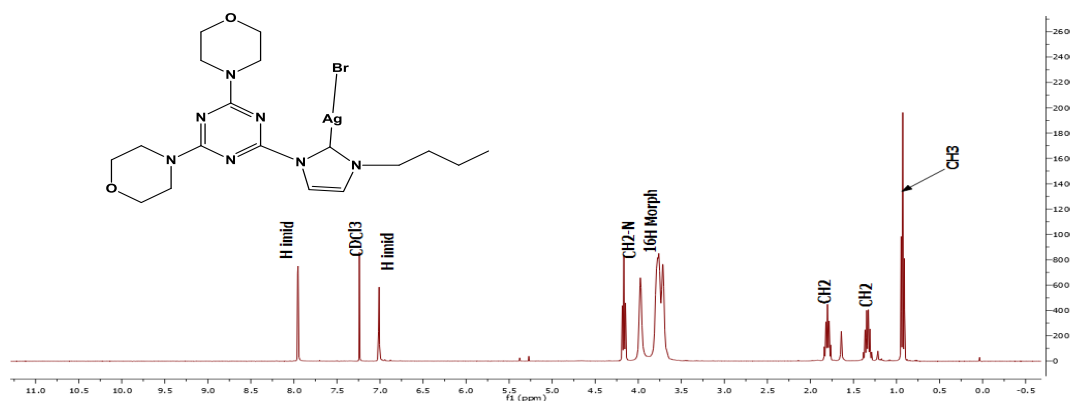


Figure (3-6) ¹H NMR spectrum of [AgBr(**2.6**)] ,**3.3**

Mass spectrometry of these complexes gives $[\text{Ag}(\text{NHC})_2]^+$ as the molecular ion, which is not uncommon for this type of complexes. [30- 33]

All the silver complexes are stable to both air and moisture and are soluble in organic solvents such as acetone, DMF, DMSO, methanol, ethanol and acetonitrile.

The ^1H NMR spectra of the Ag complexes **3.1 - 3.11** confirmed the formation of complexes by comparison with the corresponding spectra of the precursor ligands **[2.3H]Cl**, **[2.5H]Br**, **[2.6H]Br**, **[2.7H]Br**, **[2.8H]Cl**, **[2.9H]Cl**, **[2.11H]Br**, **[2.12H]Br**, **[2.13H]Cl**, **[2.14H]Br** and **[2.15H]Br**.

NMR spectra of the silver complexes show fully resolved signals corresponding to the morpholine, piperidine, diethylamine and dimethylamine resonances, i.e. four morpholine, five piperidine, four diethylamine and two dimethylamine carbon signals are observed. This is consistent with a rotational barrier about the amine–triazine bonds due to the extended π -conjugation network between the amino N-atoms and the triazine ring. [34, 35]

The ^1H NMR spectra of complexes **3.1**, **3.3**, **3.5**, **3.6**, **3.8**, and **3.11** show the absence of a peak around 10 ppm for N-CH-N. In addition to this, the peaks assigned to imidazolium protons for these complexes and complexes **3.2**, **3.4**, **3.7**, **3.9**, and **3.10** were shifted upfield in ranges 8.12 -7.91 and 7.31-6.92 ppm. Comparison with the ligand precursors in the ranges 8.75-7.94 and 8.52 -7.46 suggest a lack of resonance around the imidazoline ring (Figure 3-7).

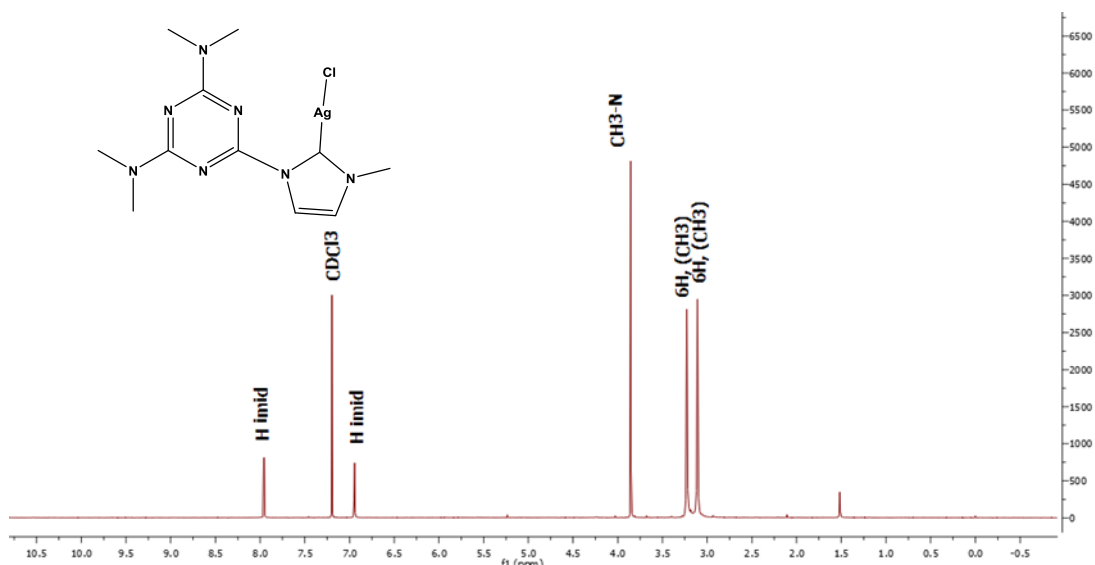


Figure (3- 7) ^1H NMR spectrum of $[\text{AgCl}(\mathbf{2.13})]$, **3.9**

^{13}C NMR spectra for complexes **3.2-3.11** confirmed the formation of complexes by the disappearance of the peak at around 137 ppm which can be attributed to C2. No signal for the $\text{Ag-C}_{\text{carbene}}$ nuclei was observed. Bergbreiter *et al.* have reported ^{13}C NMR measurements of the $\text{Ag}(\text{NHC})\text{Cl}/[\text{Ag}(\text{NHC})_2]\text{Cl}$ equilibria using ^{13}C -enriched NHC ligands. [36] We suggest that our observations herein imply a similar equilibrium taking place for complexes **3.1**. (Figure 3- 8)

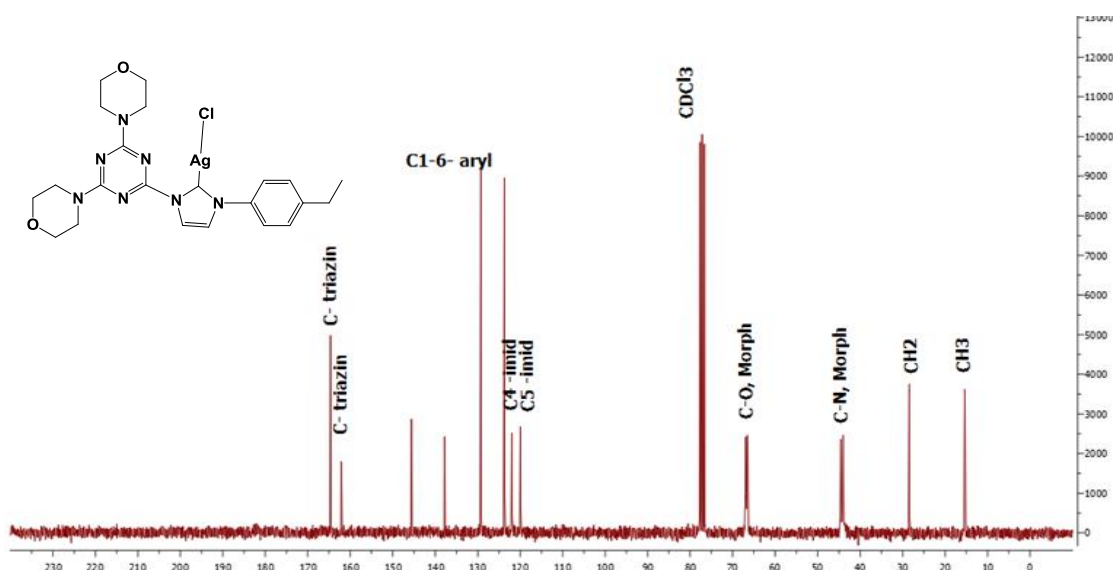


Figure (3-8) ^{13}C NMR spectrum of $[\text{AgCl}(\mathbf{2.9})]$, **3.6**

The ^{13}C NMR spectrum for **3.1** shows a resolved pair of doublets at 182.4 ppm with coupling constants of 236 Hz ($^1J_{\text{AgC}}^{107}$) and 268 Hz ($^1J_{\text{AgC}}^{109}$). The size of $^1J_{\text{AgC}}$ coupling agrees with the formation of the expected silver mono-carbene complex **3.1**. ^1H NMR spectroscopy confirmed the formation of the silver complex by the disappearance of the NCHN peak at 10.2 ppm and an upfield shift of the imidazolium protons to 6.98 and 7.93 ppm compared with 7.92 and 8.47 ppm respectively for the precursor salt [**2.3HCl**]. [37] The ^{13}C NMR spectrums for all silver complexes with morpholine substituents showed 4 peaks for morpholine carbon atoms due to a restricted rotation about the morpholine –triazine bond Fig (3-8).

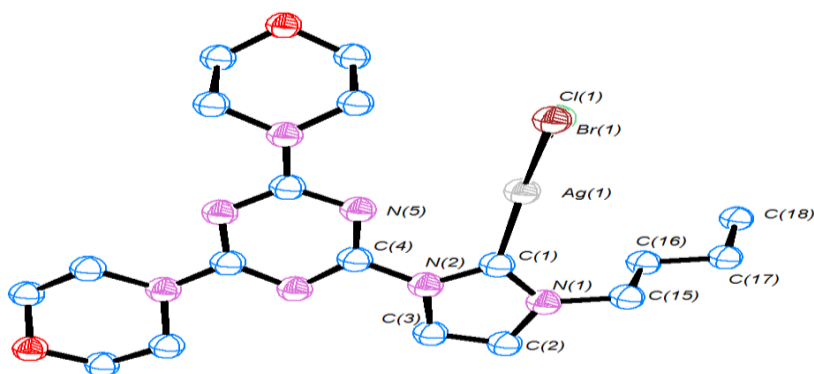
3.2.2 - X-ray Structural Determination

Attempts were made to grow crystals suitable for single crystal X-ray diffraction studies of all compounds. Suitable crystals were obtained by vapour diffusion of diethyl ether into chloroform solutions for all complexes.

Colourless block crystals were obtained for complex **3.3**. X-ray diffraction showed a mixed halide, 50% Cl 50% Br, occupation of the complex due to not completely change of bromide to chloride by adding KCl salt (Figure3-9). The C1-Ag1-X(C11,Br1) bond angles are $160.4(3)^\circ$ and $158.1(2)^\circ$ respectively due to an interaction between the metal atom and the N atom of the triazine moiety where the Ag–N triazine atom distance of 2.939 \AA is less than the sum of the van der Waals radii of the constituent atoms (3.27 \AA for sum Ag, and N). The angle between the triazine unit and the imidazolium is twisted out of the plane by 9.39° , $\text{N}_3\text{–C}_4\text{–N}_2\text{–C}_3$ $9.1(6)^\circ$. Selected bond lengths for **3.3** and angles are shown in Table (3-1).

Table (3-1) Selected bond lengths and angles for **3.3**.

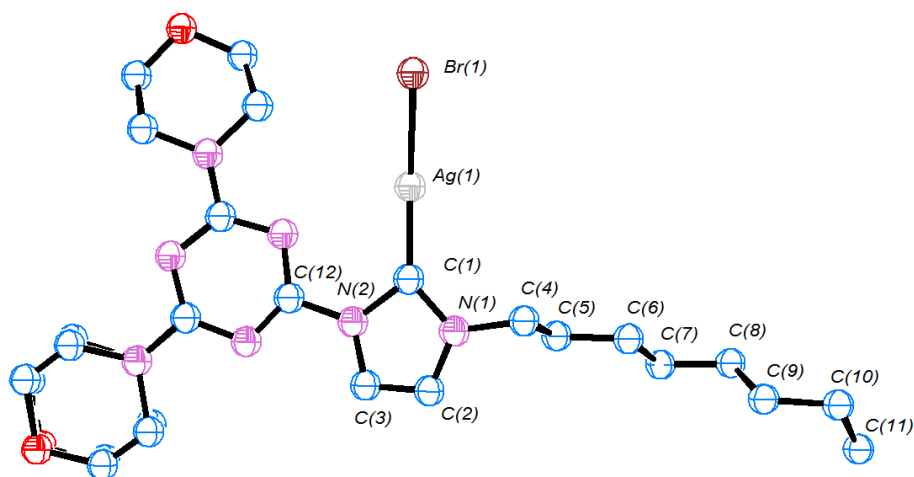
Bond Angles (°)		Bond lengths (Å)	
N1-C1-N2	103.6(3)	C1-N1	1.355(5)
N1-C1-Ag1	130.4(3)	C1-N2	1.3885(5)
N2-C1-Ag1	125.9(3)	C1- Ag1	2.1154(4)
C3-C2-N1	107.1(4)	N1-C15	1.485(5)
C1-Ag1-Br1	158. 1(2)	Cl1-Ag1	2.482(11)
C1-Ag1-Cl1	160.4(3)	Ag1- Br1	2.496(6)

**Figure (3-9)** ORTEP ellipsoid plot at 50% probability of complex **3.3**. H atoms omitted for clarity

Colourless plate crystals of **3.4** were obtained by slow diffusion of diethyl ether into concentrated chloroform solutions. X-ray diffraction showed two (NHC)AgBr in the unit cell, the morpholine moiety displays some disorder on one of the molecules in the unit. Figure (3-10) shows only one of the molecules for clarity. The complex was found to be neutral. The coordination geometry at Ag is slightly distorted from the idealised linear geometry with a C1-Ag1-Br1 angle of 162.9(4) Å due to the same previous reason. The N1-C1-N2 angle of 106.3(10) degrees is somewhat compressed when compared with previous literature as a result of coordination. the Ag–N triazine atom distance of 2.887 Å. [38] Bond lengths and angles are shown in Table (3-2).

Table (3-2) Selected bond lengths and angles for **3.4**.

Bond Angles (°)		Bond lengths (Å)	
N1-C1-N2	106.3(10)	C1-N1	1.452(16)
N1-C1-Ag1	137.9(10)	C1-N2	1.488(17)
N2-C1-Ag1	128.5(9)	C1- Ag1	1.956(14)
C3-C2- N1	107.6(11)	N1-C4	1.472(17)
C1-Ag1-Br1	162.9(4)	Ag1- Br1	2.5211(17)

**Figure (3-10)** ORTEP ellipsoid plot at 50% probability of complex **3.4**.
H atoms omitted for clarity

X-ray crystallographic data of **3.5** shows that the complex displays monodentate coordination of the imidazole ligand. The coordination geometry at Ag is slightly distorted from the idealised linear geometry with a C1-Ag1-C11 angle of $175.42(7)^\circ$ [38]. N1-C1 and N2-C1 bond distances are longer than for the precursor ligand and the corresponding N1-C1-N2 bond angle is reduced, indicative of carbene formation (Figure 3-11). The angle between the triazine unit and the imidazolium is twisted out of the plane by 26.45° . Bond lengths and angles are shown in Table (3-3).

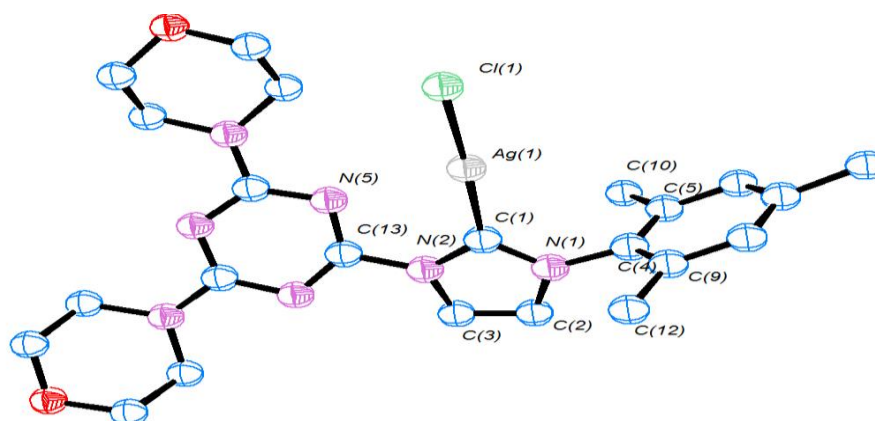


Figure (3-11) ORTEP ellipsoid plot at 50% probability of complex **3.5**.
H atoms omitted for clarity

Table (3-3) Selected bond lengths and angles for **3.5**.

Bond Angles (°)		Bond lengths (Å)	
N1-C1-N2	104.2(2)	C1-N1	1.344(4)
N1-C1-Ag1	128.84(19)	C1-N2	1.366(3)
N2-C1-Ag1	126.71(19)	C3-C2	1.350(4)
C3-C2- N1	106.3(3)	N1-C4	1.449(3)
C2-C3 -N2	106.7(2)	N2-C13	1.430(3)
C1-Ag1-Cl1	175.42(7)	Ag1-Cl1	2.3259(8)

The solid state structure of complex **3.6** shows a neutral molecule, the silver atom is associated with one N-heterocyclic carbene and one chloride atom. The coordination geometry is close to linear with the C1-Ag1-Cl1 bond angle of 174.93(6)°, the bond angle of N1-C1-N2 was reduced to 103.25 (18)° due to coordination to the silver cation. The imidazolidinyl-triazine heterocyclic moiety adopts a strictly planar geometry with the morpholine unit also displaying a planar geometry (sum of angles

= $\sim 348.95^\circ$), indicative of the N lone pairs delocalization into the triazine core. The 4-ethyl phenyl ring is oriented orthogonal to the imidazolyl ring as can be seen in figure 3-12. Bond lengths and angles are shown in Table (3-4).

Table (3-4) Selected bond lengths and angles for **3.6**

Bond Angles ($^\circ$)		Bond lengths (\AA)	
N1-C1-N2	103.25(18)	C1-N1	1.353(3)
N1-C1-Ag1	129.21(16)	C1-N2	1.369(3)
N2-C1-Ag1	127.11(16)	C3-C2	1.338(3)
C3-C2- N1	106.5(2)	N1-C4	1.438(3)
C2-C3 -N2	106.7(2)	Ag1-C1	2.077(2)
C1-Ag1-Cl1	174.93(6)	Ag1-Cl1	2.3289(7)

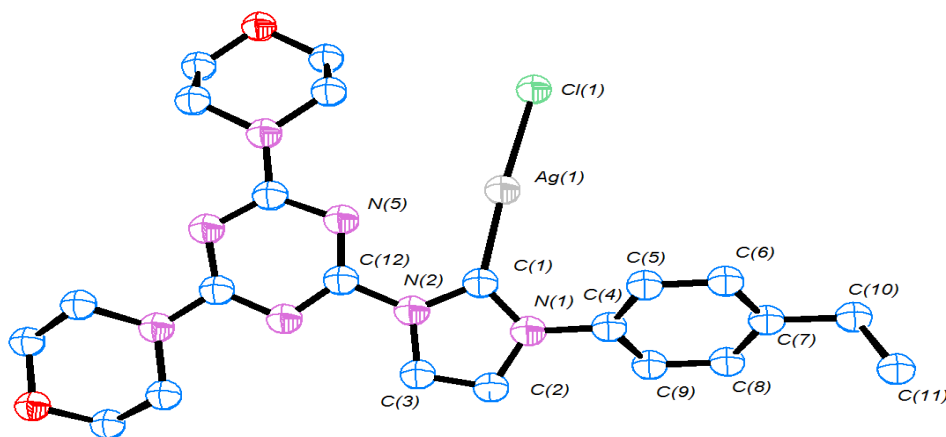


Figure (3-12) ORTEP ellipsoid plot at 50% probability of complex **3.6**.

H atoms omitted for clarity

The structure of complex **3.7** shows a neutral complex with a monodentate carbene.

The C1-Ag1-Br1 bond length of $173.38(7) \text{ \AA}$ is close to the ideal linear structure. [36]

The Bond length for N1-C1 and N2-C1 are $1.345(4) \text{ \AA}$ and $1.369(4) \text{ \AA}$ respectively,

these are elongated due to the formation of a complex (Figure 3-13). Bond lengths and angles are shown in Table (3-5).

Table (3-5) Selected bond lengths and angles for **3.7**

Bond Angles (°)		Bond lengths (Å)	
N1-C1-N2	103.2(3)	C1-N1	1.345(4)
N1-C1-Ag1	128.1(2)	C1-N2	1.378(5)
N2-C1-Ag1	128.2(2)	C3-C2	1.344(4)
C3-C2- N1	107.0(3)	N1-C17	1.479(4)
C2-C3 -N2	105.9(3)	Ag1-C1	2.086(3)
C1-Ag1-Br1	173.38(7)	Ag1-Br1	2.4496(4)

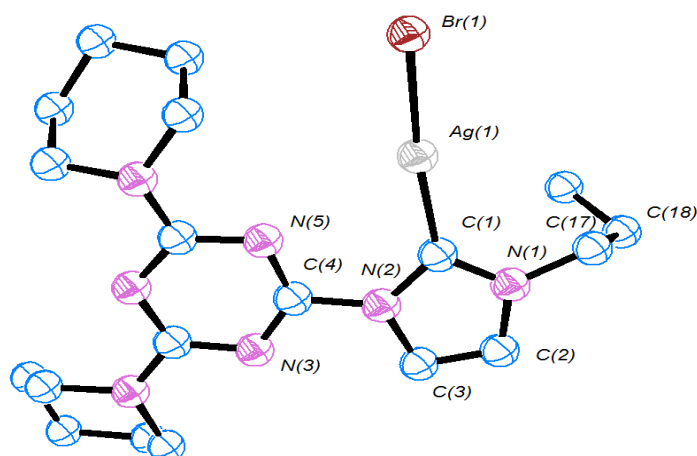


Figure (3-13)) ORTEP ellipsoid plot at 50% probability of complex **3.7**.
H atoms omitted for clarity

The X-ray diffractions for the silver complexes **3.3-3.7** showed that the coordination geometry at Ag is slightly distorted from ideally linear geometry with a $C_{NHC}-Ag-X$ angle less than 180° due to interaction between N atom on triazine and silver atom which the distances less than the sum of the van der Waals radii of the constituent atoms (3.27° for sum of Ag and N). In all the measured complexes, the imidazolidinyl-triazine heterocyclic moiety adopts a strictly planar geometry with the

exo-amine functions also displaying a planar geometry (sum of angles = $\sim 359.5^\circ$), indicative of the N lone pairs' delocalization into the triazine core.

3.3-Experimental

General remarks.

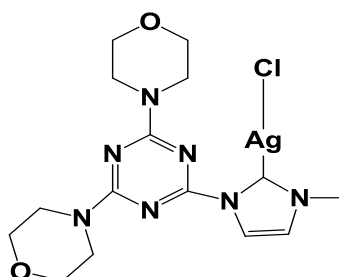
All manipulations were performed using standard glassware under Nitrogen conditions,. Solvents of analytical grade were purified using a Braun-SPS solvent purification system . Ag₂O was used as received, imidazolium salts that have been prepared in this work were used as a precursor ligand. NMR spectra were obtained using Bruker Avance AMX 250, 400, 600 (cryoprobe) and JEOL Eclipse 300 spectrometers. The chemical shifts are given as dimensionless σ values and are frequency referenced relative to TMS. Coupling constants J are given in hertz (Hz) as positive values regardless of their real individual signs. The multiplicities of the signals are indicated as s, d, and m for singlets, doublets, and multiplets, respectively. The abbreviation br is given for broadened signals, mass spectra and high resolution mass spectra were obtained in electrospray (ES) mode unless otherwise reported, on Waters LCT Premier XE instrument. Elemental Analysis worked by Elemental Analysis Service Science Centre London Metropolitan University.

X-Ray crystallographic data for 3.3, 3.4, 3.5, 3.6 and 3.7, were collected using *Rigaku AFC12* goniometer equipped with an enhanced sensitivity (HG) *Saturn724+* detector mounted at the window of an *FR-E+ SuperBright* molybdenum rotating anode generator with HF *Varimax* optics (100 μ m focus). Structural solution and refinement was achieved using *SHELXL-2013* and *SHELXL-2013* software, and absorption correction analysed using *CrystalClear-SM Expert* software

General procedure of synthesis of Ag(I)NHCs

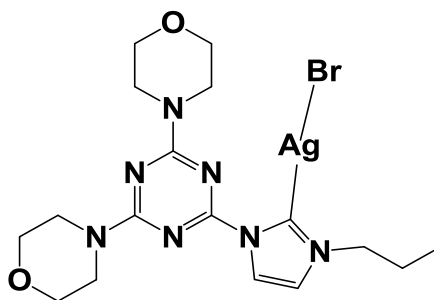
In a round bottomed flask equipped with a magnetic stirrer (1 eq) the imidazolium salt and Ag₂O (0.5 eq) were dissolved in CH₂Cl₂ (50 mL). The reaction was protected from light and stirred under nitrogen overnight at room temperature. The reaction mixture was then filtered through a bed of celite. The solvent was removed and dried in vacuo to obtain a white precipitate. The crude product was recrystallized by diffusion of diethyl ether into dichloromethane or chloroform solutions.

Synthesis of [AgCl(2.3)], 3.1



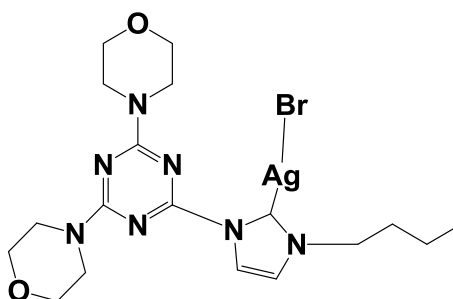
The [AgCl(2.3)], 3.1 complex was prepared using imidazolium salt [2.3H]Cl (0.809 g, 2.2 mmol) and Ag₂O (0.278 g, 1.1 mmol). Yield: 0.997 g (2.1 mmol) 96 %. ¹H NMR (300 MHz, CDCl₃, ppm), δ_H = 3.75–3.99 (br, 16 H, morpholine), 3.95 (s, 3H, CH₃), 6.98 (d, *J* = 1.8, 1 H, imid), 7.93 (d, *J* = 1.8, 1 H, imid). ¹³C NMR (150 MHz, CDCl₃) δ_C = 40.10 (CH₃), 44.0, 44.6, 66.6, 67.0 (8 × C, morpholine), 119.7, 121.9 (2 × C, imid), 162.0, 164.7 (3 × C, triazine), 182.3 (d, ¹J¹⁰⁷AgC = 236, d, ¹J¹⁰⁹AgC = 268, C_{NHC}). HRMS (ES⁺, CH₃CN), calcd mass for [Ag (NHC)₂]⁺, C₃₀H₄₂N₁₄O₄ ¹⁰⁷Ag 769.2564 measured 769.2576. Anal. Calcd for C₁₅H₂₁AgClN₇O₂ (474.29): C, 37.95; H, 4.46; N, 20.65. Found: C, 38.03; H, 4.38; N, 20.58.

Synthesis of [AgBr(2.5)], 3.2



The [AgBr(2.5)], **3.2** complex was prepared using imidazolium salt [2.5H]Br (0.5 g, 1.1 mmol) and Ag₂O (0.13 g, 0.55 mmol). Yield = 0.41g (0.74 mmol) 66 %. ¹H NMR (250 MHz, CDCl₃, ppm) δ_H = 7.97 (br, 1 H, imid), 6.99 (br, 1 H, imid), 4.11 (t, 2 H, *J* = 7, 2 H, propyl), 3.92 (m, 4 H, morpholine), 3.68 (m, 12 H, morpholine), 1.82 (m, 2 H, propyl), 0.87 (t, *J* = 7.3 Hz, 3 H, CH₃, propyl). ¹³C NMR (75 MHz, CDCl₃, ppm) δ_C = 164.7, 162.1 (3 × C, triazine), 120.7, 119.7 (2 × C, imid), 66.9, 66.9 (4 × C, morpholine), 54.9 (CH₂), 44.6, 44.0 (4 × C, morpholine), 24.5 (CH₂), 11.1 (CH₃, propyl). MS (ES⁺) calcd mass for [Ag(NHC)₂]⁺, C₃₄H₅₀N₁₄O₄¹⁰⁷Ag 825.31 (80%).

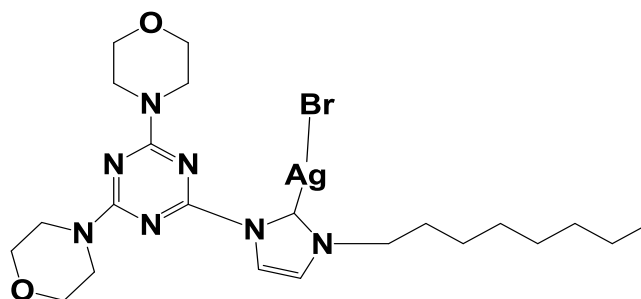
Synthesis of [AgBr(2.6)], **3.3**



The [AgBr(2.6)], **3.3** complex was prepared using imidazolium salt [2.6H]Br (0.5g, 1.1 mmol), Ag₂O (0.127 g, 0.55 mmol) and KCl (0.08 g, 1.1 mmol) Yield = 0.491g, 79 %. ¹H NMR (400 MHz, CDCl₃, ppm) δ_H = 7.92 (d, *J* = 2 Hz, 1 H, imid), 6.96 (d, *J* = 1.9 Hz, 1 H, imid), 4.13 (t, *J* = 7.2 Hz, 2 H, CH₂ - butyl), 3.94 (m, 4 H, morpholine), 3.74 (m, 8 H, morpholine), 3.68 (m, 4 H, morpholine), 1.77 (m, 2 H,

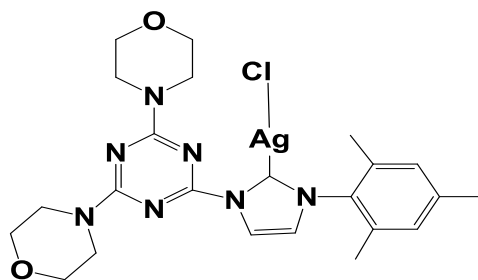
butyl), 1.29 (m, 2 H, butyl), 0.86 (t, $J = 7.2$ Hz, 3 H, CH₃ butyl). ¹³C NMR (75 MHz, DMSO, ppm) $\delta_C = 166.8$ 162.1 (3 \times C, triazine), 123.1 120.1 (2 \times C, imidazole), 66.6, 66.3 (4 \times C, morpholine), 52.6 (NCH₂, butyl), 44.4 (4 \times C, morpholine), 32.9(CH₂, butyl), 19.5 (CH₂,butyl), 14.0 (CH₃, butyl).). HRMS (ES⁺, CH₃CN), calcd mass for [Ag (NHC)₂]⁺, C₃₆H₅₄N₁₄O₄ ¹⁰⁷Ag 853.3503 measured 853.3495. Anal Anal. Calcd for [C₁₈H₂₇AgBrN₇O₂]: C, 38.52; H, 4.85; N, 17.47, found C, 38.72; H, 4.71; N, 17.56

Synthesis of [AgBr(2.7)], 3.4



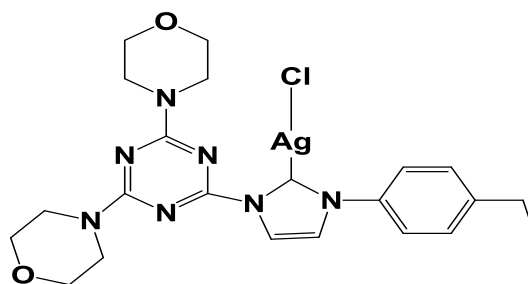
The [AgBr(2.7)], 3.4 complex was prepared using imidazolium salt [2.7H]Br (0.5g, 0.98 mmol) and Ag₂O (0.113 g, 0.49 mmol) Yield = 0.423 g (0.68 mmol) 70 %. ¹H NMR (400 MHz, CDCl₃, ppm) $\delta_H = 7.91$ (d, $J = 1.9$ Hz, 1 H, imid), 6.96 (m, 1 H, imid), 4.14 (t, $J = 7.3$ Hz, 2 H, CH₂-N), 3.94 (m, 4 H, morpholine), 3.74 (m, 4 H, morpholine), 3.68 (m, 8 H, morpholine), 1.78 (m, 2 H, CH₂, octyl), 1.22 (br, 10 H, (CH₂)₅, octyl), 0.79 (t, $J = 6.8$ Hz, 3 H, CH₃, octyl). ¹³C NMR (75 MHz, CDCl₃, ppm) $\delta_C = 164.8$, 162.1 (3 \times C-triazine), 120.7, 119.6 (2 \times C, imid), 66.6, 66.2 (4 \times C, morpholine), 53.5 (NCH₂), 44.7, 44.1 (4 \times C, morpholine), 31.8, 31.24, 29.2, 29.1, 26.5, 22.7, 14.1 (7 \times C, octyl).). HRMS (ES⁺, CH₃CN), calcd mass for [Ag (NHC)₂]⁺, C₄₄H₇₀N₁₄O₄ ¹⁰⁷Ag 965.4755 measured 965.4797.

Synthesis of [AgCl(2.8)], 3.5



The $[\text{AgCl}(\mathbf{2.8})]$, **3.5** complex was prepared similarly from $[\mathbf{2.8H}]\text{Cl}$ (0.3 g, 0.64 mmol) and Ag_2O (0.074 g, 0.32 mmol). Yield = 0.272 g (0.47 mmol) 74 %. ^1H NMR (400 MHz, CDCl_3 , ppm) $\delta_{\text{H}} = 8.12$ (d, $J = 1.2$ Hz, 1 H, imid), 6.92 (d, $J = 2.0$ Hz, 1 H, imid), 6.90 (s, 2 H, mes-CH), 3.97 (m, 4 H, morpholine), 3.70 (m, 12 H, morpholine), 2.27 (s, 3 H, CH_3), 1.95 (s, 6 H, $(\text{CH}_3)_2$). ^{13}C NMR (75 MHz, CDCl_3 , ppm) $\delta_{\text{C}} = 164.7, 162.1$ ($3 \times \text{C}$, triazine), 139.7, 135.9, 134.4, 129.9 ($6 \times \text{C}$, mesityl), 122.8, 119.7 ($2 \times \text{C}$, imid), 67.0, 66.7 ($4 \times \text{C}$, morpholine), 44.6, 44.0 ($4 \times \text{C}$, morpholine), 21.2 (CH_3), 17.9, 17.8 ($2 \times \text{C}$, CH_3). MS (ES^+) calcd mass for $[\text{Ag}(\text{NHC})_2]^+ \text{C}_{46}\text{H}_{58}\text{N}_{14}\text{O}_4$. ^{107}Ag 978.38 (95 %)

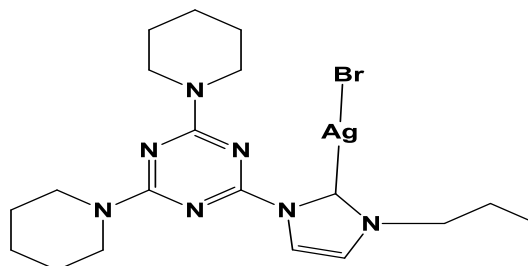
Synthesis of $[\text{AgCl}(\mathbf{2.9})]$, **3.6**



The $[\text{AgCl}(\mathbf{2.9})]$, **3.6** complex was prepared similarly from $[\mathbf{2.9H}]\text{Cl}$ (0.5 g, 1.1 mmol) and Ag_2O (0.1264 g, 0.55 mmol). Yield = 0.462 g (0.82 mmol) 75 %. ^1H NMR (400 MHz, CDCl_3 , ppm) $\delta_{\text{H}} = 8.10$ (d, $J = 1.6$ Hz, 1H, imid), 7.31 (br, 1H, imid), 7.51 (d, $J = 7.2$, 2 H, Ar), 7.32 (d, $J = 8.3$, 2 H, Ar) 3.93-3.64 (m, 16 H, morpholine), 2.69 (m, 2 H, CH_2), 1.23 (t, $J = 7.6$, 3 H, CH_3). ^{13}C NMR (100 MHz, CDCl_3 , ppm) $\delta = 164.6, 162.1$ ($3 \times \text{C}$, triazine), 145.6, 137.7, 129.8, 123.9 ($6 \times \text{C}$,

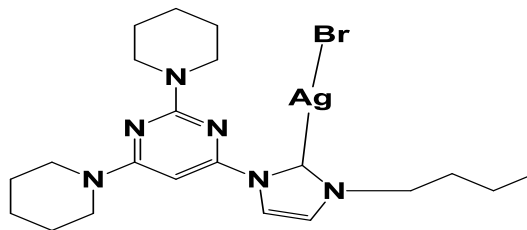
Ar), 121.9, 119.7 (2 × C, imid) 66.9, 66.5, 44.5, 44.1 (8 × C, morpholine), 28.5 (CH₂), 15.8(CH₃). MS (ES⁺) calcd mass for ⁺. [Ag (NHC)₂]⁺, C₄₄H₅₄N₁₄AgO₄¹⁰⁷Ag 949.35 (80%)

Synthesis of [AgBr(2.11)], 3.7



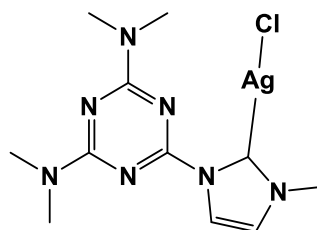
The [AgBr(2.11)], 3.7 complex was prepared similarly from [2.11H]Br (0.3 g, 0.68 mmol) and Ag₂O (0.08 g, 0.34 mmol). Yield = 0.287 g (0.53 mmol) 77 %. ¹H NMR (400 MHz, CDCl₃, ppm) δ_H = 7.94 (d, *J* = 1.6 Hz, 1H, imid), 6.93 (br, 1 H, imid), 4.10 (t, *J* = 7.2 Hz, 2 H, N-CH₂), 3.80 (m, 4 H, CH₂), 3.71 (m, 4 H, 2 × CH₂) 1.82 (m, 2 H, CH₂, propyl), 1.59 (m, 4H, (2 × CH₂), 1.53 (m, 8 H, 4 × CH₂), 0.90 (t, *J* = 7.0 Hz, 3 H, CH₃-propyl). ¹³C NMR (75 MHz, CDCl₃, ppm) δ_C = 164.4, 162.7 (3 × C, triazine), 120.1, 119.6 (2 × C, imid), 54.8 (NCH₂, propyl), 45.3, 44.1 (CH₂), 25.9 (CH₂), 25.8, 24.7 (CH₂), 23.7 (propyl), 11.0 (propyl). MS (ES⁺) calcd mass for [Ag(NHC)₂]⁺, C₃₈H₅₈AgN₁₄¹⁰⁷Ag 817.30 (30 %)

Synthesis of [Ag(2.12) Br], 3.8

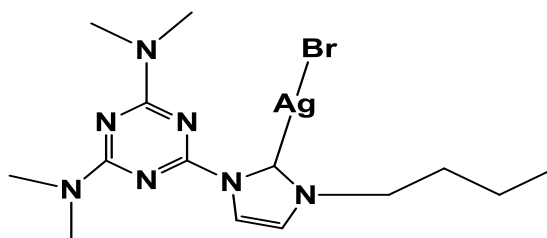


The [Ag Br (2.12)], **3.8** complex was prepared similarly from [2.12H]Br (0.5 g, 1.1mmol) and Ag₂O (0.129 g, 0.55 mmol) Yield = 0.377 g (0.67 mmol) 61 %. ¹H NMR (400 MHz, CDCl₃, ppm) δ_H = 7.94 (d, *J* = 1.6 Hz, 1 H, imid), 6.93 (br, 1 H, imid), 4.10 (t, *J* = 7.6 Hz, 2 H, CH₂-N), 3.85 (m, 4 H), 3.71 (m, 4 H), 1.82 (m, 2 H, butyl), 1.59 (m, 4 H, 2 × CH₂), 1.53 (m, 12 H), 0.93 (m, 3 H, CH₃ butyl). ¹³C NMR (75 MHz, CDCl₃, ppm) δ_C = 164.4, 161.7 (3 × C, triazine), 120.8, 119.6 (2 × C, imid), 54.8 (CH₂-N, butyl), 45.4, 44.8 (CH₂), 32.9 (butyl), 26.0 (CH₂), 24.7, 24.5 (CH₂), 21.6 (butyl), 11.0 (butyl).). HRMS (ES⁺, CH₃CN), calcd mass for [Ag (NHC)₂]⁺, C₄₄H₅₄N₁₄O₄ ¹⁰⁷Ag 949.3503 measured 949.3516.

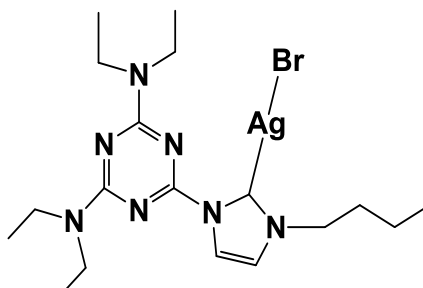
Synthesis of [Ag Cl(2.13)], **3.9**



The [Ag Cl(2.13)], **3.9** complex was prepared similarly from [2.13H]Cl (0.3 g, 1.06 mmol) and Ag₂O (0.122 g, 0.50 mmol). Yield = 0.30 g (0.73 mmol) 69 %. ¹H NMR (400 MHz, CDCl₃, ppm) δ_H = 7.96 (d, *J* = 2.0 Hz, 1 H imid), 6.94 (d, *J* = 1.9 1 H, imid), 4.85 (s, 3H, N-CH₃), 3.22 (s, 6 H, 2 × CH₃), 3.10 (s, 6 H, 2 × CH₃). ¹³C NMR (100 MHz, CDCl₃, ppm) δ_C = 163 159.3 (3 × C, triazine), 119.4, 117.8 (2 × C, imid), 37.7 (CH₃-N), 34.9, 34.6 (CH₃). MS (ES⁺) calcd mass for [Ag (NHC)₂]⁺, C₂₂H₃₄AgN₁₄ ¹⁰⁷Ag 601.18 (80 %)

Synthesis of [Ag Br(2.14)], 3.10

The [Ag Br(2.14)], **3.8** complex was prepared similarly from [2.14H]Br.10 (0.3 g, 0.81 mmol) and Ag₂O (0.094 g, 0.41 mmol). Yield = 0.294 g (0.61 mmol) 76 %. ¹H NMR (400 MHz, CDCl₃, ppm) δ_H = 7.95 (br, 1H, imid), 6.98 (br, 1H, imid), 4.14(t, J = 7.2, 2H, N-CH₂), 3.21-3.09 (br, 12 H, 2 × CH₃), 1.79 (m, 2 H, CH₂), 1.3 (m, 2 H, CH₂), 0.89 (t, J = 8HZ, 3 H, CH₃), ¹³C NMR (100 MHz, CDCl₃,ppm) δ_C = 164.9 161.3 (3 × C, triazine), 120.7 119.6 (2 × C, imid), 52.9 (CH₃-N), 37.1, 36.5 (CH₃)₄, 33.1 (CH₂), 119.6 (CH₂), 13.64 (CH₃).). HRMS (ES⁺, CH₃CN), calcd mass for [Ag (NHC)₂]⁺, C₂₈H₄₆N₁₄ ¹⁰⁷Ag 685.3081 measured 685.3067.

Synthesis of [AgBr(2.15)] 3.11

The [Ag Br(2.15)], **3.11** complex was prepared similarly from [2.15H]Br (0.5 g, 1.1 mmol) and Ag₂O (0.25 g, 0.55 mmol). Yield = 0.40 g (0.76 mmol) 64 %. ¹H NMR (400 MHz, CDCl₃, ppm) δ_H = 7.98 (d, J = 1.6 Hz, 1 H, imid), 6.96 (br, 1 H, imid), 4.19 (t, J = 7.2 Hz, 2 H, N-CH₂), 3.67 (m, 4 H, 2 × CH₂), 3.53 (m, 4 H, 2 × CH₂), 1.75 (m, 2 H, butyl), 1.30 (m, 2 H, butyl), 1.12 (m, 12 H), 0.87 (t, 3H, J = 7.2 Hz, CH₃-but). ¹³C NMR (75 MHz, CDCl₃, ppm) δ_C = 164.1, 161.5 (3 × C, triazine), 120.3

Chapter3: Synthesis and characterization of new N-heterocyclic carbene complexes of Ag (I)

119.6 (2×C, imid), 53.0 (CH₂-N), 42.2, 42.0 (CH₂), 33.2 (but), 19.7 (butyl), 14.0 (butyl), 13.9 (butyl) ppm. MS (ES⁺) calcd mass for [Ag(NHC)₂]⁺, C₃₆H₆₂AgN₁₄¹⁰⁷Ag 797.42 (80 %).

3.4-References

- (1) I. J. Line and C. S. Vasam, *Coord. Chem. Rev.* 2007, **251**, 642.
- (2) A. J. Arduengo, III, H.V. RasikaDias, J. C. Calabrese and F. Davidson. *Organometallics* 1993, **12**, 3405.
- (3) A. Caballero, E. Es-Barra, F. Galo, S. Merino and J. Tejada, *J. Organometallic. Chem.* 2001, **617-618**, 395.
- (4) M. A. Fox, M. F. Mahon, N. J. Patmore and A. S Weller, *Inorg chem.* 2002 **141**, 4567.
- (5) M. C. Chung. *Bull. Korean, Chem Soc* .2002, **23**, 921.
- (6) J. C. Garrison and W. J. Youngs, *Chem. Rev.* 2005, **105**, 3978.
- (7) I. J. line and C. S. Vasam, *Comments on Inorg Chem.* 2004, **25**, 75.
- (8) O. Guerret, S. Sole, H. Gomitzka, M. Teichert, Georges and G. Bertrand, *J. Am. Chem. Soc.* 1997, **119**, 6668.
- (9) A. A. D. Tulloch, A. A. Danopoulos, S. Winston, S. Kleinhenz and G. Easthams, *J. Chem. Soc, Dalton Trans.* 2000, **24**, 4499
- (10) H. M. J. Wang and I. J. B. Lin, *Organometallics* 1998, **17**, 972.
- (11) M. C. Liao, X. H. Duan and Y. M. Liang, *Tetrahedron Lett.* 2005, **46**, 3469.
- (12) A. O. Larsen, W. Leu, C. N. Oberhuber, J. E. Campbell and A. H. Hoveyda, *J. Am chem. Soc.* 2004, **126**, 11130.
- (13) L. G. Bonnet, R. E. Douthwaite, R. Hadgson, J. Houghton, B. M. Kariuki and S. Simonovic, *Dalton Transaction* 2004, **21**, 3528.
- (14) M. Mayr and M.R. Buchmeiser. *Macromol, Rapid Commun.* 2004, **25**,231.
- (15) Y.A. Wanniarachchi, M.A. Khan and L.M. Slaughter,. *Organometallics* 2004, **23**, 5881.

- (16) P. de Fremont, N.M. Scott, E.D. Stevens and S.P. Nolan, *Organometallics* 2005, **24**, 2411.
- (17) M. V. Baker, P. J. Barnard, S.K. Brayshaw, J.L. Hickey, B.W. Skelton and A. H. White, *Dalton Trans.* 2005, **1**, 37.
- (18) D. S. McGuinness and K. J. Cavell, *Organometallics* 2000, **19**, 741.
- (19) M. Froseth, A. Dhindsa, H. Roise and M. Tilset, *Dalton Trans.* 2003, **23**, 4516.
- (20) V. Cesar, S. Bellemin-Laponnaz and L.H. Gade, *Organometallics* 2002, **21**, 5204.
- (21) R. Wang, B. Twamley and J. M. Shreeve, *Organometallics* 2006, **71**, 426.
- (22) M. Z. Ghdayeb, R A. Haque and S. Budagumpi, *Organometallics* 2014, **757**, 42.
- (23) J. C. Garrison, R. S. Simon, C. A. Tessier, and W.J. Young, *Organometallics* 2003, **673**, 1.
- (24) J. P. Ytkowicz, S. Roland and P. Mangeney, *Organometallics* 2001, **631**, 157.
- (25) K. M. Lee, H. M. Wang, I. J. B. Lin, *J.Chem. Soc. Dalton Trans*, 2002, **14**, 2852.
- (26) C. K. Lee, K. M. Lee and I. J.B. Lin, *Organometallics*. 2002, **21**, 10
- (27) A. R. Chianese, X. Li, M.C. Janzen, J. W. Faller and R. H. Crabtree, *Organometallics* 2003, **22**, 1663.
- (28) D. C. Li and D. J. Lue, *J. Chem. Crystallorg.* 2003, **33**, 989.
- (29) S. K. Schneider, W. A. Herrmann and E. Hertweck. *Z. Anorg. Allg. Chem.* 2003, **629**, 2363.
- (30) B. Bildstein, M. Malaun, H. Kopacka, K. Wurst, M. Mitter.; K.-H. Ongania, G. Opromolla and P. Zanello, *Organometallics* 1999, **18**, 4325.

- (31) J. C. Garrison, R. S. Simons, J. M. Talley, C. Wesdemiotis, C.A. Tessier and W. J. Youngs, *Organometallics* 2001, **20**, 1276.
- (32) P. L. Arnold, A. C. Scarisbrick, A. J. Blake and C. Wilson. *Chem. Commun.* 2002, 2340.
- (33) L. G. Bonnet, R. E. Douthwaite, R. Hodgson, *Organometallics* 2003, **22**, 4384.
- (34) P. Comba, Y. D. Lampeka, A. Y. Nazarenko, A. I. Prikhod'ko and H. Pritzkow, *Eur J. Inorg Chem.* 2002, **6**, 1464.
- (35) P. Gamez, P. de Hoog, M. Lutz, A. L. Spek and J. Reedijk, *Inorg. Chim. Acta*, 2003, **351**, 319
- (36) H. L. Su, L. M. Pérez, S. J. Lee, J. H. Reibenspies, H. S. Bazzi and D. E. Bergbreiter, *Organometallics* 2012, **31**, 4063
- (37) F. Almalioti, J. Macdougall, S. Hughes, M. M. Hasson, R. Jenkins, B. D. Ward, G. J. Tizzard, S. J. Coles, D. W. Williams, S. Bamford, I. A. Fallis and A. Dervisi, *Dalton Trans.* 2013, **42**, 12370.
- (38) H. Clavier, L. Coutable, J. C. Guillemin and M. MAudit, *Tetrahedron Asymmetry.* 2005, **16**, 92.

Chapter 4

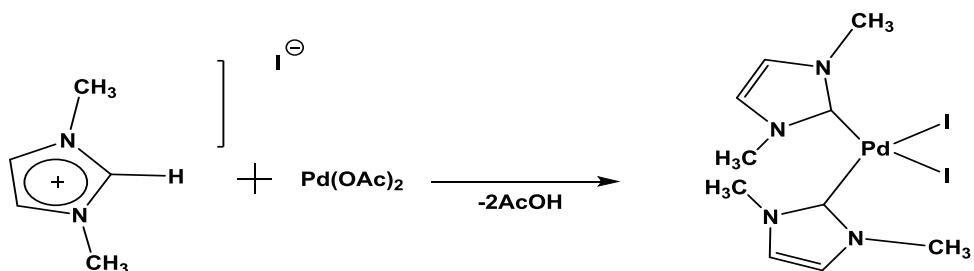
Synthesis and characterization of new Pd(II)-NHC complexes and their application in catalysis

4.1-Introduction

Palladium complexes have found particular importance as catalysts in coupling reactions to form C-C and C-N bonds. NHC ligands have been used as an alternative to phosphines for the synthesis of palladium complexes due to their properties such as thermal stability, nucleophilic behaviour, low cost and toxicity as well as their ease of preparation from azolium salts with no requirement for use of an excess of ligand to synthesise the complexes. [1]

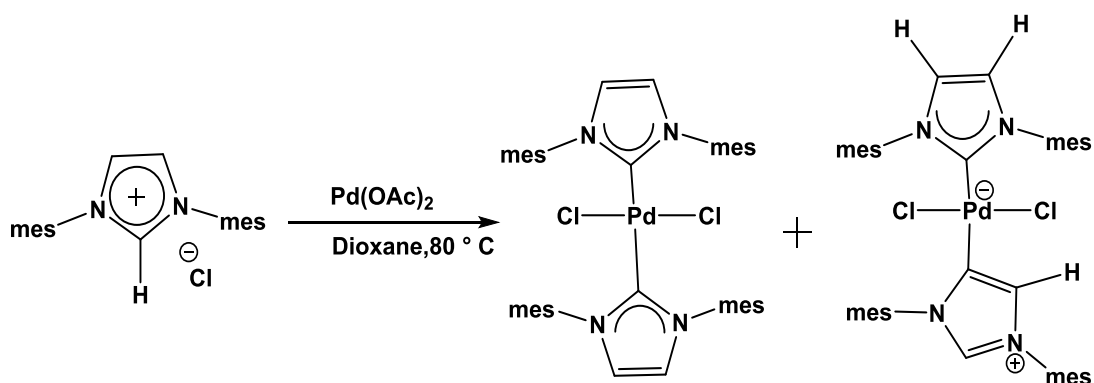
4.1.1-Synthesis of Pd-NHC complexes

The first Pd-NHC complexes were prepared by Herrmann and co-workers in 1995.[2] The complexes were obtained by reacting 1,3-dimethylimidazolium iodide or 3,3'-dimethyl-1,1'-methylene diimidazolium iodide with $[\text{Pd}(\text{OAc})_2]$. Thermally stable complexes were obtained in 40 and 70% yield respectively. Palladium acetate was used as a source of both Pd and base for the deprotonation of the azolium salts. ^{13}C NMR spectra proved the formation of complexes where carbene peaks at 168.2 and 185.5 ppm were observed respectively. In addition X-ray diffraction confirmed a distorted square planar structure for the complexes. Many Pd-NHC complexes have been synthesized since using this method (Scheme 4-1). [3, 4, 5, 6, 7]



Scheme (4-1) First examples of Pd-NHC complexes

In this method high temperature and reduced pressure is necessary for the removal of the acetic acid formed during the reaction. If the acetic acid is not removed completely, the C₄ position may be deprotonated, forming an abnormal carbene (Scheme 4-2). [8]



Scheme (4-2) Abnormal binding to Pd center.

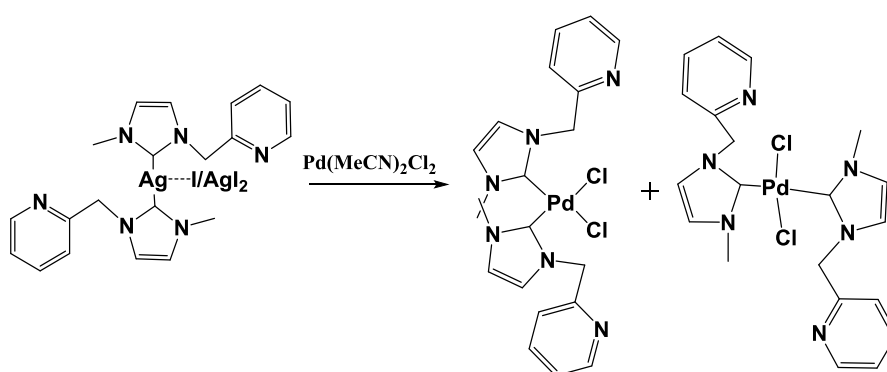
The second method for the preparation of Pd-NHC complexes involves directly reacting a PdX₂ with isolated or in situ generated NHC carbene. Free carbenes are formed using strong bases such as potassium hexamethyldisilazide or potassium tertiary butoxide (KOtBu). [9, 10, 11] Weak bases such as cesium carbonate (Cs₂CO₃), [8] sodium acetate (NaOAc) or K₂CO₃ have also been used for the deprotonation of imidazolium salts. [12] Many of the palladium complexes bearing mono- and biscarbene ligand sets were synthesized by using this method. [13]

Also, transmetallation has been used to transfer NHC ligands from silver complexes to form Pd-NHC complexes. This method can be used to avoid the harsh conditions employed in other procedures mentioned above which may result in the degradation of many ligands.

Palladium reagents such as Pd(cod)Cl₂, Pd(cod)Br₂, Pd(cod)(CH₃)Br, Pd(cod)(CH₃)Cl, [Pd(allyl)Cl]₂, PdCl₂(CH₃CN)₂ and PdCl₂(PhCN)₂ were used to obtain the Pd-NHC complexes.

These complexes can be prepared either by reacting the Pd source with an isolated Ag(NHC) or by addition of the Pd reagent to a Ag₂O/NHC.HX mixture.

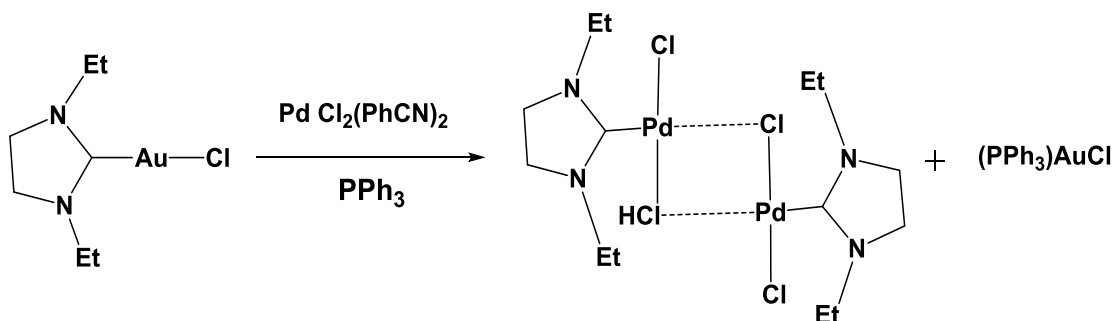
Biscarbene palladium complexes were obtained by reaction of [Ag(3-methyl-1-picolyl imidazolin-2-ylidene)₂I with Pd(MeCN)₂Cl₂ in dichloromethane in a 1:1 molar ratio. The reaction was conducted at room temperature for 1 hour to produce a white powder in 58% yield. Two isomers were found by ¹H NMR spectroscopy in a 1:2 ratio. The complex was used in a Heck reaction where excellent conversions were obtained (98%) (Scheme 4-3). [14]



Scheme (4-3) Synthesis of Pd (3-methyl-1-picolylimidazolin-2-ylidene)₂Cl₂ via a transmetallation method

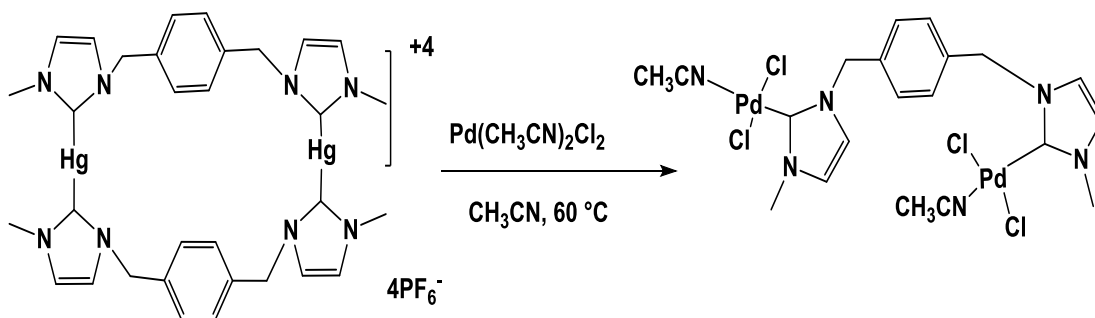
The disadvantages of this method are the high cost of silver and that the reaction must be conducted in the dark.

This method is not limited to the use of silver complexes as transfer agents for the preparation of palladium-NHC complexes. Au-NHC complexes were used as transfer agents to prepare Pd-NHC complexes by reaction of Au(NHC)Cl with PdCl₂(PhCN)₂ to produce the corresponding Pd-NHC species. The reaction was promoted by the addition of triphenylphosphine (Scheme 4-4). [15]



Scheme (4-4) Synthesis of Pd-NHC complex via Gold –NHC complex

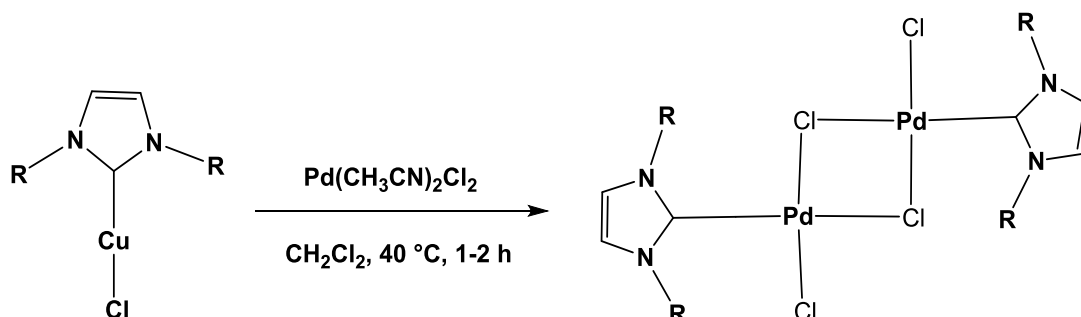
Pd-NHC complexes have also been obtained by using Hg-NHC complexes as transfer agents. The reaction was conducted by reaction of the mercury complex with 2 equivalents of Pd(CH₃CN)₂Cl₂ in acetonitrile. A yellow powder was obtained after evaporation of the solvent in 91% yield (Scheme 4-5). [16]



Scheme (4-5) Synthesis of Pd-NHC via mercury-NHC complex

Cu-NHC complexes were also used for the synthesis of Pd-NHC complexes by Cazin *et al* in 2009. Cu-NHC complexes were obtained by reacting of Cu₂O with

imidazolium salts before treatment with $\text{Pd}(\text{PhCN})_2\text{Cl}_2$ in dichloromethane to produce a Chloro-bridged dimeric species, $[\text{Pd}(\mu\text{-Cl})\text{Cl}(\text{NHC})]_2\text{NaCl}$. The low cost of copper made it an attractive alternative to silver and gold as a carbene transfer agent (Scheme 4-6). [17]



Scheme (4-6) Synthesis of Pd –NHC complex via Cu-NHC complex

Pd–PEPPSI complexes (pyridine, enhanced, pre catalyst, preparation, stabilisation and initiation) are another type of palladium N-heterocyclic carbene complex which contain mono NHC ligands. These complexes were prepared to avoid generating free carbene ligands. These complexes were obtained by reaction of the azolium salts with palladium halides in the presence of a weak base such as K_2CO_3 in pyridine at $80\text{ }^\circ\text{C}$ to produce complexes stable towards both air and moisture. The purpose of the pyridine is to increase the activity of the catalyst. Pyridine is considered a throw away ligand, thus giving way to an incoming substrate. Pd–PEPPSI complexes have proven to be highly active catalysts in various reactions such as Kumada–Tamao–Corriu (KTC), Negishi, and Suzuki–Miyaura cross-coupling reactions. [18, 19, 20]

Organ *et al* prepared series of Pd–PEPPSI complexes in 2010. The reactions were conducted by reacting various saturated and unsaturated imidazolium salts with PdCl_2 in the presence of K_2CO_3 as a base in pyridine at $80\text{ }^\circ\text{C}$ for 24 h. The complexes were

tested as catalysts in Kumada–Tamao–Corriu (KTC), Negishi, and Suzuki–Miyaura cross-coupling reactions (Figure 4-1). [21]

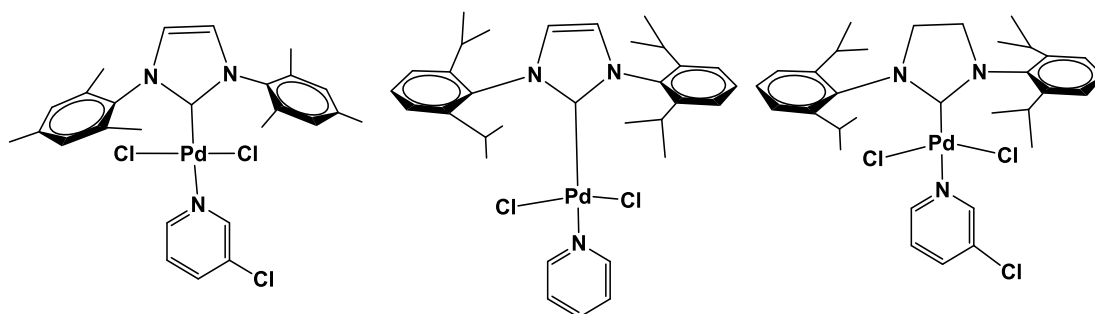


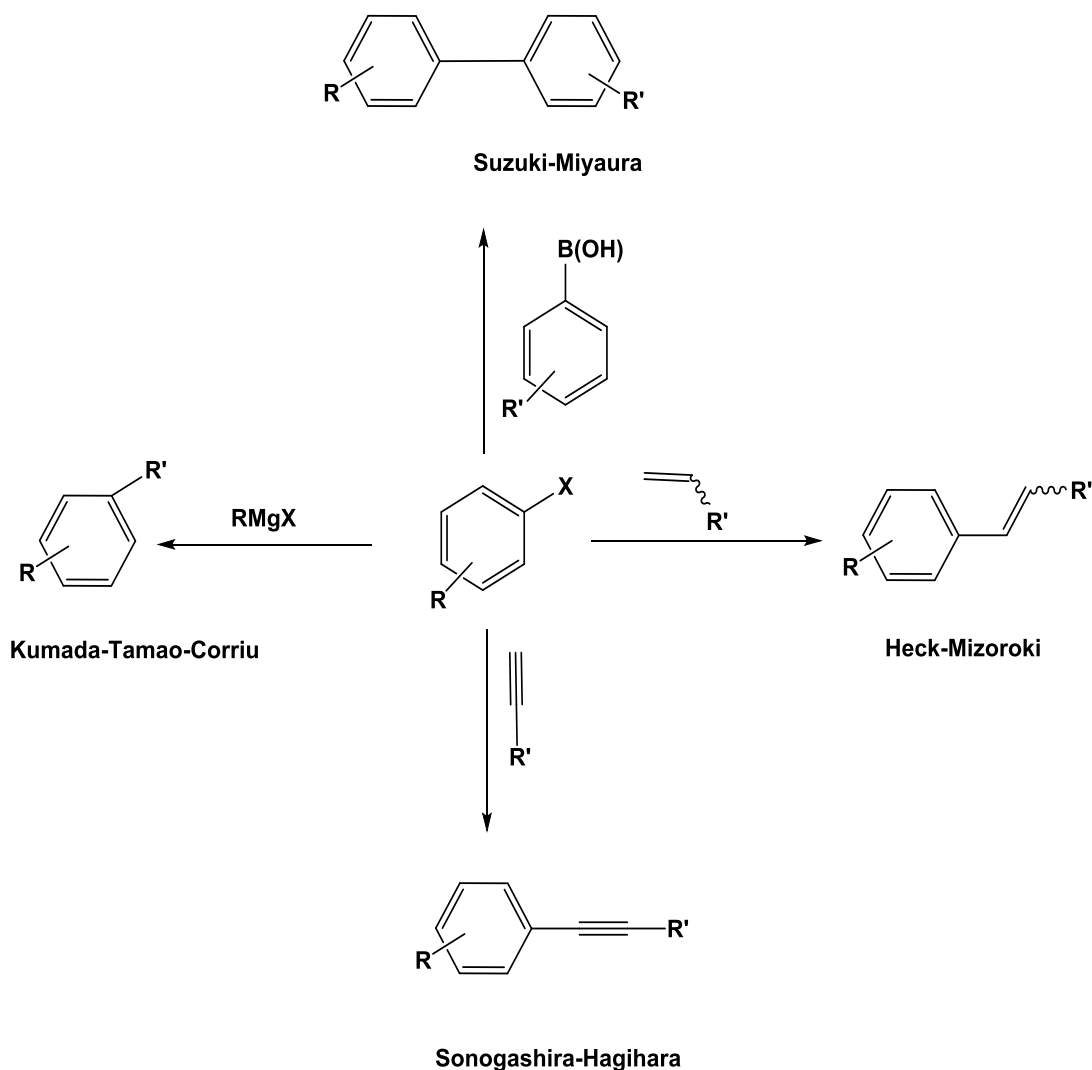
Figure (4-1) Pd–PEPPSI complexes

4.1.2- NHC–Pd cross-coupling catalysis

Cross-coupling reactions have been received much attention because of their role in the synthesis of many drugs, natural products, industrial starting materials, and optical devices. [22] The cross-coupling reaction provides a method for the formation of new C–C bonds with inorganic substrates and Pd catalysts. Pd-NHC complexes have been become alternatives to the Pd–phosphine complexes in synthetic chemistry due to strong sigma donation of NHC ligand and strong Pd- carbene bond prevents the complexes from decomposition.

Cross-coupling reactions are conducted between halogenated ($X = \text{Cl}, \text{Br}, \text{I}$) substrates and organo metal substrate to form C-C and C-Hetero atom bonds. The reactivity of the halogenated substrates is decreased in the order of $\text{R-Cl} > \text{R-Br} > \text{R-I}$ due to the value of the R–X bond dissociation enthalpies where the R-Cl bond is found to be $95.5 \text{ kcal mol}^{-1}$, while R-Br is only $80.4 \text{ kcal mol}^{-1}$ and the R-I bond is measured at $65.0 \text{ kcal mol}^{-1}$. [23]

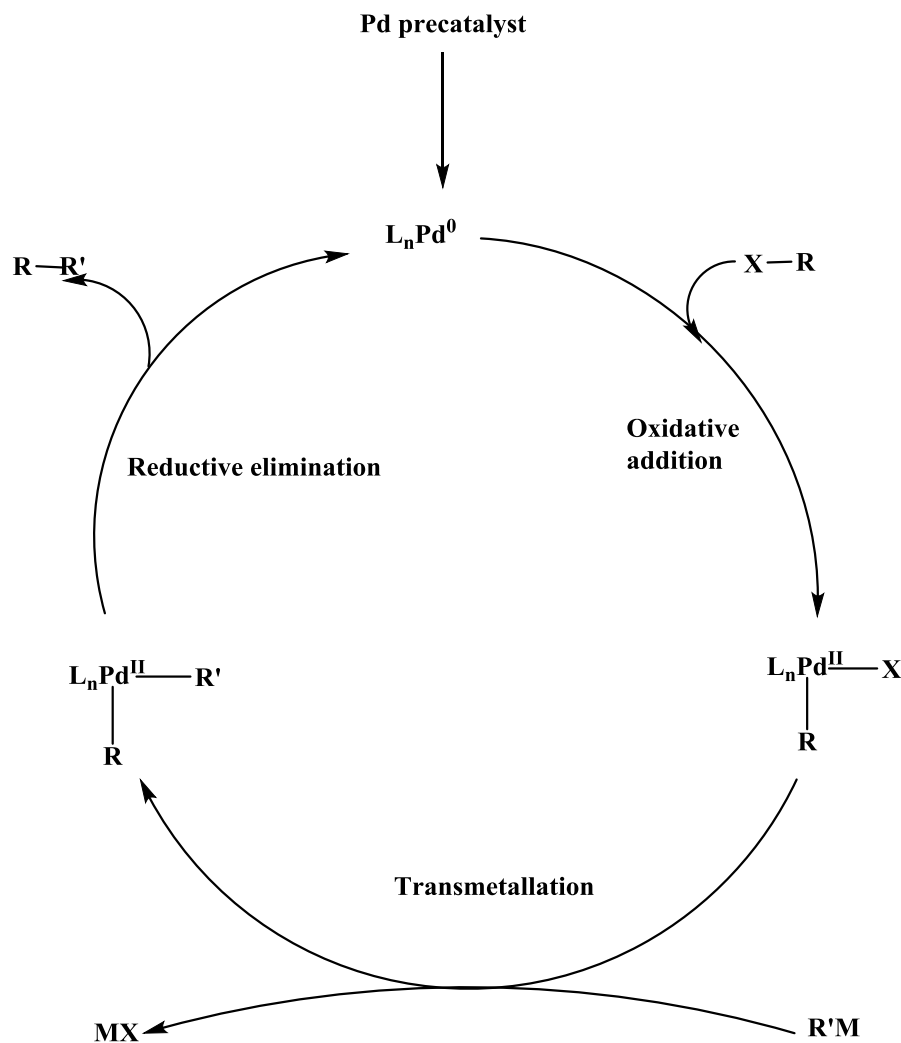
There are several types of cross-coupling reaction depending upon the organometal substrates such as Heck-Mizoroki, Suzuki-Miyaura, Corriu-Kumada-Tamao and Sonogashira-Hagihara coupling reactions (Scheme 4-7).



Scheme (4-7) Palladium catalyzed coupling reactions

Generally, the mechanism of the cross coupling reactions is similar. The mechanism consists of oxidative addition, transmetalation and reductive elimination. The oxidative addition step consists of cleavage of the Ar-X bond of an aromatic halide and formation two bonds to the palladium center from the halide and aryl moieties.

This is the rate determining step of the reaction and is highly dependent on the type of halide as mentioned above. The transmetalation step involves the reaction of this species with an organometallic substrate. The final step is reductive elimination to produce the product and reform the active palladium catalyst (Scheme 4- 8).

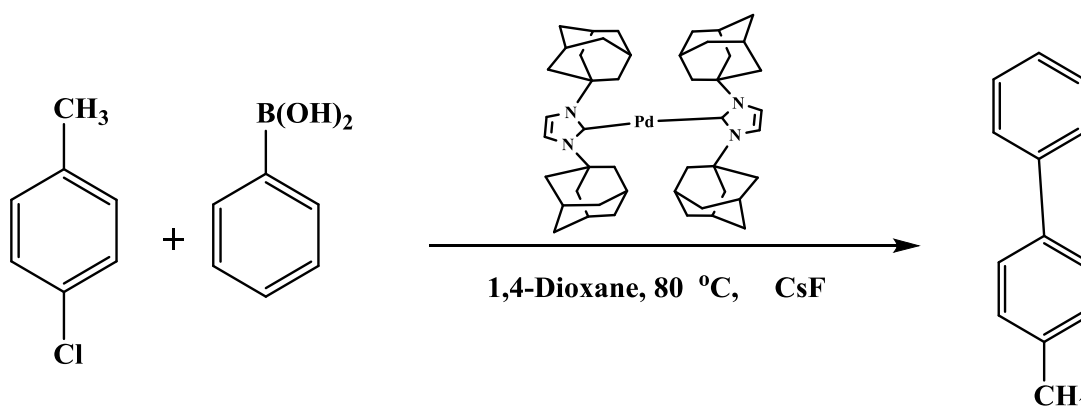


Scheme (4- 8) General mechanism of cross-coupling reactions

4.1.2.1-Suzuki Miyaura cross- coupling reaction

Pd-NHC complexes are widely used as catalysts in Suzuki cross-coupling reactions in the synthesis of a large number of drugs, [24] polymers,[25] and natural products.[26]

This reaction is conducted between aryl or vinyl halides and aryl or vinyl boronic esters and acids. [27, 28] The popularity of boronic acids in place of organometallic reagents is due to the low cost and toxicity, as well as stability towards air and moisture. [29] Pd-NHC complexes were first used as catalysts in the Suzuki reaction by Hermann *et al* in 2002. [Pd(IAd)₂] showed efficient catalytic activity in the Suzuki–Miyaura coupling of 4-chlorotoluene with phenyl boronic acid in the presence of CsF at 80 °C to produce 4-phenyltoluene. 97 % conversion was obtained within 20 minutes (Scheme 4-9). [30]



Scheme (4-9) Suzuki reaction coupling of aryl chloride with boronic acid

In 2003 Glorious used the flexible NHC ligand (IBiox) with Pd(OAc)₂ as a new strategy for catalyst preparation. Excellent catalytic activity at room temperature was observed in Suzuki-Miyaura coupling reactions. Several biaryl derivatives were obtained using aryl halides and boronic acids, high turnover numbers of up to 1370 were obtained at room temperature with less than 3 % Pd catalyst loading. The results obtained are attributed to the use of a flexible NHC ligand which plays a role in accelerating the oxidative addition step compared with Herrmann's catalyst for Suzuki-Miyaura coupling reactions. [31]

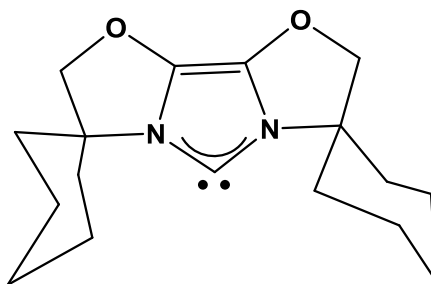


Figure (4-2) IBiox NHC ligand

Palladacycle complexes are another type of Pd - NHC complexes used in the Suzuki reaction. The reactivity of (IPr)PdCl (η^2 -N,C-C₁₂H₈NMe₂) [IPr] (*N,N*-bis(2,6-diisopropylphenyl)-imidazol-2-ylidene] has been examined in Suzuki reactions. Di- and tri-ortho-substituted biaryls have been obtained in very short reaction times by reaction of aryl chloride or triflate at room temperature in the presence of NaOt-Bu as a base. 90 % yield was obtained within 75 minutes at room temperature for biaryls formed from reaction of aryl chloride with boronic acids (Figure 4-3). [32]

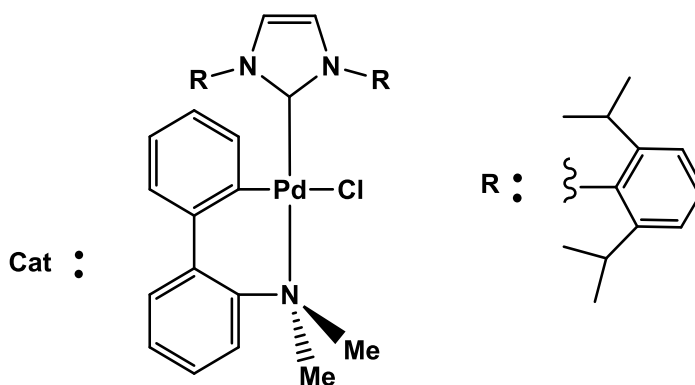


Figure (4-3) Palladacycle complexes

NHC-Pd-PEPPSI complexes (PEPPSI = pyridine-enhanced pre-catalyst, preparation, stabilization and initiation) have proven highly active in Suzuki coupling reactions. Interest in this type of complexes comes from their easy synthesis and capability to carry out Suzuki cross coupling reactions under ambient conditions. These types of complexes were prepared using the imidazolium salts with PdCl₂ in presence of a base in neat pyridine. The importance of this type of complexes comes from the

possibility of using different bases such as KOtBu, Cs₂CO₃, K₃PO₄, and K₂CO₃ to conduct Suzuki coupling reaction. This flexibility requires an appropriate choice of the base with the appropriate substrate.

Gosh and co-workers prepared a series of PEPPSI Pd–NHC complexes and tested their ability to act as catalysts in Suzuki reactions. Aryl bromide derivatives were reacted with phenyl boronic acid in the presence of K₂CO₃ in acetonitrile to produce a series of biaryl derivatives. The results showed that the aryl bromides with electron-withdrawing substituents like NO₂, CHO, and COMe moieties in the ortho and Para positions gave high yields of > 99 %. In contrast, electron - donating substituents in the ortho and para positions gave significantly lower yields (31-47%). These results reveal the role of the substituents in this reaction (Figure 4-4). [18]

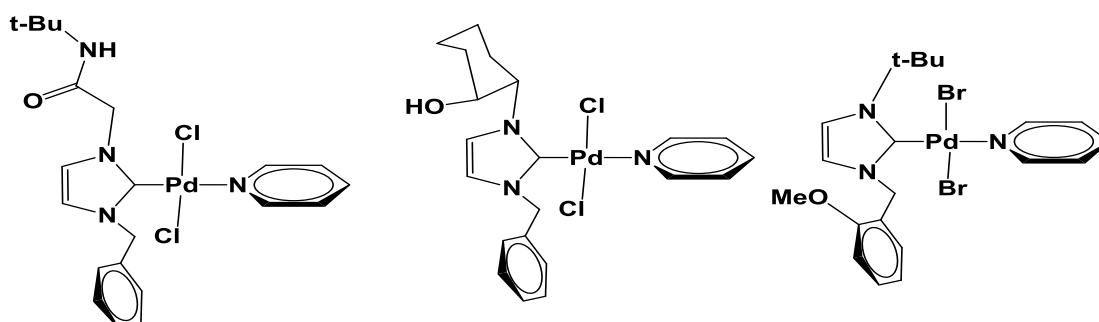
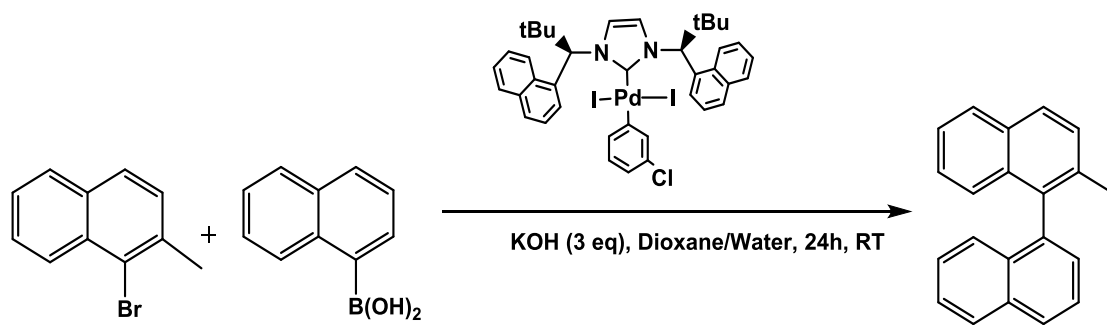


Figure (4- 4) NHC–Pd–PEPPSI complexes

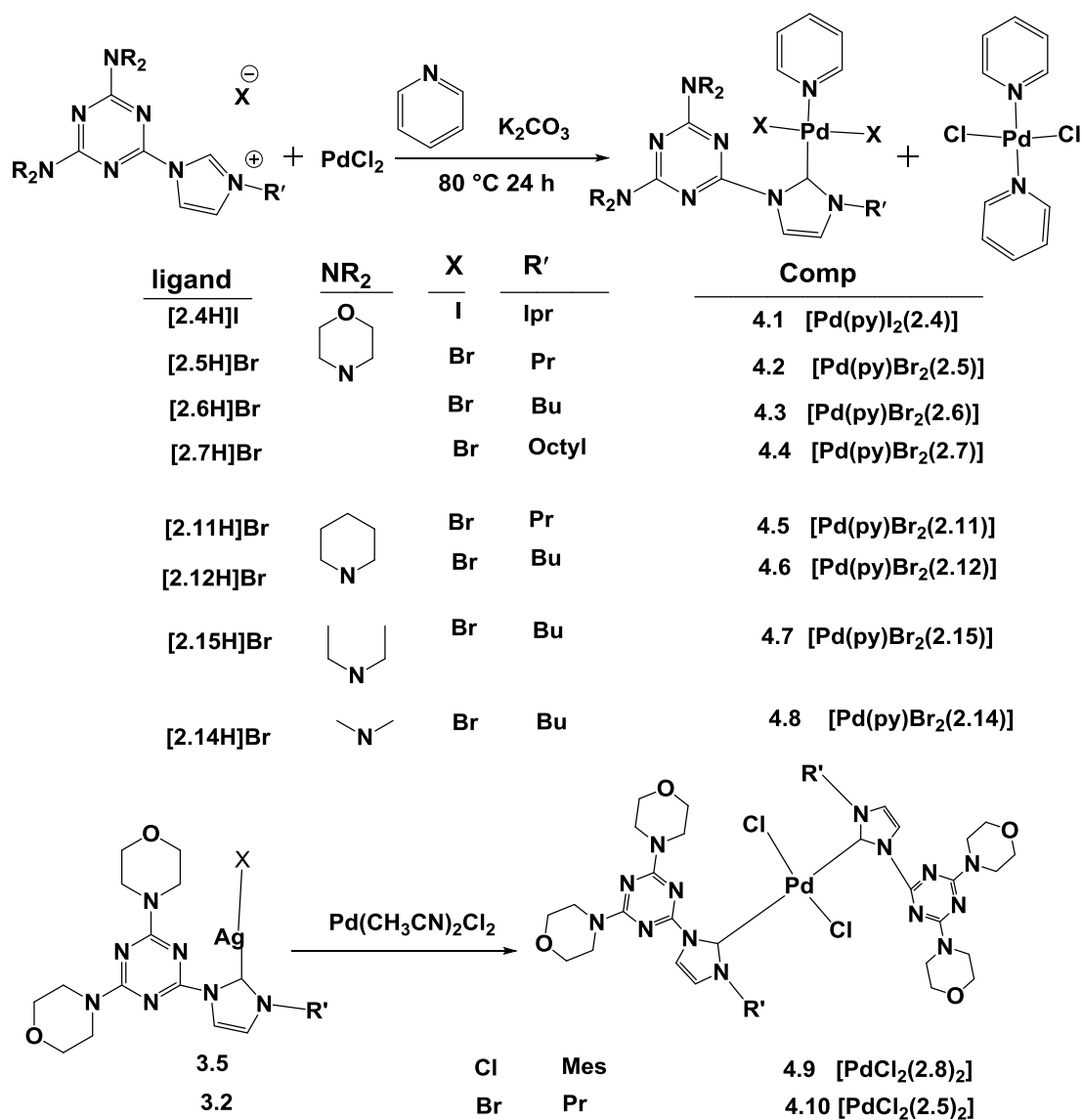
Chiral PEPPSI complexes have also been utilized in asymmetric Suzuki–Miyaura reactions by Peter *et al.* The Pd catalyzed Suzuki coupling reaction was used to synthesise atropisomeric biaryl products from the coupling of 1-halo-2-substituted naphthalene with hindered boronic acids with 3 equivalents of potassium hydroxide in a mixture of dioxane/water as a solvent. Good yields (80%) were obtained for coupling of 1-bromo-2-methyl naphthalene with naphthyl boronic acid at room temperature (Scheme 4- 10). [20]



Scheme (4-10) Synthesis of atropisomeric biaryl via Suzuki coupling reaction.

4.1.3-Aims

This chapter discusses the synthesis, characterization and catalytic reactivity of Pd-NHC complexes. Mono-NHC palladium complexes were synthesized via the reaction of NHC ligands with PdCl₂ in the presence of K₂CO₃ and pyridine as a solvent at 80 °C. Biscarbene palladium complexes were synthesized from the reaction of the corresponding silver complexes with Pd(MeCN)₂Cl₂ in dichloromethane via a transmetallation reaction. NMR spectroscopy and mass spectrometry, as well as elemental analyses and X-ray crystallography were used to confirm the formation of the complexes. Mono carbene palladium complexes were tested in Suzuki-Miyaura cross coupling reactions for the reaction of boronic acids with various aryl halides derivatives.



Scheme (4-11) Synthesis of Palladium complexes. Reagents and conditions: **(4.1 - 4.8)** 1 eq PdCl₂, 1 eq imidazolium salt, 10 eq K₂CO₃, 8 mL pyridine, 80 °C, 24 h; **(4.9, 4.10)** 2 equiv Ag(NHC)X **3.2, 3.5**, 1 eq Pd(CH₃CN)₂Cl₂, CH₂Cl₂, room temperature, 24 h.

4.2-Results and discussion

4.2.1-Synthesis of Pd-NHC complexes

[PdX₂(py)(NHC)] complexes (**4.1-4.8**) were synthesized via the reaction of PdCl₂ with the corresponding imidazolium halide salts [**2.4H**]**I**, [**2.5H**]**Br**, [**2.6H**]**Br**, [**2.7H**]**Br**, [**2.11H**]**Br**, [**2.12H**]**Br**, [**2.15H**]**Br** and [**2.14H**]**Br** in the presence of K₂CO₃ (10 eq) as an external base using pyridine as a solvent at 80 °C for 24 hours according to known procedures (Scheme 4-11). [18, 19, 20, 33]

The crude product was purified by column chromatography (silica, CHCl₃/Et₂O, 7:3) to afford the complex as a yellow powder. Suitable crystals were obtained by diffusion of diethyl ether in a chloroform solution of the complex. The complexes are stable in air and moisture, insoluble in water and readily soluble in organic solvents such as dichloromethane, chloroform, DMF, DMSO, methanol and acetonitrile.

NMR spectroscopy and mass spectrometry, as well as elemental analysis and X-ray crystallography were used to confirm the formation of the complexes.

For all of the palladium complexes reported here the imidazole proton resonances of positions 4 and 5 were shifted significantly upfield upon coordination when compared to the NHC ligand precursor, accompanied by the disappearance of the NC(H)N peak.

The ¹H NMR spectrum for complex [PdI₂(py)(**2.4**)], **4.1** is typical for the [PdX₂(py)(NHC)] complexes reported here, showing three peaks corresponding to the pyridine protons centred at 9.19, 7.68 and 7.35 ppm. Proton resonances for the imidazolium protons were observed at 7.95 and 6.93 ppm. The characteristic carbene carbon (C_{NHC}) peak at 155.6 ppm in the ¹³C NMR spectrum is consistent with

previous literature reports. [4, 6, 34, 35] For the corresponding **4.2**, **4.3**, **4.4**, **4.5**, **4.6** complexes the C_{NHC} peak appears at 153.1, 153.0, 153.1, 153.2 and 153.2 ppm respectively.

The ^1H NMR spectrum for the $[\text{PdBr}_2(\text{py})(\mathbf{2.6})]$, **4.3** complex is shown in Figure (4-5), and is a representative example for the $[\text{PdX}_2(\text{py})(\text{NHC})]$ complexes.

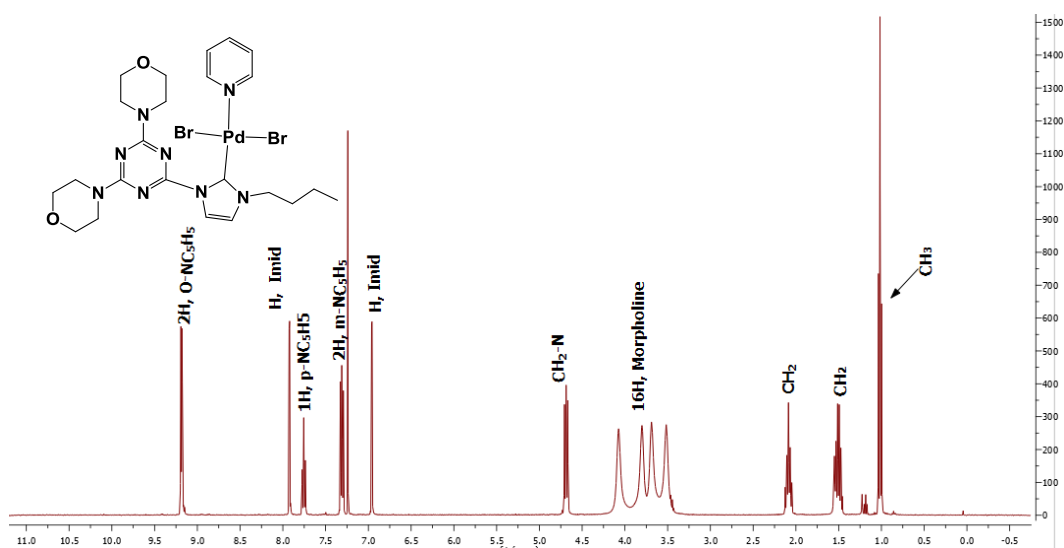


Figure (4-5) ^1H NMR spectrum for $[\text{Pd}(\text{NHC})(\text{py})\text{Br}_2]$ complex **4.3**

The ^1H NMR spectrum of complex **4.7** shows three diethyl amine peaks at 3.48, 3.79 (CH_2) and 1.12 (CH_3) ppm. In the ^{13}C NMR spectrum the resonances due to diethyl amine appear at 41.7 and 13.9 ppm.

The ^1H NMR spectrum of **4.8** shows two peaks at 3.35 and 3.10 ppm each integrating to 6H for the protons dimethyl amino groups. This is consistent with a rotational barrier about the amine–triazine bonds which is due to the extended π -conjugation network between the amino N-atoms and the triazine (Figure 4-6). The C_{NHC} peak in the ^{13}C NMR spectrum of complexes **4.7** and **4.8** appear at 153.3 and 152.0 ppm respectively.

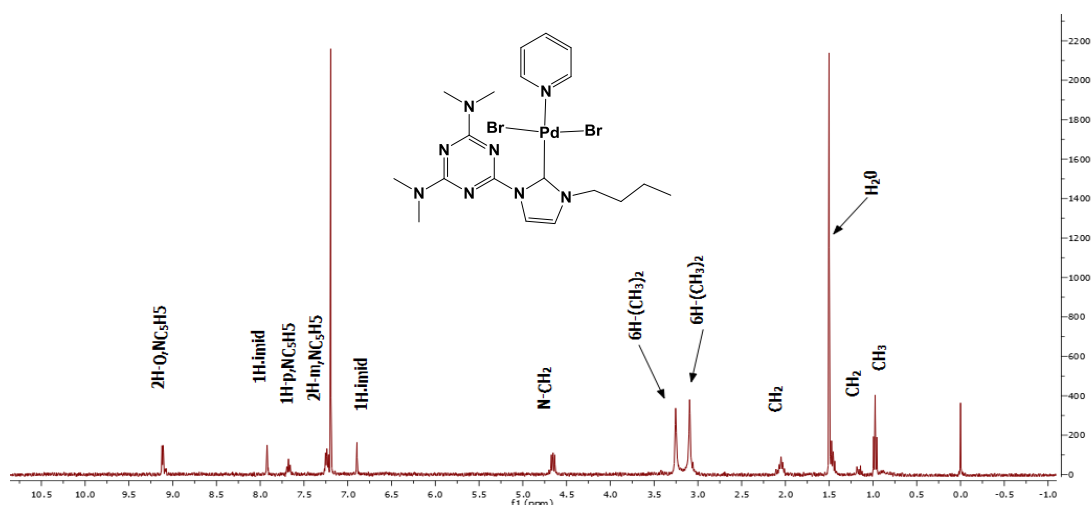


Figure (4-6) ^1H NMR spectrum for $[\text{Pd}(\text{NHC})(\text{py})\text{Br}_2]$ complex **4.8**

Attempts to prepare $[\text{PdX}_2(\text{py})(\text{NHC})]$ -type complexes with NHCs bearing aromatic substituents, such as the mesityl ligand **[2.8H]Cl**, from the direct reaction of the imidazolium salt with PdCl_2 using pyridine as solvent, have failed. This is attributed to the lower acidity of the imidazolium hydrogen of the precursor and hence the difficulty to generate the carbene ligand.

Silver transmetalation was used as an alternative method for obtaining palladium complexes with the triazine-based NHCs.

The use of 1:1 equivalent of silver complex **3.5** and $\text{Pd}(\text{MeCN})_2\text{Cl}_2$ did not result in a mono-carbene complex $[\text{Pd}(\text{MeCN})(\text{NHC})\text{Cl}_2]$, instead a mixture of unreacted $\text{Pd}(\text{MeCN})_2\text{Cl}_2$ and the bis-carbene complex $[\text{PdCl}_2(\mathbf{2.8})_2]$ was obtained. The procedure was modified by using 2 equivalents of silver complex **3.5** with 1 equivalent of $\text{Pd}(\text{MeCN})_2\text{Cl}_2$. The reaction was conducted in dichloromethane as solvent at room temperature for 24 h according to previous literature. [14, 36, 37] The reaction was wrapped with aluminum foil to exclude light from the reaction vessel. The product was filtered through celite to remove AgCl formed throughout the reaction. The residual solvent was removed by vacuum to produce a yellow powder.

The ^1H NMR spectrum was complicated indicating the presence of more than one isomer (*cis/trans*) (Figure 4-7).

Crystals of one isomer were isolated by the vapour diffusion of Et_2O into a concentrated solution of crude complex in CHCl_3 giving the *cis*-coordinated complex (Figure 4-8). The mother liquors were evaporated to dryness and recrystallised from the same solvent combination to afford the *trans*-coordinated complex (Figure 4-9). X-ray crystallography was used to confirm the isomers' structure.

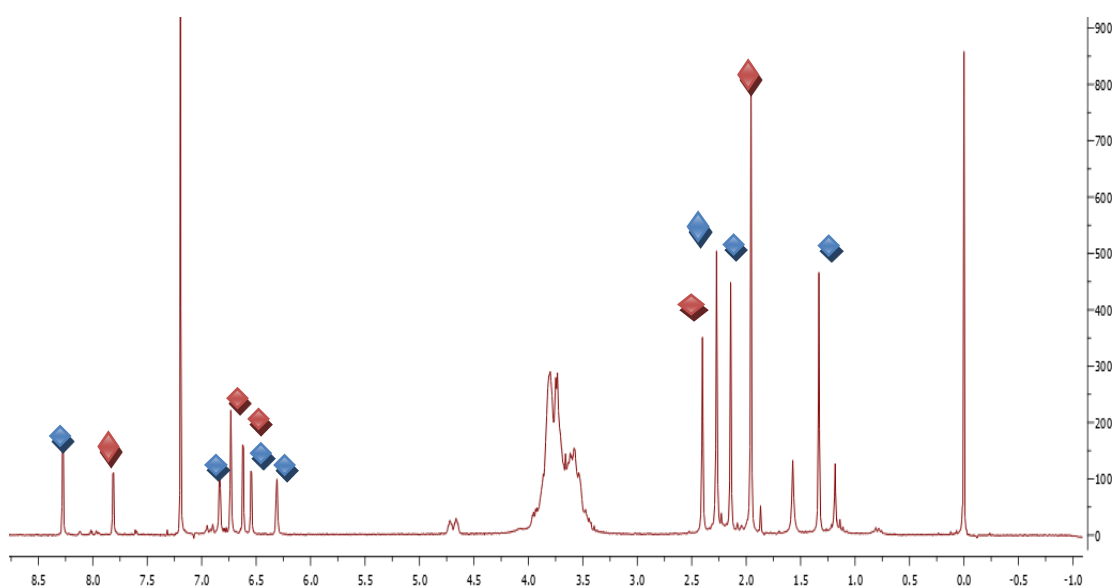


Figure (4-7) ^1H NMR spectrum of crude $[\text{Pd}(\mathbf{2.8})_2\text{Cl}_2]$, **4.9** (◆ *cis*, ◆ *trans*)

Due to restricted rotation around the Pd-Carbene and N-mesityl bonds the ^1H NMR spectrum for *cis* isomer showed two peaks corresponding to the aryl protons each one integrating to 2H at 6.88 and 6.36 ppm and three peaks for the methyl groups at 2.27 ppm, 2.14 ppm and 1.33 ppm, each peak integrating to 6 protons (Figure 4 - 8).

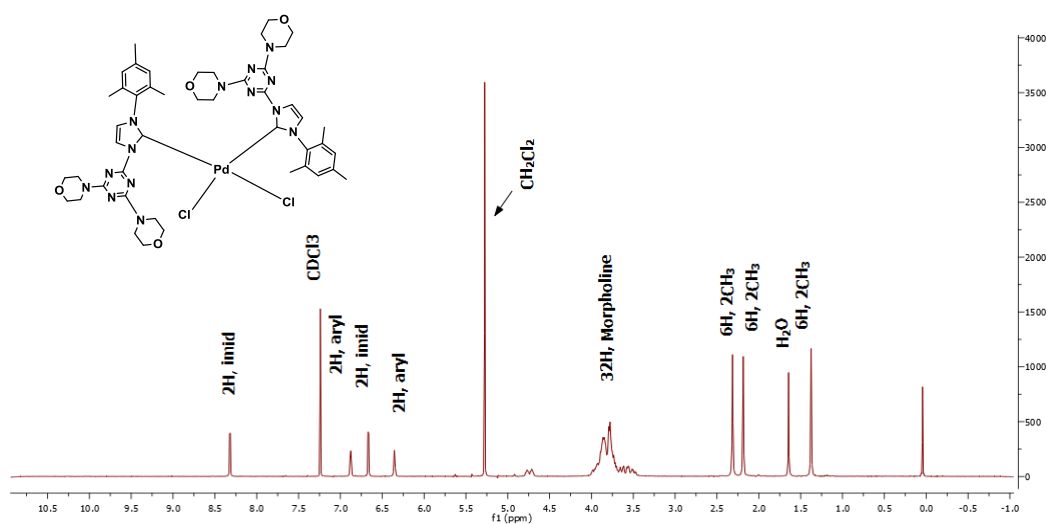


Figure (4-8) ^1H NMR spectrum of *cis*-[Pd(**2.8**) $_2$ Cl $_2$] isomer, *cis*-**4.9**

The ^1H NMR spectrum for *trans*-[Pd(**2.8**) $_2$ Cl $_2$] showed one peak for the aromatic protons as expected integrating to 4H at 6.78 ppm, and two resonances at 7.85 and 6.62 ppm for imidazolium moieties each peak integrating to 2H. Two peaks were observed at 2.45 and 2.00 ppm for methyl groups, the first peak integrating to 6H while the second one integrating to 12H, (Figure 4-9).

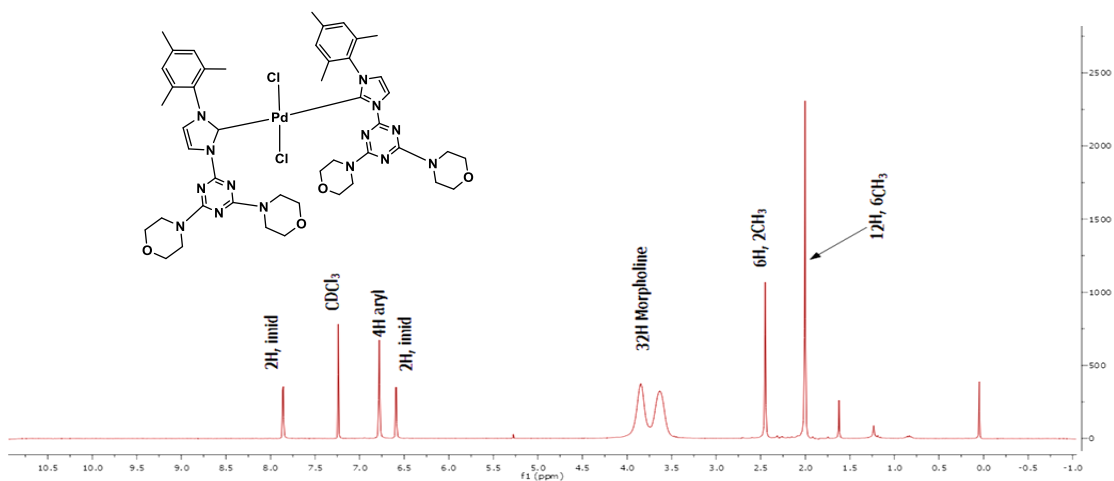


Figure (4-9) ^1H NMR spectrum of *trans*-[Pd(**2.8**) $_2$ Cl $_2$] isomer, *trans*-**4.9**

The ^{13}C NMR spectrum is complicated by the inequivalence of the carbene ligands with numerous peaks observed at 165.4, 164.3 ppm (triazine), 161.1 (Pd-C1), 138.8, 137.7, 135.9, 133.0, 129.8, 128.2 (mesityl and imidazolium), 21.3, 19.7 and 17.4 ppm

(methyl groups). Mass spectrometry (ES) supports the formation of a bis-carbene palladium complex with a fragmentation peak at 1013.33 for $[\text{Pd}(\text{NHC})_2\text{Cl}]^+$.

The complex $[\text{Pd}(\mathbf{2.5})_2\text{Cl}_2]$, **4.10**, was prepared using the transmetallation method via reaction of $[\text{Ag}(\mathbf{2.5})\text{Br}]$, **3.2**, with $\text{Pd}(\text{CH}_3\text{CN})_2\text{Cl}_2$ in dichloromethane at room temperature, in order to confirm that this was a viable procedure for the preparation of palladium bis-carbene complexes with the N-alkyl proligands $[\mathbf{2.5H}]\text{Br}$ – $[\mathbf{2.15H}]\text{Br}$. This procedure also avoided the formation of trans-dichloro bis(pyridine)palladium(II) that was always formed as a side product from the direct method.

In transmetallation reactions, the use of PdCl_2 as source of palladium failed to yield the desired complex, so $\text{Pd}(\text{CH}_3\text{CN})_2\text{Cl}_2$ was used as alternative source under a 1:2 ratio with the $[\text{AgX}(\text{NHC})]$ complexes.

Assignment of the geometry at Pd can be achieved by interpretation of the ^{13}C NMR spectrum. The *cis* and *trans* isomers display distinct chemical shifts for the carbene carbons in the $\text{Pd}(\text{NHC})_2$ complexes according to previous literature. [14] ^{13}C NMR spectroscopy for **4.10** confirmed formation of the *trans* isomer by the appearance of a new peak attributed to Pd-C at 155.95 ppm in addition to the expected other peaks corresponding to the propyl and triazine groups (Figure 4-10).

A peak at m/z 859.18 was observed in the mass spectrum of this complex and attributed to a fragmentation peak of $[\text{Pd}(\text{NHC})_2\text{Cl}]^+$ confirming the formation of a bis carbene complex.

^1H NMR analysis of complex **4.10** showed two peaks assigned to the imidazolium unit shifted upfield to 7.88 ppm and 6.95 ppm, each peak integrating to 2H and three peaks assigned to the propyl protons at 4.73, 2.05 and 1.15 ppm each integrating to

4,4 and 6H respectively. Broad peaks for the morpholine protons were observed in the range 4.32-4.73 ppm.

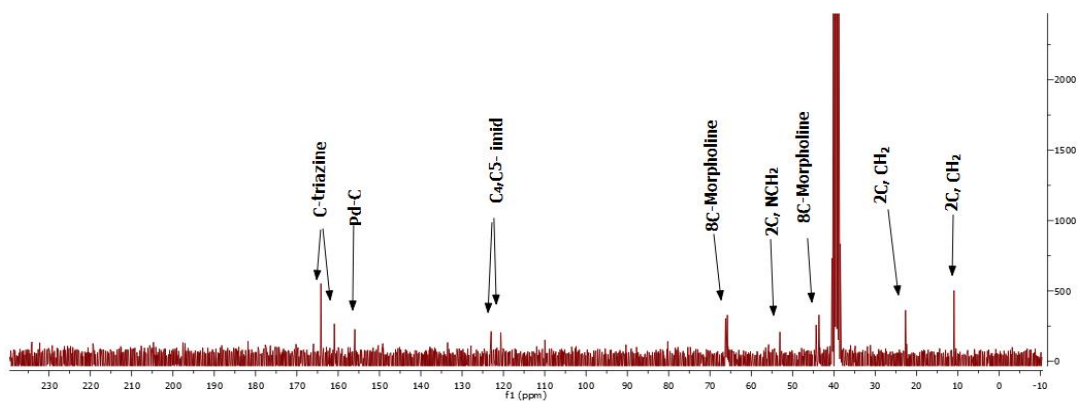


Figure (4-10) ¹³C NMR spectrum of [Pd (2.5)₂Cl₂] complex **4.10**

4.2.2-X-ray Structural Determination

Attempts were made to grow crystals suitable for single crystal X-ray diffraction studies of all compounds. For the [PdX₂(py)(NHC)]-type complexes the expected *trans*-isomers were obtained. Suitable crystals were obtained from vapour diffusion of diethyl ether into chloroform solutions for all complexes.

There are some significant structural features evident in the crystal structure of [PdCl₂(**2.6**)], **4.3**. The complex shows a distorted square planar geometry around the palladium metal centre. The bromide ligands are positioned *trans* to each other, (Br1-Pd-Br2 167.209(13)°, and the pyridine is *trans* to the carbene ligand (N8-Pd-C1 173.65(9)°. The N1-C1-N2 angle of 105.02(2)° is somewhat compressed when compared with 108.2(3)° to the corresponding precursor [**2.6H**]**Br**. The C1-N1 and C1-N2 bonds are longer at 1.339(3) and 1.367(3) Å than for the ligand at 1.324(4) and 1.332(4) Å respectively due to formation of the complex. The Pd-C1 bond 1.951(2) Å lies within the normal range of those observed for complexes that have been previously reported for PEPPSI complexes type . [38-41] The angle between the triazine unit and the imidazolium is twisted out of the plane by 18.84°. Bond lengths and angles, principally involving those around the metal centre are shown in Table (4-1).

Table (4-1) Selected bond lengths and angles for [Pd(Py)Br₂(**2.6**)] **4.3**

Bond Angles (°)		Bond lengths (Å)	
N1-C1-N2	105.02(2)	C1-N1	1.339(3)
C1-N1-Pd1	129.81(19)	C1-N2	1.367(3)
N2-C2-Pd1	124.98(17)	C3-C2	1.344(4)
C3-C2-N1	107.0(2)	N1-C15	1.467(3)
N2-C3-C2	106.5(2)	N2-C4	1.424(3)

N8-Pd1-Br1	91.84(6)	Pd1-C1	1.951(2)
N8-Pd1-Br2	92.71(6)	Pd1-N8	2.101(2)
C1-Pd1-Br1	87.99(8)	Pd-Br1	2.448(3)
C1-Pd1-Br2	88.97(7)	Pd-Br2	2.425(3)
Br1-Pd-Br2	167.209		
N8-Pd-C1	173.65		

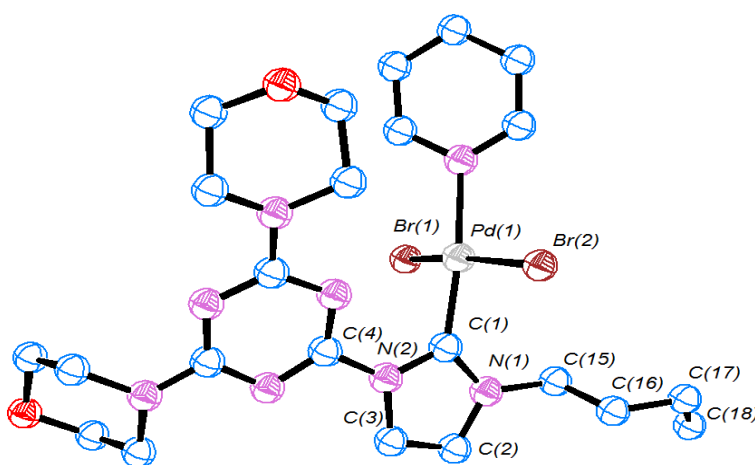
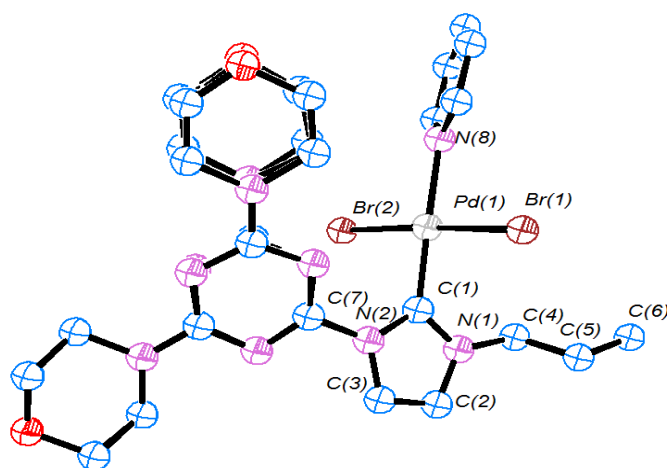


Figure (4-11) ORTEP ellipsoid plot at 50% probability of complex **4.3**. H atoms omitted for clarity

The structure of **4.2** consists of distorted square-planar molecule with a palladium center surrounded by the NHC ligand **2.5**, two bromide ligands in a *trans* configuration, and a pyridine. The structure showed some disorder for the triazine and one of morpholine moieties. The Pd-C distance is 1.9460(2) Å and Pd-pyridine distance is 2.1230(2) Å. The differences in the bond distances reflect the *trans* influence which are consistent with previous literature. [18, 20, 42] Bond lengths and angles are shown in Table (4-2).

Table (4-2) Selected bond lengths and angles for [Pd(Py)Br₂(**2.6**)] **4.2**

Bond Angles (°)		Bond lengths (Å)	
N1-C1-N2	105.0(2)	C1-N1	1.343(3)
N1-C1-Pd1	126.88(19)	C1-N2	1.362(3)
N2-C1-Pd1	128.14(19)	C3-C2	1.342(4)
C3-C2-N1	106.4(2)	N1-C4	1.463(3)
N2-C3-C2	106.5(2)	N2-C7	1.419(3)
N8-Pd1-Br1	91.11(6)	C1-Pd1	1.9460(2)
N8-Pd1-Br2	92.17(6)	Pd1-N8	2.1230(2)
C1-Pd1-Br1	88.17(7)	Pd-Br1	2.4448(3)
C1-Pd1-Br2	88.46(7)	Pd-Br2	2.4398(3)
Br1-Pd-Br2	175.7(12)		
N8-Pd-C1	177.9(10)		

**Figure (4- 12)** ORTEP ellipsoid plot at 50% probability of complex **4.2**.

H atoms omitted for clarity

The structure of *cis*-[Pd(**2.8**)₂Cl₂], *cis*-**4.9**, confirms that two carbene ligands are coordinated in a *cis* manner around a square planar Pd with a C1-Pd-C1i angle of

89.63(2)°. There is a C_2 axis of rotation bisecting the coordination plane resulting in equivalent ligands. The two mesityl carbene-triazine ligands are mutually parallel to each other driven by π - π interactions between the mesityl group of one ligand and the electron-poor triazine group of the second ligand (contact distances are in the range 3.4 – 3.7 Å). Carbene formation is supported by a decreased N1-C1-N2 bond angle (in both cases) with respect to the free ligand. In both ligands, the angle between the triazine unit and the imidazolium is twisted out of the plane by 7.43°. The dihedral angle between the mesityl and imidazole rings is 81.17°. Bond lengths and angles are shown in Table (4-3).

Table (4-3) Selected bond lengths and angles for *cis*-[Pd (**2.8**)₂Cl₂], *cis*-**4.9**

Bond Angles (°)		Bond lengths (Å)	
C1-Pd1-Cl1	89.63(10)	Pd1-Cl1	2.3781(9)
Cl1i-Pd-Cl1	178.29(10)	Pd1-Cl1i	2.3781(9)
C1-Pd1-Cl1 ⁱ	178.29(11)	Pd1-Cl1i	1.992(4)
Cl1 ⁱ -Pd1-Cl1 ⁱ	89.63(10)	Pd1-C1	1.992(4)
C1-Pd1-Cl1i	89.8(2)	N1-C1	1.361(4)
N1-C1-N2	104.2(3)	N2-C1	1.369(4)

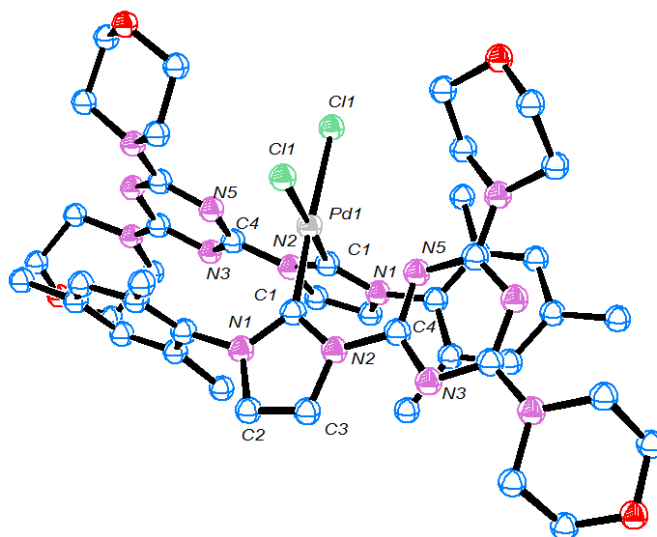
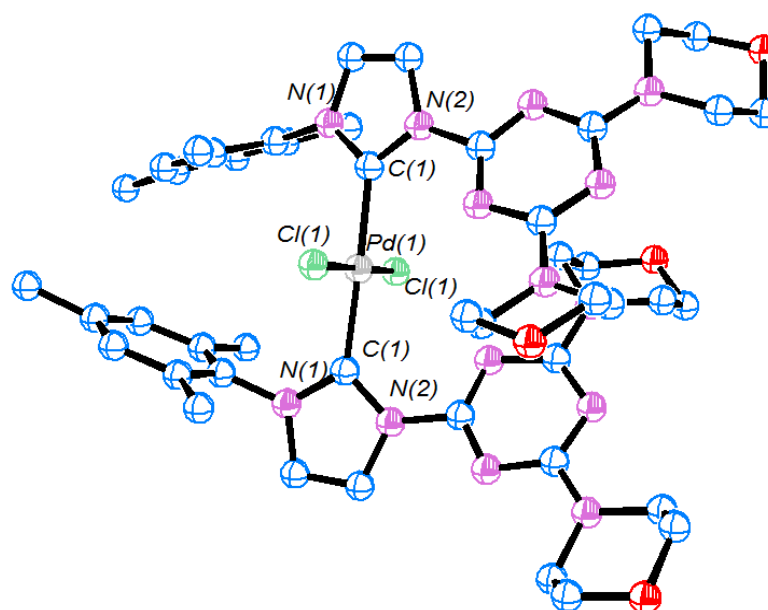


Figure (4-13) ORTEP ellipsoid plot at 50% probability of *cis*-[Pd(2.8)₂Cl₂], *cis*-**4.9** complex. H atoms omitted for clarity

A second isomer crystallised with the two carbene ligands coordinated in a *trans* manner around a square planar Pd with a C1-Pd-C1i angle of 178.10(8)°. There is C₂ axis of rotation perpendicular to the coordination plane resulting in equivalent ligands. The difference in the orientation of the aromatic imidazole substituents between the *cis* and *trans* isomers of **4.9** is that in the *cis* isomer the mesityl ring is facing the triazine ring of the 2nd carbene ligand, whereas in the *trans* isomer the mesityl rings are facing each other. No π - π interactions were observed between the aromatic rings in the *trans* isomer. In both ligands, the angle between the triazine unit and the imidazolium is twisted out of the plane by 28.50°, much greater than for the *cis*-isomer. The dihedral angle between the mesityl and imidazole rings is 78.32°. Carbene formation is supported by a decreased N1-C1-N2 bond angle (in both cases) with respect to the free ligand. Bond lengths and angles, are shown in Table (4- 4).

Table (4-4) Selected bond lengths and angles for *trans*-[Pd(**2.8**)₂Cl₂], *trans*-**4.9**

Bond Angles (°)		Bond lengths (Å)	
C1-Pd1-Cl1	91.24(4)	Pd1-Cl1	2.3266(4)
Cl1i-Pd-Cl1	88.73(4)	Pd1-Cl1i	2.3266(4)
Cl1-Pd1-Cl1i	88.73(4)	Pd1-Cl1i	2.0390(16)
Cl1i-Pd-Cl1I	91.24(4)	Pd1-Cl1	2.0390(16)
C1-Pd1-Cl1i	178.10(8)	N1-C1	1.3518(19)
N1-C1-N2	103.75(13)	N2-C1	1.373(2)

**Figure (4-14)** ORTEP ellipsoid plot at 50% probability of *trans*-[Pd(**2.8**)₂Cl₂], *trans*-**4.9** complex. H atoms omitted for clarity

Yellow block crystals were obtained for [Pd(py)Br₂(**2.12**)],**4.6**, X-ray diffraction showed a mixed halide, 30% Cl 70% Br, occupation of the complex due to incomplete exchange of bromide to chloride. As the procedure we used did not contain the addition of the excess of salt (i.e KBr) which usually used in the literature

[20] to avoid the replacement of the original counter ion. so for all compounds were made in this study we have not seen such exchange apart from the case of the complex **4.6** which tends to partly exchange of bromide by chloride (from PdCl₂) to form the complex **4.6**. The triazine moiety along with one pendant piperidine showed some disorder. The complex shows a distorted square planar geometry of ligands around the palladium metal centre. The halide ions are observed in a *trans* coordination geometry, and the pyridine with carbene ligands are also *trans* to each other (C1-Pd1-N3 179.17(10)°). The Pd–NHC and Pd–pyridine bond lengths, 1.956(3) Å and 2.112(2) Å respectively, lie in the normal range for previous literature. Bond lengths and angles, are shown in Table (4-5).

Table (4 - 5) Selected bond lengths and angles for [Pd(py)Br₂(**2.12**)], **4.6**

Bond Angles (°)		Bond lengths (Å)	
N1-C1-N2	104.6(2)	C1-N1	1.343(3)
N1-C1-Pd1	127.15(19)	C1-N2	1.392(3)
N2-C1-Pd1	128.2(2)	C3-C2	1.345(4)
C3-C2-N1	107.5(2)	N1-C9	1.469(3)
N2-C3-C2	105.9(2)	N2-C13	1.428(3)
N3-Pd1-Br1	91.99(8)	C1-Pd1	1.956(3)
N3-Pd1-Br2	91.29(10)	Pd1-N3	2.112(2)
C1-Pd1-Br1	87.98(9)	Pd-Br1	2.4344(18)
C1-Pd1-Br2	88.80(10)	Pd-Br2	2.445(2)
Br1-Pd-Br2	174.84(7)		
N3-Pd-C1	179.17(10)		

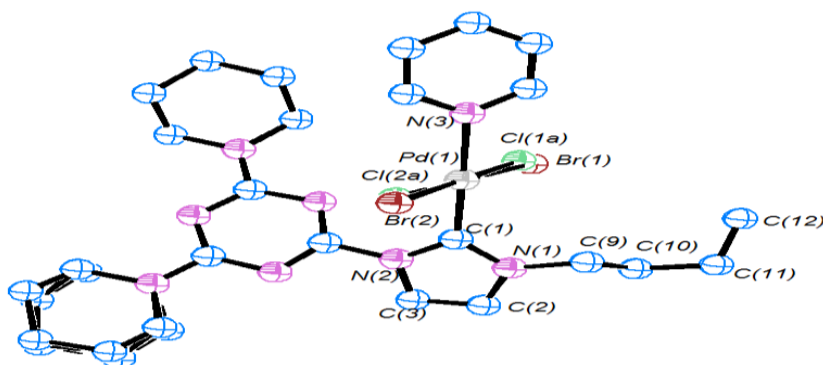


Figure (4-15) ORTEP ellipsoid plot at 50% probability of complex **4.6**.

H atoms omitted for clarity

The structure of $[\text{Pd}(\text{py})\text{Br}_2(\mathbf{2.14})]$, **4.8** shows a distorted square planar geometry of ligands around the palladium metal centre. The bond distances of Pd-N8 2.111(3) and Pd-Carbene 1.973(3) Å are consistent with other complexes in this work. The bromide ligands (and therefore the pyridine and carbene ligands) are orientated trans to one another (Br1-Pd1-Br2 177.406 (16)°). Bond lengths and angles, are shown in Table(4- 6).

Table (4-6) Selected bond lengths and angles for $[\text{Pd}(\text{py})\text{Br}_2(\mathbf{2.14})]$, **4.8**

Bond Angles (°)		Bond lengths (Å)	
N1-C1-N2	105.4(3)	C1-N1	1.346(4)
N2-C1-Pd1	127.8(2)	C1-N2	1.395(4)
N1-C1-Pd1	126.6(3)	C3-C2	1.340(5)
C3-C2-N1	107.3(3)	N1-C4	1.469(4)
N2-C3-C2	106.8(3)	N2-C8	1.425(4)
N8-Pd1-Br1	91.15(9)	C1-Pd1	1.973(3)
N8-Pd1-Br2	89.86(9)	Pd1-N8	2.111(3)
C1-Pd1-Br1	87.51(10)	Pd-Br1	2.4358(5)
C1-Pd1-Br2	91.46(10)	Pd-Br2	2.4429(5)

Br1-Pd-Br2	177.406(16)
N3-Pd-C1	178.47(12)

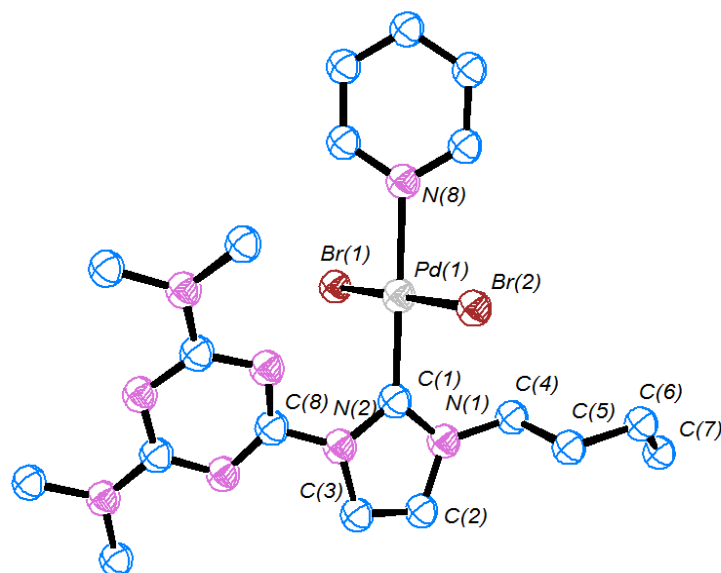


Figure (4-16) ORTEP ellipsoid plot at 50% probability of complex **4.8**.
H atoms omitted for clarity

X-ray diffraction for palladium complexes in this work were confirmed the square planar geometry around the palladium metal centre in which the bond lengths and the bond angles are consistent with the ranges previously reported for complexes of the type PEPPSI. [38-41]

4.2.3-Catalytic activity of [Pd(NHC)(py)Br₂]

We selected the nominated three complexes of palladium with three different substituents on the triazine (ie compounds **4.3**, **4.6**, and **4.8** which have dimorpholine, dipiperidine and dimethylamine respectively). The complexes have been selected to reveal the effect of the variation in the structure on the activity of these complexes toward Suzuki-Miyaura coupling of phenylboronic acid with aromatic bromides and chlorides.

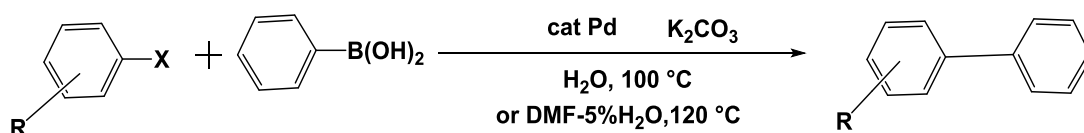
Previous studies have shown that the steric bulk of the carbene ligands which coordinate the palladium centre plays an important role in the acceleration of the reductive elimination step and completion of the reactions in short time scales. [43]

In the light of this fact palladium complexes **4.3**, **4.6**, and **4.8** have been tested for determining the ability of the NHC precursors [**2.6H**]Br, [**2.12H**]Br, and [**2.14H**]Br prepared in this work, as bulky ligands for Suzuki coupling reactions.

The results showed that the catalytic activity of the complexes depends on the steric properties of ligands regardless of the nature and position of functional groups on aryl halide [44]. This explains the similarity of the results obtained for the various substrates used (Table 4-7).

Two solvent systems were used in the cross coupling reaction; neat water and a mixture of DMF-H₂O (10-0.5 mL). The reactions were conducted at reflux under aerobic conditions in the presence of K₂CO₃ as a base.

The results obtained in both solvent systems prove that these complexes are efficient catalysts in the Suzuki reaction. The highest conversion (100%) was obtained in H₂O which is consistent with previous studies. [45-50] The results are given in table (4-7).



Scheme (4-12): Suzuki-Miyaura cross-coupling.

Several aryl halides were used with phenyl boronic acid. The results obtained are similar for all complexes used regardless of type of NHC ligand.

The highest conversion was obtained for 4-bromoacetophenone in both solvents as expected. 100% yields were obtained by reaction of 4-bromoacetophenone with phenylboronic acid with catalytic palladium complexes **4.3**, **4.6** and **4.8** within 30 minutes in water as solvent (entries 1-3). Lower yields were obtained in DMF-H₂O mixtures at about 90-94 % (entries 4-6).

The use of Pd complexes **4.3**, **4.6** and **4.8** for the cross-coupling of 4-chloroacetophenone in refluxing water afforded 26, 22 and 18 % yield after 24 h (entries 6-8) respectively.

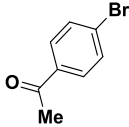
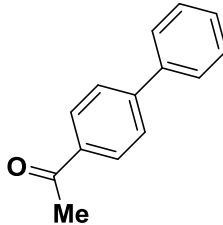
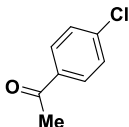
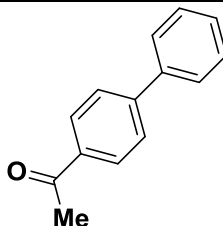
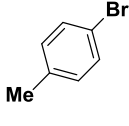
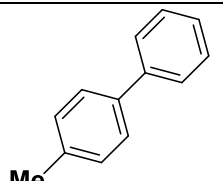
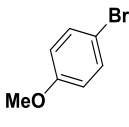
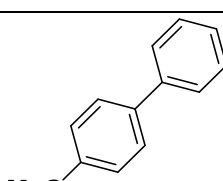
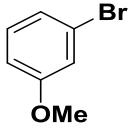
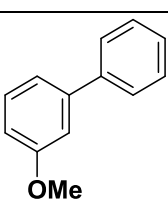
The low reactivity of 4-chloroacetophenone has been attributed to their resistance to oxidative addition because of the large Csp²-Cl bond dissociation energy. [51]

Pd catalysts **4.3**, **4.6**, **4.8** were used in the coupling of phenylboronic acid with *p*-methyl bromobenzene yielding the biphenyl product in 74, 77 and 70% yield respectively (entries 10-12). When carried out in the DMF-H₂O solvent mixture this decreased to 69, 70 and 66 % (entries 13-15). The catalytic activity of these complexes appears to be unaffected by the position of other functional groups on the bromo benzene reagent,

Similar results were achieved for the coupling of *p*-methoxy bromobenzene and *m*-methoxy bromobenzene with phenylboronic acid regardless of the position of substituents. Yields in the range 80-92% were found for both reactions (entries 16-18

and 22-24) in water, and 70-80% when carried out in DMF-H₂O (entries 19-21 and 25-27).

Table 4-7: Suzuki-Miyaura cross-coupling of aryl halides and phenyl boronic acids with complexes **4.3**, **4.6** and **4.8**.

Entry	Substrate	Cat. (mol %)	Solvent	Product	% Yield (time, h)	TON (time, h)
1		4.3 (1)	H ₂ O		100(0.5)	100(0.5)
2		4.6 (1)	H ₂ O		100(0.5)	100(0.5)
3		4.8 (1)	H ₂ O		100(0.5)	100(0.5)
4		4.3 (1)	DMF-H ₂ O		94(0.5)	94(0.5)
5		4.6 (1)	DMF-H ₂ O		92(0.5)	92(0.5)
6		4.8 (1)	DMF-H ₂ O		90(0.5)	90(0.5)
7		4.3 (1)	H ₂ O		26(24)	26(24)
8		4.6 (1)	H ₂ O		22(24)	22(24)
9		4.8 (1)	H ₂ O		18(24)	18(24)
10		4.3 (1)	H ₂ O		74(3)	74(3)
11		4.6 (1)	H ₂ O		77(3)	77(3)
12		4.8 (1)	H ₂ O		70(3)	70(3)
13		4.3 (1)	DMF-H ₂ O		69(3)	69(3)
14		4.6 (1)	DMF-H ₂ O		70(3)	70(3)
15		4.8 (1)	DMF-H ₂ O		66(3)	66(3)
16		4.3 (1)	H ₂ O		88(3)	88(3)
17		4.6 (1)	H ₂ O		92(3)	92(3)
18		4.8 (1)	H ₂ O		85(3)	85(3)
19		4.3 (1)	DMF-H ₂ O		74(3)	74(3)
20		4.6 (1)	DMF-H ₂ O		77(3)	77(3)
21		4.8 (1)	DMF-H ₂ O		70(3)	70(3)
22		4.3 (1)	H ₂ O		82(3)	82(3)
23		4.6 (1)	H ₂ O		87(3)	87(3)
24		4.8 (1)	H ₂ O		80(3)	80(3)
25		4.3 (1)	DMF-H ₂ O		77(3)	77(3)
26		4.6 (1)	DMF-H ₂ O		80(3)	80(3)
27		4.8 (1)	DMF-H ₂ O		79(3)	79(3)

^aAll reactions were carried out at 100°C (for H₂O) or 120°C (for DMF/H₂O), using 1.00 mmol of aryl halide, 1.2 mmol of phenylboronic acid, 3 mmol K₂CO₃, solvent (10 mL). Conditions were not anhydrous or air free. % yields were determined by ¹H NMR spectroscopy using 1, 3, 5-trimethoxybenzene as internal standard. Reactions were monitored at 30 minute intervals. TON = turnover number

In the comparison of catalytic activity studies of the current work with previously reported studies for other Pd complexes in Suzuki reactions under the same conditions, it is seen that the **4.3, 4.6, 4.8** complexes used in this work have relatively similar high activity as catalysts in the reactions of Suzuki reaction in both solvents H₂O and mixture DMF-H₂O (Table 4-8).

Table 4-8. Comparison of efficiency of various palladium catalysts in Suzuki reaction

Catalyst	Pd %	Temp	R	Solvent	Time	Yield %	ref
4.3, 4.6, 4.8	1	100	CH ₃ CO	H ₂ O	30min	100	This work
Palladacycles	0.01	100	CH ₃ CO	H ₂ O	15min	93	20
4.3, 4.6, 4.8	1	100	OCH ₃	H ₂ O	3h	85-92	This work
Pd@PMO-IL	0.2	60	OCH ₃	H ₂ O	2.5 h	>99	52
4.3, 4.6, 4.8	1	120	CH ₃ CO	DMF-H ₂ O	30min	90-94	This work
MPS-NHCPd	1	50	CH ₃ CO	DMF-H ₂ O	1h	94	53
PdL ₂ Cl ₂	0.01	110	CH ₃ CO	DMF-H ₂ O	1h	96	54
4.3, 4.6, 4.8	1	120	OCH ₃	DMF-H ₂ O	3h	70-74	This work
PdL ₂ Cl ₂	0.1	110	OCH ₃	DMF-H ₂ O	12h	76	54
4.3, 4.6, 4.8	1	120	CH ₃	DMF-H ₂ O	3h	66-69	This work
PdL ₂ Cl ₂	0.1	110	CH ₃	DMF-H ₂ O	3h	86	54

4.3-Experimental

General remarks.

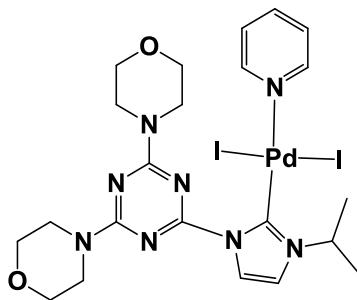
All manipulations were performed using standard glassware under Nitrogen conditions. Solvents of analytical grade were purified using a Braun-SPS solvent purification system. PdCl₂ was used as received, Pd(MeCN)₂Cl₂ was synthesised by refluxing of PdCl₂ in acetonitrile overnight under nitrogen atmosphere according to previous method. [55] Imidazolium salts that have been prepared in this work were used as a precursor ligand. NMR spectra were obtained using Bruker Avance AMX 400, 250 and JEOL Eclipse 300 spectrometers. The chemical shifts are given as dimensionless σ values and are frequency referenced relative to TMS. Coupling constants J are given in hertz (Hz) as positive values regardless of their real individual signs. The multiplicities of the signals are indicated as s, d, and m for singlets, doublets, and multiplets, respectively. The abbreviation br is given for broadened signals. High resolution mass spectra were obtained using electrospray (ES) mode unless otherwise reported, on Waters LCT Premier XE instrument. Elemental analysis worked by Elemental Analysis Service Science Centre London Metropolitan University.

X-Ray crystallographic data for **4.2**, **4.3**, **4.6**, **4.8** and **4.9**, were collected using Rigaku AFC12 goniometer equipped with an enhanced sensitivity (HG) Saturn724+ detector mounted at the window of an FR-E+ SuperBright molybdenum rotating anode generator with HF Varimax optics (70, A and 100 μ m focus). Structural solution and refinement was achieved using: SHELXL97, SHELXL-2012 and SHELXL-2014 software, and absorption correction analysed using CrystalClear-SM Expert software.

General procedure for synthesis of [PdX₂(py)(NHC)] complexes 4.1-4.8 [NHC = [2.4], [2.5], [2.6], [2.7], [2.8] [2.11], [2.12], [2.14], [2.15]

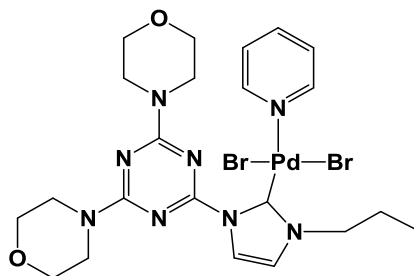
A mixture of NHC precursor (1eq), PdCl₂ (1eq) and K₂CO₃ (10 eq) in pyridine (8 mL) was heated to 80 °C with stirring for 24 hour. The solvent was removed *in vacuo*, the residue then dissolved in CH₂Cl₂ (20 mL) and filtered through a bed of celite. The product was purified by column chromatography (silica, CHCl₃/Et₂O 7:3) to give the product as a yellow powder after evaporation. Products were recrystallized by diffusion of diethyl ether in dichloromethane or chloroform.

Synthesis of [Pd(2.4)(Py)I₂], 4.1



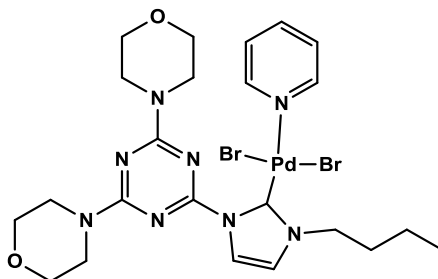
The **4.1** was prepared using imidazolium salt **[2.4H]I** (0.5 g, 1.02 mmol), PdCl₂ (0.181 g, 1.02 mmol) and K₂CO₃ (1.41 g, 10.2mmol) in pyridine (8 mL). Yield = 0.389 g (0.4 mmol) 45 %. ¹H NMR (400 MHz, CDCl₃, ppm) δ_H = 9.19 (d, *J* = 8.0 Hz, 2 H, *o*-NC₅H₅), 7.95 (d, *J* = 4.0 Hz, 1 H, imid), 7.68 (t, *J* = 8.0Hz, 1 H, *p*-NC₅H₅), 7.35 (m, 2 H, *m*-NC₅H₅), 6.93 (d, *J* = 2 Hz, 1 H, imid), 5.78 (m, 1 H, CH-N), 4.04 (m, 4 H, morpholine), 3.77 (m, 4 H, morpholine), 3.62 (m, 4 H, morpholine), 3.53 (m, 4 H, morpholine), 1.52 (d, *J* = 8.0 Hz, 6 H, 2 × CH₃). ¹³C NMR (75 MHz, CDCl₃, ppm) δ_C = 165.2, 162.2 (3 × C, triazine), 155.6 (Pd-C), 147.3 (*o*-NC₅H₅), 138.0 (*p*-NC₅H₅), 124.7 (*m*-NC₅H₅), 121.9, 117.1 (2 × C, imid), 67.3, 44.0 (4 × C, morpholine), 55.7 (CH_{isopropyl}), 44.0 (4 × C, morpholine), 22.4 (2 × C, CH₃). MS (ES⁺) for [M⁺-I], C₂₂H₃₀IN₈PdO₂ (671.51) (55%).

Synthesis of [Pd(2.5)(Py)Br₂], 4.2



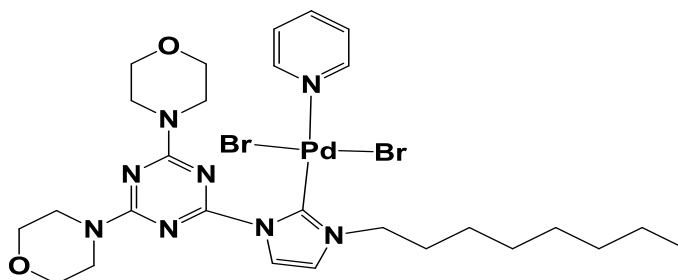
The **4.2** was prepared using imidazolium salt [**2.5H**]**Br** (1 g, 2.2 mmol), PdCl₂ (0.403 g, 2.2 mmol) and K₂CO₃ (3.1 g, 22 mmol) in pyridine (8 mL). Yield = 0.64 g (0.91 mmol) 40 %. ¹H NMR (400 MHz, CDCl₃, ppm) δ_H = 9.14 (d, *J* = 8.0 Hz, 2 H, *o*-NC₅H₅), 7.89 (d, *J* = 2.0 Hz, 1 H, imid), 7.61 (t, *J* = 7.6 Hz, 2 H, *p*-NC₅H₅), 7.28 (m, 2 H, *m*-NC₅H₅), 6.92 (d, *J* = 2.0 Hz, 1 H, imid), 4.59 (t, 2H, *J* = 2.0 Hz, 2 H, CH₂-N, propyl), 4.08 (m, 4 H, morpholine), 3.76 (m, 4 H, morpholine), 3.64 (m, 4H, morpholine), 3.47 (m, 4H, morpholine), 2.11 (m, 2 H, CH₂CH₂, propyl), 1.05 (t, *J* = 7.6 Hz, 3 H, CH₃, propyl) ppm. ¹³C NMR (75 MHz, CDCl₃, ppm) δ_C = 165.1, 161.7 (3 × C, triazine), 153.1 (Pd-C), 152.3 (*o*-NC₅H₅), 151.2 (*o*-NC₅H₅), 137.9 (*p*-NC₅H₅), 124.5 (*m*-NC₅H₅), 121.3, 121.0 (2 × C, imid) 66.9, 66.9 (4 × C, morpholine), 54.4 (N-CH₂), 44.4, 43.9 (4 × C, morpholine), 23.1 (CH₂CH₂, propyl), 11.4 (CH₃, propyl). MS (ES⁺) for [M⁺-Br], C₂₂H₃₀BrN₈PdO₂ (623.27) (40%). Anal. Calcd for C₂₂H₃₀Br₂N₈PdO₂ (704.76): C, 37.49; H, 4.29; N, 15.90. Found: C, 38.79, H, 4.82, N, 15.66.

Synthesis of [Pd (2.6)(py)Br₂], 4.3

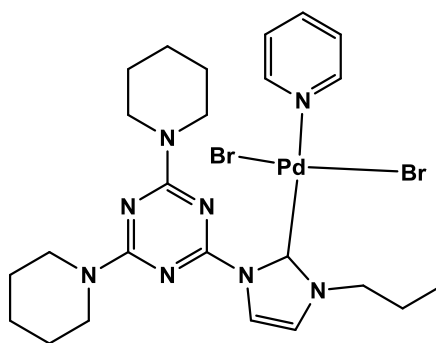


The **4.3** was prepared using imidazolium salt [**2.6H**]**Br** (0.5 g, 1.1 mmol), PdCl₂ (0.194 g, 1.1 mmol) and K₂CO₃ (1.5 g, 11 mmol) in pyridine (8 mL). Yield = 0.39 g (0.54 mmol) 50 %. ¹H NMR (400 MHz, CDCl₃, ppm) δ_H = 9.18 (d, *J* = 4.8 Hz, 2 H, *o*-NC₅H₅), 7.92 (d, 1 H, *J* = 2.4 Hz, imid), 7.75 (t, *J* = 7.6 Hz, 1 H, *p*-NC₅H₅), 7.31 (m, 2 H, *m*-NC₅H₅), 6.96 (d, *J* = 2.4 Hz, 1 H, imid), 4.69 (t, 2 H, *J* = 8 Hz, N-CH₂, butyl) 4.07 (br, 4 H, morpholine), 3.80 (br, 4 H, morpholine), 3.69 (br, 4 H, morpholine), 3.52 (br, morpholine), 2.09 (m, 2 H, CH₂, butyl), 1.51 (m, 2 H, butyl), 1.02 (t, *J* = 7.6 Hz, 3 H, CH₃-butyl). ¹³C NMR (75 MHz, CDCl₃, ppm) δ_C = 164.9, 161.7 (3 × C, triazine), 153.0 (Pd-C), 152.2 (*o*-NC₅H₅), 137.8 (*p*-NC₅H₅), 124.4 (*m*-NC₅H₅), 121.3, 121.0 (2 × C, imid), 66.6 (4 × C, morpholine), 53.5 (N-CH₂, butyl), 44.4 (4 × C, morpholine), 31.6 (CH₂, but), 20.0 (CH₂-CH₂, butyl), 13.8 (CH₃-butyl) ppm. MS (ES⁺) for [M⁺-Br], C₃₂H₃₂BrN₈PdO₂ (637.01) (32%). Anal. Calcd for C₂₃H₃₂Br₂N₈PdO₂ (718.79): C, 38.34; H, 4.49; N, 15.59. Found: C, 38.45; H, 4.58; N, 15.45.

Synthesis of [Pd (2.7)(Py)Br₂], 4.4

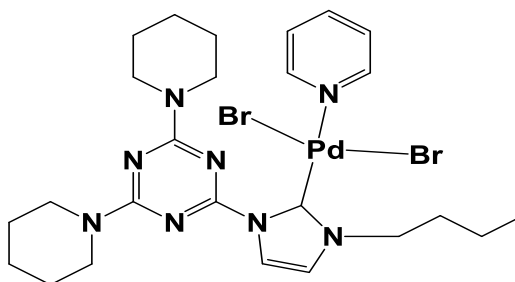


The **4.4** was prepared using imidazolium salt [**2.7H**]**Br** (0.5 g, 0.98 mmol), PdCl₂ (0.173 g, 0.98 mmol) and K₂CO₃ (1.3 g, 9.8 mmol) in pyridine (8 mL). Yield = 0.34 g (0.44 mmol) 45 %. ¹H NMR (400 MHz, CDCl₃, ppm) δ_H = 9.12 (br, 2 H, *o*-NC₅H₅), 7.88 (br, 1 H, imid), 7.71 (t, *J* = 6.4 Hz, 2 H, *p*-NC₅H₅), 7.29 (br, 2 H, *m*-NC₅H₅), 6.92 (br, 1 H, imid), 4.62 (br, 2 H, N-CH₂, Octyl), 4.02 (m, 4 H, morpholine), 3.74 (m, 4 H, morpholine), 3.63 (m, 4 H, morpholine), 3.44 (m, 4 H, morpholine), 2.09 (m, 2 H, octyl), 1.39-1.20 (br, 10 H, (CH₂)₅), 0.79 (t, *J* = 6.8, 3 H, CH₃). ¹³C NMR (75 MHz, CDCl₃, ppm) δ_C = 165.4, 161.7 (3 × C, triazine), 153.1 (Pd-C), 152.2 (*o*-NC₅H₅), 151.2 (*o*-NC₅H₅), 138.0 (*p*-NC₅H₅), 124.4 (*m*-NC₅H₅), 121.4, 121.3 (2 × C, imid) 67.0, 66.7 (4 × C, morpholine), 52.4 (N-CH₂), 44.3, 43.9 (4 × C, morpholine), 36.1, 31.8, 29.2, 26.8, 22.7, 14.18 (7 × C, octyl) ppm. (ES⁺) for [M⁺-Br+Na], C₂₇H₄₀BrNaN₈PdO₂ (716.27) (50%).

Synthesis of [Pd(2.11)(Py)Br₂], 4.5

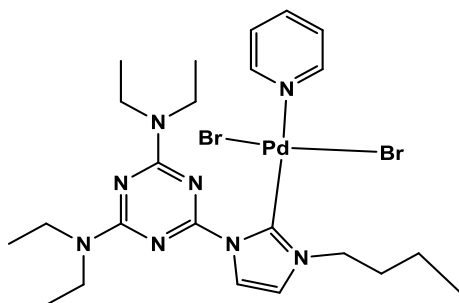
The **4.5** was prepared using imidazolium salt [**2.11H**]**Br** (0.3 g, 0.68 mmol), PdCl₂ (0.12 g, 0.68 mmol) and K₂CO₃ (0.94g, 6.8 mmol) in pyridine (8 mL). Yield = 0.20 g (0.28 mmol) 41 %. ¹H NMR (400 MHz, CDCl₃, ppm) δ_H = 9.18 (d, *J* = 8.0 Hz, 2 H, *o*-NC₅H₅), 7.93 (d, *J* = 2.4 Hz, 1 H, imid), 7.68 (t, 1 H, *J* = 8 Hz, *p*-NC₅H₅) 7.22 (m, 2 H, *m*-NC₅H₅), 6.90 (d, *J* = 2.4 Hz, 1 H, imid), 4.60 (t, *J* = 7.6 Hz, 2 H, CH₂-N), 3.96 (m, 4 H, (2 × CH₂), 3.70 (m, 4 H, (2 × CH₂), 2.06 (m, 2 H, CH₂, propyl), 1.52 (m, 4 H, (2 × CH₂), 1.48 (m, 8 H, 4 × CH₂), 1.10 (t, *J* = 7.2 Hz, 3 H, CH₃-propyl). ¹³C NMR (75 MHz, CDCl₃, ppm) δ_C = 164.6, 161.6 (3 × C, triazine), 153.2 (Pd-C), 150.4 (*o*-NC₅H₅), 137.7 (*m*-NC₅H₅), 124.3 (*p*-NC₅H₅), 121.2, 120.9 (imid), 54.3 (NCH₂), 44.8, 44.6 (4 × C, CH₂), 25.8, 25.7, 23.3 (6 × C, CH₂), 23.1 (CH₂-propyl), 11.5 (CH₃-propyl). (ES⁺) for [M⁺-Br], C₂₄H₃₄BrN₈Pd (619.11) (30 %). Anal. Calcd for C₂₄H₃₄Br₂N₈Pd (700.82): C, 41.13; H, 4.89; N, 15.99. Found: C, 42.09; H, 4.98; N, 15.95.

Synthesis of [Pd(2.12)(Py)Br₂], 4.6



The **4.6** was prepared using imidazolium salt [**2.12H**]**Br** (0.5 g, 1.1 mmol), PdCl₂ (0.19 g, 1.1 mmol), and K₂CO₃ (1.53 g, 11 mmol) in pyridine (8 mL). Yield = 0.357g (0.45 mmol) 45 %. ¹H NMR (400 MHz, CDCl₃, ppm) δ_H = 9.15 (d, *J* = 8.0 Hz, 2H, *o*-NC₅H₅), 7.92 (br, 1 H, imid), 7.69 (t, *J*_H = 8.0 Hz, 2 H, *p*-NC₅H₅), 7.27 (m, 2 H, *m*-NC₅H₅), 6.88 (br, 1 H, imid), 4.62 (m, 2 H, CH₂-N), 3.96 (m, 4 H, 2 × CH₂), 3.74 (m, 4 H, 2 × CH₂), 2.03 (m, 2 H, CH₂, butyl), 1.52 (br, 12 H, 6 × CH₂), 1.2 (m, 2 H, CH₂, butyl), 0.94 (t, *J* = 7.2 Hz, 3 H, CH₃, butyl). ¹³C NMR (75 MHz, CDCl₃, ppm) δ_C = 164.7, 161.6 (3 × C, triazine), 153.2 (Pd-C), 150.4 (*o*-NC₅H₅), 137.8 (*m*-NC₅H₅), 124.3 (*p*-NC₅H₅), 121.2, 120.9 (2 × C, imid), 52.5 (NCH₂), 44.7, 44.6 (4 × C, CH₂), 32.2 (CH₂, butyl), 25.7, 25.0 (6 × C), 20.1 (CH₂, butyl), 11.9 (CH₃, butyl). (ES⁺) for [M⁺-Br], C₂₅H₃₆BrN₈Pd (633.12) (40%). Anal. Calcd for C₂₅H₃₆Br₂N₈Pd (714.84): C, 42.01; H, 5.08; N, 15.68. Found: C, 42.13; H, 4.15; N, 15.73.

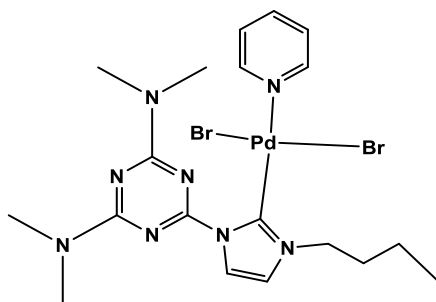
Synthesis of [Pd (2.15)(Py)Br₂], 4.7



The **4.7** was prepared using imidazolium salt [**2.15H**]**Br** (0.5 g, 1.2 mmol), PdCl₂ (0.2 g, 1.2 mmol) and K₂CO₃ (1.6 g, 12 mmol) in pyridine (8 mL). Yield = 0.4 g (0.58

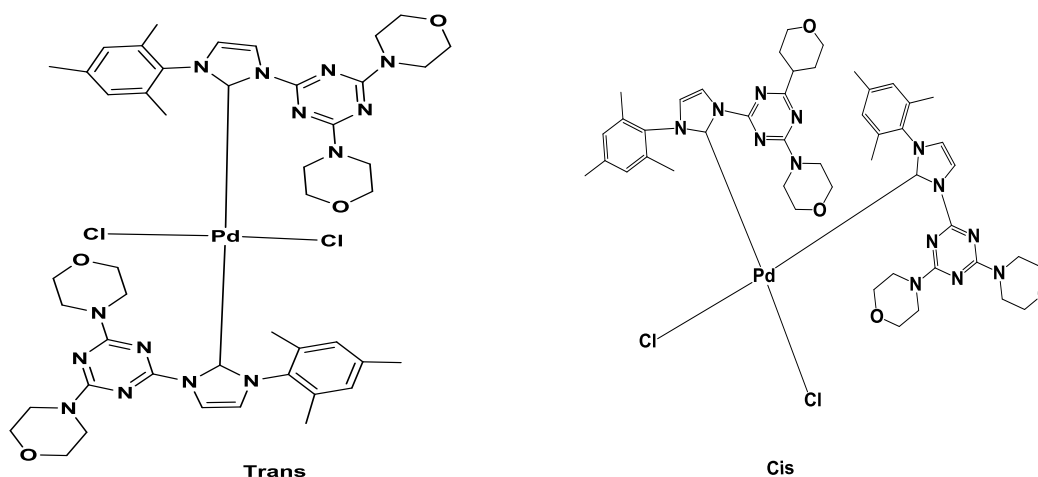
mmol) 50 %. ^1H NMR (400 MHz, CDCl_3 , ppm) $\delta_{\text{H}} = 9.24$ (d, $J = 8.0$ Hz, 2 H, *o*- NC_5H_5), 7.98 (d, $J = 1.6$ Hz, 1 H, imid), 7.68 (t, $J = 7.6$ Hz, 2 H, *p*- NC_5H_5), 7.22 (m, 2 H, *m*- NC_5H_5), 6.89 (d, $J = 2$ Hz, 1 H, imid), 4.66 (t, $J = 9.6$ Hz, 2 H, $\text{CH}_2\text{-N}$), 3.79 (m, 4 H, $2 \times \text{CH}_2$), 3.48 (m, 4 H, $2 \times \text{CH}_2$), 2.05 (m, 2 H, butyl), 1.46 (m, 2 H, butyl), 1.12 (m, 12 H, $4 \times \text{CH}_3$), 0.96 (m, 3 H, butyl). ^{13}C NMR (75 MHz, CDCl_3 , ppm) $\delta_{\text{C}} = 164.4$, 161.2 ($3 \times \text{C}$, triazine), 153.3 (Pd-C), 149.8 (*o*- NC_5H_5), 137.7 (*m*- NC_5H_5), 124.3 (*p*- NC_5H_5), 121.3 (imid), 120.8 ($2 \times \text{C}$, imid), 52.6 ($\text{CH}_2\text{-N}$), 41.7 ($4 \times \text{C}$, CH_2), 31.7 (1C, butyl), 20.2 (1C, butyl), 13.9 ($4 \times \text{C}$, CH_3), 13.10 (1 C, butyl). MS (ES^+) for $\text{C}_{22}\text{H}_{36}\text{BrN}_8\text{Pd}$ [$\text{M}^+\text{-Br}$] (610.92)(40%).

Synthesis of [Pd (2.14)(Py)(Br) $_2$], 4.8

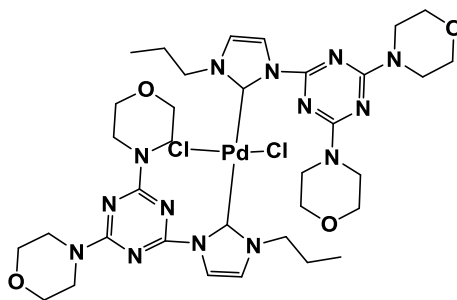


The **4.8** was prepared using imidazolium salt [**2.14H**]**Br** (0.5 g, 1.3 mmol), PdCl_2 (0.23 g, 2.4 mmol) and K_2CO_3 (1.7 g, 13 mmol) in pyridine (8 mL). Yield = 0.37 g (0.59 mmol) 44 %. ^1H NMR (250 MHz, CDCl_3 , ppm) $\delta_{\text{H}} = 9.13$ (d, $J = 6.4$ Hz, 2 H, *o*- NC_5H_5), 7.91 (d, $J = 7.6$ Hz, 1 H, imid), 7.69 (t, 1 H, $J = 8$ Hz, *p*- NC_5H_5), 7.22 (m, 2 H, *m*- NC_5H_5), 6.92 (d, $J = 7.6$ Hz, 1 H, imid), 4.60 (t, $J = 7.6$ Hz, 2 H, $\text{CH}_2\text{-N}$), 3.35, 3.10 (br, 12 H, ($4 \times \text{CH}_3$), 2.05 (m, 2 H, CH_2), 1.48 (m, 2 H, (CH_2), 1.10 (t, $J = 7.2$ Hz, 3H, CH_3 , butyl). ^{13}C NMR (100 MHz, CDCl_3 , ppm) $\delta_{\text{C}} = 164.3$, 160.1 ($3 \times \text{C}$, triazine), 152.0 (Pd-C), 149.5 (*o*- NC_5H_5), 136.6 (*m*- NC_5H_5), 123.3 (*p*- NC_5H_5), 120.0, 119.9 (imid), 51.4 (NCH_2), 35.9, 35.2 ($4 \times \text{C}$, CH_3), 30.7 ($\text{CH}_2\text{-butyl}$), 19.0 ($\text{CH}_2\text{-butyl}$), 12.8 ($\text{CH}_3\text{-butyl}$). MS (ES^+) for [M-Br] $^+$, $\text{C}_{19}\text{H}_{28}\text{BrN}_8\text{Pd}$ (554.81)(40%).

Synthesis of [Pd(2.8)₂Cl₂], 4.9



In a 50 mL conical flask, silver complex **3.5** (0.1 g, 0.173 mmol) and Pd(CH₃CN)₂Cl₂ (0.022 g, 0.086 mmol) in CH₂Cl₂ (20 mL) were stirred overnight at room temperature before filtration through celite. The solvent was removed *in vacuo* and the resulting solid recrystallised (CH₂Cl₂/Et₂O). *Trans* isomer ¹H NMR (250 MHz, CDCl₃, ppm) δ_H = 7.85 (d, *J* = 2.3 Hz, 2 H, C₅, imid), 6.78 (s, 4 H, mesityl), 6.62 (d, *J* = 2.0 Hz, 2 H, C₄, imid), 3.85-3.63 (br, 32 H, morpholine), 2.45 (s, 6 H, 2 × CH₃) 2.0 (s, 12 H, 4 × CH₃). *Cis* isomer ¹H NMR (250 MHz, CDCl₃, ppm) δ_H = 8.32 (d, *J* = 2 Hz, 2 H, C₅, imid), 6.88 (br, 2 H, mesityl), 6.67 (d, *J* = 2.3 Hz, 2H, C₄, imid), 6.36 (br, 2 H, mesityl) 4.02-3.69 (br, 32 H, morpholine), 2.31 (s, 6 H, 2 × CH₃) 2.19 (s, 6H, 2 × CH₃), 1.38 (s, 6 H, 2 × CH₃). ¹³C NMR (75 MHz, CDCl₃, ppm) δ_C = 165.4, 164.3, (3 × C, triazine), 161.1 (Pd-C), 138.8, 137.7, 135.9, 133.0, 129.8, 128.2 (mesityl), 66.9, 66.5 (8 × C, morpholine), 45.9, 44.1 (8 × C, morpholine), 21.3, 19.7, 17.4 (methyl). MS (ES⁺) for [M-Cl]⁺, C₄₆H₅₉ClN₁₄O₄Pd 1012.33 (100 %).

Synthesis of [Pd(2.5)₂Cl₂], 4.10

Prepared similarly from silver complex **3.2** (0.1 g, 0.193 mmol) and Pd(CH₃CN)₂Cl₂ (0.025 g, 0.99 mmol). ¹H NMR (400 MHz, CDCl₃, ppm) δ_H = 7.88 (br, 2H, C₅, imid), 6.95 (br, 2H, C₄, imid), 4.73 (br, 4H-NCH₂), 4.32-4.73 (br, 32 H, morpholine), 2.05 (br, 4H-CH₂), 1.15 (br, 6H, CH₃). ¹³C NMR (100 MHz, DMSO, ppm) δ_C = 164.1, 160.1 (6 × C-triazine), 155.9 (Pd-C), 66.2, 66.7, 44.3, 43.6 (16 × C, morpholine), 53.1 (2 × C, NCH₂, Propyl), 22.7 (2 × C, CH₂-propyl), 10.9 (2 × C, CH₃, propyl). MS (ES⁺) for [M⁺-Cl], C₃₄H₅₀ClN₁₄O₄Pd 859.18 (100 %).

General procedure for Suzuki coupling of aromatic

A Schlenk flask was charged with aryl halide (1 mmol), aryl boronic acid (1.2 mmol), K₂CO₃ (3 mmol), 1% catalyst, 1,3,5-trimethoxy benzene(0.33 mmol) and water (10 mL) or DMF/H₂O (10: 0.5 mL). The mixture was stirred under reflux in air for a specific time. After the reaction was stopped, the reaction mixture was extracted with diethyl ether 3 times. The organic phases were evaporated and the subsequent residue was purified by flash chromatography on silica gel.

4.4-References

- (1) S. Díez-González and S. P. Nolan, *Coord. Chem. Rev.* 2007, **251**, 874.
- (2) W. A. Herrmann, M. Elison, J. Fisher, C. Kocher and G. R. J. Artus, *Angew. Chem. Int. Ed. Engl.* 1995, **34**, 2371.
- (3) W. A. Herrmann, C. Reisinger, and M. Spiegler *Organometallics* 1998, **557**, 93.
- (4) W. A. Herrmann, J. Schwarz, M. G. Gardiner and M. Spiegler, *J. Organometallics* 1999, **575**, 80.
- (5) K. Randell, M. J. Stanford, G. J. Clarkson and J. P. Rourke, *Organometallics* 2006, **691**, 3411.
- (6) M. I G. Gardiner, W. A. Herrmann, C. Reisinger, J. Schwarz and M. Spiegler, *Organometallics* 1999, **572**, 239.
- (7) L. Li, J. Wang, C. Zhou, R. Wang and M. Hong, *Green. Chem.* 2011, **13**, 2071.
- (8) H. Lebel, M. K. Janes, A. B. Chartte and S. P. Nolan, *J. Am. Chem. Soc.* 2004, **126**, 5046.
- (9) K. S. Coleman, S. Turberville, S. I. Pascu and M. L. H. Green, *Organometallics* 2005, **590**, 653.
- (10) D. Enders and H. Gielen, *Organometallics*. 2001, **617-618**, 70.
- (11) H. M. Lee, P. L. Chiu and J.Y. Zeng, *Inorg. Chimica. Acta.* 2004, **357**, 4313
- (12) H. Lv, L. Zhu, Y. Tang and J. Lu. *Appl. Organomet. Chem.* 2014, **28**, 27.
- (13) S. P. Nolan and M. S. Viciu, *Top. Organomet. Chem.* 2005, **14**, 241.
- (14) D. S. McGuinness and K. J. Cavell, *Organometallics* 2000, **19**, 741.

- (15) S. Liu, C. Lee, C. Fu, C. Chen, Y. Liu, C. J. Elsevier, S. Peng and J. Chen, *Organometallics* 2009, **28**, 6957.
- (16) B. Murray, B. David, A. Haque, R. Haque, R.A; Skelton and B. W Allan, *J. Inclusion Phenomena and Macrocyclic Chemistry*. 2009, **65**,. 97.
- (17) M. R. L. Furst and C. S. J. Cazin, *Chem. Commun.* 2010, **46**, 6924.
- (18) L. Ray, M. M. Shaikh and P. Ghosh, *Dalton Trans.* 2007, **40**, 4546.
- (19) C. J. O'Brien, E. B. Kantchev, C. Valente, N. Hadei, G. A. Chass, A. Lough, A. C. Hopkinson and M.G. Organ, *Chem. Eur. J.* 2006, **12**, 4743.
- (20) L Benhamou, C. Besnard and E. Ndig, *Organometallics*. 2014, **33**, 260.
- (21) J. Nasielski, N. Hadei, G. Achonduh, E. Kantchev, C. J. O'Brien, A. Lough and M. G. Organ, *Chem. Eur. J.* 2010, **16**, 10844.
- (22) J. P. Corbet and G. R. Mignani, *Chem. Rev.* 2006, **106**, 2651.
- (23) Y.-R. Lou. *Comprehensive Handbook of Chemical Bond Energies CRC Press, London.* 2007.
- (24) S. R. Chemler, D. Trauner and S. J. Danishefsky, *Angew. Chem., Int. Ed.* 2001, **40**, 4544.
- (25) T. Yamamoto, K. Kobayashi, T. Yasuda, Z.-H. Zhou, I. Yamaguchi, T. Ishikawa and S. Koshihara, *Polym. Bull.* 2004, **52**, 315.
- (26) S. Lin, Z.-Q. Yang, B. H. B. Kwok, M. Koldobskiy, C. M. Crews, and S. J. Danishefsky, *J. Am. Chem. Soc.* 2004, **126**, 6347.
- (27) A. Suzuki. *J. Organomet. Chem.* 1999, **576**, 147.
- (28) S. Kotha, K. Lahiri and D. Kashinath, *Tetrahedron*. 2002, **58**, 9633.
- (29) A. F. Littke and G. C. Fu. *Angew. Chem. Int. Ed.* 2002, **41**, 4176.
- (30) C. W. K. Gst[^]ttmayr, V. P. W. B[^]hm, E. Herdtweck, M. Grosche and W. A. Herrmann, *Angew. Chem. Int. Ed.* 2002, **41**, 1363.

- (31) G. Altenhoff, R. Goddard, C. W. Lehmann and Frank Glorius, *Angew. Chem. Int. Ed.* 2003, **42**, 3690.
- (32) O. Navarro, N. Marion, Y. Oonishi, R. Kelly III and S. P. Nolan, *J. Org. Chem.* 2006, **71**, 685.
- (33) L. Ray, S. Barman, M. M. Shaikhand Pr. Ghosh, *Chem. Eur. J.* 2008, **14**, 6646.
- (34) S. Grundemann, M. Albrecht, J. A. Loch, J. W. Faller and R. H Crabtree, *Organometallics*. 2001, **20**, 5485.
- (35) W. A. Herrmann, V. P. W. Böhm, C. W. K. Gstöttmayr, M. Grosche, C. P. Reisinger and T. Weskamp. *Organometallics*. 2001, **617–618**, 616.
- (36) H. M. J. Wang, I. J. B. Lin, *Organometallics*. 1998, **17**, 972
- (37) R. Kamisue and S. Sakaguchi, *Organometallics*. 2011, **696**, 1910.
- (38) J. A. Loch, M. Albrecht, E. Peris, J. Mata, J. W. Faller and R. H. Crabtree, *Organometallics* 2002, **21**, 700.
- (39) A. Bertogg, F. Campanovo and A. Togni, *Eur. J. Inorg. Chem.* 2005, **2** 347.
- (40) A. A. Tulloch, D. S. Winston, A. A. Danopoulos, G. Eastham and M. B. Hursthouse, *Dalton.Trans.* 2003, **4**, 699.
- (41) S. Gründemann, M Albrecht, A. Kovacevic, J.W. Faller and R. H. Crabtree, *J. Chem. Soc. Dalton Trans.* 2002, 2163.
- (42) Mihai . S. Viciu, O Navarro, R F. Germaneau, R A. Kelly III, W Sommer, N Marion, E.D. Stevens, L Cavall and S P. Nolan, *Organometallics* 2004, **23**, 1629.
- (43) G. A. Grasa, M. S. Viciu, J. Huang, C. Zhang, M. L. Trudell, and Steven P. Nolan, *Organometallics*. 2002, **21**, 2866.

- (44) R. Vilar and U. Christmann, *Angew. Chem. Int. Ed.* 2005, **44**, 366.
- (45) L. Botella and C. Nájera, *Angew. Chem. Int. Ed.* 2002, **41**, 179.
- (46) Luis Botella and C. Na´jera *Organometallics*. 2002, **663**, 46.
- (47) Y. Zhang, M. Feng and J. Mei Lu, *Org. Biomol. Chem.* 2013, **11**, 2266.
- (48) W. Huang, J. Guo, Y. Xiao, M. Zhu, G. Zou and J. Tang, *Tetrahedron*. 2005, **61**, 9783.
- (49) S. K. Movahed, R. Esmatpoursalmani and A. Bazgir, *RSC. Adv.* 2014, **4**, 14586.
- (50) M. Ghiaci, M. Zarghani, A. Khojastehnezhad and F Moeinpour, *RSC Adv.* 2014, **4**, 15496.
- (51) V. V Grushin and H. Alper, *Chem. Rev.* 1994, **94**, 1047.
- (52) B. Karimi, D. Elhamifar, J. H. Clark, and A. J. Hunt, *Chem. Eur. J.* 2010, **16**, 8047.
- (53) D. Lee, J. Kim, B. Jun and H. Kang, *Org. Lett.* 2008, **10**, 1609.
- (54) W. Huang, J. Guo, Y. Xiao, M. Zhu, G. Zou and J. Tang, *Tetrahedron*. 2005, **61**, 9783
- (55) C. J. Mathews, P. J. Smith; T. Welton, *J. Mol. Catal. A Chem.* 2003, **206**, 77.

Chapter 5

Synthesis and characterization of new Ru(II)-NHC complexes and their application in transfer hydrogenation reactions

5.1-Introduction

The synthesis of Ru-NHC complexes has seen some significant development due to the wide range of accessible oxidation states and coordination geometries available to ruthenium. [1] The complexes are obtained with ease and are efficient catalysts in many applications such as hydrogen transfer, hydrogenation, hydrosilylation, isomerization and ring-closing metathesis (RCM). [2-6]

5.1.1-Types of Ru-NHC complexes

Ru-NHC complexes can be classified by the other ligand types bound to the ruthenium centre. These include hydrides (**1**), [7] arenes (**2**), [8] alkylidenes (**3**), [9] vinylidenes and indenylidenes (**4**), [10] Schiff – bases (**5**). [11] Furthermore, the NHC–Ru complex can be immobilised on a solid support (**6**) (Figure 5-1). [12]

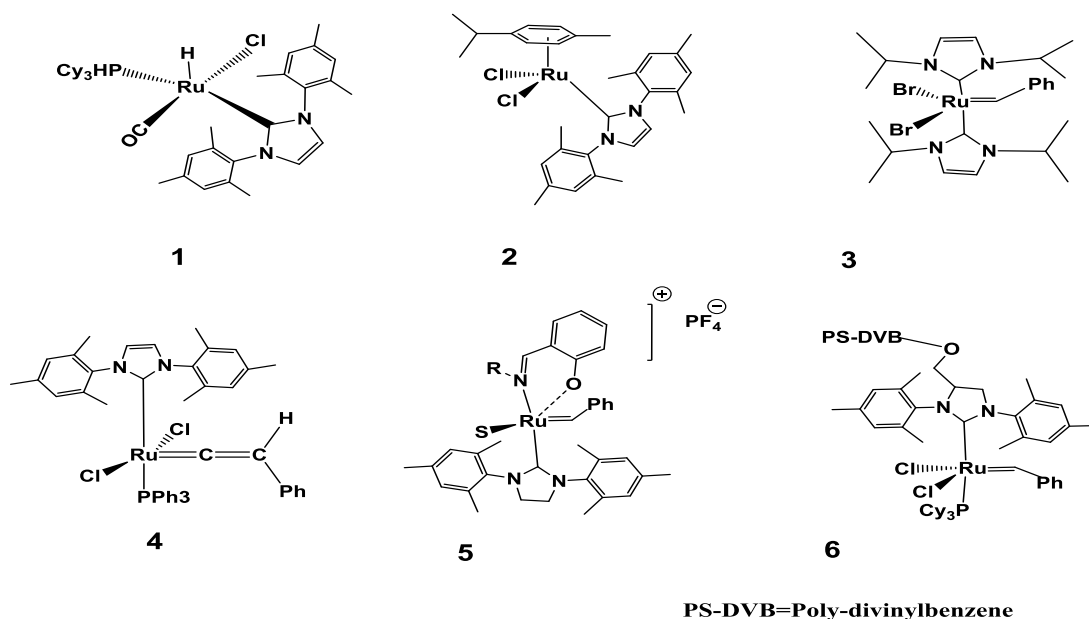
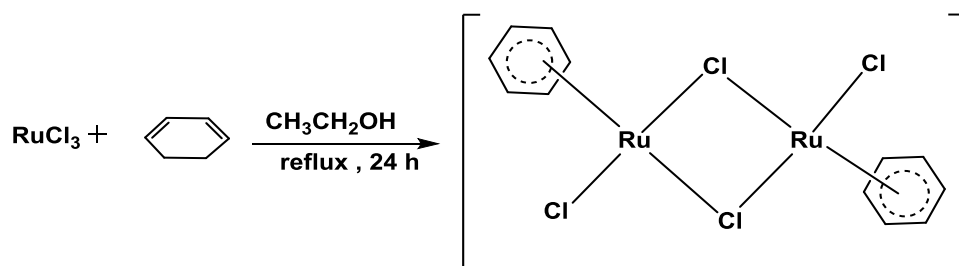


Figure (5-1) Types of Ru-NHC complexes

5.1.1.1-NHC–Ru arene complexes

Mono-carbene η^6 -arene-ruthenium complexes, $[\text{Ru}(\eta^6\text{-arene})(\text{NHC})\text{Cl}_2]$, have been received much attention due to their ease of access from the commercially available ruthenium dimer, $[(\text{arene})\text{RuCl}_2]_2$ and their stability towards both moisture and air. Many such complexes have displayed good catalytic activity in transfer hydrogenation reactions.

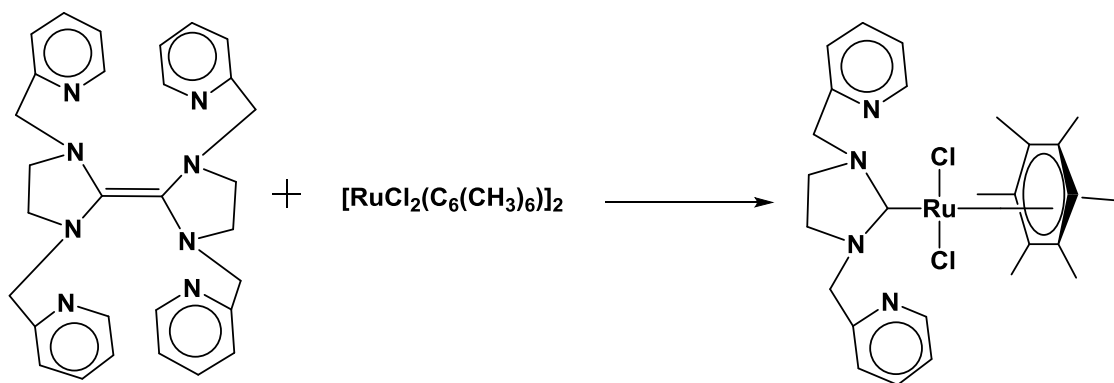
The reaction of ruthenium(III) trichloride with 1,3 or 1,4 cyclohexadiene or α -phellandrene (5-isopropyl-2-methylcyclohexane,1,3-diene) in ethanol generates $[(\eta^6\text{-benzene})\text{RuCl}_2]_2$ or $[(p\text{-cymene})\text{RuCl}_2]_2$ respectively as a brown product. These react with NHC ligands to produce complexes such as $[\text{RuCl}_2(\text{NHC})(\eta^6\text{-benzene})]$, $[\text{RuCl}_2(\text{NHC})(p\text{-cymene})]$ respectively (Scheme 5-1). [13]



Scheme (5-1) Preparation of $[(\eta^6\text{-arene})\text{RuCl}_2]_2$

The complexes are obtained by either directly reacting imidazolium salts with $[(\text{arene})\text{RuCl}_2]_2$ or *via* ligand transfer from Ag-NHC complexes. The reaction of the imidazolium salts with $[(\text{arene})\text{RuCl}_2]_2$ is conducted by refluxing the mixture for a specific time. A variety of solvents have been used for this reaction.

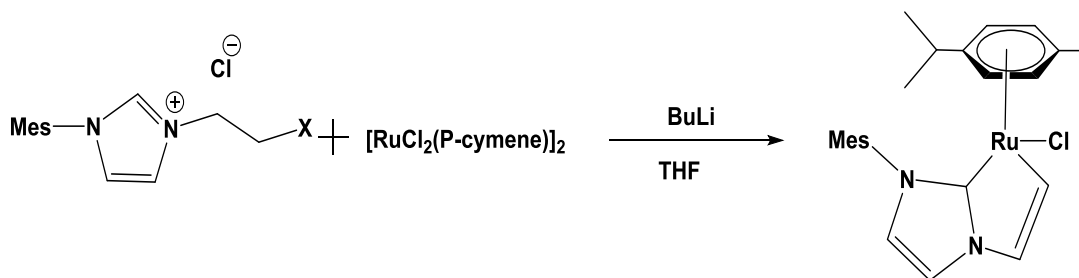
$\text{RuCl}_2(\text{NHC})(\text{arene})$ (NHC = 1,3-bis(2-picolyl) imidazolin-2-ylidene, arene = $\text{C}_6(\text{CH}_3)_6$) was obtained by Özdemir by the direct reaction of 1,3-bis(2-picolyl)imidazolin-2-ylidene with $[\text{RuCl}_2(\text{C}_6(\text{CH}_3)_6)]_2$ for 4 hours at 100 °C to produce an orange product in 87% yield (Scheme 5-2). [14]



Scheme (5-2) Synthesis of $[\text{RuCl}_2(\text{NHC})(\text{C}_6(\text{CH}_3)_6)]$

An unexpected cyclometalated ruthenium complex was obtained by Dixneuf *et al* in 2006. [15] The intramolecular product was obtained by reaction of 1-mesityl-3-halo propyl imidazolium chloride with $[\text{Ru}(p\text{-cymene})\text{Cl}_2]$ in the presence BuLi.

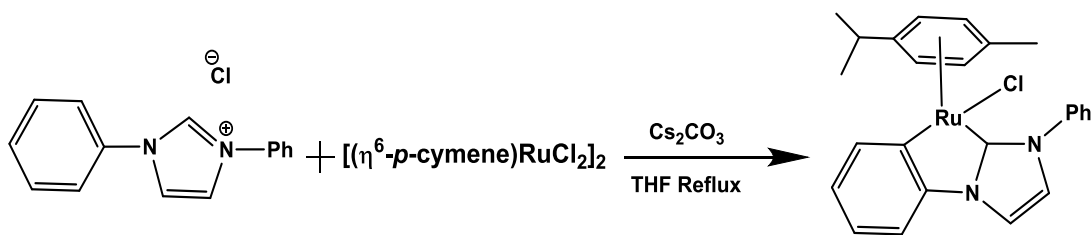
Formation of the complex proceeds *via* double deprotonation of the imidazolium salt leading to the vinyl carbene. Elimination of HCl from the coordination sphere of ruthenium yields the cyclometalated product, the structure of which has been confirmed by X-ray diffraction and is consistent with previous literature (Scheme 5-3). [16]



Scheme (5-3) Synthesis of a cyclometalated Ru complex

A series of bis-carbene complexes of ruthenium have been prepared by Paris *et al* *via* reaction of $[(\text{p-cymene})\text{RuCl}_2]_2$ with methylene bis(N-alkyl imidazolium) iodide (alkyl = methyl, neopentyl) and ethylene bis-(N-methylimidazolium) chloride. The reactions were conducted in refluxing CH_3CN and promoted by NEt_3 . The complexes were tested as catalysts for hydrogen transfer between alcohols and ketones, unfortunately the results were unsuccessful. [17]

In 2014, Wang *et al* prepared a series of NHC-based cyclometalated ruthenium complexes. The complexes were obtained by directly reacting aryl substituted imidazolium salts with $[(\text{p-cymene})\text{RuCl}_2]_2$ in the presence of Cs_2CO_3 . The complexes have been characterized by ^1H and ^{13}C NMR spectroscopy, and single-crystal X-ray diffraction analysis (Scheme 5-4). [18]



(Scheme 5-4) synthesis of $[\text{Ru Cl (NHC) (} p\text{-cymene)}]$

Ru–NHC complexes have also been prepared *via* transmetallation. Silver carbene complexes have been used as a ligand transfer agents due to their lability and fluxional behavior. This method has proven successful when Wang *et al* successfully prepared $\text{Pd}(\text{Et}_2\text{-Bimy})_2\text{-Cl}_2$, $\text{Au}(\text{Et}_2\text{-Bimy})\text{Br}$ and $[\text{Au}(\text{Et}_2\text{-Bimy})_2]\text{PF}_6$ *via* ligand transfer from $[\text{Ag}(\text{Et}_2\text{-Bimy})_2]$ $[\text{AgBr}_2]$ and $[\text{Ag}(\text{Et}_2\text{-Bimy})_2]\text{PF}_6$. [19]

Transmetalation offers many advantages over the direct route such as air stability, no requirement for the addition of base and deprotonation of the azolium salts only occurs at the C2 leaving other acidic protons in the azolium salts intact.[20]

Transmetalation can be achieved using either isolated silver complexes or alternatively the $\text{Ag}(\text{NHC})$ species can be prepared *in situ* by reacting Ag_2O with an imidazolium salt followed by addition of the Ru source in a one pot procedure.

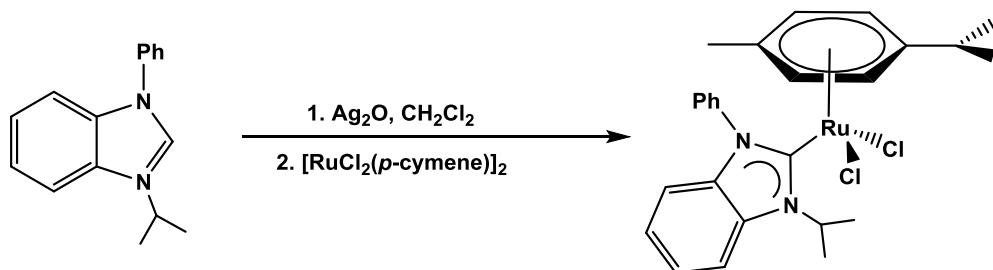
This method was used to avoid the harsh conditions required to obtain the desired complexes, and can be used where the direct reaction is unsuccessful. [21, 22]

Transmetalations are usually performed in dry solvents at room temperature, [23] care must be taken to exclude all light from the reaction mixture in order to avoid decomposition of the silver species.

Due to these advantageous features this method has been widely used for the preparation of ruthenium complexes. [24- 28]

Recently, $[\text{Ru}(p\text{-cymene})(\text{NHC})\text{Cl}_2]$ complexes have been synthesized by reacting $[\text{RuCl}_2(p\text{-cymene})]_2$ with the corresponding Ag-NHC complex. Asymmetrical

benzimidazolium salts react with Ag_2O in CH_2Cl_2 furnishing the air and moisture stable silver complex. The corresponding Ru complex was proven to be an efficient catalyst for the alkylation of amines (Scheme 5-5). [29]



Scheme (5-5) Synthesis of Ru complex *via* transmetalation

The formation of the complex was confirmed by the absence of the NCHN peak in the ^1H NMR spectrum and peak corresponding to Ru-C was observed at 189 ppm in the ^{13}C NMR. X-ray crystallography further confirmed the expected molecular structure.

The first ruthenium–NHC complex bearing sulfonate side arms was prepared by treatment of the silver complex with $[(\text{Ru}(p\text{-cymene})\text{Cl}_2)_2]$ to produce $[\text{Ru}(\text{NHC})(p\text{-cymene})\text{Cl}]\text{PF}_6$ as a yellow powder in 86% yield. The carbene was observed at 173.4 ppm in the ^{13}C NMR spectrum (Figure 5-2). [30]

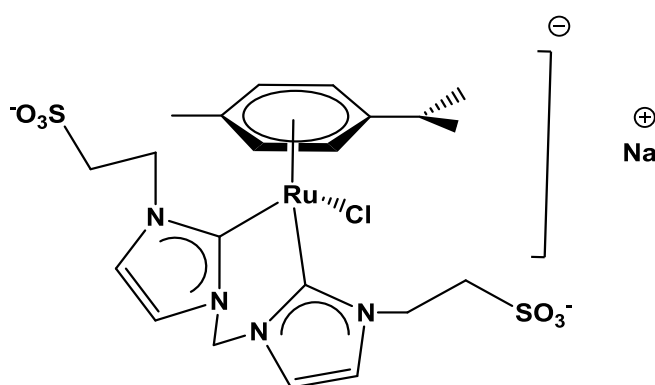


Figure (5-2) Ru complex with sulfonate chain

A cyclometalated ruthenium complex was obtained by Cross *et al* in 2011. The complex bearing a bidentate amine–NHC ligand was obtained by reaction of the

silver complex with [(*p*-cymene)RuCl₂]₂. The silver complex was prepared by reacting the aniline functionalized imidazolium salt with Ag₂O prior to addition of the ruthenium source. The product was collected in 51% yield after column chromatography. The ¹³C NMR spectrum shows peaks corresponding to the Ru-C centre at 175.9 ppm. The complex was proven to be an efficient catalyst for transfer hydrogenation reactions. [31]

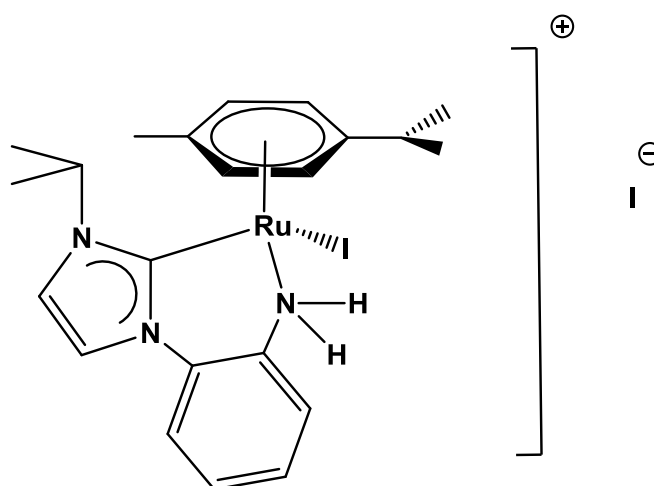
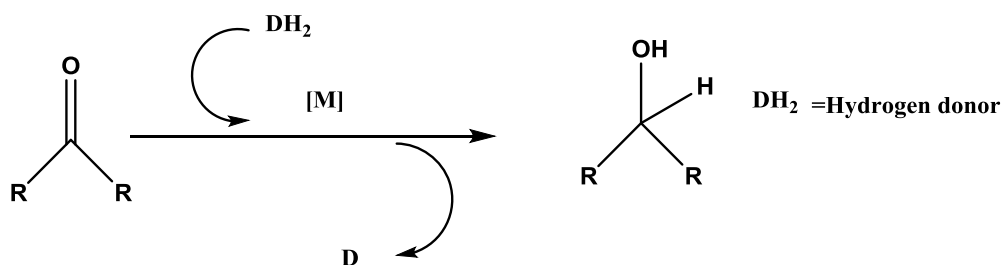


Figure (5-3) Bidentate amino-NHC Ru complex

5.1.2-Transfer hydrogenation application

Transfer hydrogenation reactions are widely used in the synthesis of many organic compounds. The reactions take place between unsaturated compounds, such as carbonyls, imines, alkenes and alkynes, with proton donor sources, such as isopropanol, which is usually present in excess as the reaction solvent. Deprotonation is facilitated by a suitable base and the reaction proceeds in the presence of a catalyst. [32- 36] Isopropanol is an ideal hydrogen source due to its stability, low toxicity and cost, its ability to dissolve many organic compounds and the ease with which it can be handled. Furthermore, the use of isopropanol leads to the production of acetone as a side product which can be easily removed (Scheme 5-6).

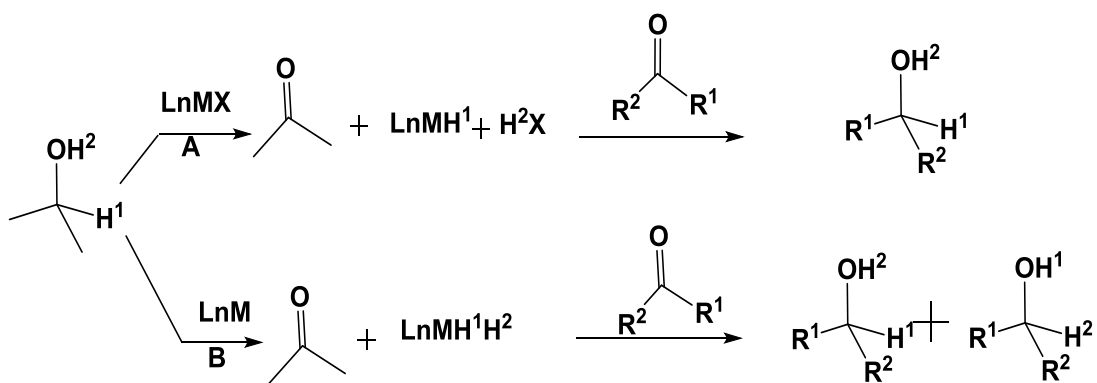


Scheme (5-6) General equation for transfer reaction

Transfer hydrogenation reactions are preferred over the use of molecular hydrogen for reduction of unsaturated compounds as it is operationally simple, environmentally benign, economical and safe, even on large scales. [37- 41]

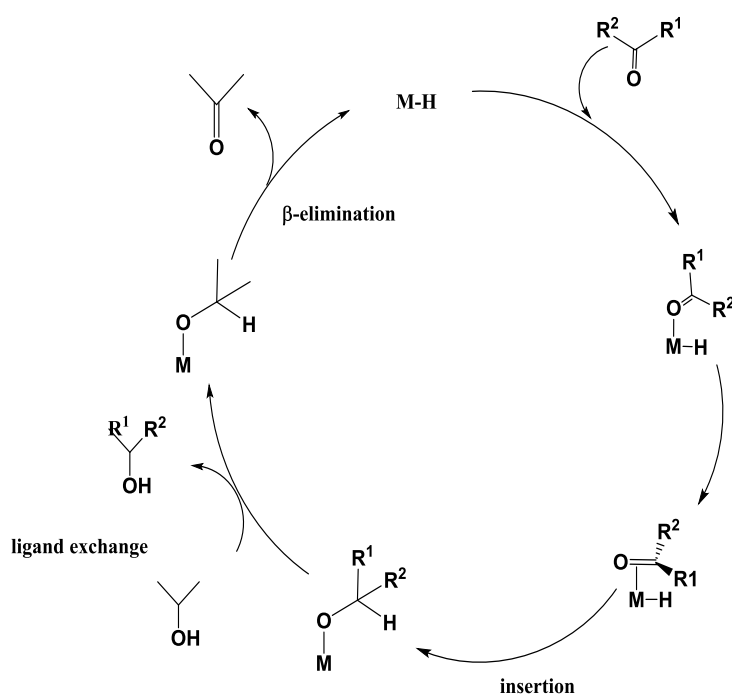
Two mechanisms have been proposed for transfer hydrogen reactions depending on the number of hydrogen atoms which are transferred from the substrate to the metal. In the monohydridic route, only one hydrogen atom is transferred from the substrate to the metal, while in the dihydridic route both hydrogen atoms are transferred to the metal (Scheme 5-7). [42, 43]

In both mechanisms the metal hydride is formed by β -hydride elimination from a donor such as 2-propanol, the hydride is then transferred to an unsaturated acceptor such as a ketone. [44]



Scheme (5-7) Monohydridic (A), dihydridic (B) mechanisms of transfer hydrogenation

The monohydric mechanism can operate by one of two routes, either an alkoxide-metal species is formed and the hydrogen is transferred from the alcohol to the metal in the inner-sphere of the metal or the hydrogens are transferred in the outer-sphere of the metal without prior formation of the alkoxide. In the inner-sphere mechanism the carbonyl first binds through π -coordination of the double bond and then inserts into the metal-hydride to form a metal-alkoxide before displacement by isopropanol to release the product. The metal-hydride is then regenerated by β -hydride elimination from the isopropanol (Scheme 5-8).



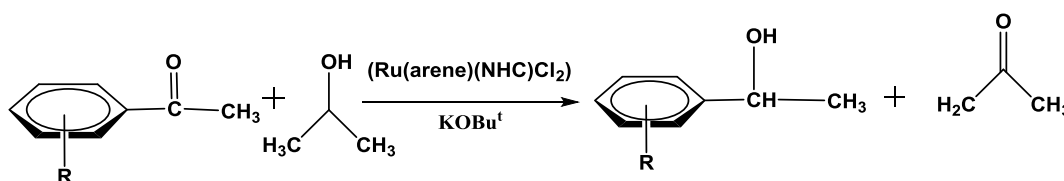
Scheme (5-8) Inner-sphere mechanism

Transition metal-NHC complexes were first used as catalytic transfer hydrogenation agents by Nolan *et al* in 2001 who prepared three Ir complexes which proved to be active catalysts for the reduction of ketones. [45]

NHC-Ru arene complexes [Ru(arene)(NHC)Cl₂] have been employed as catalysts for transfer hydrogenation in the preparation of many alcoholic compounds. This type of

ruthenium complex has proven highly efficient in transfer hydrogenation of ketones to their corresponding alcohols.

Özdemir has prepared an array of $(\text{Ru}(\text{arene})(\text{NHC})\text{Cl}_2)$ complexes and studied their use in transfer hydrogenation reactions. (Scheme 5-9) Derivatives of acetophenone have been reduced with isopropanol as a hydrogen source at 80 °C in the presence of $\text{KO}^\text{t}\text{Bu}$ to obtain the corresponding alcohols in good yields (86-99%) with the exception of *meta*-bromoacetophenone (62-78 %). [14]



Scheme (5-9) Reduction of acetophenone derivatives *via* transfer hydrogenation

Cyclometalated ruthenium complexes bearing bidentate carbene/ NH_2 and iodide ligands have been prepared and applied to transfer hydrogenation reactions. The complexes were obtained by reacting the dimers $[\text{Ru}(p\text{-cymene})\text{Cl}_2]_2$ or $[\text{RuCp}^*\text{Cl}_2]_2$ where Cp^* = pentamethylcyclopentadienylide) with the primary amine functionalized imidazolium salts. Acetophenone was reduced with isopropanol in the presence of $\text{NaO}^\text{t}\text{Bu}$ at 80 °C. High temperatures were found to be crucial; $[\text{Ru}(p\text{-cymene})(\text{C},\text{NH}_2)\text{I}]\text{I}$ gave conversions of > 90% after only 0.5 h at 80 °C, while no conversion was detected at 20 °C even after 72 h.[31]

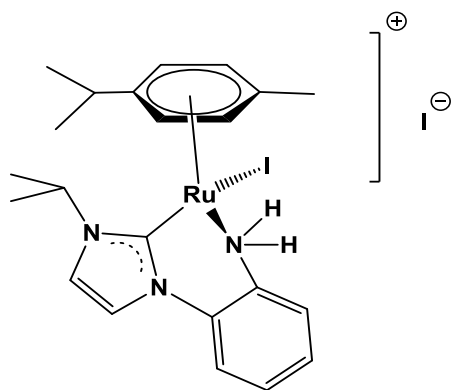


Figure (5-4) [Ru(NHC)(p-cymene)I]I

Mono and bis NHC complexes of Ru with p-cymene and benzene co-ligands were prepared by Papish *et al* and applied to transfer hydrogenation reactions. For the reduction of acetophenone with isopropanol, the highest TOF (turnover frequency) and TON (turnover number) values obtained were 3003 h^{-1} and 845 respectively. The yields were determined by ^1H NMR spectroscopy using 1,3,5-trimethoxybenzene as an internal standard. [46]

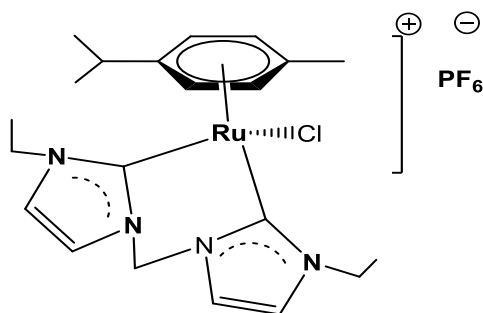
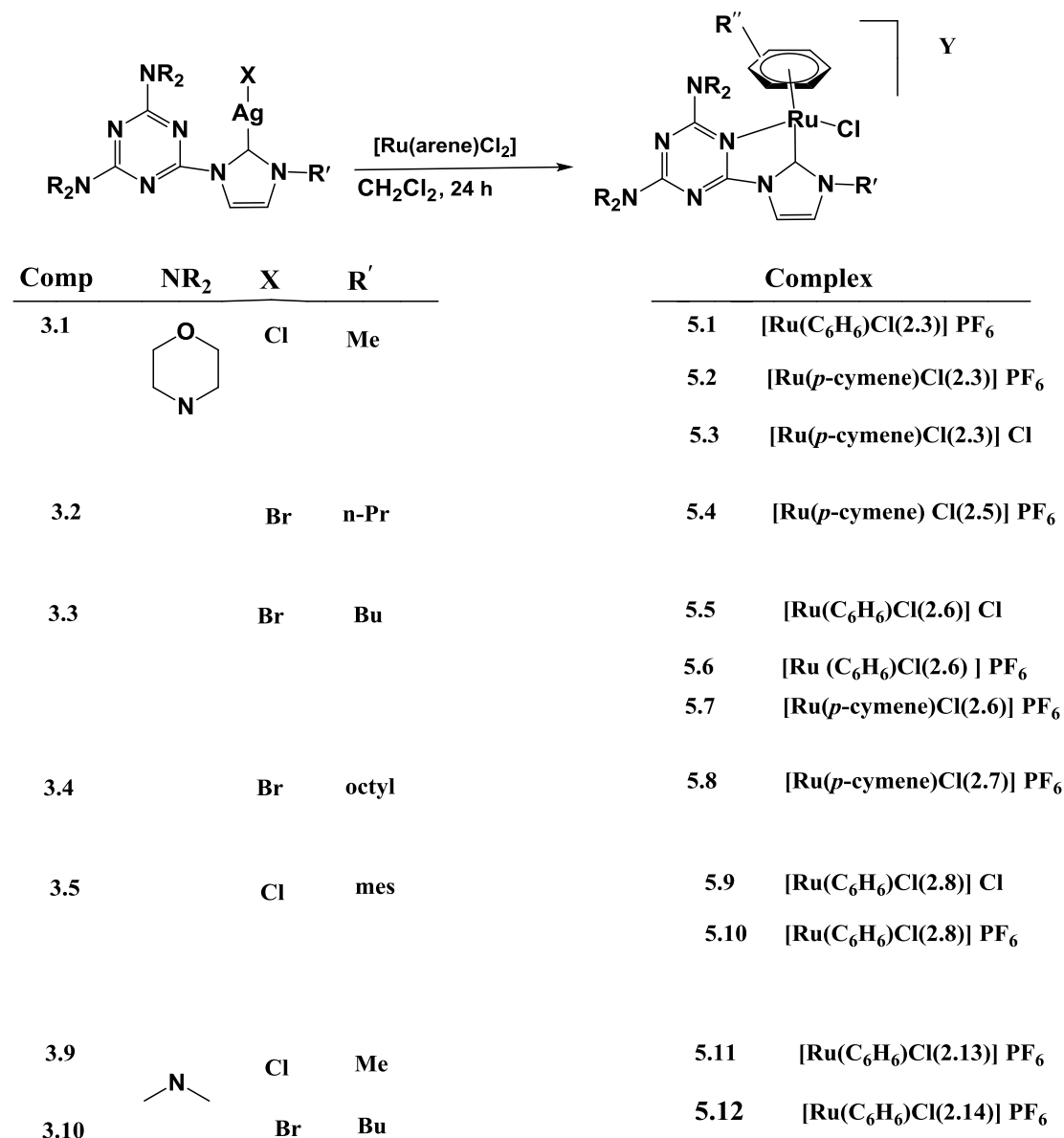


Figure (5-5) [Ru(NHC)₂(p-cymene)Cl]PF₆

5.1.3-Aim

This chapter discusses the synthesis, characterisation and catalytic reactivity of [Ru(arene)(NHC)Cl]Y complexes (where Y = Cl, PF₆ and arene = benzene, *p*-cymene). The transmetallation method was used for the synthesis of the complexes *via* the reaction of the corresponding Ag-NHC complexes with [Ru(arene)Cl₂]₂ in dichloromethane at room temperature under nitrogen. NMR spectroscopy and mass spectrometry, as well as elemental analyses and X-ray crystallography were used to confirm the formation of complexes. Ru-NHC complexes were tested in transfer hydrogenation reactions for reduction of ketones to the corresponding alcohols (Scheme 5-10).



Scheme (5-10) Preparation of Ru(II) complexes; Reagents and conditions (**5.1, 5.5, 5.6, 5.9, 5.10, 5.11, 5.12**) 0.5 eq [RuCl₂(C₆H₆)₂], Ag(NHC)X (**3.1, 3.3, 3.5, 3.9, 3.10**), (KPF₆ for **5.1, 5.10, 5.11, 5.12**), CH₂Cl₂, 24 h, room temperature.; (**5.2, 5.3, 5.4, 5.7, 5.8**) 0.5 eq [RuCl₂(*p*-cymene)₂], Ag(NHC)X (**3.1, 3.2, 3.3, 3.4**), (KPF₆ except **5.3**), CH₂Cl₂, 24 h room temperature.

5.2-Results and discussion

5.2.1-Synthesis of Ru-NHC complexes

[Ru(η^6 -arene)(NHC)Cl]Y complexes **5.1-5.12** (where arene = *p*-cymene, benzene and Y = Cl, PF₆) were synthesized by the transmetallation method. The reactions were conducted by mixing the corresponding Ag(NHC)X complex with 0.5 equivalents of [Ru(η^6 -arene)Cl₂]₂, 2 equivalents of KPF₆ in order to obtain complexes **5.1, 5.2, 5.4, 5.6, 5.7, 5.8, 5.10, 5.11, and 5.12** according to known procedures (Scheme 5-10).[19, 20, 21, 22]. While the complexes **5.3, 5.5, 5.9** were prepared following the same method but without using KPF₆. The crude products were purified by slow diffusion of diethyl ether into dichloromethane solutions of the complex. Suitable crystals were obtained for some Ru complexes which were analysed using single crystal x-ray diffraction.

NMR spectroscopy and mass spectrometry, as well as elemental analysis and X-ray crystallography were used to confirm the formation of complexes.

Cyclometalated ruthenium complexes were obtained *via* coordination of the triazine-NHC ligand in a chelating mode where both the carbene and one of the N-donors of the triazine group ligate the metal.

The H NMR spectra of the Ru complexes **5.1 - 5.12** confirmed the formation of complexes by comparison with the corresponding spectra of the precursor ligands **2.3, 2.5, 2.6, 2.7, 2.8, 2.13, 2.14**.

The H NMR spectra of complexes **5.1, 5.2, 5.3, 5.5, 5.9, and 5.10** show the absence of a peak around 10 ppm for N-CH-N. In addition to this, the peaks assigned to imidazolium protons for these complexes and complexes **5.4, 5.6, 5.7, 5.8, 5.11 and**

5.12, were shifted upfield in ranges 7.57-7.91 and 7.22-7.05 ppm in comparison with the precursor ligand in ranges 8.47-7.97 and 7.46-7.72 ppm as a result of the lack of resonance around the imidazoline ring.

The ^1H NMR spectra of the $[\text{Ru}(\text{p-cymene})(\text{NHC})\text{Cl}]\text{Y}$ (where $\text{Y} = \text{Cl}, \text{PF}_6$) complexes **5.2**, **5.3**, **5.4**, **5.7** and **5.8** gave further evidence of the formation of five membered ruthenacycle by the desymmetrization of the cymene ring, indicated by the four doublets between 6.12 and 5.34 ppm. [47] Three peaks are observed for the isopropyl group of cymene; two doublets, each integrating to 3H, of the methyl groups are found in the range 0.86-1.08 ppm and a multiplet integrating to 1H for the methine group appears between 2.41-2.24 ppm, in addition a singlet peak for the methyl group of cymene integrates to 3H and appears in the range 2.06-2.12 ppm (Figure 5-6).[30]

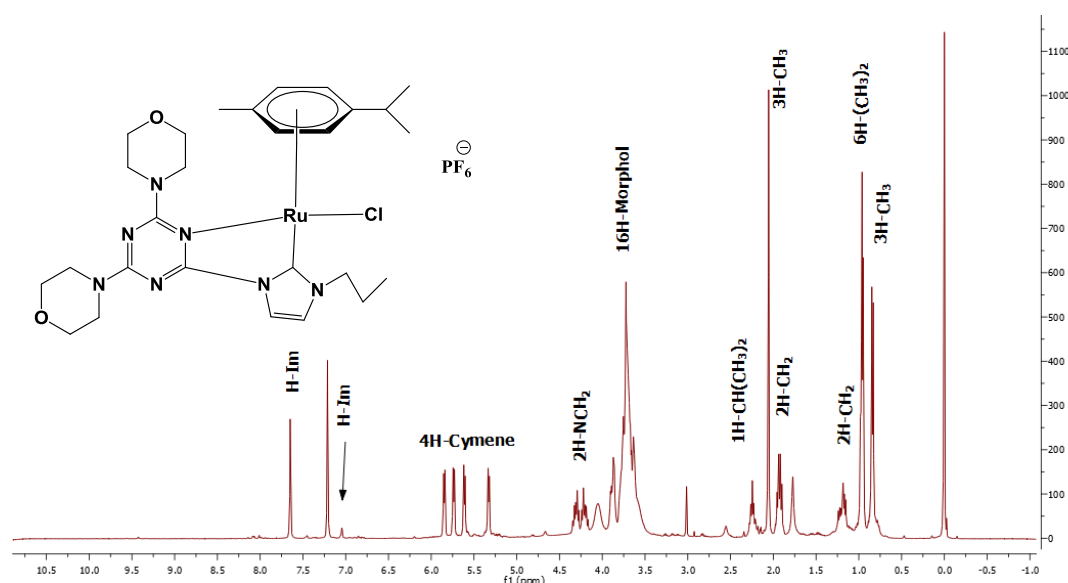


Figure (5-6) ^1H NMR spectrum for $[\text{Ru}(\text{p-cymene})\text{Cl}(\mathbf{2.5})]\text{Cl}$, **5.4**

The formation of $[\text{Ru}(\text{C}_6\text{H}_6)(\text{NHC})\text{Cl}]\text{Y}$ complexes **5.1**, **5.5**, **5.6**, **5.9**, **5.10**, **5.11** and **5.12** (where $\text{Y} = \text{Cl}, \text{PF}_6$) were confirmed by the emergence of a sharp signal between 5.92-5.39 ppm integrating to 6H and assigned to the benzene ring, which agree with

previous literature, [48] in addition to broad peaks for morpholine protons in ranges 3.5-4.08 ppm and peaks for methyl, propyl and mesityl substituents for the complexes **5.1**, **5.5**, **5.6**, **5.9**, **5.10**. Additionally, peaks were observed in ranges 3.36-3.20 attributed to methyl groups for **5.11** and **5.12** complexes (Figure 5-7)

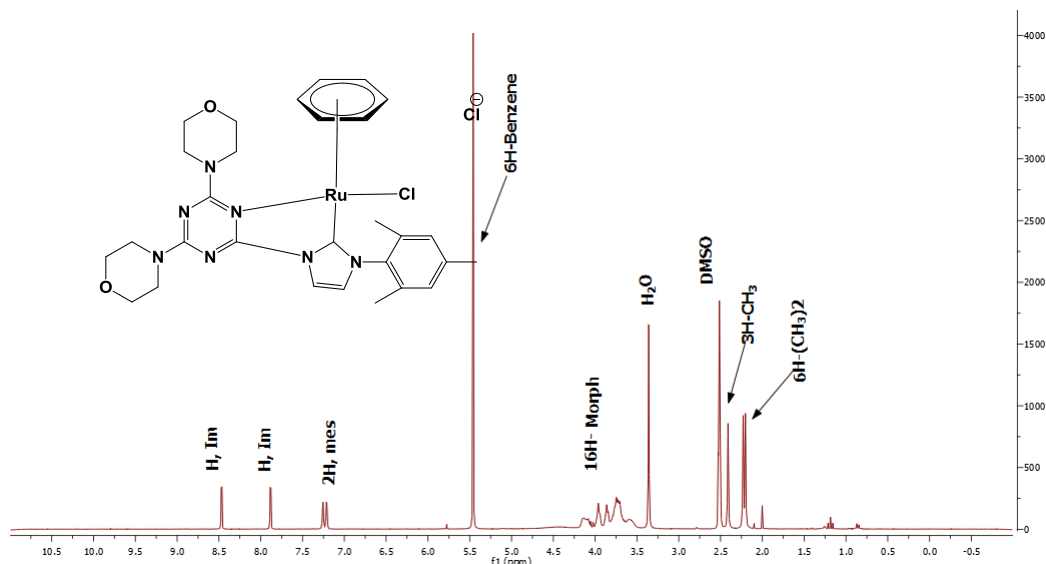


Figure (5-7) ^1H NMR spectrum for $[\text{Ru}(\text{C}_6\text{H}_6)\text{Cl}(\mathbf{2.8})]\text{Cl}$, **5.9**

The ^{13}C NMR spectra of $[\text{Ru}(\eta^6\text{-arene})(\text{NHC})\text{Cl}]\text{Y}$ complexes **5.1-5.12** display signals in the range 181.1-184.34 ppm which are consistent with the previous literature and can be attributed to the carbene carbon, confirming formation of the ruthenium complexes (Table 5-1)

Table (5-1) ^{13}C NMR data resonances in Ru-Carbene of **5.1-5.12**-compelxe

Ru complex	Ru-Carbene (ppm)
5.1	183.8
5.2	184.1
5.3,	184.3
5.4,	183.7
5.5,	182.2
5.6	183.3
5.7	183.9
5.8	183.3
5.9	184.3
5.10	183.8
5.11	181.1
5.12,	182.1

The spectra show three peaks associated with the triazine C in the range 169.7-160.7 ppm compared to the two peaks which were found with the Ag precursor, which indicates reduction of symmetry in ligands, consistent with N-coordination, which is supported by X-ray (Figure 5-8).

The ^{13}C NMR spectra of $[\text{Ru}(\text{p-cymene})(\text{NHC})\text{Cl}]\text{Y}$ **5.2**, **5.3**, **5.4**, **5.7** and **5.8** showed 6 signals attributed to the cymene aromatic ring in the range 105.4-81.7 ppm in addition to four peaks attributed to the isopropyl and methyl groups between 31.1-18.3 ppm which is consistent with the previous literature. [30, 31, 47]

The ^{13}C NMR spectra of **5.1**, **5.5**, **5.6**, **5.9**, **5.10**, **5.11** and **5.12** show sharp signals in the range 88.4-87.6 ppm corresponding to the aromatic carbon atoms (Figure 5-8).

[48]

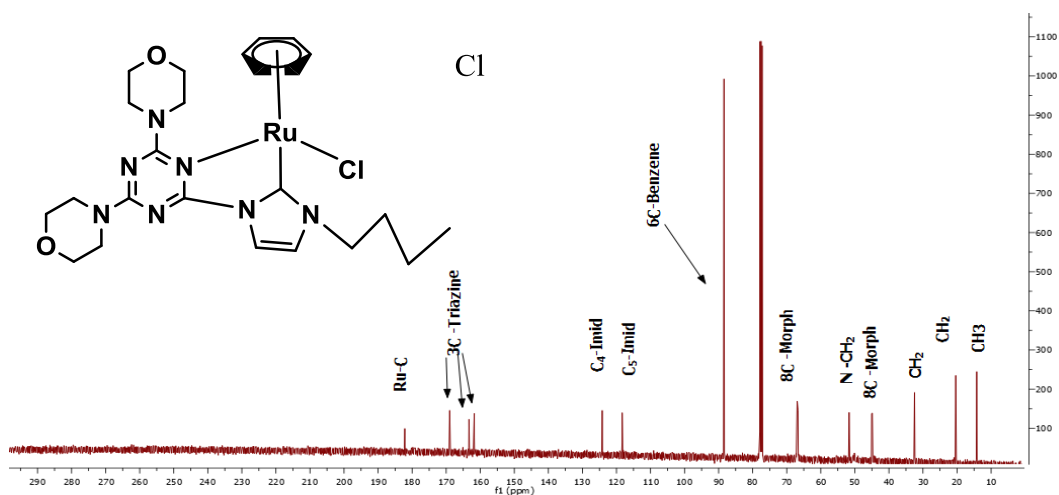


Figure (5-8) ^{13}C NMR spectrum for $[\text{Ru}(\text{C}_6\text{H}_6)\text{Cl}(\mathbf{2.6})]\text{Cl}$, **5.5**

5.2.2-X-ray Structural Determination

Attempts were made to grow crystals suitable for single crystal x-ray diffraction studies of all compounds. Suitable crystals were obtained from vapour diffusion of diethyl ether into dichloromethane solutions for some complexes.

Yellow plate crystals of $[\text{Ru}(\text{C}_6\text{H}_6)\text{Cl}(\mathbf{2.3})]\text{PF}_6$, **5.1** were obtained by slow diffusion of diethyl ether into a concentrated dichloromethane solution. X-ray diffraction showed two Yellow plate crystals of $[\text{Ru}(\text{C}_6\text{H}_6)\text{Cl}(\mathbf{2.3})]\text{PF}_6$, **5.1** were obtained by slow diffusion of diethyl ether into a concentrated dichloromethane solution. X-ray diffraction showed two $[\text{Ru}(\text{C}_6\text{H}_6)\text{Cl}(\mathbf{2.3})]\text{PF}_6$ molecules in the unit cell (Figure 5-9). One PF_6 anion displays some disorder. Complex **5.1** exhibits a piano stool geometry at the ruthenium center. The ruthenium center is bound by the chelating NHC, chloride atom and benzene ring. Coordination of the triazine N-substituent is clearly observed, with the triazine and imidazole rings adopting a coplanar geometry. The Ru-carbene bond distance of $2.01(4)\text{\AA}$ lies in the typical range for NHC–Ru complexes [25, 26, 29, 30] and the bite angle of the chelating triazine-carbene ligand C(1)-Ru(1)-N(5) is $76.42(14)^\circ$ and similar to that for the previously reported cyclometalated complex. The Ru–N_{triazine} bond distance for the cyclometalated triazine ring is $2.201(3)\text{\AA}$, which is practically identical with the reported pyridine cyclometalated complex [30]. The N morpholine units atoms are sp^2 hybridized, adopting an approximate trigonal planar geometry (sum of angles subtended at N(7)) $356.2(3)^\circ$; sum of angles subtended at N(6) $358.8(3)^\circ$, indicative of the N lone pairs' delocalization into the triazine core. The angle between morpholine unit near to the ruthencyclic and triazine unit is twisted out of the plane by 57.91° due to steric restraints. Whereas the angle between the second morpholine and triazine by only

14.07°. Bond lengths and angles, principally involving those around the metal centre, are shown in table (5-2).

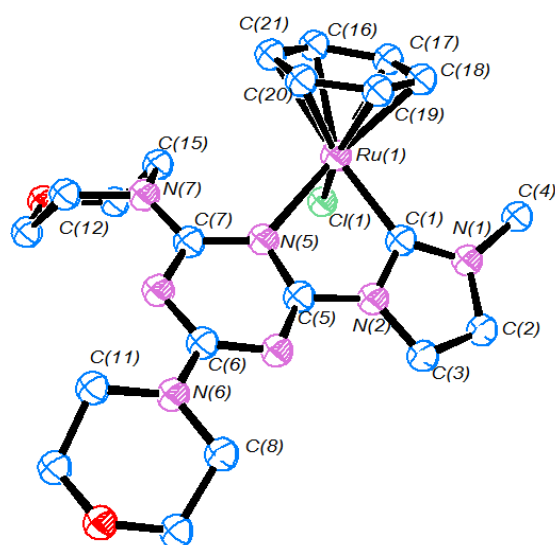


Figure (5-9) ORTEP ellipsoid plot at 50% probability of complex **5.1**. H atoms and PF_6 omitted for clarity

Table (5-2) Selected bond lengths and angles for **5.1**

Bond Angles (Å)		Bond lengths (°)	
C1–Ru1–N5	76.42(14)	Ru1–C1	2.010(4)
N5–Ru1–Cl1	90.45(8)	Ru1–N5	2.201(3)
C1–Ru1–Cl1	83.75(11)	Ru1–Cl1	2.4119(10)
C1–Ru1–C16	152.10(16)	Ru1–C16	2.255(4)
C1–Ru1–C17	115.32(16)	Ru1–C17	2.183(4)
C1–Ru1–C18	92.50(15)	Ru1–C18	2.173(4)
C1–Ru1–C19	96.43(15)	Ru1–C19	2.179(4)
C1–Ru1–C20	124.63(16)	Ru1–C20	2.176(4)

The X-ray structure of **5.4** showed one $[\text{Ru}(\text{p-cymene})\text{Cl}(\mathbf{2.5})] \text{PF}_6$ molecule with one molecule of solvent (Figure 5-10). For clarity the CH_2Cl_2 has been removed. The Ru–C1 and Ru–N5 bond distances of 2.012(3) Å and 2.180(3) Å are in the expected

ranges. Both $N_{\text{morpholine}}$ atoms are adopting planar geometry according to the sum of subtended angles at N (7) $347.2(3)^\circ$, N (6) $358.6(3)^\circ$. Angles between the Ru atom and carbene, N-triazine and chloride ligands are distorted from ideal piano-stool geometry. This observation is due to steric constraints of ligand [30] as well as the reduced flexibility as a result of coordination of the Ru centre with the N atom of the triazine. Bond lengths and angles, principally involving those around the metal centre, are shown in Table (5-3).

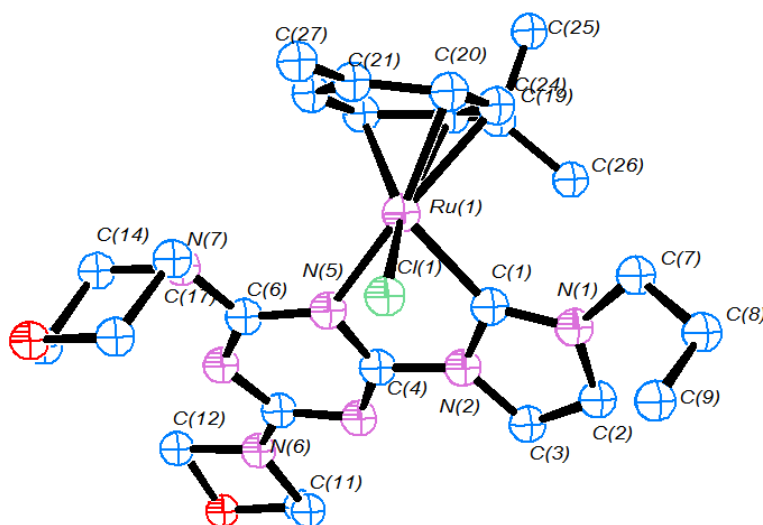


Figure (5-10) ORTEP ellipsoid plot at 50% probability of complex **5.4**. H atoms and PF_6 omitted for clarity

Table (5-3) Selected bond lengths and angles for **5.4**

Bond Angles (Å)		Bond lengths (°)	
C1–Ru1–N5	75.96(12)	Ru1–C1	2.012(3)
N5–Ru1–C11	91.77(8)	Ru1–N5	2.180(3)
C1–Ru1–C11	83.74(10)	Ru1–C11	2.4135(9)
C1–Ru1–C18	97.15(13)	Ru1–C18	2.227(4)
C1–Ru1–C19	94.21(14)	Ru1–C19	2.173(3)
C1–Ru1–C20	117.48(14)	Ru1–C20	2.179(3)
C1–Ru1–C21	154.04(14)	Ru1–C21	2.287(4)
C1–Ru1–C22	161.7(13)	Ru1–C22	2.299(4)
C1–Ru1–C21	154.04(14)	Ru1–C21	2.287(4)

The X-ray structure of **5.6** showed four [Ru(benzene)(**2.6**)Cl]PF₆ molecules in the unit cell. Figure (5-11) shows only one of the molecules for clarity. The five-membered ruthenacycle is clearly observed. The chloro ligand adopts the same orientation as the butyl chain due to steric repulsion with benzene ligand. the Ru(1)-C(1) carbene, Ru(1)-N(5) triazine bond distances of 2.018(10) Å and 2.185(8) Å are within the range for previously reported. The N atoms for both morpholine units display a planar geometry (sum of angles at = N (7) 350° (8); N (6)= 359° (7), indicative of the N lone pairs' delocalization into the triazine core. Bond lengths and angles, principally involving those around the metal centre, are shown in Table (5-4).

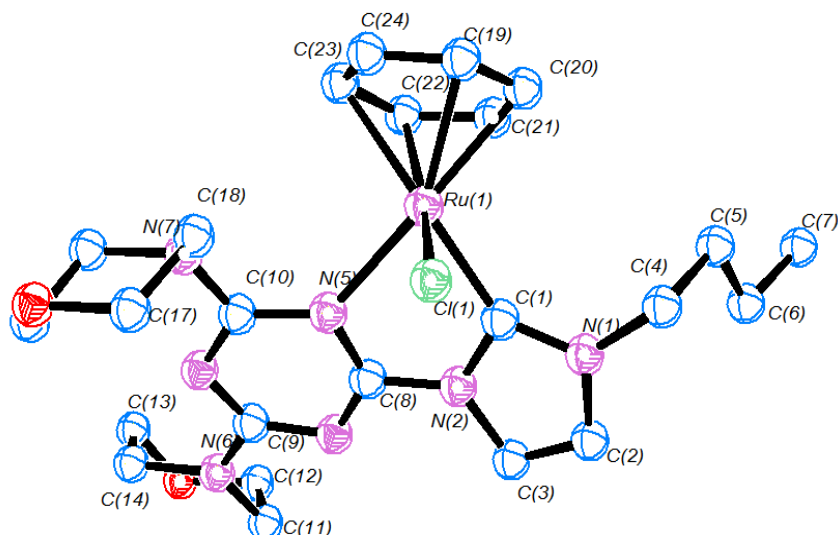


Figure (5-11) ORTEP ellipsoid plot at 50% probability of complex **5.6**. H atoms and PF_6 omitted for clarity

Table (5-4) Selected bond lengths and angles for **5.6**

Bond Angles ($^\circ$)		Bond lengths ($^\circ$)	
C1–Ru1–N5	76.6(3)	Ru1–C1	2.018(10)
N5–Ru1–C11	91.82(19)	Ru1–N5	2.185(8)
C1–Ru1–C11	83.4(3)	Ru1–C11	2.410(2)
C1–Ru1–C19	130.5(5)	Ru1–C19	2.182(10)
C1–Ru1–C20	100.5(5)	Ru1–C20	2.174(12)
C1–Ru1–C21	91.1(4)	Ru1–C21	2.157(11)
C1–Ru1–C22	110.8(4)	Ru1–C22	2.190(9)
C1–Ru1–C23	146.5 (4)	Ru1–C23	2.255(11)
C1–Ru1–C24	166.5(5)	Ru1–C24	2.271(12)

The solid state structure of complex **5.8** shows a cationic $[\text{Ru}(\text{p-cymene})(\mathbf{2.7})\text{Cl}]$ complex with a PF_6 counter ion. The structure shows disorder in the octyl chain (figure 5-12). The *p*-cymene group adopts an opposite orientation to the triazine to minimise steric repulsion. Bond lengths $\text{Ru}(1)-\text{C}(1)_{\text{NHC}} = 2.007(3) \text{ \AA}$, $\text{Ru}(1)-\text{N}(5) = 2.187(3)$ are consistent with related complexes. The imidazole and triazine rings adopt a coplanar configuration. The N atoms of morpholine units adopt a planar geometry. The angles between triazine and both morpholine are twisted out of plane by 27.02 and 73.39° . Bond lengths and angles, principally involving those around the metal centre, are shown in Table (5-5).

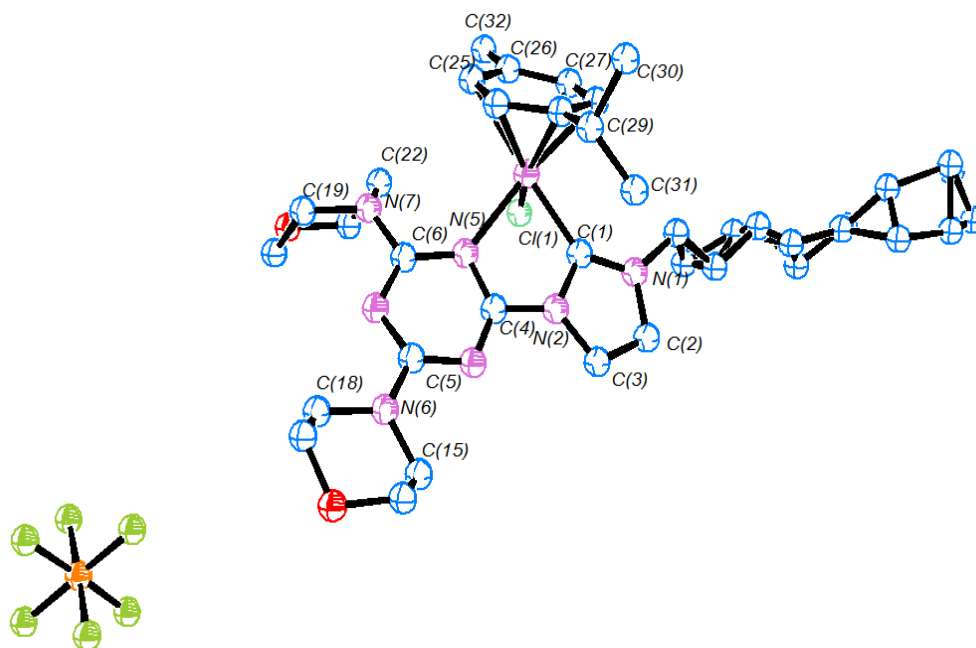


Figure (5-12) ORTEP ellipsoid plot at 50% probability of complex **5.8**. H atoms omitted for clarity

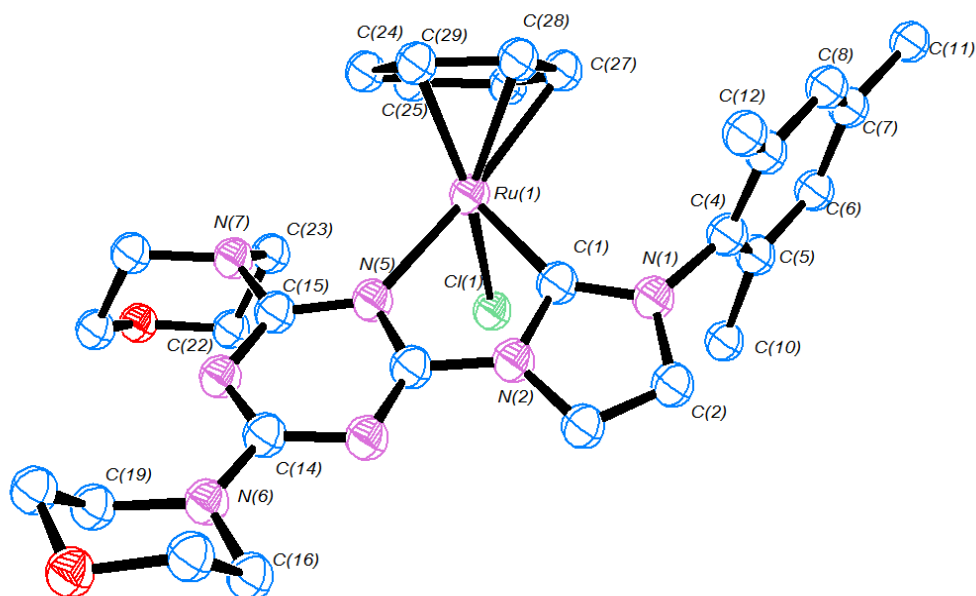
Table (5-5) Selected bond lengths and angles for **5.8**

Bond Angles (Å)		Bond lengths (°)	
C1–Ru1–N5	76.18(12)	Ru1–C1	2.007(3)
N5–Ru1–C11	90.63(8)	Ru1–C11	2.4086(9)
C1–Ru1–C11	83.33(10)	Ru1–N5	2.187(3)
C1–Ru1–C23	97.88(14)	Ru1–C23	2.240(4)
C1–Ru1–C24	125.96(14)	Ru1–C24	2.183(4)
C1–Ru1–C25	163.32(14)	Ru1–C25	2.267(4)
C1–Ru1–C26	152.51(14)	Ru1–C26	2.290(4)
C1–Ru1–C27	116.24 (14)	Ru1–C27	2.169(3)
C1–Ru1–C28	93.93(13)	Ru1–C28	2.173(3)

The solid state structure of complex **5.10** shows one molecule of $[\text{Ru}(\text{C}_6\text{H}_6)(\mathbf{2.8})\text{Cl}]\text{PF}_6$ in the unit cell. The coordination geometry is a distorted tetrahedral. The mesityl ring is orientated almost orthogonally to the imidazole ring with a dihedral angle about C(2)–N(1)–C(4)–C(5) of 94.2(4) °. Due to the steric constraints the chloride ligand adopts the same orientation as the mesityl substituent. Bond lengths Ru(1)- C(1)_{NHC} = 2.012(3) Å, Ru(1)-N(5)= 2.149(2) are consistent with related complexes. The N morpholine units atoms are sp² hybridized, adopting an approximate trigonal planar geometry (sum of angles subtended at N(7)) 350.9(3)°; sum of angles subtended at N(6)359.8(3) Bond lengths and angles, principally involving those around the metal centre are shown in Table (5-6).

Table (5-6) Selected bond lengths and angles for **5.10**

Bond Angles (Å)		Bond lengths (°)	
C1–Ru1–N5	77.13(11)	Ru1–C1	2.012(3)
N5–Ru1–C11	84.33(7)	Ru1–C11	2.3980(8)
C1–Ru1–C11	82.83(9)	Ru1–N5	2.149(2)
C1–Ru1–C24	150.39(13)	Ru1–C24	2.273(3)
C1–Ru1–C25	164.52(12)	Ru1–C25	2.285(3)
C1–Ru1–C26	127.68(13)	Ru1–C26	2.190(3)
C1–Ru1–C27	98.12(12)	Ru1–C27	2.190(3)
C1–Ru1–C28	92.73 (12)	Ru1–C28	2.177(3)
C1–Ru1–C29	114.03(13)	Ru1–C29	2.189(3)

**Figure (5-13)** ORTEP ellipsoid plot at 50% probability of complex **5.10**. H atoms and PF₆ omitted for clarity

Yellow plate crystals were obtained for complex **5.11**. The solid state structure shows one molecule of [Ru(C₆H₆)Cl(**2.13**)]PF₆ in the unit cell which clearly shows that

cyclometallation has been achieved (Figure 5-13). The Ru-carbene distance of 1.998 Å lies in the typical range for NHC–Ru complexes. The N atoms for both dimethyl units display a planar geometry (sum of angles at=N (7) 352.08°; N (6)= 357.92°. The angles between triazine and dimethyl units are out of plane by 36.79° and 16.31°. Bond lengths and angles, principally involving those around the metal centre, are shown in Table (5-7).

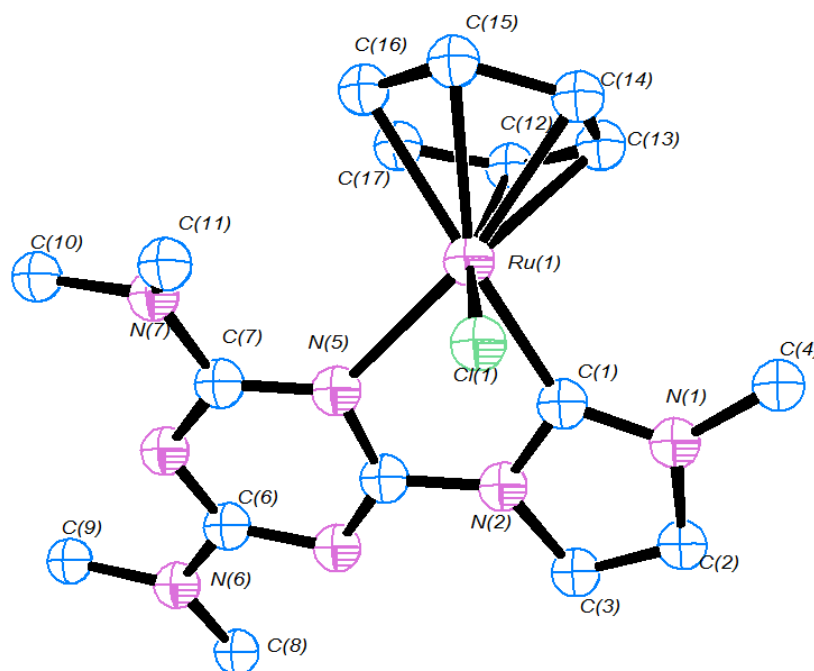


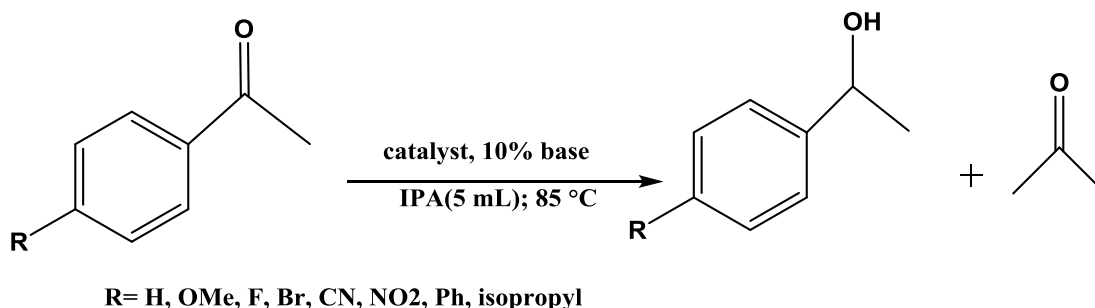
Figure (5-14) ORTEP ellipsoid plot at 50% probability of complex **5.11**. H atoms and PF₆ omitted for clarity

Table (5-7) Selected bond lengths and angles for **5.11**

Bond Angles (°)		Bond lengths (°)	
C1–Ru1–N5	75.9(6)	Ru1–C1	1.998(17)
N5–Ru1–C11	91.6(4)	Ru1–C11	2.419(5)
C1–Ru1–C12	95.8(7)	Ru1–C12	2.171(18)
C1–Ru1–C14	114.8(7)	Ru1–C14	2.188(19)
C1–Ru1–C13	91.8(7)	Ru1–C13	2.181(18)
C1–Ru1–C14	114.8(7)	Ru1–C14	2.188(19)
C1–Ru1–C15	152.2(7)	Ru1–C15	2.27(2)
C1–Ru1–C16	160.6 (6)	Ru1–C16	2.262(19)
C1–Ru1–C17	123.9(3)	Ru1–C17	2.147(19)

5.2.3-Catalytic Transfer Hydrogenation of Acetophenone

The catalytic transfer hydrogenation was examined using 2-propanol as the hydrogen source (Scheme 5-11).



Scheme (5-11) Catalytic hydrogen transfer of derivatives acetophenone

The ruthenium complexes **5.1-5.12** were tested in the transfer hydrogenation reaction of ketonic substrates and proved to be very efficient, with all complexes having this catalytic activity (Table 5-8). The complex [RuCl(p-cymene)(**2.3**)]PF₆, (**5.2**) was used to establish the optimum reaction conditions, with acetophenone as the test substrate.

The base has played an important role in this reaction for the generation of nucleophilic alkoxide ions, which would rapidly attack the ruthenium complex responsible for dehydrogenation. The three bases cesium carbonate, potassium hydroxide and tertiary butoxide were tested (entries 1, 2, 3). KO^tBu gave a yield of 79% in contrast with 53 and 57 for KOH, and Cs₂CO₃ respectively.

Under the standard catalytic conditions (i.e. 1% catalyst and 10 mol % of KO^tBu) the majority of the reactions with the Ru-cymene based catalysts were completed within four hours, typically achieving over 70 % yields within the first hour (entries 3 and 5-7). Better results were achieved with 1% catalyst loading were obtained with the Ru-benzene based catalysts (entries 8 – 11).

When comparing the effect of the PF₆ vs Cl counterion (complex **5.2** vs **5.3**; entries 3 and 4), the PF₆ ruthenium complex **5.2** is faster, with TOFs of 79 and 55 observed, respectively, after 1 hour. However, similar reaction rates were observed for both complexes after 2 hours, A rather small influence in the reaction rate was observed when varying the alkyl N-imidazole substituents. The order of activity based on the N-substituent is: Bu < Pr < Me < Octyl (run 3, 5, 6 and 7).

For the [RuCl(C₆H₆)NHC] Y complexes, **5.1**, **5.9** and **5.6**, the mesityl substituted complex was the slowest (entries 8, 10 and 12).

Next we investigated the effect of the ruthenium-coordinated arene ring on the reaction rate. Complexes with coordinated benzene showed increased activity when compared to the Ru-cymene complexes. The superiority of the benzene complexes becomes more apparent when the catalyst loading is reduced to 0.5%. For example, for the methylimidazole complexes **5.1** and **5.2** (entries 13 and 15), the TOF was 158 for **5.1** compared to only 52 for the cymene complex **5.2**.

Table (5-8) Catalytic transfer hydrogenation of acetophenone

Entry	Cat (mol %)	Yield (In 1 h)	TOF (in h ⁻¹)	Yield (time, h)	TON (time, h)
1	5.2 (1) ^b	57	57	80(2)	80(2)
2	5.2 (1) ^c	51	51	82(2)	82(2)
3	5.2 (1)	79	79	86(2)	86(2)
4	5.3 (1)	55	55	86 (2)	86 (2)
5	5.4 (1)	73	73	97 (2)	97 (2)
6	5.7 (1)	70	70	91 (2)	91 (2)
7	5.8 (1)	85	85	94 (2)	94 (2)
8	5.1 (1)	80	80	91 (2)	91 (2)
9	5.11 (1)	94	94	100 (2)	100 (2)
10	5.6 (1)	91	91	99 (1.5)	99 (1.5)
11	5.12 (1)	96	96	96 (2)	96 (2)
12	5.9 (1)	72	72	97 (3)	97 (3)
13	5.1 (0.5)	78	156	99 (3)	198 (3)
14	5.11 (0.5)	45	90	82 (3)	164 (3)
15	5.2 (0.5)	26	52	78 (4)	156 (4)
16	5.4 (0.5)	10	20	60 (7.5)	120(7.5)
17	5.6 (0.5)	78	156	100 (3)	200 (3)
18	5.12 (0.5)	82	164	90 (2)	180 (2)
19	5.6 (0.5) ^d	3	6	13 (24)	26 (24)
20	5.6 (0.1)	24	240	80 (4)	800 (4)
21	5.12 (0.1)	31	310	78 (3)	780 (3)
22	5.4 (0.005)	0	0	5 (6)	1000 (6)

^aAll reactions were carried out in isopropanol at 85 °C in air, using 2mmol acetophenone and 10 mol % of KO^tBu unless otherwise stated. Conditions were not anhydrous or air free. % yields were determined by ¹H NMR using 1,3,5-trimethoxybenzene as internal standard. Reactions were monitored at 30 minute intervals. ^bKOH as base. ^cCs₂CO₃ as base. Turnover frequency (TOF) and turnover number (TON). ^dWithout base

Next we investigated the influence of the triazine ring substituents on the catalytic activity. The comparison was made between the morpholine (**5.1**, **5.6**) and dimethyl amino (**5.11**, **5.12**) complexes (entries 8-11), where much higher activities are observed for the NMe₂ substituted complexes, **5.11** and **5.12**.

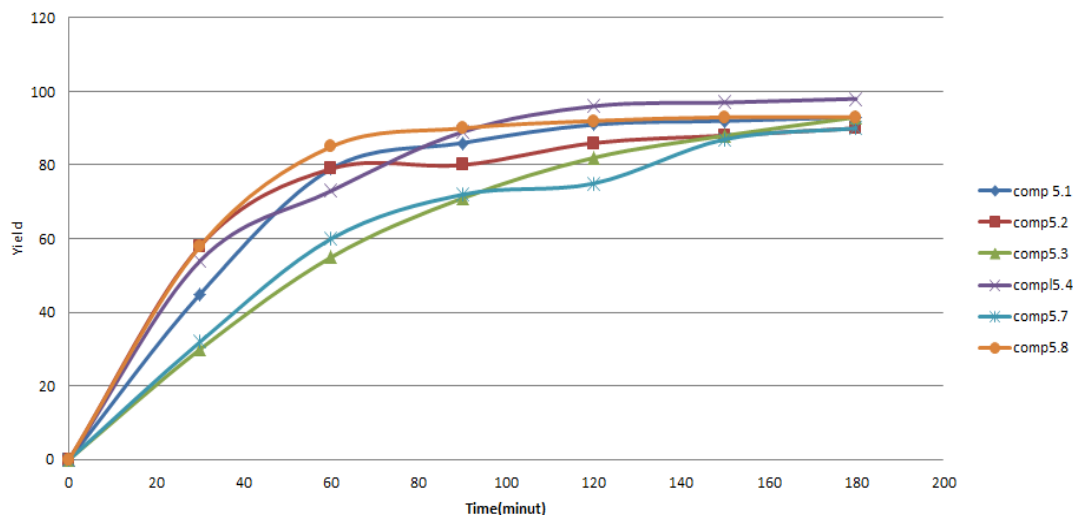


Figure (5-15) Progress of yield vs time for complexes **5.1**, **5. 2**, **5.3**, **5.4**, **5.7**and **5.18**

A common observation for the time-monitored catalytic reactions was that the reaction rate neared zero when yields reached about 80% (Fig 5-15) Addition of more ketone substrate to these reactions resulted in reactivation of the catalyst, implying that the rather weak metal-ketone binding is rate limiting.

The transfer hydrogenation activity of the Ru(arene)Cl₂(NHC) precatalysts **5.1-5.11** and **5.12** for acetophenone can be compared to that of similar Ru(arene)Cl₂(NHC) complexes in the literature. With arene = *p*-cymene, arene; NHC = ImEt,CH₂CH₂OEt, (Im,Et,Pentyl , methylenebis(ImEt)₂, our catalysts outperformed or had activity similar to that of catalysts under similar conditions.[46]

Catalytic Transfer Hydrogenation of Other Carbonyl Substrates with Precatalyst 5.2.

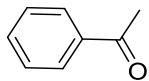
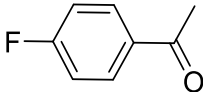
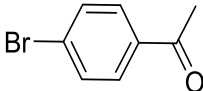
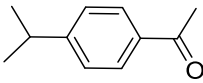
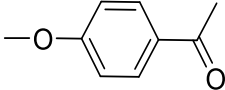
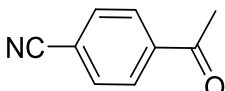
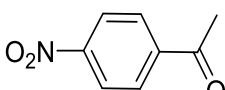
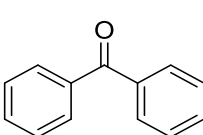
Complex **5.2** was used for the hydrogenation transfer to investigate substrate scope. These results are shown in Table (5-9). During the first hour of reaction, the non-substituted, fluoro and benzophenone derivatives (entries 1, 2, 8) have similar reaction profiles (TOF = 80). The same holds true when comparing the bromo- and isopropyl-acetophenone derivatives (TOF = 53). However, after the first hour of reaction significant deviations in the reaction profiles were observed (Table 5-9, % yield in 2h), thus allowing to establish the following activity trend for the *para*-substituted acetophenone derivatives: CN < OMe < iPr < Br < H < F < aryl.

The introduction of electron-withdrawing substituents, such as F (entry 2), to the *para* position of aryl ring of the ketone leads to a decrease in the electron density on the C=O bond. This improves the activity of (entry 2), increasing the ease of hydrogenation.[14]

The electron-rich substrate 4-methoxyacetophenone (entry 5) resulted in decreased product formation 20 % and 42 % at 1 and 2 h, suggesting that hydride transfer is slow in this case or perhaps catalyst inhibition occurs. The substrate 4-nitroacetophenone (entry 7) appears to be incompatible with base, as catalyst 5.2 led to 0% conversion at 1h with our standard conditions.

The use of benzophenone substrate (Table 3, entry 8) revealed that the steric bulk plays important role with an enhancement to 98% conversion in this reaction after 2 h.[23]

Table (5-9) Catalytic transfer hydrogenation of *para*-substituted aromatic ketone substrates

Run	Substrate	Cat (mol %)	% Yield (time, h)	TON (time, h)	% Yield (in 1 h)	TOF (in h ⁻¹)
1		5.2(1)	86 (2)	86	79	79
2		5.2 (1)	94 (2)	94	81	81
3		5.2 (1)	82 (2)	82	54	54
4		5.2 (1)	69 (2)	69	53	53
5		5.2 (1)	42 (2)	42	20	20
6		5.2 (1)	25 (2)	25	17	17
7		5.2 (1)	-		0	
8		5.2 (1)	98 (2)	98	84 (1)	84

^aAll reactions were carried out in isopropanol at 85 °C in air, using 10 mol% of KO^tBu and 1 mol% of Precatalyst **5.2**. Conditions were not anhydrous or air free. Conversions were determined by ¹H NMR spectroscopy using 1,3,5-trimethoxybenzene as internal standard. All reactions were monitored at 30 minute intervals

5.3-Experimental

General remarks.

All manipulations were performed using standard glassware under Nitrogen conditions. Solvents of analytical grade were purified using a Braun-SPS solvent purification system. $[\text{RuCl}_2(\text{C}_6\text{H}_6)_2]$ and $[\text{RuCl}_2(p\text{-cymene})_2]$ were synthesized according to a known literature procedure. [49, 50] Silver complexes that have been prepared in this work were used as a transfer agent. NMR spectra were obtained using Bruker Avance AMX 400 spectrometer. The chemical shifts are given as dimensionless σ values and are frequency referenced relative to TMS. Coupling constants J are given in hertz (Hz) as positive values regardless of their real individual signs. The multiplicities of the signals are indicated as s, d, and m for singlets, doublets, and multiplets, respectively. The abbreviation br is given for broadened signals. High resolution mass spectra were obtained using electrospray (ES) mode, on Waters LCT Premier XE instrument. Elemental analysis worked by Elemental Analysis Service Science Centre London Metropolitan University.

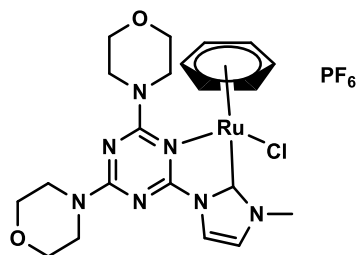
X-Ray crystallographic data for **5.1**, **5.4**, **5.6**, **5.8**, **5.10** and **5.11**, were collected using *Rigaku AFC12* goniometer equipped with an enhanced sensitivity (HG) *Saturn724+* detector mounted at the window of an *FR-E+ SuperBright* molybdenum rotating anode generator with HF *Varimax* optics (70, A and 100 μm focus). Structural solution and refinement was achieved using: *SHELXL-2013* and *SHELXL-2014* software, and absorption correction analysed using *CrystalClear-SM Expert* software.

Typical reaction procedure for the synthesis of the Ru(II) complexes 5.1-5.12

In a 50 mL conical flask and under a nitrogen atmosphere the $[\text{Ag}(\text{NHC})\text{X}]$ complex, $[\text{Ru}(\eta^6\text{-arene})\text{Cl}_2]_2$ and KPF₆ (in case **5.3**, **5.9** **5.9** without KPF₆) were dissolved in

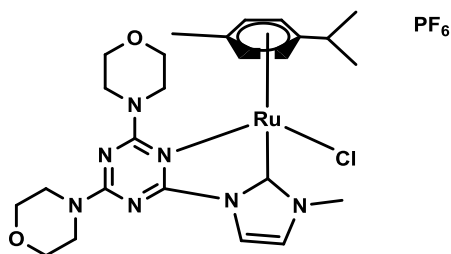
dry CH_2Cl_2 (40 mL) and left stirring overnight in the dark. The resulting mixture was filtered through celite and volatiles removed in vacuo. The orange solid obtained was recrystallized by evaporation of Et₂O in a CH_2Cl_2 solution to afford orange crystals of the ruthenium complex

Synthesis of $[\text{Ru}(\text{C}_6\text{H}_6)\text{Cl}(\mathbf{2.3})]\text{PF}_6$, **5.1**



The general procedure outlined above was followed, using silver complex **3.1** (0.1 g, 0.211 mmol), $[\text{Ru}(\text{C}_6\text{H}_6)\text{Cl}_2]_2$ (0.053g, 0.105 mmol) and KPF_6 (0.078 g, 0.42 mmol), affording $[\text{Ru}(\text{C}_6\text{H}_6)\text{Cl}(\mathbf{2.3})]\text{PF}_6$, **5.1** as an orange solid. Yield = 0.13 g (0.188 mmol) 89 %. ^1H NMR (400 MHz, CDCl_3 , ppm) $\delta_{\text{H}} = 7.65$ (d, $J = 2.0$, 1 H, C₄, imid), 7.12 (d, $J = 2.4$, 1 H, C₅, imid), 5.83 (s, 6 H, Ar), 4.08 (s, 3 H, CH₃-N), 3.70-4.10 (br, 16 H, morpholine). ^{13}C NMR (101 MHz, DMSO, ppm), $\delta = 183.8$ (C_{NHC}-Ru), 168.3, 162.9, 161.1 (3 × C, triazine ring), 126.3, 117.6 (2 × C, imid), 87.8 (6 × C, Ar), 66.5, 66.3, 44.5 (8 × C, morpholine), 37.8 (CH₃). HRMS (ES^+), calcd mass for $[\text{M}^+ - \text{PF}_6]$, C₂₀H₂₄F₆N₇O₂ 546.0942, measured 546.0942.

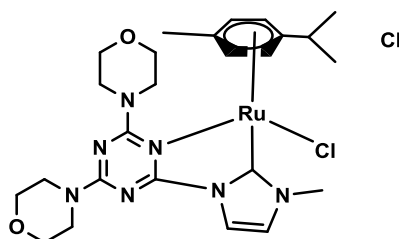
Synthesis of $[\text{Ru}(p\text{-cymene})\text{Cl}(\mathbf{2.3})]\text{PF}_6$, **5.2**



The general procedure outlined above was followed, using silver complex **3.1** (0.2g, 0.421 mmol), (0.129 g, 0.2116 mmol) $[\text{Ru}(p\text{-cymene})\text{Cl}_2]_2$, and KPF_6 (0.154g, 0.84

mmol) affording **[Ru(*p*-cymene)Cl(2.3)]PF₆, 5.2** as an orange solid Yield = 0.29 g (0.38 mmol) 90 %. ¹H NMR (400 MHz, CDCl₃, ppm) δ_H = 7.58 (d, *J* = 4.0, 1 H, C₄, imid) 7.13 (br, 1 H, C₅, imid), 5.87 (d, *J* = 4.0, 1 H, cymene), 5.83 (d, *J* = 4.0, 1 H, cymene), 5.63 (d, 1 H, *J* = 8.0, cymene) 5.41 (d, 1H, *J* = 8.0, cymene), 4.02 (s, 3H, CH₃-N), 3.62-3.95 (br, 16 H, morpholine), 2.27 (m, 1 H, CH-Me₂), 2.06 (s, 3 H, CH₃-cymene), 0.99 (d, *J* = 8.0, 3 H, CH₃, cymene), 0.86 (d, *J* = 4.0, 3 H, CH₃, cymene). ¹³C NMR (101 MHz, CDCl₃, ppm) δ_C = 184.1 (C-Ru), 168.6, 163.1, 161.2 (3 × C, triazine ring), 125.9, 117.2, (2 × C, imid), 104.7, 104.1, 93.4, 87.4, 84.2, 81.7 (6 × C, cymene), 66.5, 66.4, 44.5 (8 × C, morpholine) 37.7 (N-CH₃), 31.1 (CH-Me₂), 22.7, 21.4 (2 × CH₃, cymene) 18.3 (CH₃, cymene). HRMS (ES⁺) calcd mass for [M⁺-PF₆], C₂₅H₃₅N₇O₂ClRu 602.1584, measured 602.1557. Anal. Calcd for C₂₅H₃₅ClF₆O₂N₇PRu (747.08): C, 40.91; H, 4.72; N, 13.12. Found: C, 39.99; H, 4.58; N, 13.17.

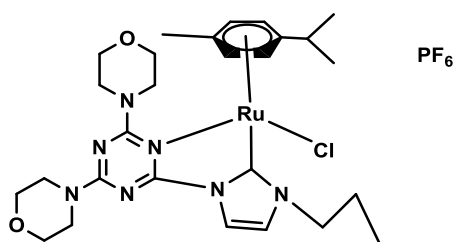
Synthesis of **[Ru(*p*-cymene)Cl(2.3)]Cl, 5.3**



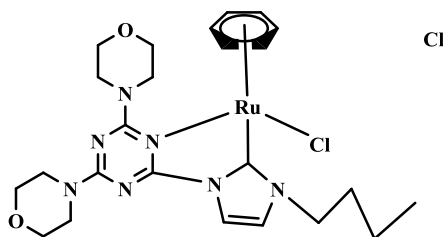
The general procedure outlined above was followed, using silver complex **3.1** (0.1 g, 0.211 mmol), [Ru(*p*-cymene)Cl₂]₂ (0.064 g 0.105 mmol), affording **[Ru(*p*-cymene)Cl(2.3)]Cl, 5.3** as an orange solid Yield = 0.117 g (0.18 mmol) 87 % as an orange solid. ¹H NMR (400 MHz, CDCl₃, ppm) δ_H = 7.65 (d, *J* = 2.0, 1 H, C₄, imid), 7.2 (d, 1 H, *J* = 2.0, C₅, imid), 6.21 (d, 1 H, *J* = 6.0, cymene), 6.15 (d, 1 H, *J* = 6.0, cymene), 5.75 (m, 2 H, cymene), 4.24 (s, 3 H, N-CH₃) 3.96-4.1 (br, 16 H, morpholine), 2.41 (m, 1 H, CH-Me₂), 2.12 (s, 3 H, CH₃, cymene), 1.08 (d, *J* = 8.0, 3 H, CH₃, cymene), 0.98 (d, *J* = 8, 3H, CH₃, cymene). ¹³C NMR (101 MHz, CDCl₃,

ppm) δ_C = 184.34 (C-Ru), 168.9, 163.4, 161.4 (3 \times C, triazine ring), 126.7, 117.4 (2 \times C, imid), 105.1, 102.6, 93.6, 87.8, 85.3, 83.2 (6 \times C-cymene) 66.8, 66.5, 44.8, 44.7 (8 \times C, morpholine), 39.0 (CH₃-N), 31.5 (CH-Me₂), 23.1, (CH₃-cymene), 22.1, (CH₃-cymene) 18.8 (CH₃-cymene). HRMS (ES⁺) for [M⁺ - Cl], C₂₅H₃₅N₇O₂ClRu 602.1568, measured 602.1557.

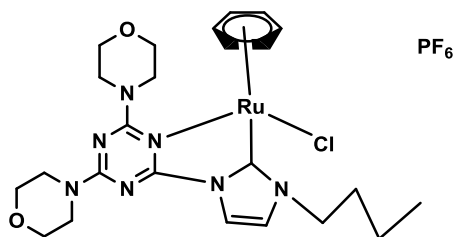
Synthesis of [Ru(*p*-cymene)Cl(2.5)]PF₆, 5.4



The general procedure outlined above was followed, using silver complex **3.2** (0.1 g, 0.18 mmol), [Ru(*p*-cymene)Cl₂]₂ (0.055g 0.09 mmol) and KPF₆ (0.066g, 0.364mmol), affording [Ru(*p*-cymene)Cl(2.5)]PF₆, **5.4** as an orange solid Yield = 0.124 g (0.16 mmol) 88 %. ¹H NMR (400 MHz, CDCl₃, ppm) δ_H = 7.64 (br, 1 H, C₄, imid), 7.2 (d, 1H, *J* = 4.0, C₅, imid), 5.85 (d, 1 H, *J* = 4.0, cymene), 5.75(d, 1H, *J* = 8.0, cymene), 5.62 (d, 1 H, *J* = 8.0, cymene), 5.34 (d, 1 H, *J* = 4.0, cymene), 4.28 (m, 2 H, N-CH₂) 3.57-4.04 (br, 16 H, morpholine), 2.24 (m, 1 H, CH-Me₂), 2.03 (s, 3 H, CH₃, cymene), 1.94 (m, 2 H, CH₂, propyl), 0.97 (m, 6 H, CH₃, cymene, CH₃, propyl), 0.85 (d, *J* = 8, 3 H, CH₃, cymene). ¹³C NMR (101 MHz, CDCl₃, ppm) δ_C = 183.7 (C-Ru), 168.4, 163.6, 161.6 (3 \times C, triazine ring), 123.5, 118.1 (2 \times C-imid), 105.1, 104.4, 93.4, 87.4, 84.5, 82.6 (6 \times C, cymene) 66.9, 66.8, 44.9,(8 \times C, morpholine), 53.0 (CH₂-N) 31.6 (CH₂, propyl), 31.6 (CH-Me₂), 23.9 (CH₂-propyl), 22.6, 21.4, 18.3 (3 \times CH₃, cymene) 11.2 (CH₃, propyl). HRMS (ES⁺) for M⁺- PF₆], C₂₇H₃₉N₇O₂ClRu 630.1897, measured 630.1761 .Anal. Calcd for C₂₇H₃₉ClF₆O₂N₇PRu (775.13): C, 41.84, H, 5.07; N, 12.65. Found: C, 42.02; H, 5.16; N, 12.64.

Synthesis of [Ru(C₆H₆)Cl(2.6)]Cl, 5.5

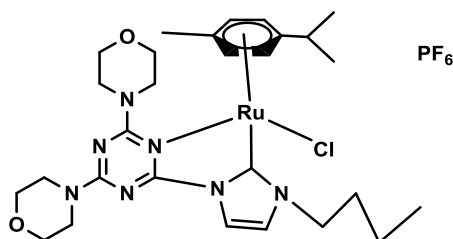
The general procedure outlined above was followed, using silver complex **3.3** (0.3 g, 0.534 mmol), [Ru(C₆H₆)Cl₂]₂ (0.13 g, 0.26 mmol), affording [Ru(C₆H₆)Cl(2.6)]Cl, **5.5** as an orange solid. Yield = 0.28 g (0.45 mmol) 85%. ¹H NMR (400 MHz, CDCl₃, ppm) δ_H = 7.69 (d, 1 H, *J* = 2.0, C₄, imid), 7.22 (d, 1 H, *J* = 2.0, C₅, imid), 5.92 (s, 6 H, Ar), 4.48 (m, 2 H, CH₂-N), 3.74-4.09 (br, 16 H, morpholine), 1.92 (m, 2 H, CH₂), 1.4 (m, 2 H, CH₂), 0.95 (t, 3 H, *J* = 7.2, CH₃). ¹³C NMR (101 MHz, CDCl₃, ppm) δ_C = 182.2 (C-Ru), 168.9, 162.6, 161.8 (3 × C, triazine), 124.2, 118.3 (2 × C, imid) 88.4 (6 × C, Ar) 66.9, 66.7, 45.1, 44.8 (8 × C, morpholine), 51.7 (CH₂-N) 32.5 (CH₂), 20.9 (CH₂), 14.2 (CH₃). HRMS (ES⁺) for [M⁺ - Cl], C₂₄H₃₃N₇O₂ClRu 588.1428, measured 588.1478.

Synthesis of [Ru(C₆H₆)Cl(2.6)]PF₆, 5.6

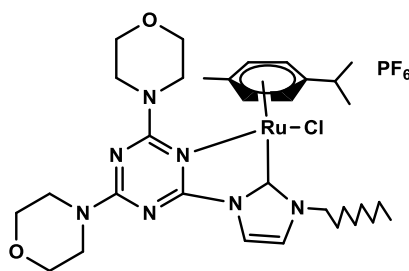
The general procedure outlined above was followed, using silver complex **3.3** (0.2g, 0.356 mmol), [Ru(C₆H₆)Cl₂]₂ (0.089g, 0.178 mmol) and KPF₆ (0.131g, 0.712 mmol), affording [Ru(C₆H₆)Cl(2.6)]PF₆, **5.6** as an orange solid. Yield = 0.193 g (0.263 mmol) 74 % as an orange solid. ¹H NMR (400 MHz, CDCl₃, ppm) δ_H = 7.63 (d, 1 H, *J* = 4.0, C₄, imid), 7.12 (d, 1 H, *J* = 4.0, C₅, imid), 5.72 (s, 6 H, Ar), 4.27 (m, 2 H, CH₂-N), 3.5-4.08 (br, 16 H, morpholine), 1.8 (m, 2 H, CH₂), 1.35 (m, 2 H, CH₂), 0.91 (t, 3

H, $J = 8.0$, CH₃). ¹³C NMR (101MHz, CDCl₃, ppm) $\delta_C = 183.3$ (C-Ru), 167.7, 162.6, 160.7 (3 \times C, triazine ring), 126.4, 117.1 (2 \times C, imid) 87.6 (6 \times C, Ar) 65.8, 64.8, 43.7 (8 \times C, morpholine), 49.4 (CH₂-N) 37.2 (CH₂), 27.4 (CH₂), 19.2 (CH₃). HRMS (ES⁺) for [M⁺ - PF₆], C₂₄H₃₃N₇O₂ClRu 588.1428, measured 588.1403. Anal. Calcd for C₂₃H₃₃ClF₆O₂N₇PRu (733.05): C, 39.32; H, 4.54; N, 13.38. Found: C, 39.22; H, 4.38; N, 13.26.

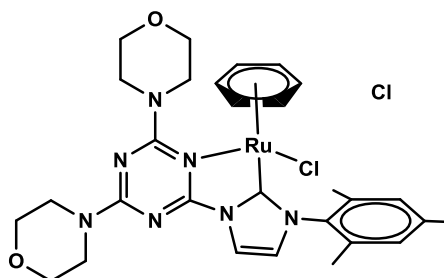
Synthesis of [Ru(*p*-cymene)Cl(2.6)]PF₆, 5.7



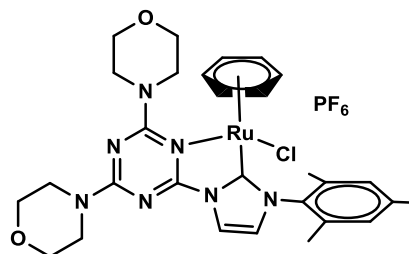
The general procedure outlined above was followed, using silver complex **3.3** (0.17 g, 0.303 mmol), [Ru(*p*-cymene)Cl₂]₂ (0.092 g, 0.151 mmol) and KPF₆ (0.111 g, 0.606 mmol) affording [Ru(*p*-cymene)Cl(2.6)]PF₆, **5.7** as an orange solid. Yield = 0.193 g (0.245 mmol) 81%. ¹H NMR (400 MHz, CDCl₃, ppm) $\delta_H = 7.62$ (d, 1 H, $J = 4.0$, C₄, imid), 7.16 (br, 1 H, C₅, imid), 5.85 (d, 1H, $J = 4.0$, cymene), 5.76 (d, 1 H, $J = 4.0$, cymene), 5.62 (d, 1 H, $J = 8.0$, cymene), 5.35 (d, $J = 4.0$, cymene), 4.35 (m, 2 H, CH₂-N), 3.5-4.0(br, 16 H, morpholine), 2.24 (m, 1 H, CHMe₂), 2.05 (s, 3 H, CH₃, cymene), 1.87 (m, 2 H, CH₂, butyl), 1.36 (m, 2 H, CH₂, butyl) 0.99 (d, 3 H, $J = 8.0$, CH₃, cymene), 0.92 (t, 3 H, $J = 4.0$, CH₃, butyl), 0.86 (d, 3 H, $J = 4.0$, CH₃-Cymene). ¹³C NMR (101 MHz, CDCl₃, ppm) $\delta_C = 183.9$ (C_(CHN)-Ru), 168.9, 163.4, 161.6 (3 \times C, triazine), 124.1, 117.9 (2 \times C, imid), 105.4, 103.8, 93.7, 87.4, 83.8 (6 \times C, cymene) 66.9, 66.7, 44.5, (8 \times C, morpholine), 51.4 (CH₂-N) 32.6 (CH₂-butyl), 31.6 (CH-Me₂), 23.2, 21.9, 18.7 (3 \times CH₃, cymene) 14.7(CH₃-butyl). HRMS (ES⁺) for [M⁺-PF₆], C₂₈H₄₁N₇O₂ClRu 644.2054, measured 644.2065.

Synthesis of [Ru(*p*-cymene)Cl(2.7)]PF₆, 5.8

The general procedure outlined above was followed, using silver complex **3.4** (0.4g, 0.65 mmol), [Ru(*p*-cymene)Cl₂]₂ (0.198 g, 0.32 mmol), and KPF₆ (0.239 g, 0.129 mmol), affording [Ru(*p*-cymene)Cl(2.7)]PF₆, **5.8** as an orange solid. Yield = 0.39 g (0.47 mmol) 72 %. ¹H NMR (400 MHz, CDCl₃, ppm) δ_H = 7.64 (d, 1H, *J* = 4.0, C₄, imid), 7.2 (br, 1 H, C₅-imid), 5.93 (d, 1 H, *J* = 8.0, cymene) 5.83 (d, 1 H, *J* = 4.0, cymene), 5.65 (d, 1 H, *J* = 8.0, cymene), 5.4 (d, 1 H, *J* = 4.0, cymene), 4.39 (m, 2 H, CH₂-N), 3.45-4.07 (br, 16 H, morpholine), 2.3 (m, 1 H, CHMe₂), 2.06 (s, 3 H, CH₃, cymene), 1.89 (m, 2H, CH₂, octyl), 1.2 (br, 10H, (CH₂)₅, octyl), 1.00 (d, 3H, *J* = 8.0, CH₃, cymene), 0.88 (d, 3 H, *J* = 8.0, CH₃, cymene), 0.81 (t, 3 H, *J* = 4.0, CH₃, octyl). ¹³C NMR (101 MHz, CDCl₃, ppm) δ_C = 183.3 (C-Ru), 168.4, 162.9, 161.3 (3 × C, triazine), 123.8, 117.7 (2 × C, imid), 104.7, 103.7, 93.2, 87.2, 84.5, 82.1 (6 × C, cymene) 66.5, 66.3, 44.5 (8 × C, morpholine), 51.3 (CH₂-N) 31.7 (CH₂-octyl), 31.1 (CHMe₂), 30.2, 29.1, 29.1, 26.6, 22.7 ((CH₂)₅-octyl), 22.6, 22.6, 18.6 (3 × CH₃, cymene) 14.1 (CH₃-octyl). HRMS (ES⁺) for [M⁺ - PF₆], C₃₂H₄₉N₇O₂ClRu 700.2680, measured 700.2766. Anal. Calcd for C₃₂H₄₉ClF₆O₂N₇PRu (845.24): C, 45.47; H, 5.84; N, 11.6. Found: C, 45.29; H, 5.76; N, 11.53.

Synthesis of [Ru(C₆H₆)Cl(2.8)]Cl, 5.9

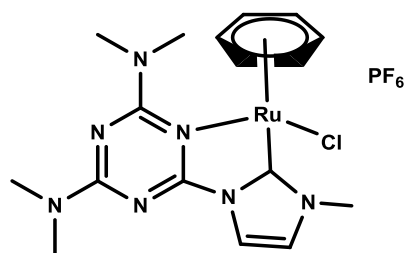
The general procedure outlined above was followed, using silver complex **3.5** (0.2 g, 0.35 mmol), and [Ru(C₆H₆)Cl₂]₂ (0.086 g, 0.17 mmol), affording [Ru(C₆H₆)Cl(2.8)]Cl, **5.9** as an orange solid. Yield = 0.21g (0.31 mmol) 90 %. ¹H NMR (400 MHz, DMSO, ppm) δ_H = 8.47 (d, 1 H, *J* = 4.0, C₄, imid), 7.89 (d, 1 H, *J* = 4.0, C₅-imid), 7.25 (s, 1 H, Ar), 7.21 (s, 1 H, Ar) 5.46 (s, 6 H, benzene), 3.59-3.9 (br, 16 H, morpholine), 2.41 (s, 3H, mesityl), 2.23 (s, 3H, CH₃, mesityl), 2.2 (s, 3H, CH₃, mesityl). ¹³C NMR (101 MHz, DMSO, ppm) δ_C = 184.3 (C-Ru), 168.5, 163.4, 160.8 (3 × C, triazine), 140.3, 136.3, 135.1, 134.8, 129.2 (6 × C, mesityl) 127.3, 118.8 (2 × C-imid), 87.9 (6 × C-benzene), 66.18, 66.05, 44.36, (8 × C, morpholine), 21.08 (CH₃), 18.78 (CH₃) 17.93 (CH₃). HRMS (ES⁺) for [M⁺ - Cl], C₂₉H₃₅N₇O₂ClRu 650.1584, measured 650.1588.

Synthesis of [Ru(C₆H₆)Cl(2.8)]PF₆, 5.10

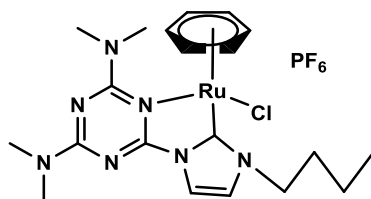
The general procedure outlined above was followed, using silver complex **3.5** (0.2 g, 0.35 mmol), [Ru(C₆H₆)Cl₂]₂ (0.086 g, 0.17 mmol), and KPF₆ (0.127, 0.69 mmol), affording [Ru(C₆H₆)Cl(2.8)]PF₆, **5.10** as an orange solid. Yield = 0.23g (0.293

mmol) 85%. ^1H NMR (400 MHz, CDCl_3 , ppm) $\delta_{\text{H}} = 7.91$ (d, 1 H, $J = 1.0$, C_4 -imid), 7.05 (d, 1H, $J = 2.0$, C_5 , imid), 7.1 (s, 1H, Ar), 7.14 (s, 1 H, Ar) 5.39 (s, 6 H, Ar), 3.59-3.9 (br, 16H, morpholine), 2.42 (s, 3 H, mesityl), 2.28 (s, 3 H, CH_3 , mesityl), 2.26 (s, 3 H, CH_3 , mesityl). ^{13}C NMR (101 MHz, CDCl_3 , ppm) $\delta_{\text{C}} = 183.8$ (C-Ru), 169.6, 163.5, 161.5 ($3 \times \text{C}$, triazine), 141.3, 137.1, 136.4, 134.7, 130.3, 129.5 ($6 \times \text{C}$, mesityl) 125.6, 118.7 ($2 \times \text{C}$, imid), 87.9 ($6 \times \text{C}$, benzene), 66.5, 44.8, 44.7, ($8 \times \text{C}$, morpholine), 21.5 (CH_3), 19.2 (CH_3) 18.1 (CH_3). HRMS (ES^+) for $[\text{M}^+ - \text{PF}_6]$, $\text{C}_{29}\text{H}_{35}\text{N}_7\text{O}_2\text{ClRu}$ 650.1584, measured 650.1569.

Synthesis of $[\text{Ru}(\text{C}_6\text{H}_6)\text{Cl}(\mathbf{2.13})]\text{PF}_6$, **5.11**



The general procedure outlined above was followed, using silver complex **3.9** (0.2 g, 0.51 mmol), $[\text{Ru}(\text{C}_6\text{H}_6)\text{Cl}_2]_2$ (0.127 g, 0.25 mmol) and KPF_6 (0.187 g, 1.02 mmol), affording $[\text{Ru}(\text{C}_6\text{H}_6)\text{Cl}(\mathbf{2.13})]\text{PF}_6$, **5.11** as an orange solid. Yield = 0.28 g (0.46 mmol) 90 %. ^1H NMR (400 MHz, CDCl_3 , ppm) $\delta_{\text{H}} = 7.57$ (d, 1 H, $J = 2.0$, C_4 , imid), 7.13 (d, 1 H, $J = 2.0$, C_5 , imid), 5.74 (s, 6 H, Ar), 4.01 (s, 3 H, CH_3), 3.17, 3.15 (s, 12 H, (CH_3)₄). ^{13}C NMR (101 MHz, CDCl_3 , ppm) $\delta_{\text{C}} = 181.1$ (C-Ru), 168.1, 161.2, 160.7 ($3 \times \text{C}$, triazine), 124.5, 116.2 ($2 \times \text{C}$, imid) 86.7 ($6 \times \text{C}$, Ar) 39.9 (CH_3), 35.9, 358 (CH_3)₄. HRMS (ES^+) for $[\text{M}^+ - \text{PF}_6]$, $\text{C}_{17}\text{H}_{23}\text{N}_7\text{ClRu}$ 462.0747, measured 462.0721. Anal. Calcd for $\text{C}_{17}\text{H}_{23}\text{ClF}_6\text{N}_7\text{PRu}$ (606.90). C, 33.64; H, 3.82; N, 16.16. Found: C, 33.69; H, 3.95; N, 16.29.

Synthesis of [Ru(C₆H₆)Cl(2.14)]PF₆, 5.12

The general procedure outlined above was followed, using silver complex **3.10** (0.3 g, 0.62 mmol) of the silver complex **3.19**, [Ru(C₆H₆)Cl₂]₂ (0.15 g, 0.31 mmol) and KPF₆ (0.23 g, 1.24 mmol), affording [Ru(C₆H₆)Cl(2.14)]PF₆, **5.12** as an orange solid. Yield = 0.34g (0.534 mmol) 85 %. ¹H NMR (400 MHz, CDCl₃, ppm) δ_H = 7.63 (br, 1 H, C₄, imid), 7.10 (br, 1 H, C₅, imid), 5.73 (s, 6 H, Ar), 4.30 (br, 2 H, N-CH₂), 3.36 (br, 6 H, (CH₃)₂), 3.20 (s, 6 H, (CH₃)₂), ¹³C NMR (101 MHz, CDCl₃, ppm) δ_C = 182.1 (C.Ru), 167.9, 161.5, 160.4 (3 × C, triazine), 124.8, 117.7 (2 × C, imid) 86.7 (6 × C, Ar) 52.1 (CH₂N, butyl) 35.9, 35.8 (CH₃)₄ (CH₂), 26.7 (CH₂), 13.7 (CH₃). HRMS (ES⁺) for [M⁺-PF₆], C₂₀H₂₉N₇ClRu 504.1216, measured 504.1217.

General procedure for transfer hydrogenation

A mixture of (2 mmol) of desired substrate (i.e. acetophenone or its derivatives or benzophenone), 10 mol% of base and (0.66 mmol) of 1,3,5-trimethoxybenzene as internal standard was dissolved in 5 mL of isopropanol followed by the addition of the catalyst solution in isopropanol. The reaction mixture was heated to 85 °C for a specific time. The reaction was left to cool to room temperature. Hexane was added to the solution and the filtered through celite. The filtrate was pumped dry in vacuo and the residue was extracted with CDCl₃. ¹H NMR spectrum was measured and the percentage yields calculated by the integration with the internal standard.

5.4-References

- (1) B. M. Trost, F. D. Toste and A. B. Pinkerton, *Chem. Rev.* 2001, **101**, 2067.
- (2) E. Fogler, E. Balaraman, Y. Ben-David, G. Leitus, L. J. W. Shimon and D Milstein, *Organometallics* 2011, **30**, 3826.
- (3) C. Gandolfi, M. Heckenroth, A. Neels, G Laurency and M. Albrecht, *Organometallics* 2009, **28**, 5115
- (4) S. V. Maifeld, M. N. Tran and D. Lee, *Tetrahedron Letters.* 2005, **46**, 105.
- (5) T. M. Trnka, and R. H. Grubbs, *Acc. Chem. Res.* 2001, **34**, 18.
- (6) L. Ackerman, A. Furstner, T. Weskamp, F. J Kohl and W. A Herrmann, *Tetrahedron Lett.* 1999, **40**, 4787.
- (7) H. M. Lee, D. C. Smith, Jr. Z. He, E. D. Stevens, C. S. Yi and S.P. Nolan, *Organometallics* 2001, **20**, 794.
- (8) A. W. Stumpf, E. Saive, A. Demonceau and A. F. Noels, *J. Chem. Soc, Chem. Commun.* 1995, 1127.
- (9) T. Weskamp, W.C. Schattenmann, M. Spiegler and W.A. Herrmann. *Angew. Chem.* 1998, **110**, 2631.
- (10) T. Opstal and F. Verpoort, *Synlett.* 2003, 314
- (11) B. De Clercq and F. Verpoort, *Organometallics* 2003, **672**, 11
- (12) J. P. Gallivan, J. P. Jordan and R. H. Grubbs, *Tetrahedron Lett.* 2005, **46**, 2577.
- (13) G. Winkhaus and H. Singer, *Organometallics* 1967, **7**, 487.
- (14) M. Yigit1, B. Yigit1, I. Özdemir1, E. Cetinkaya and B. Cetinkaya. *Appl. Organometal. Chem.* 2006, **20**, 322.

- (15) R. Cariou, C. Fischmeister, L. Toupet and P. H. Dixneuf, *Organometallics*. 2006, **25**, 2126.
- (16) B. Cetinakaya, S. Demir, I. Özdemir, L. Toupet, D. Semeril, C. Bruneau and P. H. Dixneuf, *Chem. Eur. J.* 2003, **9**, 2323
- (17) M. Poyatos, E. Mas-Marzá, M. Sanau´ and E. Peris, *Inorganic Chemistry*. 2004, **43**, 1793.
- (18) C. Ma, C. Ai, Z. Li, B. Li, H. Song, S. Xu and B. Wang, *Organometallics* 2014, **33**, 5164.
- (19) H. M. J. Wang and I. J. B. Lin, *Organometallics* 1998, **17**, 972
- (20) F. E. Hahn, and M. C. Jahnke. *Angew. Chem. Int. Ed.* 2008, **47**, 3122.
- (21) D. S. McGuinness, and K. J. Cavell, *Organometallics* 2000, **19**, 741.
- (22) A. M. Magill, D. S. McGuinness, K. J. Cavell, G. J. P. Britovsek, V. C. Gibson, A. J. P. White, D. J. Williams, A. H. White and B. W. Skelton, *Organometallics* 2001, **617**, 546.
- (23) N. Gürbüz, E. ÖzgeÖzcan, I. Özdemir, B. Çetinkaya, O. Şahin and O. Büyükgüng, *Dalton Trans.* 2012, **41**, 2330.
- (24) P. Csabai and F. Joo, *Organometallics*. 2004, **23**, 5640.
- (25) A. Prades, M. Viciano, M. Sanau´ and E. Peris, *Organometallics*. 2008, **27**, 4254.
- (26) M. Poyatos, A. Maise-François, S. Bellemin-Laponnaz, E. Peris and L. H. Gade, *Organometallics*. 2006, **691**, 2713.
- (27) P. Mathew, A. Neels and M. Albrecht. *J. Am. Chem. Soc.* 2008, **130**, 13534.
- (28) P. L. Arnold and A. C. Scarisbrick, *Organometallics*. 2004, **23**, 2519.

- (29) S. P Shan, X. Xiaoke, B. Gnanaprakasam, T. T. Dang, B. Ramalingam, H. V. Huynh and A. M. Seayad, *RSC Adv.* 2015, **5**, 4434.
- (30) D. Jantke, M. Cokoja, A. Pothig, W. A. Herrmann and F E. Kühn, *Organometallics* 2013, **32**, 741.
- (31) W. B. Cross, C G. Daly, Y. Boutadla and K Singh, *Dalton Trans.* 2011, **40**, 9722.
- (32) M. Poyatos, J. A. Mata, E. Falomir, R. H. Crabtree and E. Peris, *Organometallics* 2003, **22**, 1110.
- (33) R. Corbean, M. Sanau, and E. Peris, *Organometallics* 2007, **26**, 3492.
- (34) D. Gnanamgari, A. Moores, E. Rajaseelan and R. H. Crabtree, *Organometallics* 2007, **26**, 1226.
- (35) R. Castarlenas, M. A. Esteruelas and E. Onate, *Organometallics* 2008, **27**, 3240.
- (36) D. Gnanamgari, E. L. O.Sauer, N. D. Schley, C. Butler, C. D. Incarvito and R. H. Crabtree, *Organometallics* 2009, **28**, 321.
- (37) P. Hauwert, G. Maestri, J. W. Sprengers, M. Catellani and C. J. Elsevier, *Angew. Chem. Int. E.* 2008, **47**, 3223.
- (38) S. Gladiali and E. Alberico, *Chem. Soc. Rev.* 2006, **35**, 226.
- (39) G. Zassinovich, G. Mestroni and S. Gladiali, *Chem. Rev.* 1992, **51**, 1051.
- (40) R. Noyori and S. Hashiguchi, *Acc. Chem. Res.* 1997, **30**, 97.
- (41) H. U. Blaser, C. Malan, B. Pugin, F. Spindler and M. Steiner, *Adv. Synth. Catal.* 2003, **345**, 103.
- (42) Y. R. S. Laxmi and J- E. Bäckvall, *J. Chem. Commun.* 2000, **7**, 611.
- (43) O. Pamies, J.-E. Bäckvall, *Chem. Eur. J.* 2001, **7**, 5052.

- (44) Y. Sasson and J. Blum, *J. Org. Chem.* 1975, **40**, 1887.
- (45) A. C. Hillier, H. M. Lee, E. D. Stevens and S. P. Nolan, *Organometallic* 2001, **20**, 4249.
- (46) J. DePasquale, M. Kumar, M. Zeller and E. T. Papish, *Organometallics* 2013, **32**, 966.
- (47) M. Delgado-Rebollo, D. Canseco-Gonzalez, M. Hollering, H. Mueller-Bunz and M. Albrecht, *Dalton Trans.* 2014, **43**, 4462.
- (48) O. Saker, M. F. Mahon, J. E. Warren and M. K. Whittlesey, *Organometallics* 2009, **28**, 1976.
- (49) B. Zhu, A. Ellern, A. Sygula, R. Sygula, R. Angelici, *Organometallics* 2007, **26**, 1721.
- (50) M. A. Bennett and A. K. Smith, *J.C.S. Dalton.* 1974, **7**, 233

Chapter 6

6.1-Conclusions

A range of new imidazolium salts incorporating a triazine core have been synthesised and characterised as precursors to the corresponding NHC ligands. Cyanuric chloride was used to prepare a number of triazine derivatives, Monochlorotriazine derivatives **1a**, **1b**, **1c**, and **1d** were obtained by the reaction of morpholine, piperidine, dimethylamine and diethylamine respectively with cyanuric chloride under mildly basic aqueous conditions. The third chloride was substituted by the reaction with either 1-H-Imidazole followed by reaction with variety of alkyl halides to produce **2.4-2.7** and **2.10-2.15** or N –substituted –imidazoles to obtain salts **2.3**, **2.8**, **2.9** and **2.13** (Scheme 2-12). These methods gave good yields (61 – 85 %).

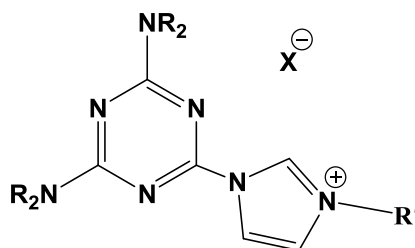


Figure (6-1) General structure of imidazolium salts

The ^1H NMR spectra typically showed three signals around 10, 8, and 7.5 ppm corresponding to the imidazole protons in addition to signals for the triazine derivatives and the second substituent on the imidazole ring. ^{13}C NMR spectroscopy confirmed the formation of salts by the appearance of two signals in the range 165-160 ppm for triazine and three signals for the imidazole ring around 123,120 and 137 ppm.

Imidazolium salts **2.4**, **2.6** and **2.10** were studied by X-ray diffraction, showed that bond lengths and bond angles for all ligands were generally in the range of expected by comparison with previous literatures.

The Ag(NHC)X complexes **3.1-3.11** were prepared in situ via the reaction of Ag₂O with an NHC precursor salt in dichloromethane to afford Ag(I)-NHC complexes. Ag₂O played two roles. First, as a base to deprotonate the azolium proton generating the free NHC and secondly it is a source of silver ions. 61-96% yields were obtained for the complexes.

NMR spectroscopy and mass spectrometry, as well as elemental analyses and X-ray crystallography were used to confirm the formation of complexes.

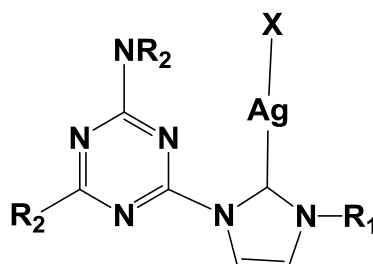


Figure (6-2) General structure of silver complexes

In the ¹H NMR spectra the imidazole proton resonances of positions 4 and 5 were shifted significantly upfield upon coordination when compared to the NHC ligand precursor, accompanied by the disappearance of the NC(H)N peak. ¹³C NMR spectra showed the disappearance of the signal corresponding to C2 in the range 137 ppm indicating formation of the complexes.

[Ag(NHC)X] complexes **3.4**, **3.5**, **3.5**, **3.6** and **3.7** were studied by X-ray diffraction. The structures consist of one NHC ligand and one halide ligand coordinated with a

single Ag center. The coordination geometry at Ag is slightly distorted from the idealised linear geometry according to $C_{\text{NHC}}\text{-Ag-X}$ bond angles.

Due to the labile nature and fluxional behaviour of silver(I)-NHCs, complexes **3.2** and **3.5** have been used as ligand transfer agents with $\text{Pd}(\text{MeCN})_2\text{Cl}_2$ for the synthesis of $[\text{Pd}(\text{NHC})_2\text{Cl}_2]$ **4.9** and **4.10**. X-ray diffraction showed both the *cis* and *trans* isomers for **4.9**.

$[\text{Pd}(\text{NHC})(\text{Py})\text{X}_2]$ complexes **4.1-4.7** have been prepared in situ via the reaction of PdCl_2 with an NHC precursor salt in the presence of K_2CO_3 in pyridine at $80\text{ }^\circ\text{C}$ giving the product in 41-68% yield.

^1H NMR spectroscopy showed that the imidazole proton resonances of positions 4 and 5 were shifted significantly upfield upon coordination when compared to the NHC ligand precursor, accompanied by the disappearance of the $\text{NC}(\text{H})\text{N}$ peak. Additionally, three new peaks for the pyridine protons were observed around 9.0, 7.5 and 7.3 ppm. New signals were observed in the ^{13}C NMR spectra attributed to Pd-C NHC around 150 ppm.

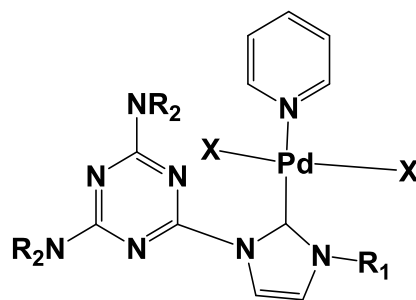


Figure (6-3) General structure of $[\text{Pd}(\text{NHC})(\text{Py})\text{X}_2]$ complexes

$[\text{Pd}(\text{NHC})(\text{Py})\text{X}_2]$ complexes **4.2**, **4.3**, **4.6** and **4.8** were studied by X-ray diffraction; the central Pd(II) is coordinated by one carbene, two bromo ligands in a *trans* configuration and a pyridine in a square planar geometry.

[Pd(NHC)(Py)X₂] complexes **4.3**, **4.6** and **4.8** were evaluated for the Suzuki-Miyaura coupling of phenylboronic acid with aromatic bromides and chlorides.

Two solvent systems were used in the cross coupling reaction; neat water and a mixture of DMF-H₂O (10-0.5 ml). The reactions were conducted at reflux under aerobic conditions in the presence of K₂CO₃ as a base.

The results obtained in both solvent systems prove that these complexes are efficient catalysts in the Suzuki reaction. The highest conversion (100%) was obtained in H₂O for 4-bromo acetophenone within 30 minute. Lower yields were obtained in DMF-H₂O mixtures at about 90-94%.

The cross-coupling for 4-chloroacetophenone in refluxing water afforded 26, 22 and 18% yield after 24h (entries 6-8) respectively. The low reactivity of 4-chloroacetophenone has been attributed to their resistance to oxidative addition because of the large Csp²-Cl bond dissociation energy.

Ag(NHC)X **3.1**, **3.2**, **3.3**, **3.4**, **3.5**, **3.9** and **3.10** have been also used to prepare [Ru(η⁶-arene)(NHC)Cl]Y **5.1-5.12** complexes (where Y= PF₆, Cl) by transmetallation from the silver complexes with either [Ru(p-cymene)Cl₂]₂ or [Ru(C₆H₆)Cl₂]₂ in dichloromethane to produce cyclometalated ruthenium complexes via coordination of the triazine-NHC ligand in a chelating mode where both the carbene and one of the N-donors of the triazine group ligate the metal.

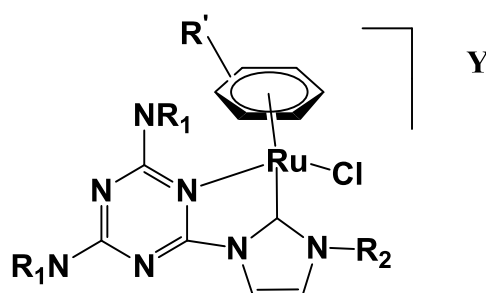


Figure (6-4) General structure of [Ru(η⁶-arene)(NHC)Cl]Y complexes

^1H NMR spectra of the $[\text{Ru}(\text{p-cymene})(\text{NHC})\text{Cl}]\text{Y}$ (where $\text{Y} = \text{Cl}, \text{PF}_6$) complexes **5.2**, **5.3**, **5.4**, **5.7** and **5.8** confirmed the formation of five membered ruthenacycle by the desymmetrization of the cymene ring, indicated by the four doublets between 6.12 and 5.34 ppm. The formation of $[\text{Ru}(\text{C}_6\text{H}_6)(\text{NHC})\text{Cl}]\text{Y}$ complexes **5.1**, **5.5**, **5.6**, **5.9**, **5.10**, **5.11** and **5.12** (where $\text{Y} = \text{Cl}, \text{PF}_6$) were confirmed by the emergence of a sharp signal between 5.92-5.39 ppm integrating to 6H and assigned to the benzene ring. ^{13}C NMR spectra of $[\text{Ru}(\eta^6\text{-arene})(\text{NHC})\text{Cl}]\text{Y}$ complexes **5.1-5.12** display signals in the range 181.1-184.3 ppm attributed to the carbene carbon, confirming formation of the ruthenium complexes.

$[\text{Ru}(\eta^6\text{-arene})(\text{NHC})\text{Cl}]\text{Y}$ **5.1**, **5.4**, **5.6**, **5.8**, **5.10** and **5.11** were studied by X-ray diffraction and showed that the ruthenium center is bound by the chelating NHC, chloride atom and η^6 -arene ring. Coordination of the triazine N-substituent is clearly observed.

The ruthenium complexes **5.1-5.12** were tested in the transfer hydrogenation reaction of ketonic substrates and proved to be very successful.

The reaction takes place between a variety of ketones and isopropanol as a solvent and proton source at 85 $^{\circ}\text{C}$ under basic conditions.

Publication from this Thesis

Dalton
Transactions

RSC Publishing

PAPER

[View Article Online](#)

[View Journal](#) | [View Issue](#)

Cite this: *Dalton Trans.*, 2013, **42**, 12370

Convenient syntheses of cyanuric chloride-derived NHC ligands, their Ag(I) and Au(I) complexes and antimicrobial activity†

Foteini Almalioti,^a James MacDougall,^a Stephen Hughes,^a Mohammed M. Hasson,^{a,d} Robert L. Jenkins,^a Benjamin D. Ward,^a Graham J. Tizzard,^b Simon J. Coles,^b David W. Williams,^c Sarah Bamford,^c Ian A. Fallis^{*a} and Athanasia Dervisi^{*a}

Convenient syntheses of mono- and bis-imidazolium 1,3,5-triazine derivatives bearing piperidine and morpholine substituents are reported. *In situ* deprotonation of the mono-imidazolium salts and reaction with Ag₂O or Au(tht)Cl (tht = tetrahydrothiophene) precursors affords the corresponding Ag(NHC)Cl and Au(NHC)Cl carbene complexes. In the presence of Ag(I) or Au(I) salts the bis-imidazolium pincers eliminate the imidazolium group to afford –OMe or –NMe₂ substituted triazines depending on the solvent used. In solution, the Ag(I) and Au(I) complexes show a barrier to rotation about the C_{triazine}–N_{amine}

X-Ray crystal structure data

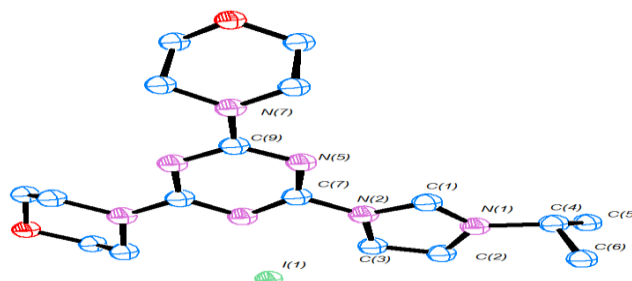
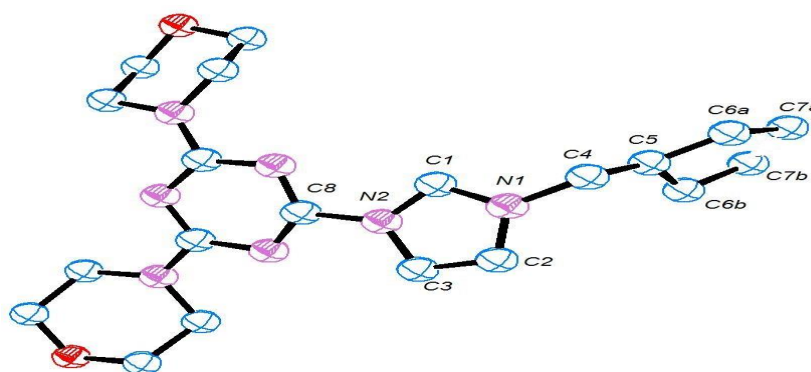
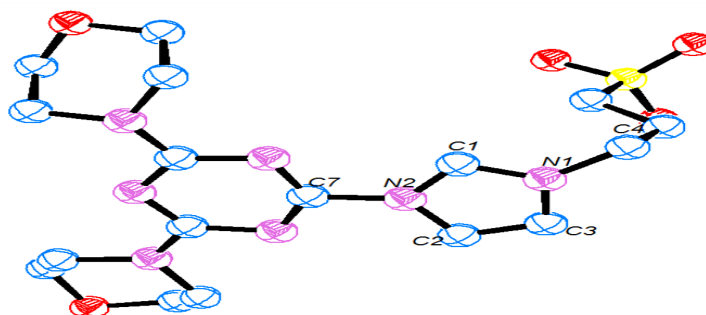


Table A.1: Crystal data and structure refinement for [1- TzMorph₂-3-IPr- Im]I, (2.4)

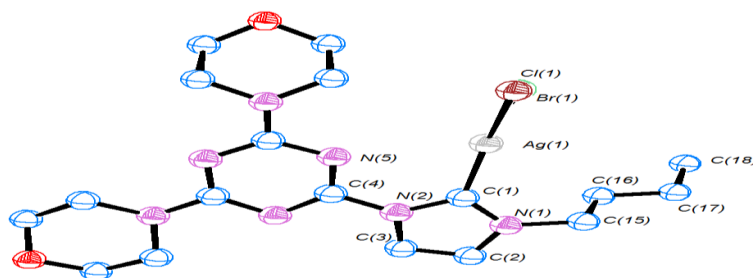
Identification code	2012ncs0915a	
Empirical formula	C ₁₉ H ₂₉ IN ₈ O ₂	
Formula weight	528.40	
Temperature	100(2) K	
Wavelength	0.71075 Å	
Crystal system	Triclinic	
Space group	<i>P</i> -1	
Unit cell dimensions	<i>a</i> = 9.9931(4) Å	<i>α</i> = 103.828(7) °
	<i>b</i> = 10.9576(4) Å	<i>β</i> = 108.497(8) °
	<i>c</i> = 11.7851(8) Å	<i>γ</i> = 97.432(7) °
Volume	1158.46(10) Å ³	
<i>Z</i>	2	
Density (calculated)	1.515 Mg / m ³	
Absorption coefficient	1.414 mm ⁻¹	
<i>F</i> (000)	536	
Crystal	Block; colourless	
Crystal size	0.05 × 0.04 × 0.03 mm ³	
<i>θ</i> range for data collection	3.00 – 27.49°	
Index ranges	–12 ≤ <i>h</i> ≤ 12, –14 ≤ <i>k</i> ≤ 14, –15 ≤ <i>l</i> ≤ 15	
Reflections collected	36531	
Independent reflections	5293 [<i>R</i> _{int} = 0.0339]	
Completeness to <i>θ</i> = 27.49°	99.8 %	
Absorption correction	Semi-empirical from equivalents	
Max. and min. transmission	0.9588 and 0.9327	
Refinement method	Full-matrix least-squares on <i>F</i> ²	
Data / restraints / parameters	5293 / 0 / 274	
Goodness-of-fit on <i>F</i> ²	1.046	
Final <i>R</i> indices [<i>F</i> ² > 2σ(<i>F</i> ²)]	<i>R</i> 1 = 0.0248, <i>wR</i> 2 = 0.0581	
<i>R</i> indices (all data)	<i>R</i> 1 = 0.0276, <i>wR</i> 2 = 0.0593	
Largest diff. peak and hole	0.826 and –0.811 e Å ⁻³	

**Table B.1:** Crystal data and structure refinement for [1-TzMorph₂-3-Bu-Im]Br, (**2.6**)

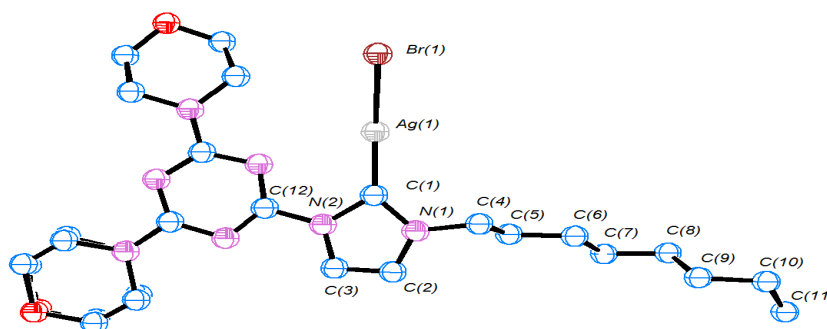
Identification code	2012ncs0913ab
Empirical formula	C ₁₉ H ₂₉ BrCl ₃ N ₇ O ₂
Formula weight	573.75
Temperature	100(2) K
Wavelength	0.71075 Å
Crystal system	Monoclinic
Space group	<i>P</i> 2 ₁ / <i>c</i>
Unit cell dimensions	<i>a</i> = 14.7565(10) Å $\alpha = 90^\circ$ <i>b</i> = 11.2256(8) Å $\beta = 110.606(3)^\circ$ <i>c</i> = 16.6420(11) Å $\gamma = 90^\circ$
110.606(3)°	
Volume	2580.4(3) Å ³
<i>Z</i>	4
Density (calculated)	1.477 Mg / m ³
Absorption coefficient	1.933 mm ⁻¹
<i>F</i> (000)	1176
Crystal	Block; Colorless
Crystal size	0.160 × 0.050 × 0.040 mm ³
θ range for data collection	2.921 – 27.461°
Index ranges	–12 ≤ <i>h</i> ≤ 19, –14 ≤ <i>k</i> ≤ 14, –21 ≤ <i>l</i> ≤ 21
Reflections collected	17306
Independent reflections	5869 [<i>R</i> _{int} = 0.0802]
Completeness to $\theta = 25.242^\circ$	99.6 %
Absorption correction	Semi-empirical from equivalents
Max. and min. transmission	1.000 and 0.619
Refinement method	Full-matrix least-squares on <i>F</i> ²
Data / restraints / parameters	5869 / 0 / 310
Goodness-of-fit on <i>F</i> ²	1.095
Final <i>R</i> indices [<i>F</i> ² > 2σ(<i>F</i> ²)]	<i>R</i> 1 = 0.0464, <i>wR</i> 2 = 0.0937
<i>R</i> indices (all data)	<i>R</i> 1 = 0.0768, <i>wR</i> 2 = 0.1067
Extinction coefficient	n/a
Largest diff. peak and hole	0.574 and –0.519 e Å ⁻³

**Table C.1:** Crystal data and structure refinement [1-TzMorph₂-3-sulfonat-Im], (2.10)

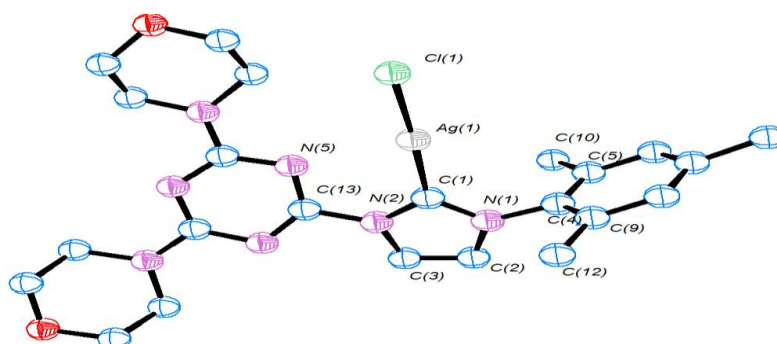
Empirical formula	C ₁₈ H ₂₈ N ₇ O _{5.50} S	
Formula weight	462.53	
Temperature	100(2) K	
Wavelength	0.71075 Å	
Crystal system	Monoclinic	
Space group	<i>P</i> 2 ₁ / <i>c</i>	
Unit cell dimensions	<i>a</i> = 13.5640(9) Å	$\alpha = 90^\circ$
	<i>b</i> = 15.9055(6) Å	$\beta = 97.959(7)^\circ$
	<i>c</i> = 9.8977(3) Å	$\gamma = 90^\circ$
Volume	2114.78(17) Å ³	
<i>Z</i>	4	
Density (calculated)	1.453 Mg / m ³	
Absorption coefficient	0.203 mm ⁻¹	
<i>F</i> (000)	980	
Crystal	Block; Colourless	
Crystal size	0.08 × 0.08 × 0.08 mm ³	
θ range for data collection	3.02 – 27.49°	
Index ranges	–17 ≤ <i>h</i> ≤ 16, –20 ≤ <i>k</i> ≤ 20, –8 ≤ <i>l</i> ≤ 12	
Reflections collected	14624	
Independent reflections	4827 [<i>R</i> _{int} = 0.0397]	
Completeness to $\theta = 27.49^\circ$	99.6 %	
Absorption correction	Semi-empirical from equivalents	
Max. and min. transmission	0.9840 and 0.9840	
Refinement method	Full-matrix least-squares on <i>F</i> ²	
Data / restraints / parameters	4827 / 0 / 300	
Goodness-of-fit on <i>F</i> ²	1.077	
Final <i>R</i> indices [<i>F</i> ² > 2σ(<i>F</i> ²)]	<i>R</i> 1 = 0.0399, <i>wR</i> 2 = 0.1005	
<i>R</i> indices (all data)	<i>R</i> 1 = 0.0608, <i>wR</i> 2 = 0.1055	
Largest diff. peak and hole	0.405 and –0.502 e Å ⁻³	

**Table D.1:** Crystal data and structure refinement for [AgBr(2.6)],(3.3)

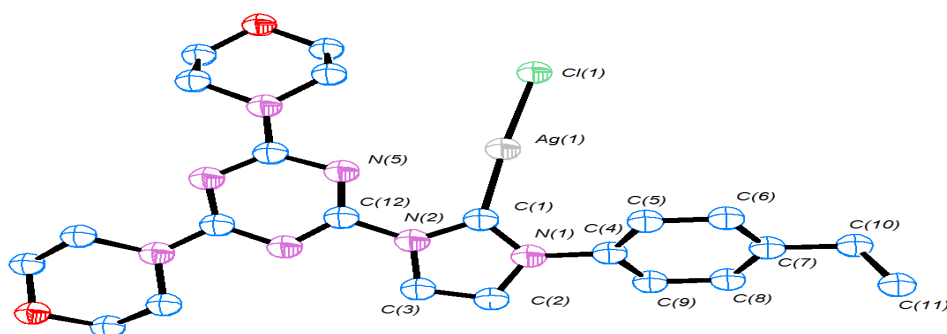
identification code	2012ncs0914dlsba	
Empirical formula	C ₁₈ H ₂₇ AgBr _{0.50} Cl _{0.50} N ₇ O ₂	
Formula weight	539.01	
Temperature	100(2) K	
Wavelength	0.68890 Å	
Crystal system	Monoclinic	
Space group	P21/c	
Unit cell dimensions	<i>a</i> = 13.932(15) Å	$\alpha = 90^\circ$
	<i>b</i> = 17.533(17) Å	$\beta = 103.147(15)^\circ$
	<i>c</i> = 8.981(9) Å	$\gamma = 90^\circ$
Volume	2136(4) Å ³	
<i>Z</i>	4	
Density (calculated)	1.676 Mg / m ³	
Absorption coefficient	1.971 mm ⁻¹	
<i>F</i> (000)	1092	
Crystal	Block; Colorless	
Crystal size	0.090 × 0.030 × 0.010 mm ³	
θ range for data collection	3.121 – 24.203°	
Index ranges	–16 ≤ <i>h</i> ≤ 14, –20 ≤ <i>k</i> ≤ 20, –8 ≤ <i>l</i> ≤ 10	
Reflections collected	11862	
Independent reflections	3611 [<i>R</i> _{int} = 0.0618]	
Completeness to $\theta = 24.415^\circ$	93.3 %	
Absorption correction	Semi-empirical from equivalents	
Max. and min. transmission	1.000 and 0.625	
Refinement method	Full-matrix least-squares on <i>F</i> ²	
Data / restraints / parameters	3611 / 0 / 272	
Goodness-of-fit on <i>F</i> ²	1.060	
Final <i>R</i> indices [<i>F</i> ² > 2σ(<i>F</i> ²)]	<i>R</i> 1 = 0.0487, <i>wR</i> 2 = 0.1316	
<i>R</i> indices (all data)	<i>R</i> 1 = 0.0539, <i>wR</i> 2 = 0.1382	
Extinction coefficient	n/a	
Largest diff. peak and hole	1.646 and –1.382 e Å ⁻³	

**Table e.1:** Crystal data and structure refinement for [AgBr(2.7)] (3.4)

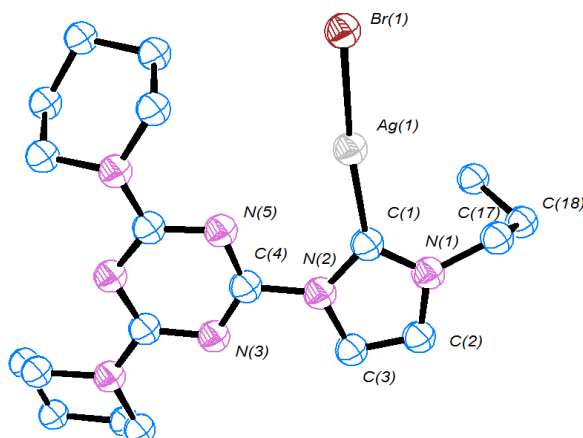
Identification code	2013ncs0524r1aa	
Empirical formula	C ₂₂ H ₃₅ Ag ₁ Br ₁ N ₇ O ₂	
Formula weight	617.34	
Temperature	100(2) K	
Wavelength	0.71075 Å	
Crystal system	Monoclinic	
Space group	P121/c1	
Unit cell dimensions	<i>a</i> = 9.2025(5) Å	$\alpha = 90^\circ$
	<i>b</i> = 17.0845(11) Å	$\beta = 90.837(2)^\circ$
	<i>c</i> = 31.998(2) Å	$\gamma = 90^\circ$
Volume	5030.2(5) Å ³	
Z	8	
Density (calculated)	1.630 Mg / m ³	
Absorption coefficient	2.423 mm ⁻¹	
<i>F</i> (000)	2512	
Crystal	Plate; Colourless	
Crystal size	0.14 × 0.1 × 0.01 mm ³	
θ range for data collection	2.251 – 27.483°	
Index ranges	–11 ≤ <i>h</i> ≤ 11, –21 ≤ <i>k</i> ≤ 22, –38 ≤ <i>l</i> ≤ 41	
Reflections collected	45795	
Independent reflections	11325 [<i>R</i> _{int} = 0.1083]	
Completeness to $\theta = 27.500^\circ$	98.1 %	
Absorption correction	Semi-empirical from equivalents	
Max. and min. transmission	1.000 and 0.578	
Refinement method	Full-matrix least-squares on <i>F</i> ²	
Data / restraints / parameters	11325 / 1254 / 643	
Goodness-of-fit on <i>F</i> ²	1.121	
Final <i>R</i> indices [<i>F</i> ² > 2σ(<i>F</i> ²)]	<i>R</i> 1 = 0.1195, <i>wR</i> 2 = 0.3040	
<i>R</i> indices (all data)	<i>R</i> 1 = 0.1465, <i>wR</i> 2 = 0.3180	
Extinction coefficient	n/a	
Largest diff. peak and hole	5.102 and –3.221 e Å ⁻³	

**Table F.1:** Crystal data and structure refinement [AgCl(**2.8**)],(3.5)

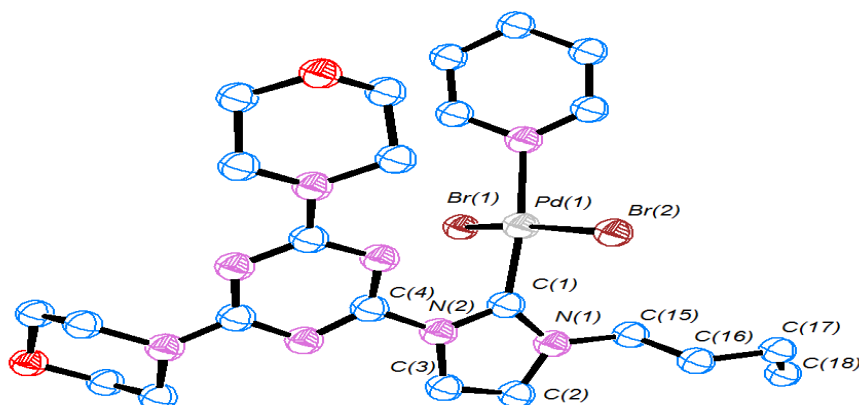
Identification code	2013ncs0050a	
Empirical formula	C ₂₃ H ₂₉ AgClN ₇ O ₂	
Formula weight	578.85	
Temperature	100(2) K	
Wavelength	0.71075 Å	
Crystal system	Triclinic	
Space group	<i>P</i> -1	
Unit cell dimensions	<i>a</i> = 8.8720(5) Å	<i>α</i> = 93.981(4) °
	<i>b</i> = 10.0035(7) Å	<i>β</i> = 105.976(5) °
	<i>c</i> = 15.4909(11) Å	<i>γ</i> = 104.748(5) °
Volume	1263.72(15) Å ³	
<i>Z</i>	2	
Density (calculated)	1.521 Mg / m ³	
Absorption coefficient	0.937 mm ⁻¹	
<i>F</i> (000)	592	
Crystal	Block; Colorless	
Crystal size	0.050 × 0.040 × 0.020 mm ³	
<i>θ</i> range for data collection	3.111 – 27.474°	
Index ranges	–11 ≤ <i>h</i> ≤ 11, –12 ≤ <i>k</i> ≤ 12, –20 ≤ <i>l</i> ≤ 20	
Reflections collected	17001	
Independent reflections	5762 [<i>R</i> _{int} = 0.0397]	
Completeness to <i>θ</i> = 25.242°	99.8 %	
Absorption correction	Semi-empirical from equivalents	
Max. and min. transmission	1.000 and 0.834	
Refinement method	Full-matrix least-squares on <i>F</i> ²	
Data / restraints / parameters	5762 / 0 / 310	
Goodness-of-fit on <i>F</i> ²	1.027	
Final <i>R</i> indices [<i>F</i> ² > 2σ(<i>F</i> ²)]	<i>R</i> 1 = 0.0371, <i>wR</i> 2 = 0.0989	
<i>R</i> indices (all data)	<i>R</i> 1 = 0.0408, <i>wR</i> 2 = 0.1011	
Extinction coefficient	n/a	
Largest diff. peak and hole	2.469 and –0.711 e Å ⁻³	

**Table F.1:** Crystal data and structure refinement [AgCl(2.9)],(3.6)

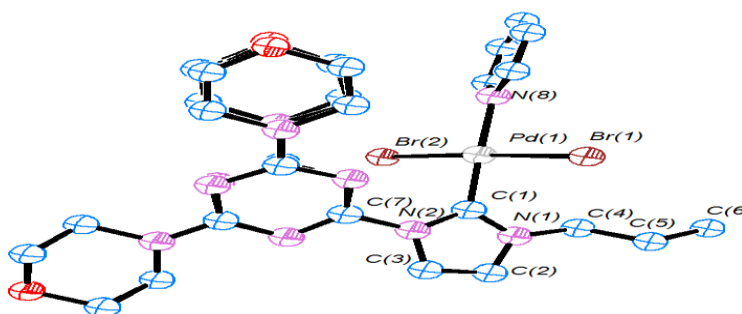
Identification code	2013ncs0763a	
Empirical formula	$C_{22}H_{27}AgClN_7O_2$	
Formula weight	564.82	
Temperature	100(2) K	
Wavelength	0.71075 Å	
Crystal system	Monoclinic	
Space group	$P121/n1$	
Unit cell dimensions	$a = 7.5969(5)$ Å	$\alpha = 90^\circ$
	$b = 19.9498(14)$ Å	$\beta = 101.972(2)^\circ$
	$c = 15.9396(11)$ Å	$\gamma = 90^\circ$
Volume	$2363.2(3)$ Å ³	
Z	4	
Density (calculated)	1.588 Mg / m ³	
Absorption coefficient	1.000 mm ⁻¹	
$F(000)$	1152	
Crystal	Fragment; Brownish	
Crystal size	$0.07 \times 0.05 \times 0.03$ mm ³	
θ range for data collection	2.424 – 27.485°	
Index ranges	$-9 \leq h \leq 7, -25 \leq k \leq 17, -20 \leq l \leq 18$	
Reflections collected	16975	
Independent reflections	5409 [$R_{int} = 0.0361$]	
Completeness to $\theta = 27.500^\circ$	99.6 %	
Absorption correction	Semi-empirical from equivalents	
Max. and min. transmission	1.000 and 0.740	
Refinement method	Full-matrix least-squares on F^2	
Data / restraints / parameters	5409 / 0 / 299	
Goodness-of-fit on F^2	1.019	
Final R indices [$F^2 > 2\sigma(F^2)$]	$R1 = 0.0292, wR2 = 0.0688$	
R indices (all data)	$R1 = 0.0405, wR2 = 0.0735$	
Extinction coefficient	n/a	
Largest diff. peak and hole	0.544 and -0.545 e Å ⁻³	

**Table F.1:** Crystal data and structure refinement [AgBr(2.11)], (3.7)

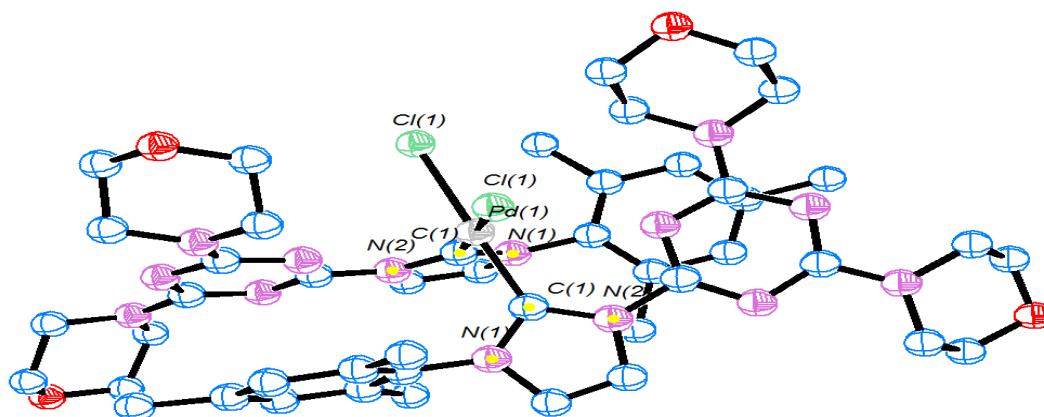
Empirical formula	$C_{19}H_{29}AgBrN_7$	
Formula weight	543.27	
Temperature	100(2) K	
Wavelength	0.71075 Å	
Crystal system	Monoclinic	
Space group	$P121/c1$	
Unit cell dimensions	$a = 11.5086(8)$ Å	$\alpha = 90^\circ$
	$b = 9.9376(7)$ Å	$\beta = 99.830(2)^\circ$
	$c = 18.9003(13)$ Å	$\gamma = 90^\circ$
Volume	$2129.9(3)$ Å ³	
Z	4	
Density (calculated)	1.694 Mg / m ³	
Absorption coefficient	2.842 mm ⁻¹	
$F(000)$	1096	
Crystal	Block; colourless	
Crystal size	$0.05 \times 0.03 \times 0.03$ mm ³	
θ range for data collection	$2.323 - 27.455^\circ$	
Index ranges	$-14 \leq h \leq 9, -12 \leq k \leq 11, -22 \leq l \leq 24$	
Reflections collected	14299	
Independent reflections	4850 [$R_{int} = 0.0326$]	
Completeness to $\theta = 25.242^\circ$	99.6 %	
Absorption correction	Semi-empirical from equivalents	
Max. and min. transmission	1.000 and 0.690	
Refinement method	Full-matrix least-squares on F^2	
Data / restraints / parameters	4850 / 0 / 254	
Goodness-of-fit on F^2	1.023	
Final R indices [$F^2 > 2\sigma(F^2)$]	$R1 = 0.0310, wR2 = 0.0701$	
R indices (all data)	$R1 = 0.0417, wR2 = 0.0739$	
Extinction coefficient	n/a	
Largest diff. peak and hole	0.913 and -0.998 e Å ⁻³	

**Table G.1:** Crystal data and structure refinement [Pd(py)Br₂(**2.6**)].(4.3)

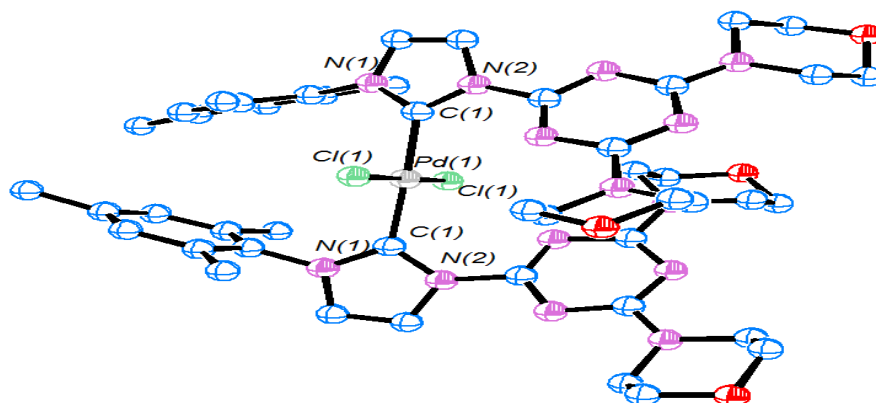
Identification code	2013ncs0032a	
Empirical formula	C ₂₄ H ₃₃ Br ₂ Cl ₃ N ₈ O ₂ Pd	
Formula weight	838.15	
Temperature	100(2) K	
Wavelength	0.71075 Å	
Crystal system	Triclinic	
Space group	<i>P</i> -1	
Unit cell dimensions	<i>a</i> = 9.0549(2) Å	<i>α</i> = 76.609(5) °
	<i>b</i> = 12.6900(2) Å	<i>β</i> = 77.973(6) °
	<i>c</i> = 14.2332(10) Å	<i>γ</i> = 84.223(6) °
Volume	1553.74(12) Å ³	
<i>Z</i>	2	
Density (calculated)	1.792 Mg / m ³	
Absorption coefficient	3.464 mm ⁻¹	
<i>F</i> (000)	832	
Crystal	Block; Yellow	
Crystal size	0.15 × 0.13 × 0.09 mm ³	
<i>θ</i> range for data collection	3.00 – 27.48°	
Index ranges	–11 ≤ <i>h</i> ≤ 11, –16 ≤ <i>k</i> ≤ 15, –18 ≤ <i>l</i> ≤ 18	
Reflections collected	35205	
Independent reflections	7126 [<i>R</i> _{int} = 0.0321]	
Completeness to <i>θ</i> = 27.48°	99.8 %	
Absorption correction	Semi-empirical from equivalents	
Max. and min. transmission	0.7457 and 0.6246	
Refinement method	Full-matrix least-squares on <i>F</i> ²	
Data / restraints / parameters	7126 / 6 / 379	
Goodness-of-fit on <i>F</i> ²	1.043	
Final <i>R</i> indices [<i>F</i> ² > 2σ(<i>F</i> ²)]	<i>R</i> 1 = 0.0298, <i>wR</i> 2 = 0.0762	
<i>R</i> indices (all data)	<i>R</i> 1 = 0.0311, <i>wR</i> 2 = 0.0771	
Largest diff. peak and hole	2.568 and –1.383 e Å ⁻³	

**Table H.1:** Crystal data and structure refinement Pd(py)Br₂(2.5).(4.2)

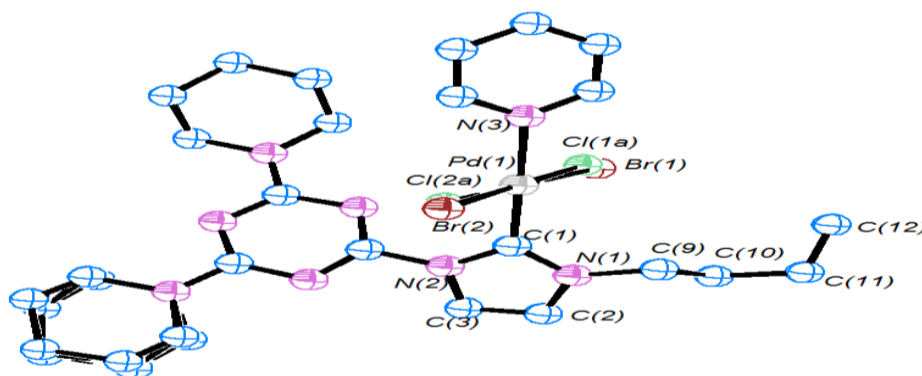
Empirical formula	C ₂₂ H ₃₀ Br ₂ N ₈ O ₂ Pd	
Formula weight	704.76	
Temperature	100(2) K	
Wavelength	0.71075 Å	
Crystal system	Monoclinic	
Space group	<i>P</i> 121/ <i>n</i> 1	
Unit cell dimensions	<i>a</i> = 12.7034(9) Å	$\alpha = 90^\circ$
	<i>b</i> = 8.7709(5) Å	$\beta = 96.803(2)^\circ$
	<i>c</i> = 23.7349(17) Å	$\gamma = 90^\circ$
Volume	2625.9(3) Å ³	
<i>Z</i>	4	
Density (calculated)	1.783 Mg / m ³	
Absorption coefficient	3.786 mm ⁻¹	
<i>F</i> (000)	1400	
Crystal	Block; yellow	
Crystal size	0.13 × 0.12 × 0.05 mm ³	
θ range for data collection	2.478 – 27.485°	
Index ranges	–16 ≤ <i>h</i> ≤ 16, –11 ≤ <i>k</i> ≤ 11, –30 ≤ <i>l</i> ≤ 19	
Reflections collected	17392	
Independent reflections	5933 [<i>R</i> _{int} = 0.0286]	
Completeness to $\theta = 25.242^\circ$	98.9 %	
Absorption correction	Semi-empirical from equivalents	
Max. and min. transmission	1.000 and 0.727	
Refinement method	Full-matrix least-squares on <i>F</i> ²	
Data / restraints / parameters	5933 / 0 / 393	
Goodness-of-fit on <i>F</i> ²	1.044	
Final <i>R</i> indices [<i>F</i> ² > 2σ(<i>F</i> ²)]	<i>R</i> 1 = 0.0264, <i>wR</i> 2 = 0.0645	
<i>R</i> indices (all data)	<i>R</i> 1 = 0.0343, <i>wR</i> 2 = 0.0683	
Extinction coefficient	n/a	
Largest diff. peak and hole	0.564 and –0.515 e Å ⁻³	

**Table I.1:** Crystal data and structure refinement for *cis*-[Pd(**2.8**)₂Cl₂], *cis*-**4.9**

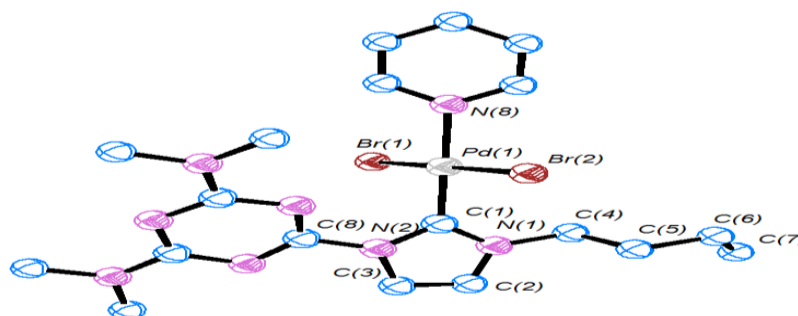
Identification code	2013ncs0520a	
Empirical formula	C ₄₆ H ₅₈ Cl ₂ N ₁₄ O ₄ Pd	
Formula weight	1048.36	
Temperature	100(2) K	
Wavelength	0.71075 Å	
Crystal system	Orthorhombic	
Space group	<i>Pccn</i>	
Unit cell dimensions	<i>a</i> = 12.5125(9) Å	$\alpha = 90^\circ$
	<i>b</i> = 18.9010(13) Å	$\beta = 90^\circ$
	<i>c</i> = 19.4406(14) Å	$\gamma = 90^\circ$
Volume	4597.7(6) Å ³	
<i>Z</i>	4	
Density (calculated)	1.515 Mg / m ³	
Absorption coefficient	0.582 mm ⁻¹	
<i>F</i> (000)	2176	
Crystal	Needle; colourless	
Crystal size	0.13 × 0.01 × 0.01 mm ³	
θ range for data collection	2.095 – 27.411°	
Index ranges	–15 ≤ <i>h</i> ≤ 16, –21 ≤ <i>k</i> ≤ 24, –25 ≤ <i>l</i> ≤ 25	
Reflections collected	31555	
Independent reflections	5233 [<i>R</i> _{int} = 0.0902]	
Completeness to $\theta = 25.242^\circ$	99.9 %	
Absorption correction	Semi-empirical from equivalents	
Max. and min. transmission	1.000 and 0.667	
Refinement method	Full-matrix least-squares on <i>F</i> ²	
Data / restraints / parameters	5233 / 0 / 306	
Goodness-of-fit on <i>F</i> ²	1.038	
Final <i>R</i> indices [<i>F</i> ² > 2σ(<i>F</i> ²)]	<i>R</i> 1 = 0.0460, <i>wR</i> 2 = 0.1004	
<i>R</i> indices (all data)	<i>R</i> 1 = 0.0895, <i>wR</i> 2 = 0.1176	
Extinction coefficient	n/a	
Largest diff. peak and hole and hole	0.607 and –0.785 e Å ⁻³ Largest diff. peak 0.564 and –0.515 e Å ⁻³	

**Table J.1:** Crystal data and structure refinement for *trans*-[Pd(**2.8**)₂Cl₂], *trans*-**4.9**

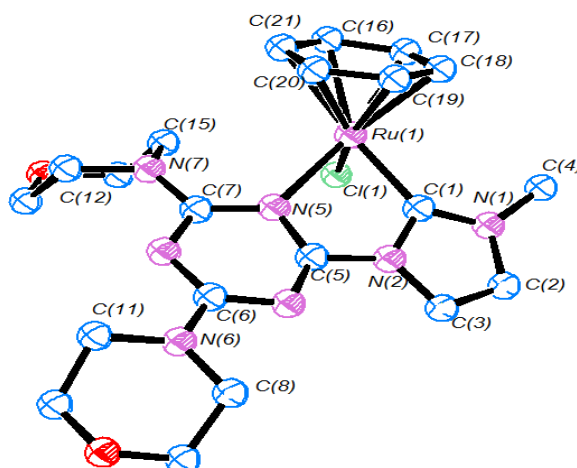
Identification code	2013ncs0513r1a	
Empirical formula	C ₄₈ H ₆₀ Cl ₈ N ₁₄ O ₄ Pd	
Formula weight	1287.10	
Temperature	100(2) K	
Wavelength	0.71075 Å	
Crystal system	Orthorhombic	
Space group	<i>Pbcn</i>	
Unit cell dimensions	<i>a</i> = 17.6748(11) Å	$\alpha = 90^\circ$
	<i>b</i> = 26.6161(19) Å	$\beta = 90^\circ$
	<i>c</i> = 12.3891(9) Å	$\gamma = 90^\circ$
Volume	5828.3(7) Å ³	
<i>Z</i>	4	
Density (calculated)	1.467 Mg / m ³	
Absorption coefficient	0.740 mm ⁻¹	
<i>F</i> (000)	2640	
Crystal	Block; colourless	
Crystal size	0.19 × 0.1 × 0.09 mm ³	
θ range for data collection	2.25 – 27.48°	
Index ranges	–22 ≤ <i>h</i> ≤ 22, –34 ≤ <i>k</i> ≤ 33, –16 ≤ <i>l</i> ≤ 14	
Reflections collected	29749	
Independent reflections	6669 [<i>R</i> _{int} = 0.0347]	
Completeness to $\theta = 25.242^\circ$	99.7 %	
Absorption correction	Semi-empirical from equivalents	
Max. and min. transmission	1.000 and 0.822	
Refinement method	Full-matrix least-squares on <i>F</i> ²	
Data / restraints / parameters	6669 / 0 / 342	
Goodness-of-fit on <i>F</i> ²	1.047	
Final <i>R</i> indices [<i>F</i> ² > 2σ(<i>F</i> ²)]	<i>R</i> 1 = 0.0264, <i>wR</i> 2 = 0.0664	
<i>R</i> indices (all data)	<i>R</i> 1 = 0.0345, <i>wR</i> 2 = 0.0686	
Extinction coefficient	n/a	
Largest diff. peak and hole	0.346 and –0.437 e Å ⁻³	
	0.564 and –0.515 e Å ⁻³	

**Table K.1:** Crystal data and structure refinement for [Pd(py)Br₂(**2.12**)], **4.6**

Identification code	2013ncs0651a	
Empirical formula	C ₂₅ H ₃₆ Br _{1.39} Cl _{0.61} N ₈ Pd	
Formula weight	687.67	
Temperature	100(2) K	
Wavelength	0.71075 Å	
Crystal system	Triclinic	
Space group	<i>P</i> -1	
Unit cell dimensions	<i>a</i> = 8.4667(5) Å	<i>α</i> = 88.798(5) °
	<i>b</i> = 12.1907(9) Å	<i>β</i> = 79.162(4) °
	<i>c</i> = 13.8571(10) Å	<i>γ</i> = 86.720(4) °
Volume	1402.37(17) Å ³	
<i>Z</i>	2	
Density (calculated)	1.629 Mg / m ³	
Absorption coefficient	2.728 mm ⁻¹	
<i>F</i> (000)	694	
Crystal	Block; yellow	
Crystal size	0.04 × 0.04 × 0.03 mm ³	
<i>θ</i> range for data collection	2.62 – 27.48°	
Index ranges	-10 ≤ <i>h</i> ≤ 10, -15 ≤ <i>k</i> ≤ 15, -17 ≤ <i>l</i> ≤ 17	
Reflections collected	18354	
Independent reflections	6394 [<i>R</i> _{int} = 0.0461]	
Completeness to <i>θ</i> = 27.500°	99.5 %	
Absorption correction	Semi-empirical from equivalents	
Max. and min. transmission	1.000 and 0.790	
Refinement method	Full-matrix least-squares on <i>F</i> ²	
Data / restraints / parameters	6394 / 0 / 352	
Goodness-of-fit on <i>F</i> ²	1.030	
Final <i>R</i> indices [<i>F</i> ² > 2σ(<i>F</i> ²)]	<i>R</i> 1 = 0.0344, <i>wR</i> 2 = 0.0841	
<i>R</i> indices (all data)	<i>R</i> 1 = 0.0457, <i>wR</i> 2 = 0.0910	
Extinction coefficient	n/a	
Largest diff. peak and hole	0.902 and -0.866 e Å ⁻³	

**Table L.1:** Crystal data and structure refinement for [Pd(py)Br₂(2.14)], **4.8**

Identification code	2014ncs0636a	
Empirical formula	C ₁₉ H ₂₈ Br ₂ N ₈ Pd	
Formula weight	634.71	
Temperature	100(2) K	
Wavelength	0.71075 Å	
Crystal system	Triclinic	
Space group	<i>P</i> -1	
Unit cell dimensions	<i>a</i> = 9.1101(11) Å	<i>α</i> = 82.785(8)°
	<i>b</i> = 11.2952(11) Å	<i>β</i> = 87.938(7)°
	<i>c</i> = 12.1936(17) Å	<i>γ</i> = 70.853(6)°
Volume	1175.9(2) Å ³	
<i>Z</i>	2	
Density (calculated)	1.793 Mg / m ³	
Absorption coefficient	4.210 mm ⁻¹	
<i>F</i> (000)	628	
Crystal	Block; Colourless	
Crystal size	0.07 × 0.04 × 0.02 mm ³	
<i>θ</i> range for data collection	2.367 – 27.470°	
Index ranges	-11 ≤ <i>h</i> ≤ 11, -14 ≤ <i>k</i> ≤ 14, -14 ≤ <i>l</i> ≤ 15	
Reflections collected	15732	
Independent reflections	5341 [<i>R</i> _{int} = 0.0533]	
Completeness to <i>θ</i> = 25.242°	99.8 %	
Absorption correction	Semi-empirical from equivalents	
Max. and min. transmission	1.000 and 0.571	
Refinement method	Full-matrix least-squares on <i>F</i> ²	
Data / restraints / parameters	5341 / 0 / 276	
Goodness-of-fit on <i>F</i> ²	1.036	
Final <i>R</i> indices [<i>F</i> ² > 2σ(<i>F</i> ²)]	<i>R</i> 1 = 0.0411, <i>wR</i> 2 = 0.1031	
<i>R</i> indices (all data)	<i>R</i> 1 = 0.0491, <i>wR</i> 2 = 0.1099	
Extinction coefficient	n/a	
Largest diff. peak and hole	0.847 and -0.697 e Å ⁻³	

**Table M.1:** Crystal data and structure refinement FOR [Ru(C₆H₆)Cl(2.3)] PF₆, (5.1)

Identification code	2014ncs0110a	
Empirical formula	C ₂₁ H ₂₈ ClF ₆ N ₇ O ₃ PRu	
Formula weight	707.99	
Temperature	100(2) K	
Wavelength	0.71073 Å	
Crystal system	Monoclinic	
Space group	P121/n1	
Unit cell dimensions	<i>a</i> = 11.4046(2) Å	$\alpha = 90.0^\circ$
	<i>b</i> = 33.5674(7) Å	$\beta = 93.836(2)^\circ$
	<i>c</i> = 13.8115(4) Å	$\gamma = 90.0^\circ$
Volume	5275.5(2) Å ³	
<i>Z</i>	8	
Density (calculated)	1.783 Mg / m ³	
Absorption coefficient	0.839 mm ⁻¹	
<i>F</i> (000)	2856	
Crystal	Plate; Yellow	
Crystal size	0.06 × 0.04 × 0.01 mm ³	
θ range for data collection	2.162 – 27.483°	
Index ranges	–15 ≤ <i>h</i> ≤ 15, –39 ≤ <i>k</i> ≤ 46, –18 ≤ <i>l</i> ≤ 19	
Reflections collected	46225	
Independent reflections	12066 [<i>R</i> _{int} = 0.0510]	
Completeness to $\theta = 27.500^\circ$	99.7 %	
Absorption correction	Semi-empirical from equivalents	
Max. and min. transmission	1.00000 and 0.81301	
Refinement method	Full-matrix least-squares on <i>F</i> ²	
Data / restraints / parameters	12066 / 126 / 795	
Goodness-of-fit on <i>F</i> ²	1.025	
Final <i>R</i> indices [<i>F</i> ² > 2σ(<i>F</i> ²)]	<i>R</i> 1 = 0.0486, <i>wR</i> 2 = 0.1071	
<i>R</i> indices (all data)	<i>R</i> 1 = 0.0701, <i>wR</i> 2 = 0.1163	
Extinction coefficient	n/a	
Largest diff. peak and hole	1.212 and –0.862 e Å ⁻³	

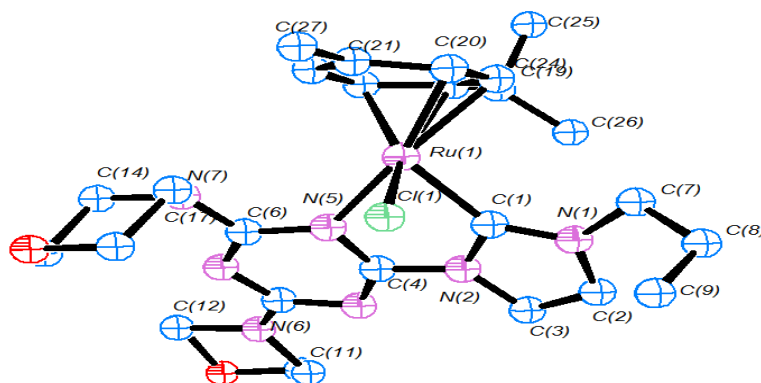
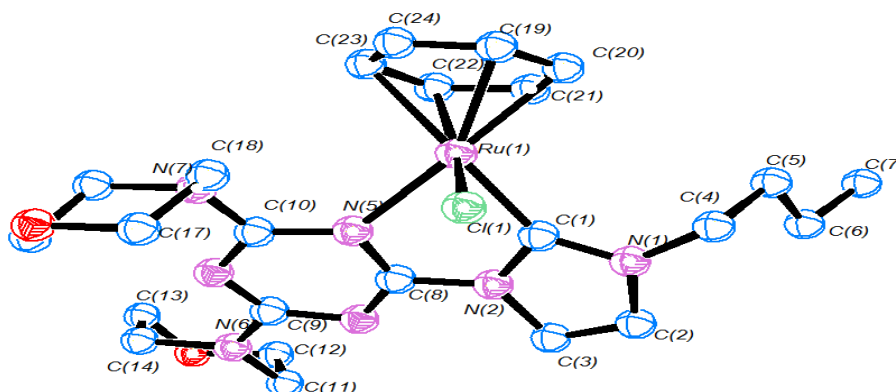
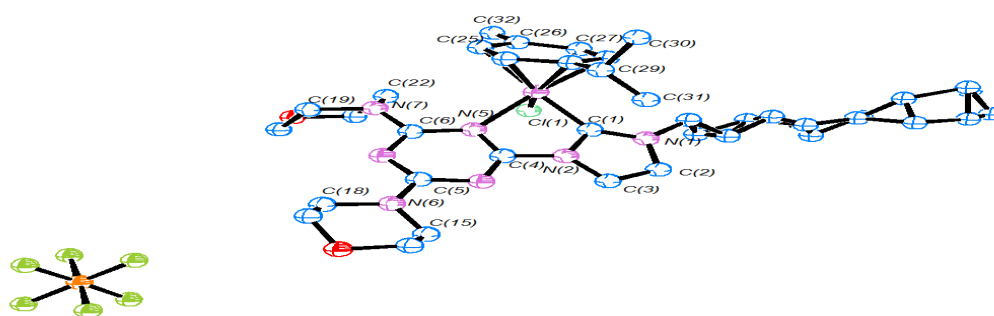


Table N.1: Crystal data and structure refinement for [[Ru (p-cymene)Cl(2.5)] PF₆, (5.4)

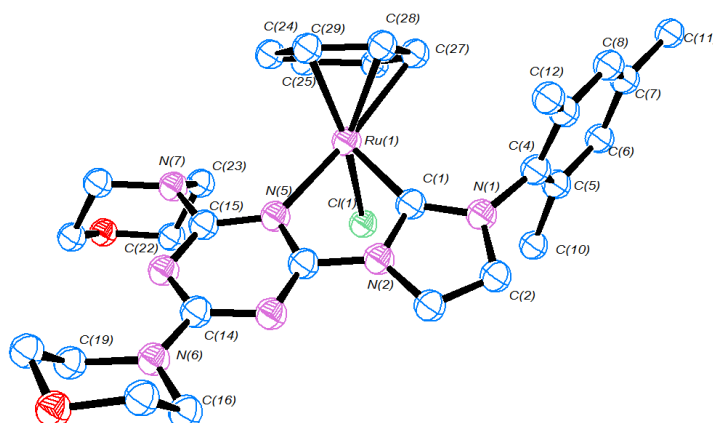
Identification code	2013ncs0839a	
Empirical formula	C ₂₈ H ₄₁ Cl ₃ F ₆ N ₇ O ₂ P ₁ Ru ₁	
Formula weight	860.07	
Temperature	100(2) K	
Wavelength	0.71075 Å	
Crystal system	Monoclinic	
Space group	P121/c1	
Unit cell dimensions	$a = 11.4445(8) \text{ \AA}$	$\alpha = 90^\circ$
	$b = 15.0619(11) \text{ \AA}$	$\beta =$
	$c = 21.0597(15) \text{ \AA}$	$\gamma = 90^\circ$
Volume	3516.6(4) Å ³	
Z	4	
Density (calculated)	1.624 Mg / m ³	
Absorption coefficient	0.790 mm ⁻¹	
$F(000)$	1752	
Crystal	Plate; Yellow	
Crystal size	0.08 × 0.04 × 0.01 mm ³	
θ range for data collection	2.281 – 27.482°	
Index ranges	–14 ≤ h ≤ 14, –18 ≤ k ≤ 19, –26 ≤ l ≤ 27	
Reflections collected	24503	
Independent reflections	8044 [$R_{int} = 0.0584$]	
Completeness to $\theta = 27.500^\circ$	99.6 %	
Absorption correction	Semi-empirical from equivalents	
Max. and min. transmission	1.000 and 0.574	
Refinement method	Full-matrix least-squares on F^2	
Data / restraints / parameters	8044 / 0 / 437	
Goodness-of-fit on F^2	1.032	
Final R indices [$F^2 > 2\sigma(F^2)$]	$R1 = 0.0475$, $wR2 = 0.1154$	
R indices (all data)	$R1 = 0.0734$, $wR2 = 0.1264$	
Extinction coefficient	n/a	
Largest diff. peak and hole	0.819 and –0.764 e Å ⁻³	

**Table O.1:** Crystal data and structure refinement for [Ru (C₆H₆)Cl(2.6)] PF₆, (5.6)

Identification code	2014ncs0109a	
Empirical formula	C ₂₄ H _{33.50} ClF ₆ N ₇ O _{2.25} PRu	
Formula weight	737.57	
Temperature	100(2) K	
Wavelength	0.71075 Å	
Crystal system	Monoclinic	
Space group	P121/c1	
Unit cell dimensions	<i>a</i> = 29.950(7) Å	<i>α</i> = 90°
	<i>b</i> = 14.365(3) Å	<i>β</i> = 107.174(4)°
	<i>c</i> = 28.015(7) Å	<i>γ</i> = 90°
Volume	11516(5) Å ³	
Z	16	
Density (calculated)	1.702 Mg / m ³	
Absorption coefficient	0.770 mm ⁻¹	
<i>F</i> (000)	5992	
Crystal	Lozenge; Yellow	
Crystal size	0.13 × 0.06 × 0.04 mm ³	
<i>θ</i> range for data collection	2.602 – 27.526°	
Index ranges	−38 ≤ <i>h</i> ≤ 38, −18 ≤ <i>k</i> ≤ 17, −35 ≤ <i>l</i> ≤ 36	
Reflections collected	73960	
Independent reflections	25963 [<i>R</i> _{int} = 0.0777]	
Completeness to <i>θ</i> = 25.242°	98.1 %	
Absorption correction	Semi-empirical from equivalents	
Max. and min. transmission	1.000 and 0.697	
Refinement method	Full-matrix least-squares on <i>F</i> ²	
Data / restraints / parameters	25963 / 0 / 1529	
Goodness-of-fit on <i>F</i> ²	1.069	
Final <i>R</i> indices [<i>F</i> ² > 2σ(<i>F</i> ²)]	<i>R</i> 1 = 0.1028, <i>wR</i> 2 = 0.2430	
<i>R</i> indices (all data)	<i>R</i> 1 = 0.1790, <i>wR</i> 2 = 0.3027	
Extinction coefficient	n/a	
Largest diff. peak and hole	7.693 and −2.080 e Å ⁻³	

**Table P.1:** Crystal data and structure refinement for [Ru(C₆H₆)Cl(2.7)] PF₆, (**5.8**)

Identification code	2013ncs0802a	
Empirical formula	C ₃₂ H ₄₉ Cl ₁ F ₆ N ₇ O ₂ P ₁ Ru ₁	
Formula weight	845.27	
Temperature	100(2) K	
Wavelength	0.71075 Å	
Crystal system	Monoclinic	
Space group	P121/c1	
Unit cell dimensions	$a = 11.3960(8) \text{ \AA}$	$\alpha = 90^\circ$
	$b = 15.5257(11) \text{ \AA}$	$\beta = 98.700(2)^\circ$
	$c = 20.5939(15) \text{ \AA}$	$\gamma = 90^\circ$
Volume	3601.8(4) Å ³	
Z	4	
Density (calculated)	1.559 Mg / m ³	
Absorption coefficient	0.626 mm ⁻¹	
$F(000)$	1744	
Crystal	Plate; Yellow	
Crystal size	0.04 × 0.03 × 0.01 mm ³	
θ range for data collection	2.234 – 27.485°	
Index ranges	–14 ≤ h ≤ 12, –20 ≤ k ≤ 20, –26 ≤ l ≤ 26	
Reflections collected	24540	
Independent reflections	8222 [$R_{int} = 0.0619$]	
Completeness to $\theta = 25.242^\circ$	99.6 %	
Absorption correction	Semi-empirical from equivalents	
Max. and min. transmission	1.000 and 0.663	
Refinement method	Full-matrix least-squares on F^2	
Data / restraints / parameters	8222 / 3 / 478	
Goodness-of-fit on F^2	1.047	
Final R indices [$F^2 > 2\sigma(F^2)$]	$R1 = 0.0492$, $wR2 = 0.0952$	
R indices (all data)	$R1 = 0.0808$, $wR2 = 0.1085$	
Extinction coefficient	n/a	
Largest diff. peak and hole	0.911 and –0.712 e Å ⁻³	

**Table Q.1:** Crystal data and structure refinement for [Ru(C₆H₆)Cl(2.8)] PF₆, (5.10)

Identification code	2014ncs0150x_twin1_hklf4	
Empirical formula	C ₂₉ H ₃₅ ClF ₆ N ₇ O ₂ PRu	
Formula weight	795.13	
Temperature	100(2) K	
Wavelength	0.71073 Å	
Crystal system	Triclinic	
Space group	<i>P</i> -1	
Unit cell dimensions	<i>a</i> = 8.8859(3) Å	<i>α</i> = 82.024(3) °
	<i>b</i> = 13.2681(4) Å	<i>β</i> = 75.430(3) °
	<i>c</i> = 13.8230(6) Å	<i>γ</i> = 87.225(3) °
Volume	1561.89(10) Å ³	
<i>Z</i>	2	
Density (calculated)	1.691 Mg / m ³	
Absorption coefficient	0.716 mm ⁻¹	
<i>F</i> (000)	808	
Crystal	Block; orange	
Crystal size	0.21 × 0.13 × 0.05 mm ³	
<i>θ</i> range for data collection	2.483 – 27.517°	
Index ranges	–11 ≤ <i>h</i> ≤ 11, –17 ≤ <i>k</i> ≤ 17, –17 ≤ <i>l</i> ≤ 17	
Reflections collected	11085	
Independent reflections	11085 [<i>R</i> _{int} = ?]	
Completeness to <i>θ</i> = 25.242°	99.8 %	
Absorption correction	Semi-empirical from equivalents	
Max. and min. transmission	1.00000 and 0.80175	
Refinement method	Full-matrix least-squares on <i>F</i> ²	
Data / restraints / parameters	11085 / 0 / 428	
Goodness-of-fit on <i>F</i> ²	1.078	
Final <i>R</i> indices [<i>F</i> ² > 2σ(<i>F</i> ²)]	<i>R</i> 1 = 0.0392, <i>wR</i> 2 = 0.1084	
<i>R</i> indices (all data)	<i>R</i> 1 = 0.0400, <i>wR</i> 2 = 0.1090	
Extinction coefficient	n/a	
Largest diff. peak and hole	1.338 and –1.222 e Å ⁻³	

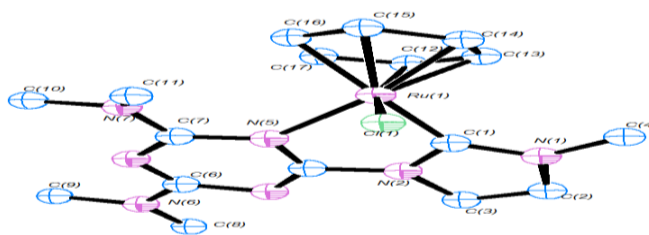


Table R.1: Crystal data and structure refinement [Ru(C₆H₆)Cl(2.13)] PF₆, (5.11)

Identification code	2014ncs0638a	
Empirical formula	C ₁₇ H ₂₃ ClF ₆ N ₇ PRu	
Formula weight	606.91	
Temperature	100(2) K	
Wavelength	0.71075 Å	
Crystal system	Monoclinic	
Space group	P121/n1	
Unit cell dimensions	$a = 13.406(7) \text{ \AA}$	$\alpha =$
90°	$b = 11.741(5) \text{ \AA}$	$\beta =$
107.968(6)°	$c = 14.525(7) \text{ \AA}$	$\gamma =$
90°		
Volume	2174.7(18) Å ³	
Z	4	
Density (calculated)	1.854 Mg / m ³	
Absorption coefficient	0.990 mm ⁻¹	
$F(000)$	1216	
Crystal	Plate; Yellow	
Crystal size	0.07 × 0.06 × 0.02 mm ³	
θ range for data collection	2.358 – 25.028°	
Index ranges	–17 ≤ h ≤ 16, –15 ≤ k ≤ 15, –18	
≤ l ≤ 18		
Reflections collected	5699	
Independent reflections	3739 [$R_{int} = ?$]	
Completeness to $\theta = 25.000^\circ$	97.5 %	
Absorption correction	Semi-empirical from	
equivalents		
Max. and min. transmission	1.000 and 0.414	
Refinement method	Full-matrix least-squares on F^2	
Data / restraints / parameters	3739 / 348 / 304	
Goodness-of-fit on F^2	1.089	
Final R indices [$F^2 > 2\sigma(F^2)$]	$R1 = 0.1244$, $wR2 = 0.3239$	
R indices (all data)	$R1 = 0.1719$, $wR2 = 0.3528$	
Extinction coefficient	n/a	
Largest diff. peak and hole	3.384 and –1.551 e Å ⁻³	